The Role of Glucocorticoid Receptor Signaling in Zebrafish Development

by

Dinushan Nesan

A thesis
presented to the University of Waterloo
in fulfillment of the
thesis requirement for the degree of
Doctor of Philosophy
in
Biology

Waterloo, Ontario, Canada, 2013

AUTHOR'S DECLARATION

I hereby declare that I am the sole author of this thesis. This is a true copy of the thesis, including any required final revisions, as accepted by my examiners.

I understand that my thesis may be made electronically available to the public.

Abstract

These studies present a series of novel roles for glucocorticoid signaling in the developing zebrafish embryo. The best-characterized roles of cortisol, the primary circulating corticosteroid in teleost fish, are known to occur by the activation of the glucocorticoid receptor (GR) in the post-hatch animal to mobilize energy reserves for response and recovery from stressful situations. For the first time, evidence is presented that GR and cortisol are key developmental regulators in the pre-hatch zebrafish embryo and that glucocorticoid signaling modulates multiple critical developmental pathways and affects embryogenesis in diverse ways.

Prior to these experiments, very little was known regarding the developmental role of glucocorticoids in lower vertebrates. In mammalian models, there has been extensive study of the action of these steroids in late-stage organ maturation, and they have a variety of clinical and biomedical applications. However, in fish, there was a relative dearth of information regarding the basic dynamics and potential functional roles of cortisol and GR in embryogenesis. Zebrafish are a popular model for developmental study, with optically transparent embryos that allow for reliable observation. Additionally, the zebrafish genome is fully sequenced and extensively annotated, and a variety of molecular biology techniques are well-established in the existing literature. The zebrafish is also now recognized as an advantageous model for endocrine and stress axis studies, as it expresses a single GR gene, unique among teleosts but comparable to mammals. Preliminary studies published in the literature described cortisol and GR as deposited in the zebrafish embryo prior to fertilization, and showed their expression declining prior to hatch, then rising significantly as larvae approach the stage of first feeding. This dynamic expression of both ligand and receptor during embryogenesis, combined with knowledge from mammalian models, led to the hypothesis that glucocorticoid signaling may be functionally relevant in zebrafish development.

A variety of techniques were used to examine the roles of cortisol and GR in the zebrafish embryo. Morpholino oligonucleotides were injected into one-cell embryos to block GR protein translation, allowing for the identification of GR-responsive developmental events and putative GR target genes. High-density microarray analysis of GR morphants presented numerous novel genes and pathways that are modulated by glucocorticoid signaling in the embryo. The ability to microinject molecules into a newly-fertilized zygote also allowed for other manipulations, including the addition of exogenous cortisol or the use of a cortisol-specific antibody to sequester

maternally deposited cortisol. These studies provided the first evidence regarding the functional importance of the maternal cortisol deposition in the zebrafish oocyte prior to fertilization.

The detailed temporal and spatial expression of GR mRNA and protein in the developing embryo has been characterized for the first time. GR expression is widespread, especially in developing mesoderm, and *de novo* GR transcription in the zebrafish embryo begins within 12 hours post fertilization. Lack of GR protein expression in the developing zebrafish embryo causes reduced growth, delayed somitogenesis, altered myogenesis, and severely reduces post-hatch survival. Additionally, GR modulates the expression of bone morphogenetic proteins, a family of morphogens that are involved in major developmental events including dorsoventral patterning, somitogenesis, myogenesis, and organogenesis. Reduction in GR protein content in the developing embryo is also linked to other major developmental processes including neurogenesis, eye formation, cellular adhesion, and development and function of the hypothalamic-pituitary-interrenal (HPI) axis.

Cortisol in the early embryo, which is contributed entirely by maternal deposition prior to fertilization, is an important regulator of cardiogenesis and development of the HPI axis. Modulation of cortisol content in the early embryo causes an impairment of the post-hatch response to a physical stressor, as larvae exposed to increased cortisol during embryogenesis displayed an inability to increase heart rate in response to an acute physical stress, and did not display the classical increase in cortisol that follows a stressor challenge. Embryos that experience lowered glucocorticoid signaling in development tend to have a heightened post-hatch response to stress, further supporting the conclusion that HPI axis development is regulated by glucocorticoid signaling. These studies have identified key cardiogenic and HPI axis genes that are GR-responsive, providing mechanistic explanations for these phenotypic changes. Together these findings indicate that maternal deposition of cortisol in the embryo can pattern the post-hatch larva and has definitive impacts on performance as the offspring begin locomotion and approach feeding stages.

In total, these studies demonstrate that glucocorticoid signaling is critically important to zebrafish embryogenesis, defining novel roles that are completely independent of the classical vertebrate stress response. These functions have significant effects on diverse developmental pathways and processes, and with the potential applicability of the zebrafish model to studies in higher vertebrates, may have important biomedical applications.

Acknowledgements

There may not be enough words to express my gratitude to those who have helped me make it through what has been the most challenging experience of my life, but I will try.

My deepest thanks to Dr. Matt Vijayan, my supervisor and friend, who gave me this opportunity, trusted me to see it through, gave me endless support both personally and professionally, and bought many pitchers of beer when they were most needed. I also need to thank my committee members, Dr. Mungo Marsden and Dr. David Spafford, for their invaluable kindness, support, input, and reason.

I am indebted to the great scientists who lent me their wisdom: Dr. Derek Alsop taught me to work with zebrafish; Dr. Maryam Kamkar taught me microinjection; and my dear friend Dr. Neel Aluru taught me to be a functional graduate student.

I could not be more thankful to the members of Dr. Vijayan's Stressed Lab that have shared space with me for the last five years. Without you, I surely would not have made it through this. Special thanks to the rest of the core four who started with me in 2007 as coworkers and are now cherished friends: Laura Dindia, Brian Chow, and Navdeep Sandhu. Love and high-fives to the others who have made the lab/offices into a second home and tolerated/encouraged my insanity and endless distractions, especially Erin Faught, Nataliya Melnyk-Lamont, Eunmi Park, Lynsi Henrickson, Liz Drolle, Darryl Jones, Wendy Guan, and Carol Best. My best wishes to Jen Ings, Nita Modi, Oana Birceanu, Edna Leung, Sarah Alderman, Anju Philip and so many others who passed through my life these past 5 years.

To my parents, I owe everything. I don't know where I would be if it wasn't for your love, guidance, and support, but it certainly wouldn't be here. Thank you.

Finally, and most importantly, to the woman who has been my source of support, grace, understanding, and love, Nicole Henderson, who had to listen to my endless complaints, tolerate piles of journal articles around our home, and put up with an exhausted absentee partner for far too long: Thank you is not meaningful enough, but it will have to do.

Dedication

For Nicole.

For my friends and family.

For all who believed in me when I didn't believe in myself.

Table of Contents

AUTHOR'S DECLARATION ii
Abstract iii
Acknowledgements v
Dedication vi
Table of Contents vii
List of Figures xi
List of Tables xiii
Chapter 1 General Introduction 1
1.1 Introduction 2
1.2 The corticosteroid stress axis in teleosts 5
1.3 Zebrafish as a model for corticosteroid research 11
1.4 Early zebrafish development 12
1.5 Roles of bone morphogenetic proteins in development 19
1.6 Development of the zebrafish corticosteroid stress axis 19
1.6.1 Structure and development of the hypothalamus 19
1.6.2 Structure and development of the pituitary 20
1.6.3 Structure and development of the interrenal tissue 22
1.7 Ontogeny of stress response in zebrafish 25
1.8 Developmental role for glucocorticoid signaling 28
1.8.1 Developmental roles of glucocorticoids in mammals 28
1.8.2 Developmental role of glucocorticoids in non-mammalian models 29
1.9 Major techniques utilized in zebrafish developmental studies 30
1.9.1 Morpholino oligonucleotides 30
1.9.2 Microinjection into single-cell zebrafish embryos 31
1.10 Objectives 34
Chapter 2 Glucocorticoid receptor signaling is essential for mesoderm formation and muscle development in zebrafish 35
2.1 Overview 36
2.2 Introduction 36
2.3 Materials & Methods 38
2.3.1 Zebrafish care 38

2.3.2 Embryo GR expression 38
2.3.3 GR promoter activation 39
2.3.4 GR knockdown 40
2.3.5 Western blotting 40
2.3.6 Gene expression 41
2.3.7 Embryo survival and morphology 44
2.3.8 Zebrafish GR mRNA synthesis and rescue 44
2.3.9 Promoter analysis 45
2.3.10 Statistical analysis 45
2.4 Results 45
2.4.1 Temporal GR expression in zebrafish embryos 45
2.4.2 GR knockdown 50
2.4.3 GR signaling is important for embryo growth and survival 54
2.4.4 GR signaling is essential for mesoderm patterning 61
2.5 Discussion 74
2.6 Acknowledgements 77
Chapter 3 Embryo exposure to elevated cortisol level leads to cardiac performance dysfunction in zebrafish 78
3.1 Overview 79
3.2 Introduction 79
3.3 Materials and Methods 81
3.3.1 Zebrafish care 81
3.3.2 Cortisol injection 81
3.3.3 Embryo morphology 82
3.3.4 Cardiac performance 82
3.3.5 Cortisol ELISA 83
3.3.6 Gene expression 83
3.3.7 Protein expression 85
3.3.8 Statistical analysis 85
3.4 Results 85
3.4.1 Cortisol levels 85
3.4.2 GR expression and signaling 88

3.4.3 Cardiac morphogenesis 91
3.4.4 Marker genes for cardiac development 94
3.4.5 Cardiac performance 97
3.5 Discussion 100
3.6 Acknowledgement 103
Chapter 4 Knockdown of glucocorticoid receptor protein expression significantly alters global gene expression in developing zebrafish 104
4.1 Overview 105
4.2 Introduction 105
4.3 Materials and Methods 107
4.3.1 Zebrafish care and breeding 107
4.3.2 Morpholino microinjection 107
4.3.3 RNA extraction 108
4.3.4 Microarray scanning and analysis of resulting data 108
4.3.5 Quantitative PCR 109
4.4 Results 112
4.4.1 Major trends and characteristics of microarray results 112
4.4.2 Results of pathway analysis 120
4.4.3 Confirmation by quantitative PCR 131
4.5 Discussion 136
4.5.1 Confirmation that the BMP signaling pathway is GR responsive 137
4.5.2 Novel pathways identified for the GR knockdown phenotype 138
4.5.3 Neurogenesis and eye formation affected by GR knockdown 140
4.5.4 Effects of GR knockdown on endocrine signaling 143
4.5.5 GR knockdown disrupts expression of cell-adhesion molecules 145
4.5.6 Conclusions 146
4.5.7 Acknowledgement 147
Chapter 5 Maternal cortisol is critical for stress axis development in zebrafish 148
5.1 Overview 149
5.2 Introduction 149
5.3 Materials and Methods 152
5.3.1 Zebrafish care and breeding 152

5.3.2 Treatment injections 152
5.3.3 Characterization of embryo phenotypes 153
5.3.4 Stressor exposure 153
5.3.5 Cortisol extraction and quantification 154
5.3.6 Gene expression 154
5.3.7 Statistical analysis 156
5.4 Results 156
5.4.1 Confirmation of antibody efficacy 156
5.4.2 Observation and characterization of embryo phenotypes 159
5.4.3 Embryo cortisol concentration throughout development 166
5.4.4 Quantifying the response to a physical stressor 169
5.4.5 Expression of HPI axis genes 172
5.5 Discussion 178
5.5.1 Characterization and validation of treatments 178
5.5.2 Developmental cortisol dynamics in our treated embryos 179
5.5.3 Reduced embryonic cortisol availability enhances the larval stress response 180
5.5.4 Exogenous cortisol addition reduces HPI axis stress response capacity 181
5.5.5 Potential disruptions to embryo fitness as a result of altered maternal cortisol deposition 182
5.5.6 Conclusions 182
5.6 Acknowledgement 183
Chapter 6 General Conclusions 184
6.1 Summary of findings 185
6.2 Perspectives and avenues for further research 189
6.3 Conclusions 191
Appendix A Chapter 2 Supplemental Information and Figures 192
Appendix B Expanded Methods and Protocols 202
Appendix C Complete List of Significantly Changed Genes from Chapter 4 Microarray Analysis 205
Publication Permissions 263
References 266

List of Figures

All figures in this thesis are original works by Dinushan Nesan.

Chapter 1: Introduction

Figure 1. Schematic diagram of the hypothalamic-pituitary-interrenal (HPI) axis……....7
Figure 2. Schematic diagram of classical glucocorticoid receptor activation……....9
Figure 3. Representative images of key milestones in zebrafish development……18
Figure 4. Summary of zebrafish hypothalamus-pituitary-interrenal development……24
Figure 5. Structures of DNA and morpholino oligonucleotides……33

Chapter 2: Glucocorticoid receptor signaling is essential for mesoderm formation and muscle development in zebrafish

Figure 1. Glucocorticoid receptor (GR) gene and protein expression in wild-type embryos……...48
Figure 2. Glucocorticoid receptor protein knockdown by morpholino injection……..52
Figure 3. Effect of glucocorticoid receptor knockdown on embryo survival and development……...56
Figure 4. Effects of glucocorticoid receptor knockdown on morphogenesis……59
Figure 5. Effects of glucocorticoid receptor knockdown on expression of developmental genes……64
Figure 6. Effects of glucocorticoid receptor knockdown on expression of BMP signaling markers…67
Figure 7. Effects of glucocorticoid receptor knockdown on expression of myogenic transcription factors……69
Figure 8. Effects of glucocorticoid receptor knockdown on mRNA abundance of muscle specific proteins……..71
Figure 9. GR receptor knockdown and mRNA rescue of disrupted expression of myogenic genes…73

Chapter 3: Embryo exposure to elevated cortisol level leads to cardiac performance dysfunction in zebrafish

Figure 1. Whole body cortisol content……..87
Figure 2. Glucocorticoid receptor and glucocorticoid responsive gene expressions……90
Figure 3. Heart deformity phenotypes……..…..93
Figure 4. mRNA abundance of cardiac genes……...96
Figure 5. Cardiac performance……..99

Chapter 4: Knockdown of glucocorticoid receptor protein expression significantly alters global gene expression in developing zebrafish

Figure 1. Numbers of statistically significant genes upregulated and downregulated at 24 and 36 hpf in response to GR knockdown……117

Figure 2. Distribution of fold-change for statistically significant genes at 24 and 36 hpf in response to GR knockdown……119

Figure 3. Functional annotation (using Ingenuity Pathway Analysis software) of genes that were upregulated and downregulated by GR knockdown……...124

Figure 4. Interactome networks of select pathways identified as GR responsive by Ingenuity Pathway Analysis software……126

Figure 5. Confirmation of microarray findings by qPCR analysis……..134

Chapter 5: Maternal cortisol is critical for stress axis development in zebrafish

Figure 1. Confirmation of antibody efficacy……...158

Figure 2. Representative images of treated embryos……...161

Figure 3. Quantification of embryo length……..163

Figure 4. Quantification of embryo extension……165

Figure 5. Embryo cortisol content of treated embryos during development……..……168

Figure 6. Cortisol response to a physical stressor in treated larvae……171

Figure 7. Altered expression of HPI axis genes……..174

Chapter 6: General Conclusions

Concluding Figure. Summary of known glucocorticoid-responsive genes and pathways in zebrafish development. ……..188

Appendix A: Chapter 2 supplemental information and figures

Figure A1. Glucocorticoid receptor-green fluorescent protein (GR-GFP) reporter construct……....194

Figure A2. Putative GR promoter sequence……196

Figure A3. Fluorescence images of GR promoter activation in developing embryos……199

Figure A4. Putative non-functional glucocorticoid response elements in MyoD and IGF promoter regions……201

List of Tables

Chapter 1: Introduction

Table 1. Animal stress axis signaling reviews from the primary literature…….....3
Table 2. Reviews pertaining to stress axis interactions with major physiological systems……..10
Table 3. Reviews regarding the use of the zebrafish model in developmental study……16
Table 4. The time of first onset of stress axis signal synthesis and stress responsiveness in various model animals in relation to total gestation/hatching time (shown as percentage) ……..27

Chapter 2: Glucocorticoid receptor signaling is essential for mesoderm formation and muscle development in zebrafish

Table 1. Primers used for RT-PCR and qPCR (bold) and their amplicon size and melting temperatures (Tm)…….43

Chapter 3: Embryo exposure to elevated cortisol level leads to cardiac performance dysfunction in zebrafish

Table 1. Primers used for qPCR and their amplicon size and melting temperatures (Tm) ……..84

Chapter 4: Knockdown of glucocorticoid receptor protein expression significantly alters global gene expression in developing zebrafish

Table 1. Details of primer pairs for qPCR, including forward and reverse nucleotide sequences, melting temperatures, and amplicon length…….111
Table 2. Select genes (top ranked based on fold-change) that were significantly upregulated in response to GR knockdown at 24 and 36 hpf, with their respective fold-change values and p-values from statistical comparisons……113
Table 3. Select genes (top ranked based on fold-change) that were significantly downregulated in response to GR knockdown at 24 and 36 hpf, with their respective fold-change values and p-values from statistical comparisons ……..114
Table 4. Functional grouping (based on Ingenuity Pathway Analysis and Gene Ontology databases) of select genes that were significantly affected by GR knockdown at both 24 and 36 hpf, with their fold-change values at each timepoint…….…….115

Table 5. Gene-regulatory networks that are GR responsive, identified by Ingenuity Pathway Analysis software at 24 hpf and the calculated IPA score (higher scores denote more strongly affected pathways)……121
Table 6. Gene-regulatory networks that are GR responsive, identified by Ingenuity Pathway Analysis software at 36 hpf and the calculated IPA score (higher scores denote more strongly affected pathways)……122
Table 7. List of genes confirmed using microarray and qPCR with fold-changes and p-values……132

Chapter 5: Maternal cortisol is critical for stress axis development in zebrafish
Table 1. Primer pair sequences, characteristics, and applicable references used for qPCR……155

Appendix C: **Complete List of Significantly Changed Genes from Chapter 4 Microarray Analysis**
Table C1. Significantly changed genes at 24 hpf in response to GR knockdown……...207
Table C2. Significantly changed genes at 36 hpf in response to GR knockdown……...241

Chapter 1
General Introduction

1.1 Introduction

Activation of the vertebrate corticosteroid stress axis involves a highly conserved set of coordinated signaling events between various organs leading to hormonal release in response to stressor insult (see Table 1 for reviews). In teleosts the main circulating stress steroid is cortisol and this hormone binds to glucocorticoid receptor (GR) which acts as a transcription factor upon ligand binding to affect gene expression in target tissues (Bury and Sturm, 2007; Prunet et al., 2008). It has recently been shown in zebrafish (*Danio rerio*), GR mRNA abundance is differentially regulated during embryogenesis (Alsop and Vijayan, 2008; 2009). Cortisol is also present in the newly fertilized embryo (Alsop and Vijayan, 2008), and the combined presence of both receptor and ligand leads to interesting questions of potential glucocorticoid signaling actions in development.

It should be noted that cortisol can also bind and activate teleost mineralocorticoid receptors (MR) *in vitro* (Prunet et al., 2006; Pippal et al., 2011). However, the extent to which it acts in tissues *in vivo* is unclear, as research has shown the co-expression of MR with the cortisol-converting enzyme 11-hydroxysteroid dehydrogenase 2 (*11hsd2*) indicating that cortisol-MR binding may be similar to that in mammals where active cortisol is often spatially separate from MR expressing tissues (Edwards et al., 1988; Pascual-Le Tallec and Lombes, 2005; Sturm et al., 2005). Teleosts do not synthesize aldosterone, and the primary ligand for MR remains unknown (Sturm et al., 2005; Pippal et al., 2011). As with GR, MR expression is also dynamic in the early embryo (Alsop and Vijayan, 2008), but without a clear understanding of basic function and activation, it is difficult to assess its importance. For these reasons, this introductory chapter and this dissertation in total will focus on the role of cortisol and its activation of the glucocorticoid receptor.

While the role of GR activation on downstream molecular responses has been explored to a large extent by expression analysis of targeted glucocorticoid-responsive genes and/or by microarrays examination of transcriptomic changes in teleosts (Mommsen et al., 1999; Vijayan et al., 2005; Aluru and Vijayan, 2007; Aluru and Vijayan, 2009), the role of cortisol and the GR signaling in developmental programming is far from clear. This introductory chapter will describe general zebrafish embryogenesis and some key developmental processes and regulatory pathways, as well as the development of the zebrafish stress axis organs and what is known about the role of glucocorticoid signaling in the development of a variety of animals.

Table 1 – Animal stress axis signaling reviews from the primary literature

Major Subject/Animal(s)	**Reference**
Fish	(Wendelaar Bonga, 1997)
Fish	(Mommsen et al., 1999)
Fish	(Schreck et al., 2001)
Fish	(Barton, 2002)
Fish	(Prunet et al., 2006)
Fish	(Bury and Sturm, 2007)
Fish	(Prunet et al., 2008)
Fish	(Aluru and Vijayan, 2009)
Fish	(Pankhurst, 2011)
Amphibians	(Rollins-Smith, 2001)
Amphibians	(Denver et al., 2002)
Amphibians/reptiles	(Moore and Jessop, 2003)
Reptiles	(Greenberg, 1990)
Reptiles	(Lance, 1990)
Birds	(Siegel, 1980)
Birds	(Harvey and Hall)
Birds	(Hess, 2006)
Birds	(Martin and Rubenstein, 2008)
Mammals	(Boonstra, 2005)
Mammals	(Reeder and Kramer, 2005)
Humans	(Zhou and Cidlowski, 2005)
Humans	(Nicolaides et al., 2010)

Table 1 (Continued) – Animal stress axis signaling reviews from the primary literature

Major Subject/Animal(s)	Reference
Vertebrates	(Dallman et al., 1992)
Vertebrates	(Johnson et al., 1992)
Vertebrates	(Ottaviani and Franceschi, 1996)
Vertebrates	(Chrousos, 2000)
Vertebrates	(Sapolsky et al., 2000)
Vertebrates	(Tsigos and Chrousos, 2002)
Vertebrates	(Charmandari et al., 2004b)
Vertebrates	(Chrousos, 2006)
Vertebrates	(Smith and Vale, 2006)
Vertebrates	(Wada, 2008)
Vertebrates	(Denver, 2009)
Vertebrates	(Tort and Teles)
Molecular mechanisms	(Burnstein and Cidlowski, 1989)
Molecular mechanisms	(Adcock, 2001)
Molecular mechanisms	(Schaaf and Cidlowski, 2002)
Molecular mechanisms	(Yudt and Cidlowski, 2002)
Molecular mechanisms	(Schoneveld et al., 2004)
Molecular mechanisms	(Heitzer et al., 2007)
Molecular Mechanisms	(Mormede et al., 2011)

1.2 The corticosteroid stress axis in teleosts

The vertebrate stress response is highly conserved and well characterized in a variety of different animals (see Table 1). In general, perception of a stressor leads to the release of corticotropin-releasing hormone (CRH) (or corticotropin-releasing factor (CRF) in fish) from the hypothalamus (Feist and Schreck, 2001; Tsigos and Chrousos, 2002). This neuropeptide acts on the anterior pituitary and stimulates the release of adrenocorticotropic hormone (ACTH), which acts on the adrenal gland (or interrenal tissue in fish) to release corticosteroids, including cortisol or corticosterone (Schmidt and Litwack, 1982; Wendelaar Bonga, 1997; Levine, 2001; Charmandari et al., 2004b), into circulation. Together, this interconnected network of organs is known as the hypothalamus-pituitary-interrenal (HPI; see Figure 1 for a schematic) axis in fish and their functioning is critical for evoking a cortisol stress response (Chrousos and Gold, 1992; Rehan, 1996). A key metabolic role for corticosteroids is to mobilize energy substrate stores and produce glucose to cope with immediate energy demands during stressor exposure, and also to replenish glycogen stores during recovery (Ballard and Ballard, 1974; Chrousos and Gold, 1992; Johnson et al., 1992; Wendelaar Bonga, 1997; Charmandari et al., 2004b; Schreck, 2010). However, glucocorticoids also act on other systems, including nervous, muscle, reproductive, and immune systems, to affect behavior, growth, metabolism, reproduction, and/or health of the animal (see Table 2 for reviews). This action is mediated predominantly by binding to intracellular corticosteroid receptors (Funder, 1997), including GR and MR (Mommsen et al., 1999). Corticosteroid binding activates GR, and results in dimerization and translocation into the nucleus, where the activated-complex modulates target gene expression by binding to glucocorticoid response elements (GREs) upstream of target genes (Funder, 1993; Mommsen et al., 1999; Charmandari et al., 2004a) (see Figure 2 for a schematic). Mammals express a single GR gene, which is under variable regulation by multiple phosphorylation sites (Webster et al., 1997). Humans express two splice variants, GRα and GRß (Bamberger et al., 1995), that exhibit different transcriptional activities, and GRß is activated even in the absence of ligand binding (Kino et al., 2009). Unlike other vertebrates, most teleost fish exhibit multiple GR genes as a result of genome-wide duplication events and this has been reviewed recently (Meyer and van de Peer, 2005).

Figure 1 – Schematic diagram of the hypothalamic-pituitary-interrenal (HPI) axis
The HPI axis is the coordinated stress axis in teleosts and consists of the hypothalamus which recognizes a stressor and produces corticotropin-releasing factor (CRF) that acts on the anterior pituitary to cause the release of adrenocorticotrophic hormone (ACTH), that is released into general circulation and causes the release of cortisol from the interrenal tissue. Cortisol then acts on a variety of tissues to mobilize energy stores and affect metabolic and other pathways to prepare for a recovery from stressor challenge.

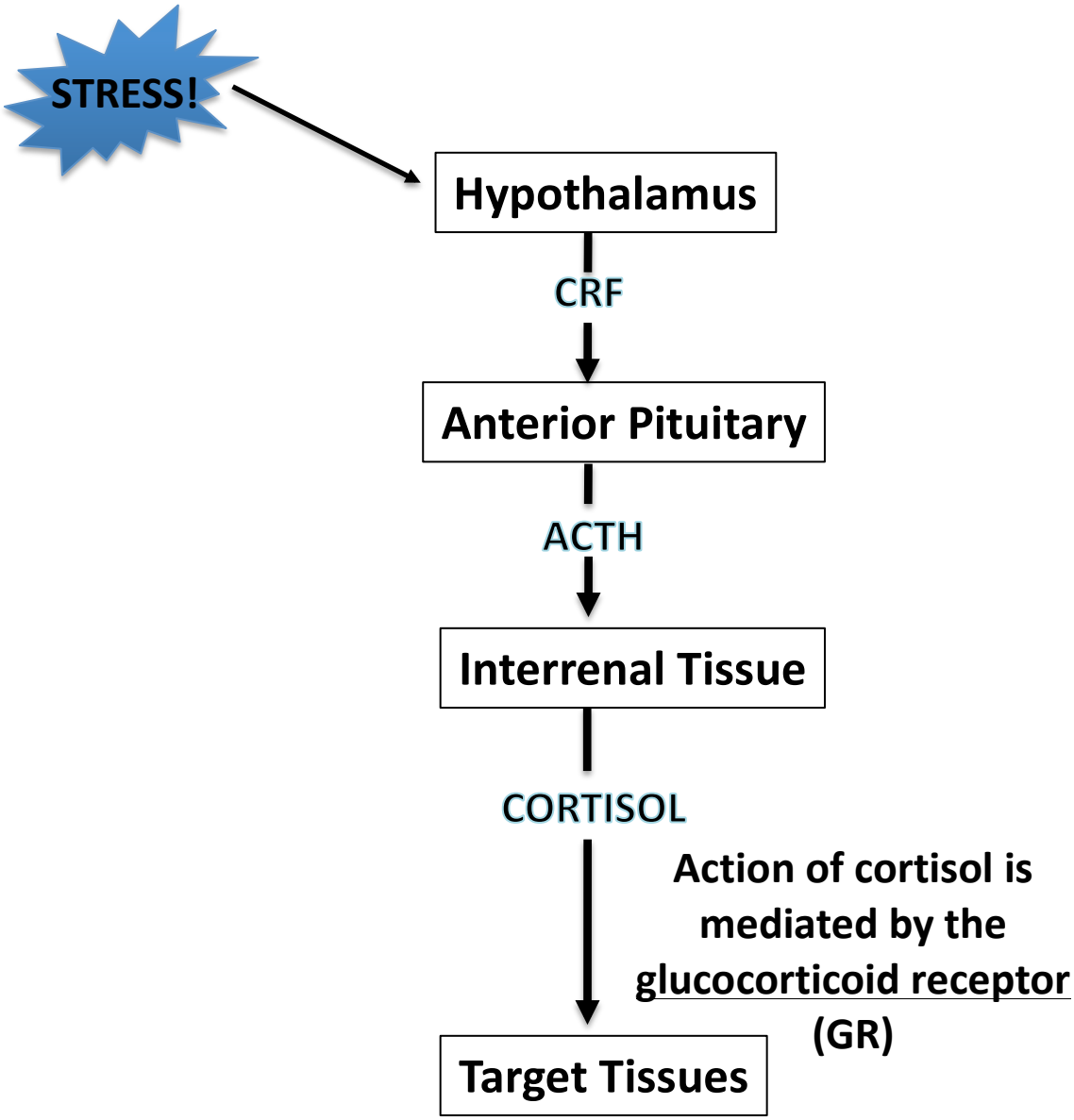
STRESS!
Hypothalamus
CRF
Anterior Pituitary
ACTH
Interrenal Tissue
CORTISOL
Action of cortisol is mediated by the glucocorticoid receptor (GR)
Target Tissues

Figure 2 – Schematic diagram of classical glucocorticoid receptor activation

After the release of cortisol into circulation from the interrenal tissue, it crosses membranes readily due to its hydrophobic steroid structure. It then binds to the cytosolic glucocorticoid receptor (GR) which is thought to be bound by molecular chaperones in teleosts. Cortisol binding causes the shedding of these chaperones and the dimerization of the activated receptor which then translocates to the nucleus to act as a transcription factor and modulate target gene expression.

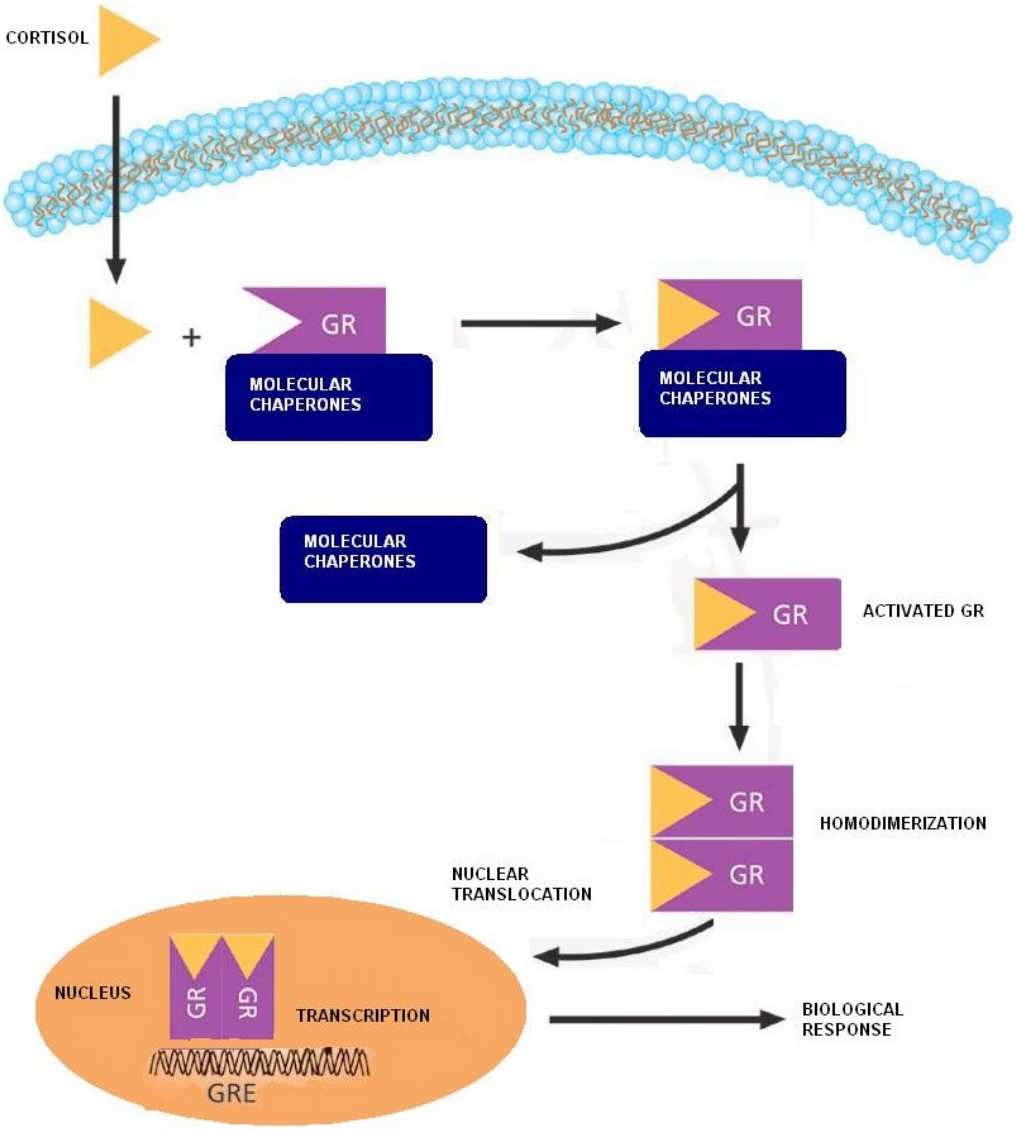
CORTISOL
GR
MOLECULAR CHAPERONES
GR
MOLECULAR CHAPERONES
MOLECULAR CHAPERONES
GR
ACTIVATED GR
GR
GR
HOMODIMERIZATION
NUCLEAR TRANSLOCATION
NUCLEUS
GR
GR
TRANSCRIPTION
GRE
BIOLOGICAL RESPONSE

Table 2 – Reviews pertaining to stress axis interactions with major physiological systems

Target System	**Reference**
Behaviour	(O'Connor et al., 2000)
Behaviour	(Summers, 2002)
Behaviour	(Summers et al., 2005)
Behaviour	(Wolkowitz et al., 2009)
Behaviour	(Ellis et al., 2012)
Feeding	(Bernier and Peter, 2001)
Immune system	(Dohms and Metz, 1991)
Immune system	(Weyts et al., 1999)
Immune system	(Rollins-Smith, 2001)
Immune system	(Padgett and Glaser, 2003)
Immune system	(Bauer, 2005)
Immune system	(Tort, 2011)
Metabolism	(van der Boon et al., 1991)
Metabolism	(Kyrou and Tsigos, 2009)
Metabolism/Cardiovascular	(Maxwell et al., 1994)
Metabolism/Cardiovascular	(Walker, 2007)
Metabolism/Growth	(Thakore and Dinan, 1994)
Metabolism/Growth	(van Weerd and Komen, 1998)
Osmoregulation	(McCormick, 2001)
Reproduction	(Tilbrook et al., 2000)
Reproduction	(Wingfield and Sapolsky, 2003)
Reproduction	(Tetsuka, 2007)
Reproduction	(Borell et al., 2007)
Reproduction	(Milla et al., 2009)
Reproduction	(Leatherland et al., 2010)
Reproduction	(Schreck, 2010)
Reproduction	(Vrekoussis et al., 2010)

1.3 Zebrafish as a model for corticosteroid research

Considering the depth of knowledge and study that has been focused on the role of circulating glucocorticoids in animals, it is surprising that detailed investigation of glucocorticoid action during early development has only recently been explored. Some of this is likely due to the relative opacity of embryogenesis in mammalian models as the early developmental events occur *in utero* limiting the accessibility of the embryo for visual observation. As an alternative to the primary mammalian model, the mouse, the zebrafish is a prominent model organism for developmental study (Lele and Krone, 1996; Grunwald and Eisen, 2002; Berman et al., 2005). Zebrafish embryos are optically clear and develop externally over a short period of time; they hatch within 2 days of fertilization and are mobile and feeding within 5 days of fertilization (Kimmel, 1989; Kimmel et al., 1995). The adult fish are hardy, breed readily and in large numbers, and there exist numerous continuing strains that allow for controlled experiments on genetically identical animals (Segner, 2009). In addition, the zebrafish genome is sequenced and well characterized and annotated, allowing the usage of advanced genetic techniques to investigate the effects of specific genes or proteins in developmental processes (Aleström et al., 2006). Specifically, forward and reverse genetic techniques, such as gene or protein silencing, can be used readily to identify molecular mechanisms and isolate developmental roles for genes of interest (Nasevicius and Ekker, 2000; Löhr and Hammerschmidt, 2011).

Unlike most teleost species, which express multiple glucocorticoid receptor genes in their genome, the zebrafish has only a single GR gene, as seen in mammals (Alsop and Vijayan, 2008; Schaaf et al., 2008). The single zebrafish GR gene is expressed as two splice-variant isoforms (GRα and GRß) that are very similar in structure to those found in humans, although the role of the newly identified GRß variant remains unclear (Schaaf et al., 2008). The implications of this genomic profile are still being investigated, but it provides a promising framework to examine corticosteroid effects during development in humans. In addition, *de novo* cortisol synthesis in zebrafish embryos begins only around hatching (Alsop and Vijayan, 2008; 2009), meaning that glucocorticoid signaling during early development is due only to maternally deposited cortisol. This allows for easier identification of glucocorticoid-responsive developmental processes than in mammalian systems, where fetal glucocorticoid concentrations are more dynamic, and protection from maternal glucocorticoids is dependent on enzymatic degradation at the placenta (Yang, 1997). Together, these attributes underscore the utility of zebrafish as a valuable model for developmental and endocrine disorders, with potentially significant application to human health and disease (Dooley and Zon, 2000; Schaaf et al., 2009; Schoonheim et al., 2010).

1.4 Early zebrafish development

Vertebrate development is complex, but is reasonably well conserved, with numerous patterning processes and morphogenic movements occurring in diverse animals, including gastrulation, somitogenesis, and general body axis patterning (de Robertis et al., 2000; Altmann and Brivanlou, 2001; Yin et al., 2009; Mallo et al., 2010; Maroto et al., 2012). The zebrafish has emerged as a prominent model organism for developmental studies (see Table 3 for reviews) due to a number of useful attributes. Zebrafish are hardy fish that spawn large clutches of eggs readily in laboratory settings, and these eggs are optically clear allowing for ready observation of developmental processes (Lele and Krone, 1996; Lawrence, 2007). In this section the broad morphogenetic stages of pre-hatch zebrafish development will be outlined. All staging times are from standard incubation experiments and observations of zebrafish carried out at 28.5 C, which is considered the optimal temperature for zebrafish embryo incubation and development (Kimmel et al., 1995; Westerfield, 2007).

Many different factors are present in the zebrafish oocyte prior to fertilization, including cortisol and GR transcripts as mentioned previously, and the consensus is that they are highly active in early development (Pelegri, 2003; Abrams and Mullins, 2009; Fuentes and Fernández, 2010). After fertilization, the newly-created zygote remains a single cell for approximately 40 minutes, then the first cell division begins (Kimmel et al., 1995). The initial cell represents the animal pole of the cell and sits atop the yolk cell, and the yolk region most distant from the fertilized cell is the vegetal pole (Marlow and Mullins, 2008). The cleavage stage begins after the completion of first division, and cells divide synchronously every 15 minutes (Kimmel et al., 1995). The whole mass of cells is termed the blastodisc at this stage (Kimmel and Law, 1985a). Zebrafish cell division is meroblastic, with dividing daughter cells (termed blastomeres) sitting atop the large yolk cell (Solnica-Krezel and Driever, 1994). Meroblastic division means that some cells remain incompletely divided, and are linked to each other by cytoplasmic connections (Kimmel and Law, 1985a). During these cleavage events, cytoplasmic streaming of yolk content into the newly formed blastomeres brings deposited factors into the developing embryo (Howley and Ho, 2000). This process is particularly advantageous for experiments that attempt to manipulate the early embryo environment, as changes in the yolk content can have functional action on the early embryo. The cleavage stage ends after the sixth division creating a 64-cell embryo, and for the first time there is more than a single layer of cells lying atop the yolk (Kimmel et al., 1995).

As the cells begin to layer they are renamed the blastula, marking the onset of the blastula period at the 128-cell stage (~2 hours post fertilization [hpf]). During the blastula period, cell division becomes less coordinated with waves of division moving across the cell mass forming a domed mass on top of the yolk (Kimmel et al., 1995). Midway through the blastula period, two distinct and important developmental events occur: the formation of the yolk syncytial layer (YSL) and the mid-blastula transition (MBT) (Kane and Kimmel, 1993; Carvalho and Heisenberg, 2010). The YSL is thought to be unique to teleosts and is a layer formed from the marginal cells of the blastula, those cells still connected from early cleavage events, which degrade and release their cytoplasm into the yolk (Kimmel and Law, 1985b; Chen and Kimelman, 2000). These cells continue nuclear division and remain positioned just under the developing blastula and appear to act as an organizing center for mesoderm and endoderm differentiation as well as later events in embryogenesis (Carvalho and Heisenberg, 2010). The MBT marks the onset of *de novo* transcription in the embryo and the degradation of most of the maternally deposited mRNA (Kane and Kimmel, 1993; Pelegri, 2003; Giraldez et al., 2006). The MBT is characterized by a lengthening of the cell cycle and a slowing of division rate, and seems to be triggered by a threshold ratio between the amount of nuclear and cytoplasmic material (Kane and Kimmel, 1993). In addition, the MBT is an early cell-fate differentiation point (Kimmel et al., 1990). As these processes occur, the cells, now termed the blastoderm, continue to divide and amass atop the yolk, until they begin to spread thinly across the surface of the yolk hemisphere late in the blastula period (Ho, 1992). This process is termed epiboly; Figure 3 shows the difference between embryos before (A) and during (B) epiboly, the movement of the blastoderm cells down towards the vegetal pole can be seen (arrows indicate boundary). Epiboly is classified by the percent of yolk covered by the spreading blastula cells, and marks the transition from blastula to gastrula period at approximately 5 hpf (Kimmel et al., 1995). At 50% epiboly, gastrulation begins and cells at the edges of the spreading blastoderm begin the process of involution, in which they fold inward and form a second layer underneath the spreading cells (Ho, 1992). As involution occurs, the blastoderm also continues to spread across the surface of the yolk towards the vegetal pole, eventually achieving near complete coverage of the yolk at the end of epiboly (Kimmel et al., 1995). Gastrulation events coincide with cell fate determination and studies have established fate maps of the embryo at 50% epiboly (Kimmel et al., 1990; Ho, 1992). Gastrulation also marks the primary period of dorsoventral patterning, beginning with the creation of the thickened shield region that will act as an organizing centre and becomes the dorsal region of the developing embryo (Ho, 1992; Schier, 2001; Montero, 2005). A number of well-characterized developmental morphogens are involved in dorsoventral patterning, including

members of the fibroblast growth factor family (Furthauer, 2004), the hedgehog family (Johnson et al., 1994; Ekker et al., 1995), nodal-related genes (Rebagliati et al., 1998) and the bone morphogenetic proteins (BMPs; Hammerschmidt and Mullins, 2002). As involution continues and after the movements of epiboly are complete, the embryo thickens to form a ring-like region surrounding the yolk (see Figure 3C) that will soon become recognizable as the developing animal with a classical vertebrate body plan (Kimmel et al., 1995). Gastrulation ends at approximately 10 hpf with the embryo displaying a distinct axis and recognizable body shape, including a thickened head region at the shield and a smaller thickening at the tail (Ho, 1992; Kimmel et al., 1995).

After gastrulation, the next major stage of zebrafish development is the segmentation period. During this period the somitogenesis occurs and the tail becomes recognizable as the embryo develops and uncurls from around the yolk (Figure 3D; Schroter et al., 2008). Somites develop in bilateral pairs on either side of the developing notochord, which is the vertebral region progenitor tissue and also produces signals that will induce neural tissue formation (Glickman et al., 2003). Somite pairs form every 30 minutes until 30 pairs are complete after ~24 hpf (Stickney et al., 2000). Somites differentiate into the skeleton and skeletal muscle, as well as cartilage and epithelial tissue and develop a classical chevron shape as myosin chains form and elongate (Kimmel and Warga, 1987; Kimmel et al., 1995; Stickney et al., 2000; Patterson et al., 2010). Organogenesis also begins during the segmentation period, with the specification and organization of multiple organ primordia, including the kidneys, eyes, and brain (Kimmel et al., 1995; Mueller and Wullimann, 2003). The neural plate thickens in response to signals from the developing notochord and eventually forms the neural tube, the source of the central nervous system tissue (Glickman et al., 2003; Mueller and Wullimann, 2003; Maier et al., 2011). As the segmentation period ends at approximately 24 hpf, the embryo begins random movements in the tail region as the developing muscle fibres contract and expand (Stickney et al., 2000).

The pharyngula period follows segmentation and many of the processes that began before 24 hpf continue as the embryo enters the second day of development. The neural tube hollows and enlarges in the dorsal region to become the brain, forming five distinct lobe regions that will become the telencephalon, the diencephalon, the midbrain, the cerebellum, and the epiphysis (Kimmel and Law, 1985a; Mueller and Wullimann, 2003; 2005). Organogenesis also continues as the lateral line forms (Kimmel et al., 1995; Wada et al., 2010), the heart chambers enlarge and the preliminary cardiac tube loops (Chen and Fishman, 1996; Glickman and Yelon, 2002; Brand, 2003), and the gastrointestinal tract differentiates and extends along with associated organs such

as the liver and pancreas (Field et al., 2003; Wallace et al., 2005). Most importantly, the embryo develops towards hatching with increased muscle contraction rate and strength, and the development of the hatching gland (Kimmel et al., 1995). The pharyngula period ends at approximately 48 hpf, which marks the beginning of the hatching period and the transition to larval stages as the animal begins to move, grow, and approaches feeding stages (Kimmel et al., 1995; Lawrence, 2007).

Table 3 – Reviews regarding the use of the zebrafish model in developmental study

Major Topic	Reference
Angiogenesis	(Childs et al., 2002)
Aquaculture	(Aleström et al., 2006)
Behaviour	(Gerlai, 2003)
Biomedicine	(Barut and Zon, 2000)
Biomedicine	(Zon and Peterson, 2005)
Biomedicine (Endocrinology)	(Löhr and Hammerschmidt, 2011)
Biomedicine (Endocrinology)	(Schoonheim et al., 2010)
Biomedicine (Muscle)	(Lin, 2012)
Biomedicine (Skin)	(Li et al., 2011)
Cardiovascular	(Chico et al., 2008)
Cardiovascular	(Stainier and Fishman, 1994)
Circadian Rhythm	(Vatine et al., 2011)
Development	(Driever et al., 1994)
Development	(Eisen, 1996)
Development	(Grunwald and Eisen, 2002)
Endocrinology	(Bourque and Houvras, 2011)
Endocrinology	(McGonnell and Fowkes, 2006)
Endocrinology	(Schaaf et al., 2009)
Endocrinology	(Steenbergen et al., 2011)
Immune System	(Traver et al., 2003)
Myelopoiesis	(Berman et al., 2005)
Myogenesis	(Chong et al., 2009)
Neurogenesis	(Abraham et al., 2009)
Neuroscience	(Friedrich et al., 2010)
Physiology	(Briggs, 2002)
Toxicology	(Ali et al., 2011)
Toxicology	(Lele and Krone, 1996)
Toxicology	(Segner, 2009)

Figure 3 – Representative images of key milestones in zebrafish development

Certain major developmental stages in zebrafish embryogenesis are readily assessed by simple microscopy. In this figure, we show images of the pre-epiboly zebrafish embryo (A), the 50% epiboly (B; arrow indicates blastoderm border), the post-gastrulation embryo (C), and the 24 hpf embryo with fully developed somite pairs (D; arrow indicates developed somites).

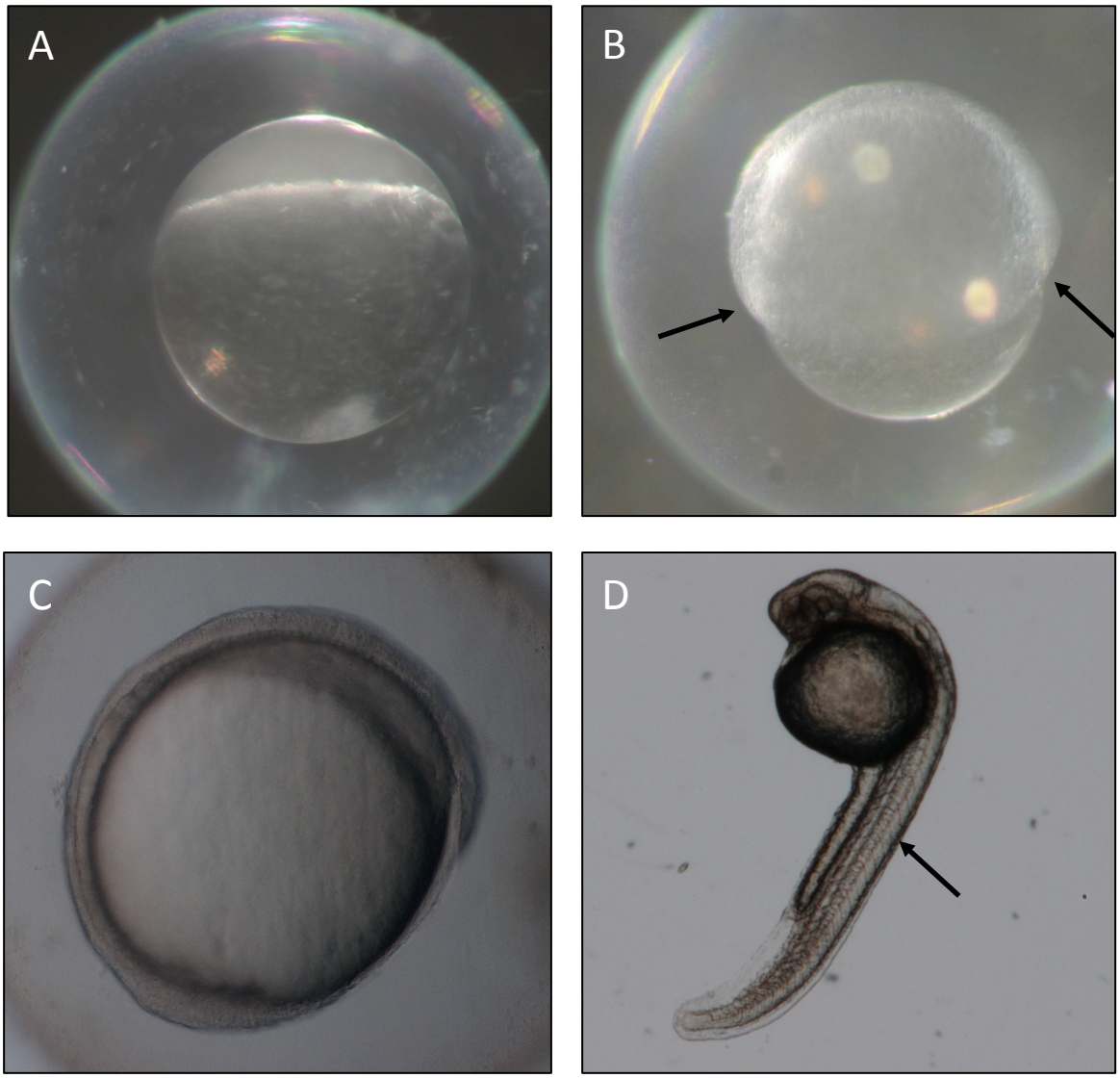
A
B
C
D

1.5 Roles of bone morphogenetic proteins in development

One of the major findings of this dissertation is that signaling by the bone morphogenetic proteins (BMPs) may be modulated by glucocorticoids. The BMPs are a family of conserved proteins that are active developmental morphogens in a variety of animals (Nikaido et al., 1997; Miyazono et al., 2005; Yanagita, 2005; Wagner et al., 2010). BMP ligands are members of the transforming growth factor-*β* (TGF*β*) family of developmental signaling molecules (Miyazono et al., 2005). BMP ligands bind to integral membrane BMP receptors, which then cause the activation of members of the Smad family of signaling proteins that act as transcription factors to affect gene expression (Bubnoff and Cho, 2001; Miyazono et al., 2005; Wagner et al., 2010). BMP signaling regulation is complex, with specific Smad molecules producing either inhibitory or excitatory signals (Dick et al., 1999; Zhang et al., 2007) as well as numerous other antagonizing pathways and molecules that act to oppose BMP signaling (Miyazono et al., 2005; Yanagita, 2005; Walsh et al., 2010; Sylva et al., 2011). To date, 14 BMP ligands, 5 BMP receptors, and 10 Smad molecules have been identified in zebrafish (ZFIN Staff, 2006) and together they play roles in a diverse array of embryogenic events. In addition to early axial patterning (Kishimoto et al., 1997; Hammerschmidt and Mullins, 2002), BMP signaling is implicated in a variety of processes throughout development, including myogenesis (Patterson et al., 2010), angiogenesis (David et al., 2009), organogenesis (Shin et al., 2007; Chung et al., 2008; McCulley et al., 2008), and craniofacial development (Nie et al., 2006).

1.6 Development of the zebrafish corticosteroid stress axis

In this section we present an overview of the known molecular mechanisms regulating stress axis development in zebrafish. Specifically we will highlight the formation of the hypothalamus, pituitary, and interrenal tissue in zebrafish, noting the time at which precursors are determined, the morphogenic movements that occur, and major molecular signaling molecules that are involved (see Figure 4 for summary). Very little is known about cortisol regulation of key genes involved in the development of the HPI axis. This would be an area of intense interest given the findings that cortisol content can vary in teleost oocytes due to maternal stressor exposure (Stratholt et al., 1997; McCormick, 1998; Eriksen et al., 2007; Giesing et al., 2011).

1.6.1 Structure and development of the hypothalamus

The hypothalamus is a major regulating center for control of bodily functions, and activation of this region of the brain is the first step in the whole organism cortisol-mediated response to stress (Wendelaar Bonga, 1997; Charmandari et al., 2004b; de Kloet et al., 2005; Chrousos, 2006). It is

located at the posterior basal region of the forebrain, positioned between the thalamus and the pituitary (Mueller and Wullimann, 2003; 2005). There are two major cell groups in the zebrafish hypothalamus, dopaminergic neurons and OXT-like neurons, which are analogous to mammalian parvocellular and magnocellular neurons, respectively (Blechman et al., 2007). OXT-like neurons, named for the *oxtl* (oxytocin-like) transcripts that mark their specification, produce neurohormones, including oxytocin and vasopressin (Machluf et al., 2011). Dopaminergic neurons produce trophic hormones that act on the pituitary, including corticotropin-releasing hormone (CRH) and gonadotropin-releasing hormone (Machluf et al., 2011).

The regulation of hypothalamic development is unclear in teleosts, but the diencephalon develops from the anterior neuroectoderm, migrating from the neural plate inward during early somitogenesis stages (~12 hpf; (Russek-Blum et al., 2009)). Hypothalamic neurons develop later in development, with dopaminergic neurons specified during gastrulation and directly observed by 18 hpf, and OXT-like neurons detectable at 36 hpf (Russek-Blum et al., 2008; Machluf et al., 2011). Some of the most well studied developmental signaling pathways have been implicated in hypothalamic neurogenesis. For instance, release of *nodal*, *bmp7*, and *wnt* from the prechordal plate induces the hypothalamus to develop (Dale et al., 1997; Mathieu et al., 2002; Machluf et al., 2011), and *lef1*, a member of the Wnt pathway, restricts and determines dopaminergic neuron specification (Kapsimali, 2004; Lee et al., 2006). The forebrain marker *fezf2*, which is regulated by the Wnt pathway, is required for dopaminergic neuron development and regulates other neurogenic morphogens, including neurogenin 1 (*ngn1*), and the two zebrafish paralogs of orthopedia homolog (*otp*), a well-characterized mammalian hypothalamic developmental regulator (Wang and Lufkin, 2000; Del Giacco et al., 2006; Jeong et al., 2006; Del Giacco et al., 2008).

1.6.2 Structure and development of the pituitary

The morphology of the pituitary is well known and has been characterized in zebrafish (Herzog et al., 2004b; Chapman et al., 2005). In general, the pituitary has two subregions, termed the neurohypophysis and the adenohypophysis. The neurohypophysis, also known as the posterior pituitary, is a neural component that contains projections of the dopaminergic cells that originate in the hypothalamus (Chapman et al., 2005). The adenohypophysis, or anterior pituitary, is an endocrine gland containing cells producing a variety of hormones, including thyroid stimulating hormone, follicular stimulating hormone, luteinizing hormone, and ACTH, that act on target tissues (Chrousos, 2000). Adenohypophyseal release of hormones occurs in response to hypothalamic stimulation via trophic hormones from OXT-like neurons. The pituitary is located

in a pocket of the skull, just below the hypothalamus (Chapman et al., 2005). There are some structural differences between the teleost and mammalian HP axis. In teleosts, the neurohypophysis is positioned dorsal to the adenohypophysis, instead of the posterior-anterior positioning seen in mammals (Mueller and Wullimann, 2005). Another major difference is that teleosts lack the hypothalamo-hypophyseal portal system that is found in higher vertebrates (Pogoda and Hammerschmidt, 2007). The portal system is a network of blood vessels that transport the trophic hormones released by the hypothalamus directly to the adenohypophysis, bypassing general circulation. Instead of this system, the teleost adenohypophysis is directly innervated by input from the hypothalamus, similar to the neurohypophysis (Pogoda and Hammerschmidt, 2007).

The development of the adenohypophysis has been extensively studied in zebrafish (Herzog et al., 2003; 2004b; Pogoda and Hammerschmidt, 2007). The first determination of adenohypophyseal cells begins at approximately 10 hpf in the anterior region of the pre-placodal ectoderm (Dutta et al., 2005). By 18-20 hpf, the first adenohypophysis-specific markers are expressed in the newly thickened placodal ectoderm; specifically *lim3*, a Lim-domain homeobox gene, and *pit1*, a Pou-domain homeobox gene (Glasgow et al., 1997; Nica et al., 2004). By 24 hpf, the pituitary is structurally distinct from the brain and surrounding region (Chapman et al., 2005; Pogoda and Hammerschmidt, 2007). Over the next few hours the cells migrate internally as a solid mass of cells towards the final position below the hypothalamus (Chapman et al., 2005; Pogoda and Hammerschmidt, 2007; 2009). This is different from the mammalian and avian model, in which the cells form a hollow outpocket (Rathke's pouch) that eventually fuses to form the solid pituitary (Sheng, 1997). Within the developing zebrafish pituitary, the corticotrope cells differentiate early in the lateral regions, and begin to express the ACTH precursor proopiomelanocortin (POMC) as early as 18-20 hpf, with strong expression observable by 24-26 hpf (Herzog et al., 2003; Liu et al., 2003a). Specific genes have been identified as necessary for pituitary formation; a key factor being *pitx3* (Dutta et al., 2005). There are numerous *pitx* genes found in mice, with overlapping functions, but only *pitx3* is expressed in zebrafish, and it appears to assume all the developmental functions necessary for pituitary formation (Dutta et al., 2005). Signaling from the hedgehog system is also required for adenohypophysis specification, with requirements for both sonic hedgehog (*shh*) and tiggy winkle hedgehog (*twhh*) (Herzog et al., 2003; Sbrogna et al., 2003). Other genes necessary for pituitary cell survival are fibroblast growth factor 3 (*fgf3*), which seems to prevent regional apoptosis (Herzog et al., 2004a), *ascl1a*, which is necessary for all adenohypophyseal hormone production (Pogoda et al., 2006), and *eya1*, which signals with *shh* to induce corticotrope cell specification (Nica et al., 2006).

1.6.3 Structure and development of the interrenal tissue

Another major difference between mammalian and teleost stress axis organs is that piscine models lack a distinct adrenal gland. Instead, steroidogenic and chromaffin cells are dispersed in the interrenal tissue, located in the head kidney region in the dorsal region of the body cavity, posterior to the post-cardinal vein (Wendelaar Bonga, 1997). Interrenal development begins at 22 hpf, as cells are specified within the pronephric primordia, which are two regions on either side of the developing neural crest (Hsu et al., 2003). From 24-36 hpf, the presumptive interrenal cells migrate to the midline and merge together (Hsu et al., 2003). At 28 hpf, steroidogenesis commences, marked by increased expression of key steroidogenic marker genes, including cytochrome P450 side chain cleavage enzyme (*p450scc*), steroidogenic acute regulatory protein (*star*), and 3-beta-hydroxysteroid dehydrogenase (*3ß-HSD*) in discrete regions of the migrating cells (Liu, 2007; To et al., 2007; Alsop and Vijayan, 2008; 2009). Chromaffin cells develop relatively late in the process, and are not detectable until 48 hpf, and by 72 hpf they have interspersed with the steroidogenic cells and interrenal development is complete (Liu, 2007; To et al., 2007). As with the pituitary, there are similarities in the genetic contributors to interrenal development in mammals and teleosts. In mammals, the primary driver of adrenal development is the *sf1* gene, a Ftz-F1 gene identified as an orphaned nuclear receptor (Chai and Chan, 2000; Savage et al., 2003; Ishimoto and Jaffe, 2011). In zebrafish, two orthologs have been identified, *ff1b* and *ff1d* (Chai and Chan, 2000). *ff1b* is the earliest visible marker of interrenal cells, and its knockdown results in a complete lack of interrenal tissue formation (Chai et al., 2003). While *ff1b* is required for specific interrenal development, other signaling molecules are required both prior to and after the initial specification. For example, the formation of the pronephric primordia requires *wt1*, and without it no further development of pronephros or the interrenals occurs (Hsu et al., 2003). Later on, *dax1* and *prox1* are required for the development of steroidogenic cells (Liu et al., 2003b; Zhao et al., 2006). The mechanisms that regulate these genes, and whether any hormonal input is involved, remain unclear and require further examination.

Figure 4 – Summary of zebrafish hypothalamus-pituitary-interrenal development.
The hypothalamus (HT), pituitary (adenohypophysis [AH], and neurohypophysis [NH]), and interrenal (IR) develop simultaneously during development, and in advance of the activation of the coordinated response to stress. HT develops from 12-36 hpf, and corticotropin-releasing factor (CRF) transcripts are maternally deposited in the oocyte. AH formation occurs from 10-26 hpf, with corticotropes distinguishable in the lateral AH regions at 24-26 hpf. IR tissue develops initially from 22-36 hpf, with steroidogenic ontogeny occurring at 28 hpf. Chromaffin cells develop late, differentiating at 48 hpf and interspersing with the established steroidogenic cells by 72 hpf. The earliest coordinated response to a perceived stressor leading to the release of cortisol occurs at around 72 hpf in zebrafish.

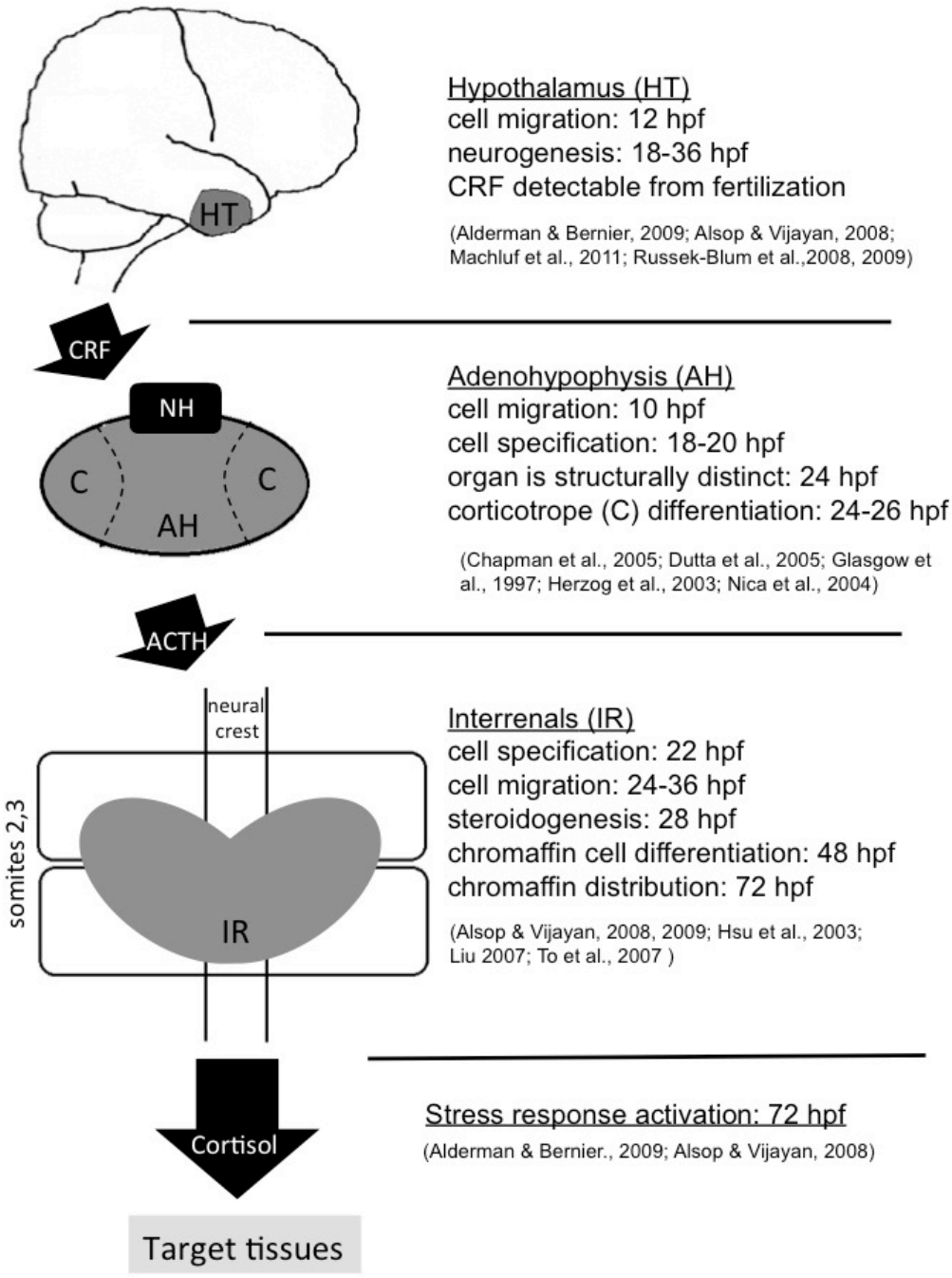

Hypothalamus (HT)
cell migration: 12 hpf
neurogenesis: 18-36 hpf
CRF detectable from fertilization

(Alderman & Bernier, 2009; Alsop & Vijayan, 2008; Machluf et al., 2011; Russek-Blum et al.,2008, 2009)

Adenohypophysis (AH)
cell migration: 10 hpf
cell specification: 18-20 hpf
organ is structurally distinct: 24 hpf
corticotrope (C) differentiation: 24-26 hpf

(Chapman et al., 2005; Dutta et al., 2005; Glasgow et al., 1997; Herzog et al., 2003; Nica et al., 2004)

Interrenals (IR)
cell specification: 22 hpf
cell migration: 24-36 hpf
steroidogenesis: 28 hpf
chromaffin cell differentiation: 48 hpf
chromaffin distribution: 72 hpf

(Alsop & Vijayan, 2008, 2009; Hsu et al., 2003; Liu 2007; To et al., 2007)

Stress response activation: 72 hpf

(Alderman & Bernier., 2009; Alsop & Vijayan, 2008)

1.7 Ontogeny of stress response in zebrafish

Although the signaling and steroidogenic components of the zebrafish HPI axis are present around the time of hatching (see Figure 4 for summary), the earliest induction of a stress response occurs at 72 hpf (Alderman and Bernier, 2009; Alsop and Vijayan, 2009). This delay in the ability to perceive a stressor and evoke a cortisol surge, despite the presence of the molecular signaling components of the HPI axis, is common in teleost species, having been observed in rainbow trout (*Onchorynchus mykiss*; (Barry et al., 1995)), yellow perch (*Perca flavscens*; (Jentoft et al., 2002)), tilapia (*Oreochromis mossambicus*; (Pepels and Balm, 2004)), common carp (*Cyprinus carpio*; (Stouthart et al., 1998)) and chinook salmon (*Oncorhynchus tshawytscha*; (Feist and Schreck, 2001)). All of these fish display a classical response to stress some time after hatching. There is a similar stress hyporesponsive period in both mice and rats, which are unable to respond to a stressor for an extended period after birth (Levine, 2001; Schmidt et al., 2003). It is unclear whether this delay in stressor responsiveness is functionally relevant. However, it can be hypothesized that if glucocorticoids are developmental regulators, the delay in HPI/HPA activation may be protective, as stress-activated cortisol or corticosterone surges may disrupt glucocorticoid-sensitive developmental pathways. Interestingly, the general pattern and timing of stress axis organogenesis and activation is relatively well conserved, when controlled for gestational time, in vertebrates (see Table 4). This pattern, along with the similarity in stress axis activation and the molecular markers involved in HPA axis organogenesis, indicates that the ontogeny of the stress response and the developmental role of corticosteroid identified in zebrafish may be conserved in higher vertebrates.

Cortisol and GR are maternally deposited into the zebrafish oocyte and decrease in concentration during pre-hatch embryogenesis, then begin to rise after hatching (Alsop and Vijayan, 2008; Alderman and Bernier, 2009; Alsop and Vijayan, 2009; Pikulkaew et al., 2009).This variation in cortisol concentration prior to hatching is conserved in teleosts (de Jesus et al., 1991; Hwang and Wu, 1993; Barry et al., 1995; Sampath-Kumar et al., 1995; Stouthart et al., 1998; Nechaev et al., 2006). Interestingly CRF is also present in the oocyte, along with its receptors and binding proteins, although whether this deposition is functionally relevant remains unknown (Alderman and Bernier, 2009). Although the ACTH precursor POMC is not expressed until approximately 18-24 hpf (Liu et al., 2003a), a potential role for the CRF system in the early development of a functional corticotropic system remains to be examined, as well as whether CRF has other independent developmental roles. Steroidogenic enzymes are not measurable until after 28 hpf, indicating that early glucocorticoid effects are only due to maternally deposited

cortisol, not zygotically synthesized steroids (Liu et al., 2003a; To et al., 2007; Alsop and Vijayan, 2008; 2009).

Table 4 – The time of first onset of stress axis signal synthesis and stress responsiveness in various model animals in relation to total gestation/hatching time (shown as percentage).

	Gestation time (%)				
Species (Gestation or Hatching time**)**	**CRF/CRH**	**ACTH**	**GC**	**Stress**	**References**
Danio rerio (~ 48 h)	0-13	50	75-100	150	(Liu, 2007; Alsop and Vijayan, 2008; Alderman and Bernier, 2009; Alsop and Vijayan, 2009)
Gallus gallu (22 days)	63	45	45	113	(Jenkins and Porter, 2004; Saito et al., 2005)
Musculus musculus (20 days)	65	93	75	160	(Keegan et al., 1994; Sheng, 1997; Heikkila et al., 2002; Schmidt et al., 2003)
Rattus norvegicus (21 days)	80	76	86	166	(Chatelain et al., 1979; Baram and Lerner, 1991; Mitani et al., 1999; Levine, 2001)

CRF: corticotropin-releasing factor; CRH: corticotropin-releasing hormone; ACTH: adrenocorticotropic hormone; GC: glucocorticoid.

1.8 Developmental role for glucocorticoid signaling

The presence of HPI signaling molecules and receptors in zebrafish oocytes, and their persistence throughout embryogenesis, indicates that they may be developmentally active. In this section we will detail established roles for glucocorticoid in organogenesis based on mammalian studies, as well as indications from other egg-laying species and what little is known in zebrafish. The conservation of the stress axis signaling between teleosts and mammals and the presence of a similar GR gene expression and splicing profile to humans suggests that evidence from zebrafish study may be applicable to human health and disease.

1.8.1 Developmental roles of glucocorticoids in mammals

In mammals, numerous known developmental effects of glucocorticoids center on organogenesis. Glucocorticoid signaling has been implicated in the maturation and functional activation of multiple organ structures, including the heart, lungs, gut, pancreas, and kidneys, with research conducted in a variety of animals (Rall et al., 1977; Majumdar and Nielsen, 1985; Liggins, 1994; Pierce et al., 1995; Langdown et al., 2003; Gesina et al., 2004; Lumbers et al., 2005). Synthetic glucocorticoids are often given to prematurely-born infants to help speed organ development (Chrousos and Gold, 1992; Rehan, 1996). In various mammals, glucocorticoids have been shown to increase respiratory surfactant production and accelerate overall lung development (Ballard and Ballard, 1974; Mescher et al., 1975; Pierce et al., 1995; Bolt et al., 2001). In mice, knockout of the GR gene fatally impairs lung development, causing complete prenatal mortality (Cole et al., 2001). There have been a number of other identified roles for corticosteroids in developmental organogenesis in varied mammalian models. Glucocorticoids have been found to accelerate renal tissue development (Celsi et al., 1993; Wang et al., 1994; Djouadi et al., 1996), modulate pancreatic development (Rall et al., 1977; Sangild et al., 1994; Gesina et al., 2004), regulate cell communication in the small intestine (Schaeffer et al., 2000), and to increase osteoblast activity (Shalhoub et al., 1992; Boden et al., 1996). Glucocorticoids also have detrimental effects on the brain, delaying development of neurons and glial cells, slowing myelination, and impairing vascularization (Huang et al., 1999; 2001). However, little is known about the mechanism of action of corticosteroid in these processes. Organogenesis is a complex process, and the transcription factors and/or morphogens that respond to glucocorticoid treatment in the maturation or activation of these developmental processes are still unclear. Attempts to determine the mechanistic action of GR-mediated cortisol signaling in mammalian embryos has been difficult due to lack of understanding behind the specific molecular signaling pathways of organogenesis as well as the difficulty in studying changes *in utero*.

Glucocorticoid programming is a known consequence of elevated pre-natal glucocorticoids in mammals, referring to effects that last into adulthood, and has been identified as the cause of various human disease states (Seckl, 2001; Matthews, 2002; Seckl and Meaney, 2004). For instance, pre-natal elevation of glucocorticoid levels affects the cardiovascular system, resulting in chronic hypertension and cardiovascular risk, modulating cardiac genes such as PPARγ and calreticulin (Seckl, 2001; Langdown et al., 2003). Elevated glucocorticoids during development also result in lasting disruption of brain function, via altered hippocampal neuronal content and reduced corticosteroid receptor expression (Welberg and Seckl, 2001; Welberg et al., 2001). Other major programming effects involve the priming of the stress response (Matthews, 2002), and disruption of glucose metabolism, the effects of which persist for multiple generations in treated rats (Drake et al., 2005). As with the direct effects of prenatal glucocorticoids on embryogenesis, the opacity of mammalian fetal development models obscures the mechanisms at work to create these lasting effects.

1.8.2 Developmental role of glucocorticoids in non-mammalian models

In teleost species, maternal stress and/or increased steroid deposition in the oocyte is associated with a reduction in larval performance and survival (McCormick, 1998; Mccormick, 1999; Li et al., 2010; Sloman, 2010; Åberg Andersson et al., 2011). The deposition of cortisol, GR, and possibly CRF and its receptors, could be a mechanism for transmitting this message from stressed mothers to progeny. This kind of maternal-embryonic communication is a common concept in avian models, where steroid deposition into egg affects priming of the stress response, decreasing the sensitivity of the HPA axis (Hayward and Wingfield, 2004), and in reptiles, where it can affect growth and philopatry (Shine and Downes, 1999; De Fraipont et al., 2000). In zebrafish, exposure of embryos to exogenous glucocorticoids has revealed novel glucocorticoid-responsive genes that have known developmental roles. Glucocorticoids modulate specific members of the matrix metalloproteinase (MMPs) family that act in degradation of the extracellular matrix, such as *mmp2*, *mmp9*, and *mmp13*, the latter of which is required for somitogenesis and craniofacial development (Hillegass et al., 2007; 2008). Matrix metalloproteinases are involved in a variety of cell remodeling actions that occur in development (Zhang et al., 2003; Yoong et al., 2007; Rozario and DeSimone, 2009), and GR-mediated alteration of their expression could cause widespread disruption of embryogenesis and birth defects. In combination, these actions of glucocorticoids in development provide interesting avenues for further exploration. However, comparatively little is known regarding glucocorticoid effects on development of birds and lower vertebrates, especially teleosts, when compared to mammals.

1.9 Major techniques utilized in zebrafish developmental studies

This section will summarize two prominent techniques that are used in studies of zebrafish embryogenesis but may not be particularly common to many researchers: the use of morpholino oligonucleotides for the blocking of protein translation; and the use of microinjection for the delivery of morpholino oligonucleotides and other molecules into the developing zebrafish embryo. Other common techniques in this thesis that are better established, such as quantitative polymerase chain reaction (qPCR) and *in situ* hybridization (ISH) for transcript analysis or western blotting and immunohistochemistry for protein expression quantification, are described in the methods of each individual chapter, but an exploration of the theory behind them was deemed redundant due to their familiarity to most developmental, physiological, and molecular biology researchers.

1.9.1 Morpholino oligonucleotides

Morpholino oligonucleotides (MOs) are short sequences of modified nucleic acid that are commercially available from GeneTools, LLC in California. MOs are modified by the replacement of the deoxyribose or ribose sugars normally found in DNA or RNA with a nuclease resistant morpholine ring (see Figure 5 for structure; (Summerton and Weller, 1997)). MOs are designed against regions that will disrupt either transcription or translation and render cell unable to express the target protein for periods of time (Summerton and Weller, 1997). In this thesis (Chapters 2 and 4), an MO was targeted against the start site of translation from the zebrafish *gr* mRNA product. The binding of the MO at this region prevents ribosomal assembly and establishes what is termed a "knockdown" of GR protein (Nasevicius and Ekker, 2000). Another option is to block an intron/exon boundary to disrupt the splicing of the mRNA after transcription and prevent a functional protein from being produced (Summerton and Weller, 1997). This is a useful technique if one does not have a functional antibody for the protein of interest, as PCR amplification of the disrupted transcript can describe the efficacy of the MO (Eisen and Smith, 2008). Controls for MO studies can be specific or non-specific. Specific MO controls are usually in the form of a mispair (MP) MO, in which 5 random basepairs are changed (out of the 20-25 bp MO sequence), which is enough to affect the binding of the MO to the target sequence (Summerton and Weller, 1997; Eisen and Smith, 2008). Non-specific controls either use a standard oligo for a given species, meant to control for any effects of the morpholine ring; or by the use of a p53 coinjected-MO to suppress p53 activity, as MOs are known to cause non-specific effects via p53 mediated mechanism (Heasman, 2002; Eisen and Smith, 2008). In the studies presented in subsequent chapter, the primary control used is a 5 bp mispair oligonucleotide

specifically designed to control for effects of the MO designed against the start site of GR translation, although we also use a p53 MO co-injection in chapter 2 as a further control for non-specific effects.

1.9.2 Microinjection into single-cell zebrafish embryos

The optically clear nature of zebrafish embryos makes them ideal for developmental study, and the previously mentioned delay in first cleavage (~40 minutes), meroblastic cleavage pattern, and cytoplasmic streaming (Kimmel et al., 1995) mean that injection into the yolk of zebrafish embryos is an excellent and minimally traumatic way to alter the content of the fertilized zygote and the initial daughter cells. No puncturing of cells is required, and contents are rapidly taken up into the first daughter cells and then subsequently divided during cleavage and blastula stages (Kimmel and Law, 1985a; Nasevicius and Ekker, 2000). It should be noted that the length of time of clearance of molecules in the developing embryo is highly variable, with some MO sequences remaining effective up to 48-72 hpf (Nascevicius and Ekker, 2000), but dynamics in the embryo must be characterized, preferably by quantification of target molecules.

Figure 5 – Structures of DNA and morpholino oligonucleotides

This schematic shows the difference in chemical structure between a DNA nucleotide and morpholino nucleotide. Morpholinos have the deoxyribose sugar replaced with a morpholine ring to confer resistance from nuclease degradation. The phosphodiester bond in DNA is therefore replaced with a phosphorodiamidate linkage.

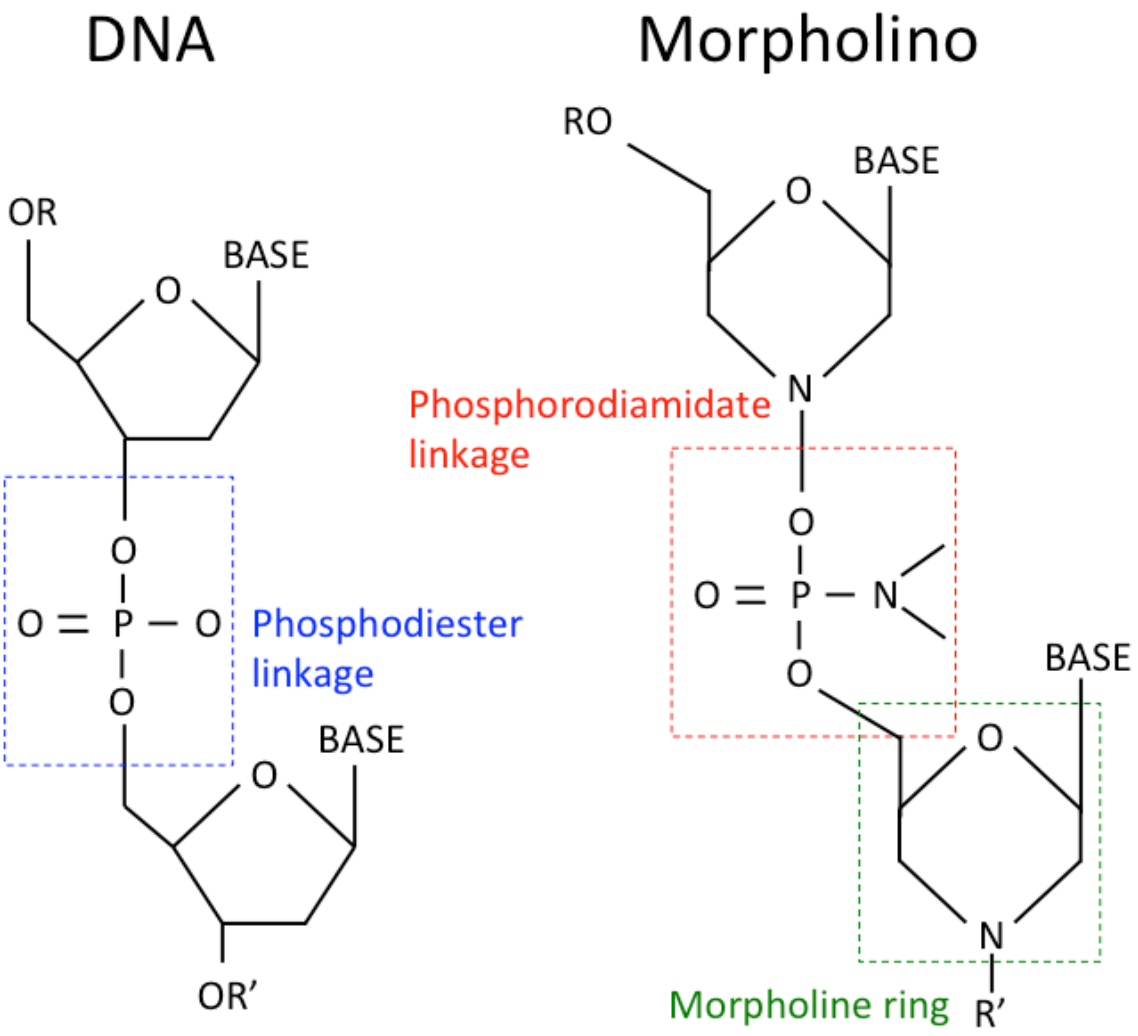
DNA
Morpholino
OR
BASE
O
O
O = P – O
O
Phosphodiester
linkage
BASE
O
OR'
RO
BASE
O
N
Phosphorodiamidate
linkage
O
O = P – N
O
BASE
O
N
Morpholine ring
R'

1.10 Objectives

Generally, this chapter has attempted to highlight the relative lack of knowledge about the role of glucocorticoids in early vertebrate development relative to the well known, conserved, and characterized pathways of morphogenesis. The major objectives of this thesis stem from the primary hypothesis that the presence of cortisol and GR in the oocyte is functionally relevant, and that glucocorticoid signaling is important in zebrafish embryogenesis. This chapter also highlighted the utility of zebrafish as an excellent model for testing the above hypothesis.

The specific objectives of this thesis are as follows:

1) Characterize the broad actions of GR on early zebrafish development.

   This objective is addressed throughout the dissertation, but is the primary finding of Chapter 2, examined by the use of morpholino oligonucleotides to inhibit GR signaling.

2) Identify novel developmental pathways and genes that are GR-modulated.

   This objective is studied throughout this thesis, with findings in Chapters 2, 3, and 4. Major pathways are identified in Chapter 4 by high-density microarray analysis of changes in global gene expression in response to morpholino knockdown of GR.

3) Determine the effect of abnormal maternal cortisol deposition on early zebrafish development.

   This objective is examined in Chapter 3, by use of exogenous cortisol administration that mimics elevated maternal deposition.

4) Determine the role of maternal cortisol on zebrafish stress axis development and functioning.

   This objective is examined in Chapter 5, by use of exogenous cortisol administration to mimic elevated maternal deposition and a cortisol-specific antibody that sequesters the yolk-deposited cortisol, mimicking decreased maternal deposition.

Chapter 2

Glucocorticoid receptor signaling is essential for mesoderm formation and muscle development in zebrafish

Specific coauthor contributions:

J Burrows and Dr. IC Scott contributed *in situ* hybridization data and images to Figures 1 and 2

Dr. M Kamkar designed the GR-GFP construct and contributed to GR rescue mRNA construct creation

Some imaging for Figures 1 and 2 was carried out in Dr. M Marsden's lab.

2.1 Overview

Glucocorticoid receptor (GR) signaling is thought to play a key role in embryogenesis, but its specific developmental effects remain unclear. In zebrafish (*Danio rerio*), *de novo* cortisol synthesis takes place only after hatching, indicating that pre-hatch cortisol signaling events are of maternal origin. Using early zebrafish developmental stages, we tested the hypothesis that GR signaling is critical for embryo growth and hatching. In zebrafish, maternal GR mRNA is degraded quickly, followed by zygotic synthesis of the receptor. GR protein is widely expressed throughout early development and we were able to knock down this protein using morpholino oligonucleotides. This led to a >70% reduction in mRNA abundance of *mmp13*, a glucocorticoid-responsive gene, supporting suppressed GR signaling. The GR morphants displayed delayed somitogenesis, defects in somite and tail morphogenesis, reduced embryo size, and rarely survived after hatch. This correlated with altered expression of myogenic markers, including myogenin, myostatin, and specific myosin heavy chain and troponin genes. A key finding was a 70-90% reduction in the mRNA abundance of bone morphogenetic proteins (BMPs), including *bmp2a, bmp2b*, and *bmp4* in GR morphants. Bioinformatics analysis confirmed multiple putative glucocorticoid response elements upstream of these BMP genes. GR morphants displayed reduced expression of BMP modulated genes, including *eve1* and *pax3*. Zebrafish GR mRNA injection rescued the GR morphant phenotype and reversed the disrupted expression of BMPs and myogenic genes. Our results for the first time indicate that GR signaling is essential for zebrafish muscle development, and we hypothesize a role for BMP morphogens in this process.

2.2 Introduction

Glucocorticoid signaling in adults has been extensively studied, and the functioning of the hypothalamic-pituitary-adrenal axis is essential for stress adaptation (Sapolsky et al., 2000). However, comparatively little is known about the developmental roles of glucocorticoid hormone and its signaling molecule, the glucocorticoid receptor (GR), a cytosolic ligand-bound transcription factor. Cortisol signaling is essential for late-term organ development (Liggins, 1994), and GR knockout mice did not survive after birth due to impaired lung development (Cole et al., 2001). Also, exposure of the developing fetus to elevated glucocorticoid levels leads to lowered fetal birth weight and disrupted glucocorticoid responsiveness later in life (Ward, 2004). While these studies clearly implicate a critical role for corticosteroid signaling in fetal development, the role of glucocorticoid receptor activation on developmental programming events are far from clear.

Zebrafish (*Danio rerio*) is an excellent model to identify the early developmental effects associated with GR signaling. This is because *de novo* synthesis of cortisol, the primary GR ligand, happens only after hatch in this species, leading to maternal cortisol as the sole contributor for early developmental programming (Alsop and Vijayan, 2008). This was further reinforced by the gradual decrease in maternal cortisol and GR transcripts prior to hatching in zebrafish (Alsop and Vijayan, 2008). Also, unlike other teleosts that have multiple copies of GR, zebrafish only has a single GR gene in the genome (Alsop and Vijayan, 2008; Schaaf et al., 2008), making the species amenable for genetic manipulations. Additionally, a GRß splice variant, similar to humans, was recently discovered in zebrafish, leading to the proposal that this species is an excellent model for biomedical research, especially pertaining to developmental abnormalities associated with glucocorticoid excess or resistance to this hormone action (Schaaf et al., 2008; Schoonheim et al., 2010). Also, a recent study demonstrated that knocking down maternal GR leads to developmental defects in mesoderm formation in zebrafish (Pikulkaew et al., 2011).

Zebrafish embryogenesis has been extensively characterized and several transcription factors, including MyoD (Ochi and Westerfield, 2007; Chong et al., 2009), and insulin-like growth factors (IGFs) (Duan et al., 2010) have been associated with early muscle development. Also the temporal expression of morphogens, including the bone morphogenetic proteins (BMPs) and their signaling is essential for mesoderm differentiation and dorsoventral patterning in the developing zebrafish embryo (Nikaido et al., 1997; Pyati et al., 2005). BMP signaling is highly conserved and upregulates the Smad family of proteins (Bubnoff and Cho, 2001; Miyazono et al., 2005) and specific BMPs, including *bmp2a*, *bmp2b*, and *bmp4* also affect myogenesis, angiogenesis, and organogenesis during zebrafish development (Stickney et al., 2000; Brand, 2003; Chung et al., 2008; Patterson et al., 2010). Consequently, transient expression of BMPs are essential for mesoderm differentiation, dorsoventral patterning, and embryo survival (Stickney et al., 2000; Pyati et al., 2005; Patterson et al., 2010). Several endogenous regulators of BMPs have been identified, including their receptor antagonists that play key roles in affecting embryogenesis (Bubnoff and Cho, 2001; Little and Mullins, 2006).

Here we tested the hypothesis that glucocorticoid receptor signaling is essential for fetal programming of mesoderm formation and muscle development in zebrafish. This was tested by assessing the phenotypic traits in response to reduced GR signaling, by knocking down this receptor protein expression and investigating changes in developmental and myogenic gene expression prior to hatching in zebrafish. Given the established role of BMPs in mesoderm formation and differentiation (Patterson et al., 2010), we also examined the expression of *bmp2a*,

bmp2b, and *bmp4*, and markers of their downstream signaling events to ascertain if these morphogens are regulated by GR signaling in zebrafish. Our results underscore a critical role for GR signaling in the fetal programming of mesoderm formation and myogenesis in zebrafish. Our results lead us to propose that BMPs may be involved in the developmental changes associated with GR knockdown in zebrafish.

2.3 Materials & Methods

2.3.1 Zebrafish care

Adult zebrafish were maintained in 10L tanks at 28.5^{o}C in a recirculating system (Aquatic Habitats) with a 14h light: 10h dark photoperiod and were fed 2-3 times daily with dry pellets (Zeigler). Egg traps were placed just before the start of the dark period and embryos were collected within 30 min of light and reared in embryo medium (Westerfield, 2007) with added methylene blue (3 ppm) in 10 cm petri dishes at 28.5^{o}C with medium replaced at 12 and 36 hours post-fertilization (hpf). The zebrafish protocol was approved by the animal care committee at the University of Waterloo, and is in accordance with the Canadian Council for Animal Care guidelines.

2.3.2 Embryo GR expression

Wild-type zebrafish embryos were collected to determine GR gene and protein expression by whole-mount *in-situ* hybridization (ISH) and immunohistochemistry (IHC), respectively. Embryos were fixed in 4% paraformaldehyde (PFA) in phosphate buffered saline (PBS) overnight at 4^{o}C, dehydrated in 100% methanol (MeOH), and frozen at -20^{o}C. Prior to analysis, embryos were thawed and rehydrated with a series of 5 min washes: 75% MeOH/25% PBS, 50% MeOH/50% PBS, 25% MeOH/75% PBS, and 100% PBS. ISH was performed according to standard protocols (Thisse and Thisse, 2008). Riboprobes were created with the DIG RNA labeling kit (Roche) as follows:

GRLEFT 5'-GGAAGAACTGCCCTGCCTGTCG-3'

GRRIGHT 5' CACCCACCAAGTCGTGCATGG-3'

The embryos were bright-field imaged using a Leica MZ16 microscope with a Leica DFC 320 camera. ISH was used to identify GR mRNA abundance in wild-type embryos at the following time-points: 16-cell, 4, 6, 8, 10, 12, 24, and 48 hpf. Sense strand hybridizations at each time-point ensured probe specificity.

The primary antibody used for both IHC and later western blotting was a custom-made affinity-purified polyclonal rabbit antibody generated against a peptide fragment (KIKDNGDLILSSPKC) of zebrafish GR protein (Genscript Corp.). The specificity of the antibody was confirmed by western blotting of serially diluted zebrafish and rainbow trout tissues.

For whole mount IHC, rehydrated embryos were rinsed for 15 min (repeated 3x) in PBS with 1% Triton-X100 (PBST), then rinsed in blocking solution of PBST with 10% fetal bovine serum for 1 h (3x). Primary antibody (polyclonal rabbit anti-zebrafish GR, 1:500 dilution) incubation was for16 h at 4^{o}C. Embryos were then rinsed in blocking solution for 1 h (3x). Secondary antibody incubation (Alexa-fluor 594 coupled goat anti-rabbit, Invitrogen; 1:2000 dilution) was for 3 h in the dark. Embryos were rinsed for 15 min (3x) with blocking solution and 15 min (3x) in PBST in the dark. All rinses and incubations were carried out with gentle rocking. Images were taken with a Zeiss Lumar V.12 stereomicroscope. IHC was used to identify distribution of GR protein in wild-type zebrafish embryos at 24, 36 and 48 hpf.

2.3.3 GR promoter activation

To confirm the temporal and regional onset of *de novo* GR mRNA synthesis, a GR promoter-GFP reporter construct was created. A ~3.5 kb segment upstream of the zebrafish GR start codon was identified as the putative promoter region and coupled to the enhanced green fluorescent protein (EGFP) coding sequence. The primers used to amplify the putative promoter region are shown in Table 1 (see GR Promoter), while the sequence and annotations of the amplified region are provided in the Appendix A. PCR was carried out with DNA extracted from adult zebrafish tail and each 25 μL reaction mixture contained 2.5 μL 5x Reaction Buffer, 0.5 μL of 10mM dNTPs, 1.5 μL of 25mM $MgCl_2$, 0.13 μL Taq Polymerase (all from MBI Fermentas), 17.87 μL of RNase free water (Qiagen), 1.25 μL of 10 μM primer pair, and 1.25 μL of DNA template. The PCR conditions were as follows: 2 min at 95^{o}C; 35 cycles of 30s at 94^{o}C, 4 min at 58^{o}C, and 5 min at 72^{o}C; and a final 10 min at 72^{o}C. The resulting PCR product was run on an agarose gel and purified with the Qiaquick Gel Extraction kit (Qiagen). The PCR product was ligated into pCRII-Topo vector with the Topo-TA cloning kit (Invitrogen). Both the GR (in pCRII-Topo) and a pEGFP-1 vector (Clonetech) were digested with XhoI and BamHI restriction enzymes, then ligated overnight at 16^{o}C using ligase enzyme (MBI Fermentas). The construct was sequenced (York University DNA Sequencing Facility) to ensure that the correct cassette was inserted. The construct was microinjected into the cell of 1-cell embryos using a nitrogen-powered microinjector (Narishige). The injection concentration was 100 μg/μL in sterile water, and

approximately 500 pL was injected into the cell. Control embryos were injected with a promoter-less pEGFP-1 vector. The embryos were imaged at 12, 15, and 18 hpf with an AZ100 microscope, Intensilight fluorescent module and DS-Ri1 camera (all from Nikon).

2.3.4 GR knockdown

Morpholino oligonucleotides (MO; Gene-Tools) were targeted to the start site of translation for the zebrafish GR gene, while a 5 bp mispair (MP) served as the control. The sequences of the MO and MP are:

MO – 5'-CTCCAGTCCTCCTTGATCCATTTTG-3';

MP – 5'TGcTATgTTTAcTCTCgATACgTG-3',

small letters indicate mismatched basepairs.

The MO was fluorescein-tagged to track dispersion in the embryo. The oligonucleotides were dissolved in sterile water to 1.0 mM with added phenol red. Titration studies (0.1, 0.25, 0.5 and 1.0 M) were carried out to establish the MO concentration that did not result in early embryo mortality. The MO and MP were injected into the yolk of 1-2 cell embryos and the concentration used in this study (0.5 M; 4.4 ng/nL) allowed the embryos to survive beyond 12 hpf. As a further control, a p53 morpholino was co-injected with the GR morpholino. The resulting double morphants displayed the same characteristics as those injected with the GR-MO alone, indicating that the observed GR knockdown effects were specifically caused by reduced GR protein translation, independent of any non-specific MO effects due to the loss of p53. The effectiveness of GR knockdown was established by whole-mount ISH, IHC, western blotting, and quantitative real-time PCR (qPCR).

2.3.5 Western blotting

Pools of 24 hpf MP and MO embryos were dissected to isolate the tails to prevent yolk protein contamination and sonicated for 10s on ice with a Model 60 Sonic Dismembrator (Fisher Scientific). Sample protein concentration was determined by the bicinchoninic acid method with bovine serum albumin (Sigma) standards. The resulting homogenate was diluted with Laemmli's buffer and 30 μg of protein was loaded onto an 8% SDS-PAGE gel and electrophoresed and immunodetected exactly as described before (Boone and Vijayan, 2002). The proteins were transferred onto a nitrocellulose membrane and were probed with the rabbit anti-zebrafish GR primary antibody (1:750 dilution) and goat anti-rabbit HRP-conjugated secondary antibody (1:3000 dilution, Bio-Rad) for 1 h each at room temperature with gentle rocking. Protein bands

were detected with ECL Plus western blotting detection reagent (GE Healthcare) and the intensity of the bands scanned with the Typhoon Variable Mode Imager (GE Healthcare) and quantified using AlphaEase software (Alpha Innotech).

2.3.6 Gene expression

RNA extraction was carried out on pools of embryos with the RNeasy Mini Kit (Qiagen) with DNase treatment (Qiagen) to remove genomic DNA contamination. RNA quantification was performed with a Nanodrop spectrophotometer at 260 nm (Thermo Scientific) and 1 μg of total RNA was reverse transcribed with the First Strand cDNA Synthesis Kit (MBI Fermentas) using M-MuLV reverse transcriptase to produce a 20 μL mixture according to the manufacturer's protocol.

RT-PCR was performed on 24 and 36 hpf MP and MO embryos to assess the transcript expression of the following genes: *igf1*, *igf2*, *bmp2a*, *bmp2b*, and *bmp4*, with *β-actin* as a control for equal loading. 1.25 μL of the cDNA mixture was used for RT-PCR analysis. The PCR conditions were: 94^{o}C for 3 min, 40 cycles of 30s at 94^{o}C, 30s at Tm (Table 1), and 30s at 72 ^{o}C; followed by 10 min at 72 ^{o}C. PCR mixtures were run on agarose gels with added SYBR Safe gel stain (Invitrogen) and imaged with an AlphaImager (Alpha Innotech).

Primers used for real-time quantitative PCR (qPCR) analysis are listed in Table 1, in bold. The 25 μL qPCR mixture contained: 0.75 μL of template, 12.5 μL iQ SYBR green supermix (Bio-Rad), 0.75 μL of 10 μM primers, 11μL RNase free water (Qiagen). The sample mixtures were run in triplicate on an iCycler iQ thermocycler (Bio-Rad) using the following conditions: 94^{o}C for 2 min, 40 cycles of 30s at 95^{o}C, and 30s at Tm (see Table 1, bold), followed by 10 min at 72^{o}C. To assess the effectiveness of the GR knockdown, the mRNA abundance of GR and matrix metalloproteinase-13 (*mmp13*), a known GR-responsive gene (Hillegass et al., 2007), was quantified from pools of 24 hpf MP and MO embryos. Standard curves were created for GR and *mmp13* by insertion of the amplicon into a PGEM-Teasy vector (Promega) using established protocols (Aluru et al., 2010). qPCR was also used to measure observed changes in the mRNA abundance of BMP genes (*bmp2a*, *bmp2b*, *bmp4*) and markers of BMP signaling (*eve1, pax3, pax7*). To determine changes in expression related to altered mesodermal formation, we quantified the mRNA abundance of the following myogenic markers: *myod*, myogenin (*myog*), myostatin (*mstnb*), slow muscle myosin heavy chain 1 (*smyhc1*), fast muscle specific myosin heavy chain (*myhz2*), slow muscle troponin C (*stnnc*), and fast muscle troponin I (*tnni2a*). qPCR primers for all myogenic marker genes other than *myod* were previously characterized

(Palstra et al., 2010). The mRNA abundance of these genes was quantified from pools of 24 and 36 hpf MP and MO embryos using the delta-delta Ct method of quantification (Livak and Schmittgen, 2001) using *β-actin* as the housekeeping gene (values were similar across samples).

Table 1: Primers used for RT-PCR and qPCR (bold) and their amplicon size and melting temperatures (Tm).

Gene	Forward Primer (5'-3')	Reverse Primer (5'-3')	Amplicon Size (bp)	Tm (^{o}C)
bmp2a	**AGGCTGGAATGACTGGATTG**	**TTGCTGTTCACCGAGTTCAC**	**140**	**55**
bmp2b	**CTGAAAACGATGACCCGAAC**	**TCGTATCGTGTTTGCTCTGC**	**88**	**55**
bmp4	**CTTTGAGACCCGTTTTACCG**	**TTTGTCGAGAGGTGATGCAG**	**147**	**57**
eve1	**GGGAACAGCTGACTCGTCTC**	**TGTCCTTCATTCTCCGGTTC**	**141**	**53**
mmp13	**ATGGTGCAAGGCTATCCCAAGAGT**	**GCCTGTTGTTGGAGCCAAACTCAA**	**289**	**60**
mstnb	**AGACCGCTGTGGCTGCTCAT**	**GCGGAAAGCACTGGTAATGT**	**107**	**60**
myod	TCAGACGAGAAGACGGAACA	CACGATGCTGGACAGACAAT	117	60
myhz2	**GCCTGAGCTGATTGAAATGACGC**	**GCTCCTCACGCTGCTTCTGCTT**	**232**	**57**
myog	**AGTGGACAGCATAACGGGAACAG**	**GCTGGTCTGAAGGTAACGGTGAG**	**99**	**60**
igf1	CCACGATCTCTACGAGCACA	TCGGCTCGAGTTCTTCTGAT	113	60
igf2	TGCAGGTCATTCCAGTGATG	TAGCCTCTGAGCAGCCTTTC	109	60
gr	**ACAGCTTCTTCCAGCCTCAG**	**CCGGTGTTCTCCTGTTTGAT**	**116**	**60**
GR promoter	ATGGCGTTGGAAGAAATGCA	GATTTGCTCGTTTTCGGCCA	3444	58
pax3	**AACCCAAGCAGAGCACAACT**	**TTATTCCGATCGCAGATTCC**	**127**	**60**
pax7	**CTGAAGGACGGAGTGTGTGA**	**AAGGTCTGGCTCTGACTCCA**	**230**	**57**
smyhc1	**GAGCCGTGATTCAGGACCCA**	**TGGCTTCACAACAAACAAACTCGT**	**78**	**60**
stnnc	**GCAAGATCGACTACGACGAGTTCT**	**AGGCAGCATTGGTTCAGGGA**	**95**	**57**
tnni2a	**GGTATGGACGGCAGGAAGAAGA**	**GGAACGGGAGGTTTACAGGACAG**	**123**	**57**
β-actin	**TGTCCCTGTATGCCTCTGGT**	**AAGTCCAGACGGAGGATG**	**120**	**60**

2.3.7 Embryo survival and morphology

Embryos were counted, imaged and sampled at 12, 24, 36 and 48 hpf and dead or unfertilized embryos were removed. Bright-field embryo images were captured and processed after dechorionation with a Nikon AZ-100 microscope and DS-Ri1 camera. By annotation with NIS-elements software (Nikon), the number of formed somites was counted at 12 and 15 hpf, and the embryo length (as measured around the dorsal edge from head to tail) and the head-trunk angle (as measured between the eye-ear axis and the notochord) were measured at 24 hpf.

2.3.8 Zebrafish GR mRNA synthesis and rescue

To synthesize the GR coding sequence mRNA, a ~2.2 kb region was amplified using the following primers:

F 5'-ATG GAT CAA GGA GGA CTG GA-3'

R 5'- TCA TTT CTG GTG AAA GAG CAG C-3'

PCR and cloning of the amplicon was performed as noted above for the GR-GFP construct. The resulting vector was transformed into competent DH5α *E. coli* cells by heat shock (15s, 42^{o}C), which were grown on lysogeny broth (LB) media plates with 10 mM ampicillin for 14h at 37^{o}C. Transformed colonies were grown in LB media for 14h at 37^{o}C. Plasmids were eluted in sterile water with the GenElute Plasmid Miniprep Kit (Sigma), following manufacturer protocols. Plasmids were quantified on a Nanodrop spectrophotometer (Thermo Scientific). To ensure proper insertion, the plasmid was sequenced (York University DNA Sequencing Facility). Before in vitro transcription, the plasmid was linearized with EcoRV restriction enzyme (1 hour, 37 ^{o}C). The mMessage mMachine T7 kit (Ambion) was used to create capped mRNA according to the manufacturer's protocol and diluted to 1 µg/µL in sterile water.

GR mRNA was diluted to 50 pg/nL and 200 pg/nL for initial titration and assessment of rescue. As 200 pg/nL was found to rescue a higher percentage of embryos, with no adverse effects on embryos when injected alone, this concentration was used for further rescue injections. One-cell embryos were injected with 1 nL of GR MO, GR MP, GR mRNA alone, or GR mRNA and MO co-injections. Embryos were grown as noted previously, and survival, somite development, and growth were measured exactly as before. Gene expression of rescue embryos was analyzed at 36 hpf by qPCR exactly as described for MO knockdown embryos, quantifying the mRNA abundance of *bmp2a*, *bmp2b*, *bmp4*, *myog*, and *smyhc1*.

The following abbreviations are used in the text: MP - embryos injected with mispair only; MO - GR morphants, only injected with morpholino; RNA - embryos injected with GR mRNA only; and MO+RNA - the morpholino and mRNA coinjection rescue embryos. MP and MO groups presented as part of the GR mRNA rescue data are independent from those presented as part of the examination of GR receptor knockdown effects, as they represent separate injection trials.

2.3.9 Promoter analysis

A bioinformatics approach was used to analyze the regions upstream of the transcriptional start sites of *myod*, *igf1*, *igf2*, *bmp2a*, *bmp2b*, and *bmp4*. For each gene, a 7.5 kb regions was identified using NCBI's Entrez Gene and Sequence Viewer (*myod*: NC_007136.5; *igf1*: NC_007115.5; *igf2*: NC_007118.5; *bmp2a*: NW_003040445.1; *bmp2b*: NW_001878149.2; *bmp4*: NW_001877808.2). These sequences were analyzed using the Matinspector software suite (Genomatix), and the Transcription Element Search System (TESS) to identify putative glucocorticoid response elements (GREs). Only regions that were identified by both software packages were accepted as likely sites.

2.3.10 Statistical analysis

All data are presented as mean ± standard error of the mean (SEM). Data comparison for two samples (MO and MP) utilized Student's t-test, while multiple treatments were compared using either one-way analysis of variance (ANOVA) or two-way ANOVA (Sigmastat, Systat Software). A probability value of $p<0.05$ was considered significant.

2.4 Results

2.4.1 Temporal GR expression in zebrafish embryos

GR mRNA was observed in embryos at the 16-cell stage (Fig. 1A I) and at 4 hpf (Fig 1A II), but at 6 and 8 hpf, no GR mRNA were detectable in the developing embryo (Figs. 1A III and IV). GR mRNA transcripts were detected again at 10 hpf in the anterior end (Fig. 1A V), and were widely expressed by 12 hpf (Fig. 1A VI). GR mRNA was seen throughout the developing embryo with strong detection in the somites at 24 hpf (Fig 1A VII). By 48 hpf, the GR mRNA expression is reduced in the tail and is predominantly localized in the developing head and trunk (Fig 1A VIII, see arrow). Sense strand hybridizations at 24 and 48 hpf (Figs. 1A IX and X) confirm the specificity of the GR riboprobes. Similar to GR transcripts, GR protein expression was also

widely expressed throughout the embryo at 24 and 36 hpf (Fig. 1B I and II), but reduced at 48 hpf and was detectable only in discrete regions in the head, trunk, and tail (Fig. 1B, III, see arrows).

We used a GR-GFP reporter construct (see Appendix A for sequence and diagrams, Fig. A1) to confirm the zygotic expression of GR. Using this construct the earliest *de novo* GR promoter activation was observed at 15 hpf in the ventral midtrunk region. By 18 hpf, GFP was also visible at somite boundaries. Negative control embryos showed no GFP fluorescence. Representative images are included in supplemental data (See Appendix A, Fig. A2).

Figure 1 – Glucocorticoid receptor (GR) gene and protein expression in wild-type embryos. GR mRNA and protein exhibit dynamic spatial expression during early embryogenesis. (A) Spatial GR mRNA abundance in wild-type (WT) embryos at 16-cell (I), 4 hpf (II), 6 hpf (III), 8 hpf (IV), 10 hpf (V), 12 hpf (VI), 24 hpf (VII), and 48 hpf (VIII) stages (n=10-15 embryos at each stage). Sense strand hybridizations at 24 hpf (IX) and 48 hpf (X) display probe specificity. (B) Spatial GR protein expression in WT embryos (n=10-12 embryos) at 24 hpf (I), 36 hpf (II), and 48 hpf (III). Fluorescent images (left) show GR protein distribution detected by specific antibody (polyclonal rabbit anti-zebrafish GR) binding, bright-field images (middle) display whole embryo shape, and negative control images (right) show specificity of fluorescence in embryo tissue.

A

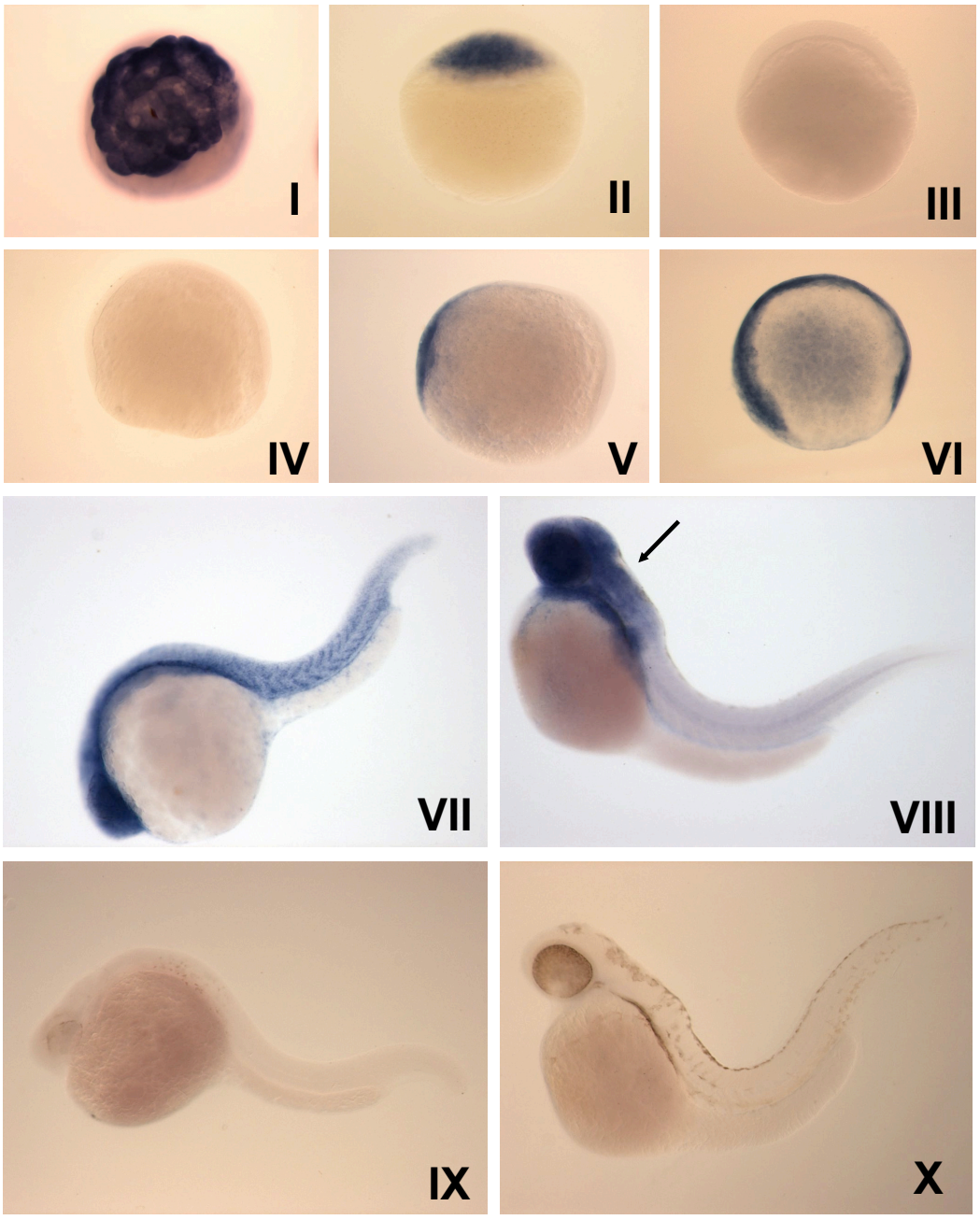


B
GR IHC
Bright-Field
Neg. Ctrl.
I) 24 hpf
II) 36 hpf
III) 48 hpf

2.4.2 GR knockdown

The post-injection dispersion of morpholinos (MO) was observed by microscopic observation of fluorescein tagged-GR MO embryos. Fluorescein was ubiquitously spread throughout the cells from the two-cell stage, and continued to be observable until 40 hpf (data not shown). The knockdown of GR protein was confirmed by whole-mount immunohistochemistry (IHC; Fig. 2A) and western blotting (Fig. 2B). There was a >50% reduction in GR protein content in the MO embryo at 24 hpf by western blotting (Fig. 2B) and this was also confirmed by a decrease in GR protein expression observed by IHC at 24 and 36 hpf (Figs. 2A I and II). Essentially no GR protein expression was seen in the tail after morpholino injection (Fig. 2A, see dashed inset). GR mRNA abundance was not affected by MO injection as seen by *in situ* hybridization (ISH; Fig. 2C) and qPCR (Fig. 2D). MMP-13 expression was suppressed by >70% in the MO embryos compared to the MP embryos at 24 hpf (Fig. 2E) confirming a functional knockdown of GR signaling.

Figure 2 – Glucocorticoid receptor protein knockdown by morpholino injection.
Injection of morpholino oligonucleotides (MO) causes a significant decrease in GR protein expression in developing embryos, but does not affect GR mRNA content.
(A) Whole-mount immunohistochemistry shows widespread loss of GR protein in morpholino-injected (MO, right) embryos compared to mispair-injected embryos (MP, left) at both 24 hpf (I) and 36 hpf (II). Reduced GR protein expression in the developing somites at 24 hpf is shown in the expanded dashed inset. (B) A representative western image of GR protein expression in the tail of MP and MO embryo is shown and the band intensity (% MP) is displayed as a histogram (n=4 pools of 30 embryo tails). (C) GR mRNA expression was unchanged in 24 hpf wild-type (WT, left) and MO embryos (right) (n=10 embryos each). (D) GR mRNA abundance (n=5 pools of 16 embryos) of 24 hpf MO and MP embryos expressed as percentage of MP. (E) Matrix metalloproteinase-13 (MMP-13; a known GR-responsive gene) mRNA abundance in 24 hpf embryos expressed as percentage of MP (n=4 pools of 16 embryos). All values shown are mean ± standard error of mean (SEM); * significantly different (Student's t-test, $p<0.05$).

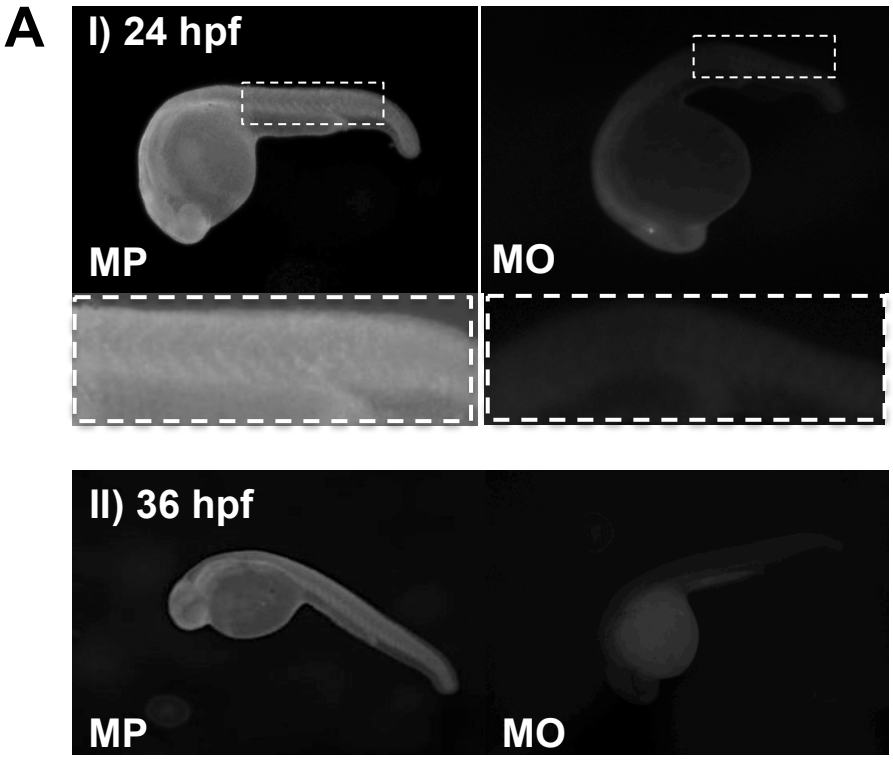
A
I) 24 hpf
MP
MO
II) 36 hpf
MP
MO

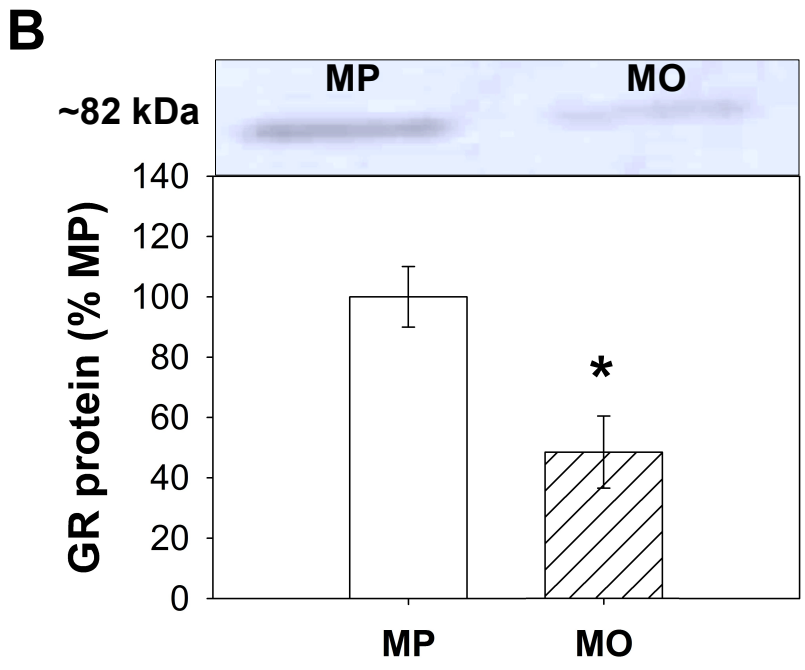
B
MP
MO
~82 kDa
GR protein (% MP)
140
120
100
80
60
40
20
0
*
MP
MO

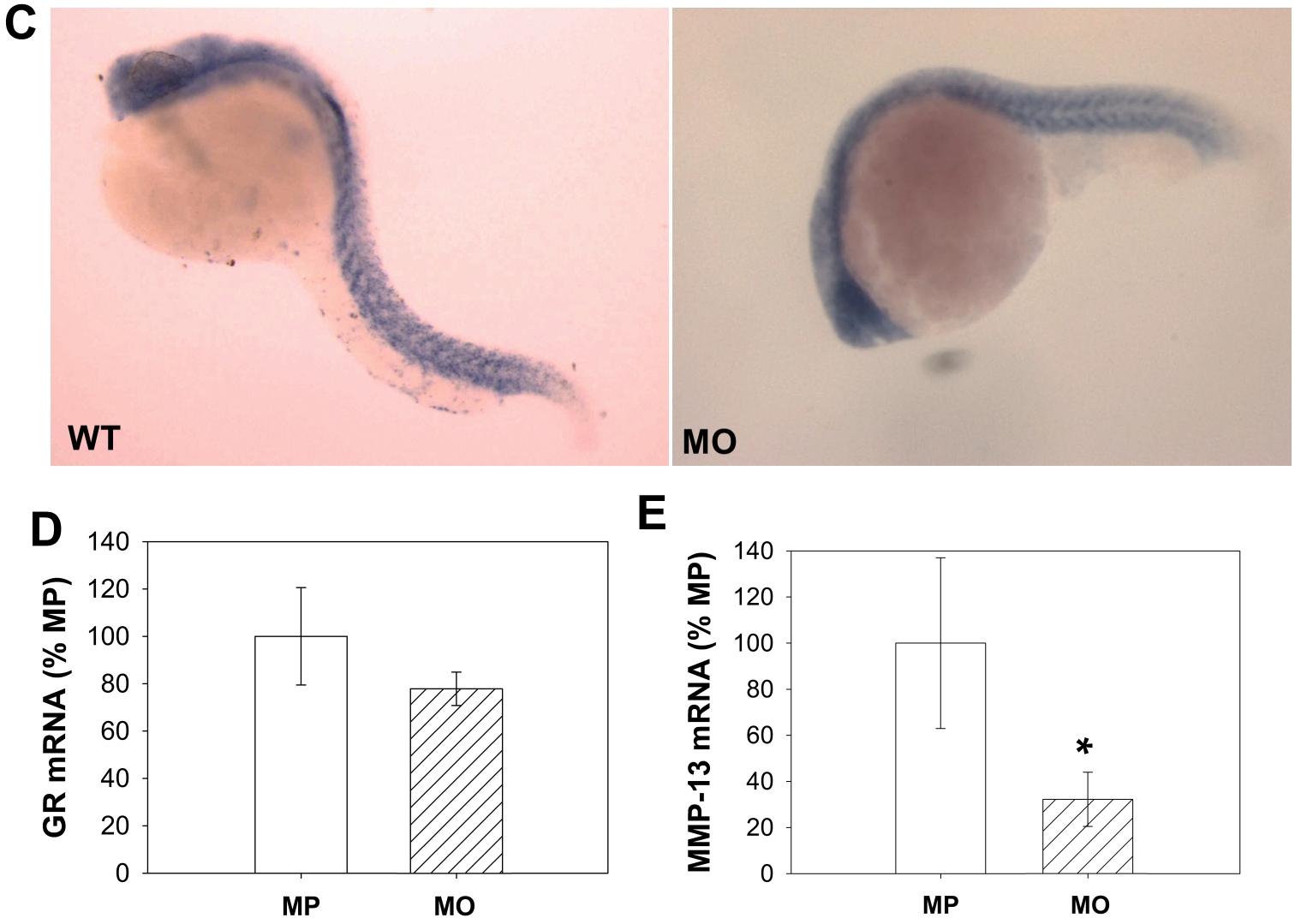
C
WT
MO
D
GR mRNA (% MP)
140
120
100
80
60
40
20
0
MP
MO
E
MMP-13 mRNA (% MP)
140
120
100
80
60
40
20
0
*
MP
MO

2.4.3 GR signaling is important for embryo growth and survival

There was embryo mortality associated with microinjection compared to uninjected wild-type (WT) embryos (Fig. 3A, 3B). However, there were no differences in embryo survival or morphology between the WT and mispair (MP) embryos at any time point (Figs. 3A and 3B). Hence, all data comparisons included only MP control and MO embryos. There was no significant difference in embryo survival between the MO and MP group at 12 hpf (Fig. 3A I). GR knockdown reduced embryo survival compared to the MP control by ~30% at 24 hpf (Fig. 3A II) and by >90% at 48 hpf (Fig. 3A III). Growth and early developmental rate was also affected by GR knockdown. A significant decrease in embryo length (Fig. 4C) and head-trunk angle (Fig. 4D) was seen in the MO compared to MP embryos. There was a significant decrease in the rate of somite formation in the MO embryos at 12 and 15 hpf compared to the MP group (Figs. 3C I and 3D I). In addition to slower rates of somite formation, morphant embryos often exhibited more prominent tail formation defects (Fig. 4A and 4B). At 24 hpf (Fig. 4A), GR knockdown embryos often exhibited kinked tails compared to the normal smooth and straight extension displayed by MP embryos. At 36 hpf (Fig. 4B), in addition to tail malformations (see arrows), MO embryos were seen to exhibit misshapen and unusually sized somites (see dashed inset). Low-magnification images of embryos are included to show the common nature of these defects in only the GR morphants (Fig. 4B).

The injection of 200 pg of GR mRNA along with the MO was able to rescue most of the morphant phenotypes. There was no significant difference in survival between the controls and rescued embryos at either 24 or 48 hpf (Fig. 3B II and III). The rate of somite formation was also rescued by mRNA injection. At both 12 and 15 hpf (Fig. 3C II and 3D II), the number of somites was significantly higher in the rescue embryos relative to the MO embryos. Later in development, the rescue embryos displayed far fewer morphological defects (Fig. 4A and 4B). The rescued embryos were similar to MP embryos with fewer tail disruptions, including kinked tails and somite patterning and shape at 24 and 36 hpf (Fig. 4A and 4B). The relative rarity of defects in all groups other than the GR knockdown embryos can be seen from the low magnification images of multiple embryos (Fig. 4A, II, see arrows). The coinjection of GR mRNA also rescued the significant reduction in embryo length (Fig. 4C) and head-trunk angle (Fig. 4D) that was evident in the 24 hpf MO embryos.

Figure 3 – Effect of glucocorticoid receptor knockdown on embryo survival and development.

GR morphants display increased mortality and slowed somitogenesis, but these effects are reversed with GR mRNA rescue. (A) Embryo survival at 12 hpf, (I), 24 hpf (II), and 48 hpf (III), comparing mispair-injected (MP, n=9 pools of 86-351 embryos) and morpholino-injected embryos (MO, n=14 pools of 84-218 embryos). Data is presented as percentage of wild-type (WT) survival (n=19 pools of 33-356 embryos). (B) Embryo survival was similarly measured after mRNA rescue, comparing MP (n=6 pools of 56-113 embryos), MO (n=8 pools of 42-136 embryos), RNA-injected (RNA, n=6 pools of 89-149 embryos), and RNA and MO co-injected embryos (RNA+MO, n=10 pools of 56-149 embryos). Data is presented as a percentage of WT survival (n=5 pools of 33-224 embryos). (C) Number of formed somites in 12 hpf MP and MO embryos (I, n=11-15 embryos) and 12 hpf MO, MP, RNA, and RNA+MO embryos (II, n=8-22 embryos). (D) Number of formed somites in 15 hpf MP and MO embryos (I, n=11-15 embryos) and 15 hpf MO, MP, RNA, and RNA+MO embryos (II, n=8-22 embryos). Representative images are shown (arrows indicate region of formed somites). Values shown are mean ± SEM; * significantly different (Student's t-test, $p<0.05$); bars with different letters are statistically different (ANOVA, $p<0.05$).

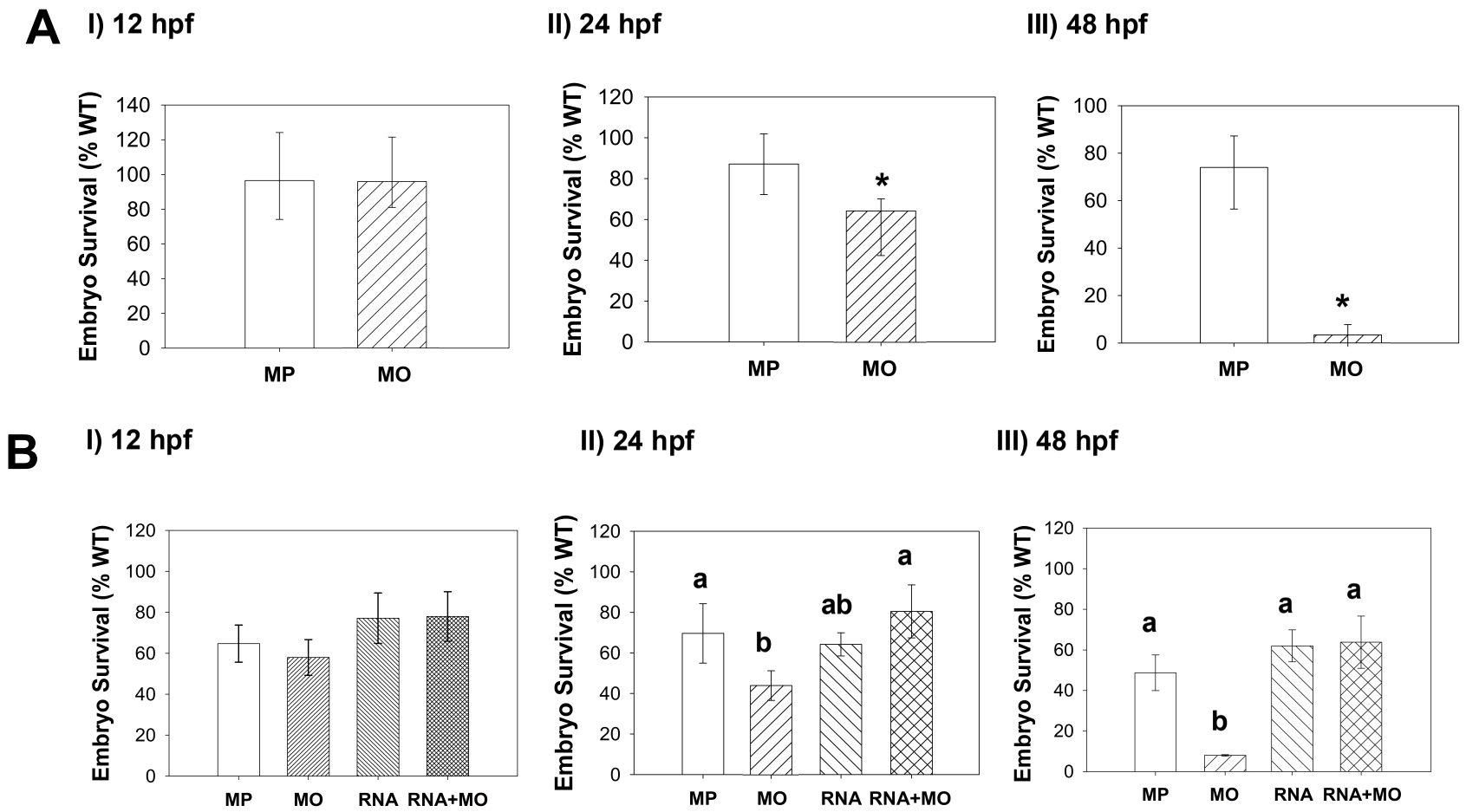
A
I) 12 hpf
II) 24 hpf
III) 48 hpf
Embryo Survival (% WT)
MP
MO
*
B
I) 12 hpf
II) 24 hpf
III) 48 hpf
RNA
RNA+MO
a
b
ab

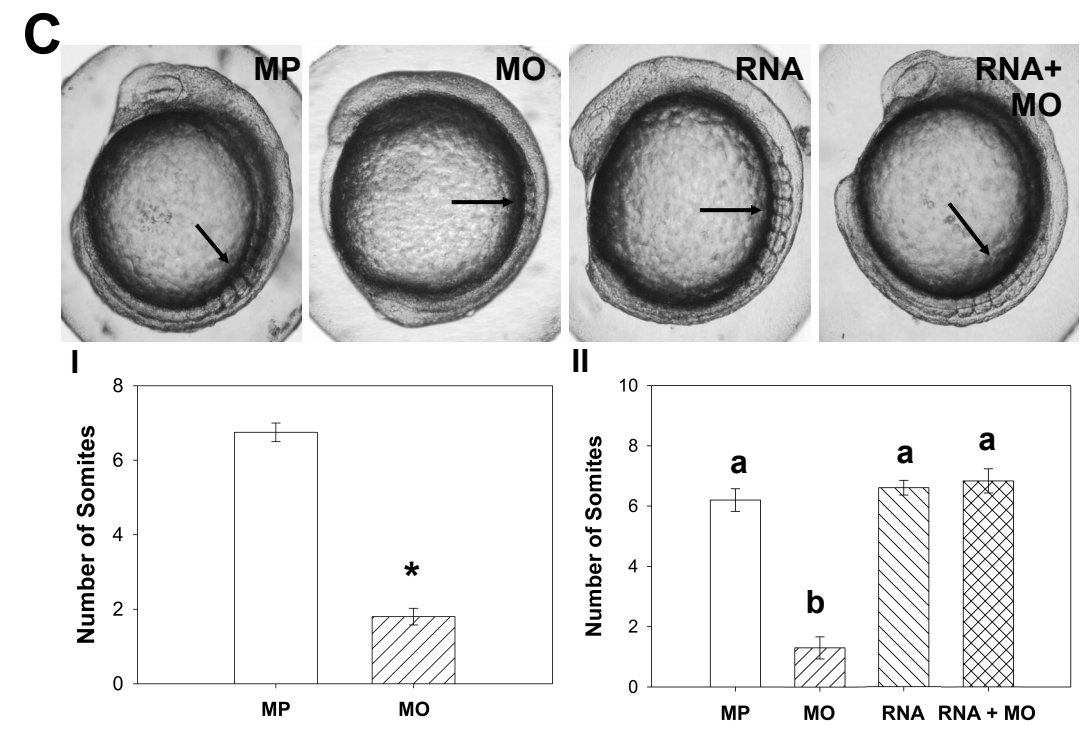
C
MP
MO
RNA
RNA+ MO
I
Number of Somites
8
6
4
2
0
*
MP
MO
II
Number of Somites
10
8
6
4
2
0
a
b
a
a
MP
MO
RNA
RNA + MO

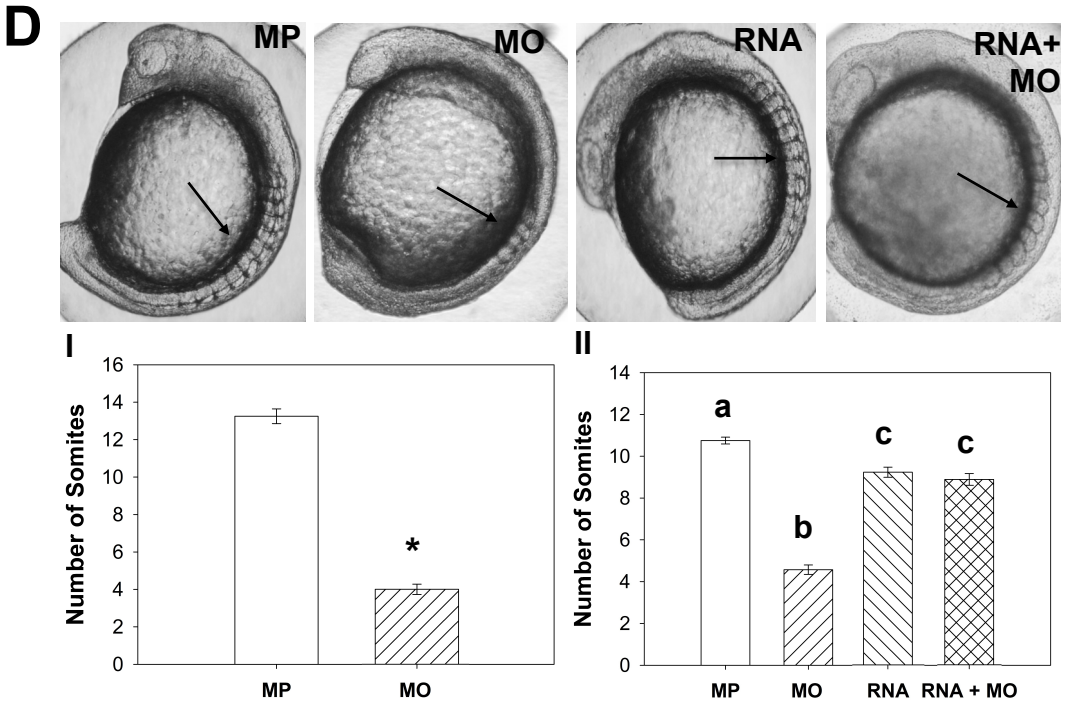
D
MP
MO
RNA
RNA+ MO
I
Number of Somites
16
14
12
10
8
6
4
2
0
*
MP
MO
II
Number of Somites
14
12
10
8
6
4
2
0
a
b
c
c
MP
MO
RNA
RNA + MO

Figure 4 – Effects of glucocorticoid receptor knockdown on morphogenesis.

GR morphants display disrupted tail structures and reduced growth; these characteristics are corrected by GR mRNA coinjection.

Representative images of tail morphological abnormalities in 24 hpf (A) and 36 hpf (B) morpholino-injected embryos (MO) compared to mispair-injected embryos (MP), mRNA-injected embryos (RNA), and mRNA and MO co-injected embryos (RNA+MO); arrows indicate malformed tails. Malformed somites are shown in the magnified dashed inset (B, center). Low-magnification images (B, bottom half) are shown to indicate the common nature of defects in the GR morphants. (C) Length of 24 hpf MP and MO embryos, as measured along the outer edge of the embryo (representative image, white line; n=6-12 embryos). (D) Head-trunk angle of 24 hpf MO, MP, RNA, and RNA+MO, embryos, as measured between the eye-ear axis and the notochord (representative image, white line; n=6-12 embryos). Values shown are mean ± SEM; bars with different letters are statistically different (ANOVA, $p<0.05$).

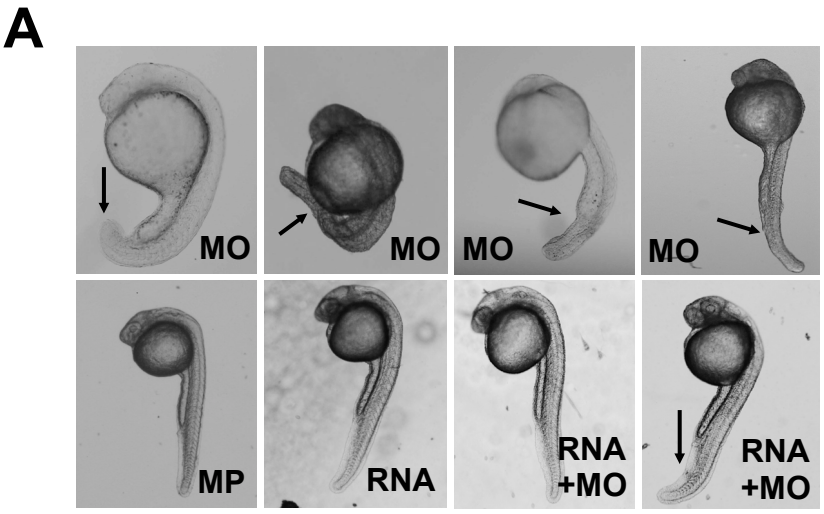
A
MO
MO
MO
MO
MP
RNA
RNA
+MO
RNA
+MO

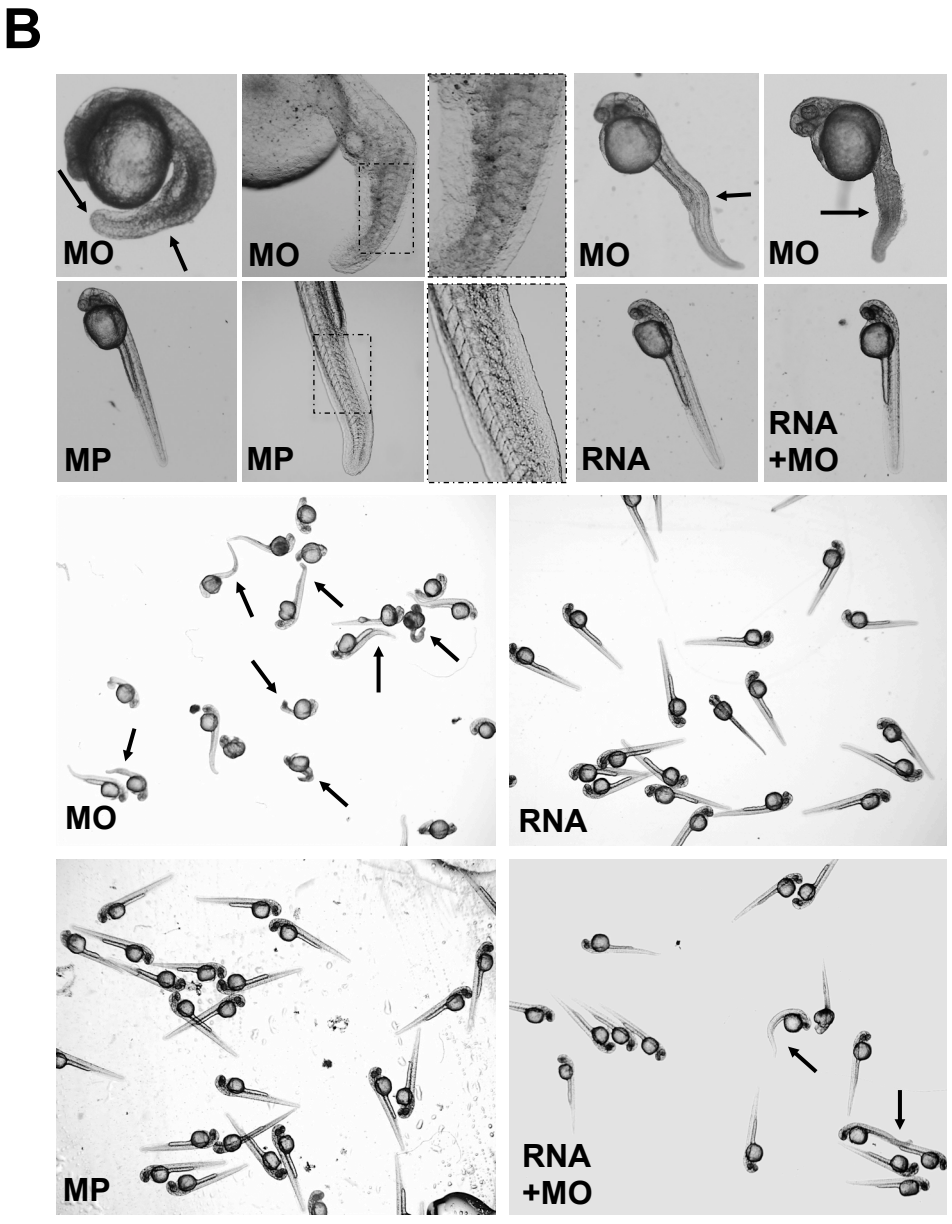
B
MO
MO
MO
MO
MP
MP
RNA
RNA
+MO
MO
RNA
MP
RNA
+MO

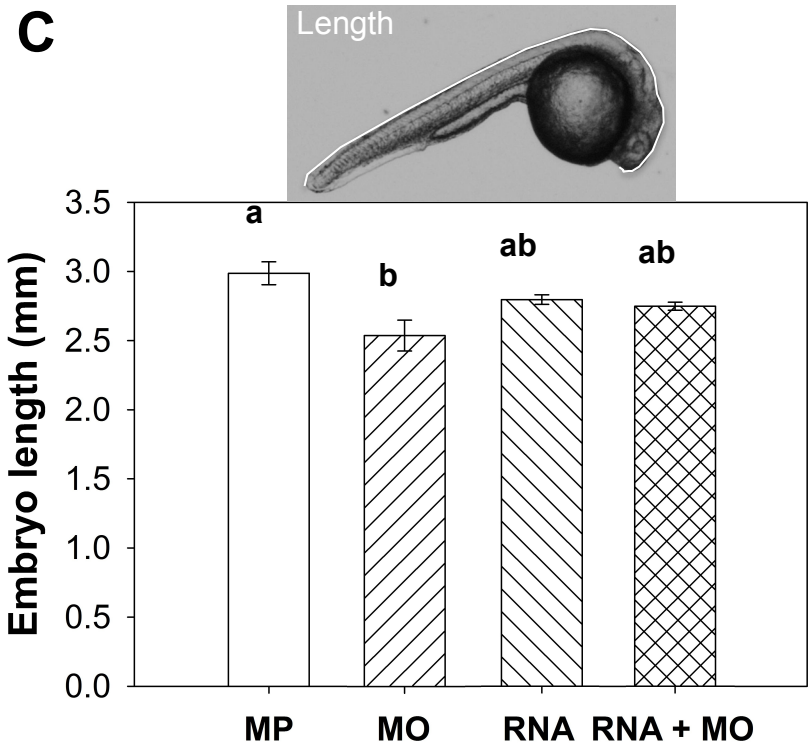
C
Length
Embryo length (mm)
3.5
3.0
2.5
2.0
1.5
1.0
0.5
0.0
a
b
ab
ab
MP
MO
RNA
RNA + MO

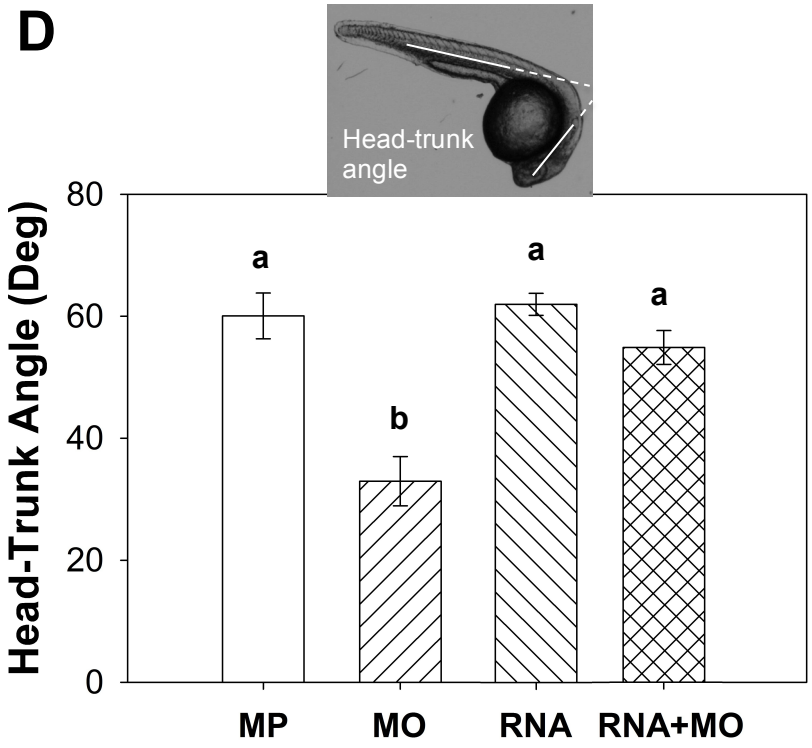
D
Head-trunk angle
Head-Trunk Angle (Deg)
80
60
40
20
0
a
b
a
a
MP
MO
RNA
RNA+MO

2.4.4 GR signaling is essential for mesoderm patterning

Due to defects in the mesodermally-derived tissues, we examined the expression of a suite of genes that are well established mesoderm and growth markers. RT-PCR showed no discernible differences in *igf1* or *igf2* mRNA abundances in the MO group compared to MP control groups at either 24 or 36 hpf (Fig. 5A). However, *bmp2a*, *bmp2b*, and *bmp4* expression was strongly reduced in the MO at both 24 and 36 hpf (Fig. 5A), and this was further confirmed using qPCR. *bmp2a* (Fig. 5B I), *bmp2b* (Fig. 5B II), and *bmp4* (Fig. 5B III) mRNA abundances were all significantly reduced by ~70-90% in GR morphants compared to the MP control at both 24 hpf and 36 hpf. A time-dependent change in gene expression between 24 and 36 hpf was seen only for *bmp2b*, but not for *bmp2a* and *bmp4* (Figs. 5B I-III). For *bmp2b*, mRNA abundance of MP, but not MO embryos were significantly reduced at 36 hpf compared to 24 hpf (Fig. 5B II). In addition, we show that the expression of *eve1* is downregulated in GR morphants at both 24 and 36 hpf (Fig. 6A).

To determine if reduced GR signaling is involved in the disrupted mesoderm phenotype, we examined key marker genes involved in myogenesis in the morphant embryos at 24 and 36 hpf. *pax3* mRNA abundance (Fig. 6B) was reduced by 90% in GR morphants at 24 hpf only, with no significant change observed at 36 hpf. *pax7* mRNA abundance was unchanged in GR morphants (Fig. 6C). *Myod* mRNA abundance was unchanged at both 24 and 36 hpf (Fig. 7A). However, the mRNA abundance of myogenin (*myog*; *Fig*. 7B) and myostatin (*mstnb*; Fig. 7C) were both significantly different in GR morphants at 36 hpf. Myogenin expression was increased by a factor of 2, while myostatin was decreased by a factor of 3. Expression of slow muscle myosin heavy chain 1 (*smyhc1*; Fig. 8A) was increased by ~60% at 24 hpf and by ~30% at 36 hpf in GR morphants, but there was no change in mRNA abundance of fast muscle myosin (*myhz2*; Fig. 8B) at either time points. Also, both slow muscle troponin C (*stnnc*; Fig. 8C) and fast muscle troponin I 2a (*tnni2a*; Fig. 8D) were significantly increased by ~150% at 24 hpf, but remained unchanged in GR morphants at 36 hpf.

GR mRNA rescue completely abrogated the suppression of BMP gene expressions (Fig. 5C) and two selected myogenic genes (Fig. 9) seen in the MO group. For all three BMP genes, the rescued embryos had significantly higher mRNA abundance relative to MO embryos, and were not statistically different from the MP (exception was *bmp2a*) or mRNA control groups (5C I-III). The rescued embryos also showed significantly lower mRNA abundance of *myog* (Fig. 9A) and *smyhc1* (Fig. 9B) compared to MO embryos, but were not statistically different from the MP or mRNA control groups. In addition, bioinformatics analysis of the region upstream of *bmp2a,*

bmp2b and *bmp4* coding sequences indicate that there are multiple putative GREs within a 7.5 kb region upstream of each gene (Fig. 5D I-III). Bioinformatics analysis also indicated two putative GRE sites upstream of each of *igf1*, *igf2*, and *myod* (base pair regions are shown in Appendix A, Fig. A3), but there was no change in gene expression following GR knockdown (Fig. 5A; Fig 7A).

Figure 5 – Effects of glucocorticoid receptor knockdown on expression of developmental genes.

GR knockdown reduced expression of BMPs but not other developmental genes. BMP expression in the morphants is rescued by GR mRNA injection. (A) RT-PCR images of *igf1*, *igf2*, *β-actin*, *bmp2a*, *bmp2b*, and *bmp4* mRNA expression in 24 and 36 hpf mispair (MP) and morpholino (MO) injected embryos (n=4 pools of 25 embryos). (B) mRNA abundance of *bmp2a* (I), *bmp2b* (II), and *bmp4* (III) measured by qPCR in 24 hpf and 36 hpf MP and MO embryos (GR gene knockdown; n=4 pools of 25 embryos) or (C) MP, MO, RNA injected (RNA), and RNA and MO co-injected (RNA+MO) embryos (GR mRNA rescue; n=4 pools of 25 embryos). Values shown are mean ± SEM; bars with different letters are statistically different (ANOVA, $p<0.05$). (D) Schematics of putative glucocorticoid response elements (GREs; number starting base pair) upstream of BMP2A (I), BMP2B (II) and BMP4 (III).

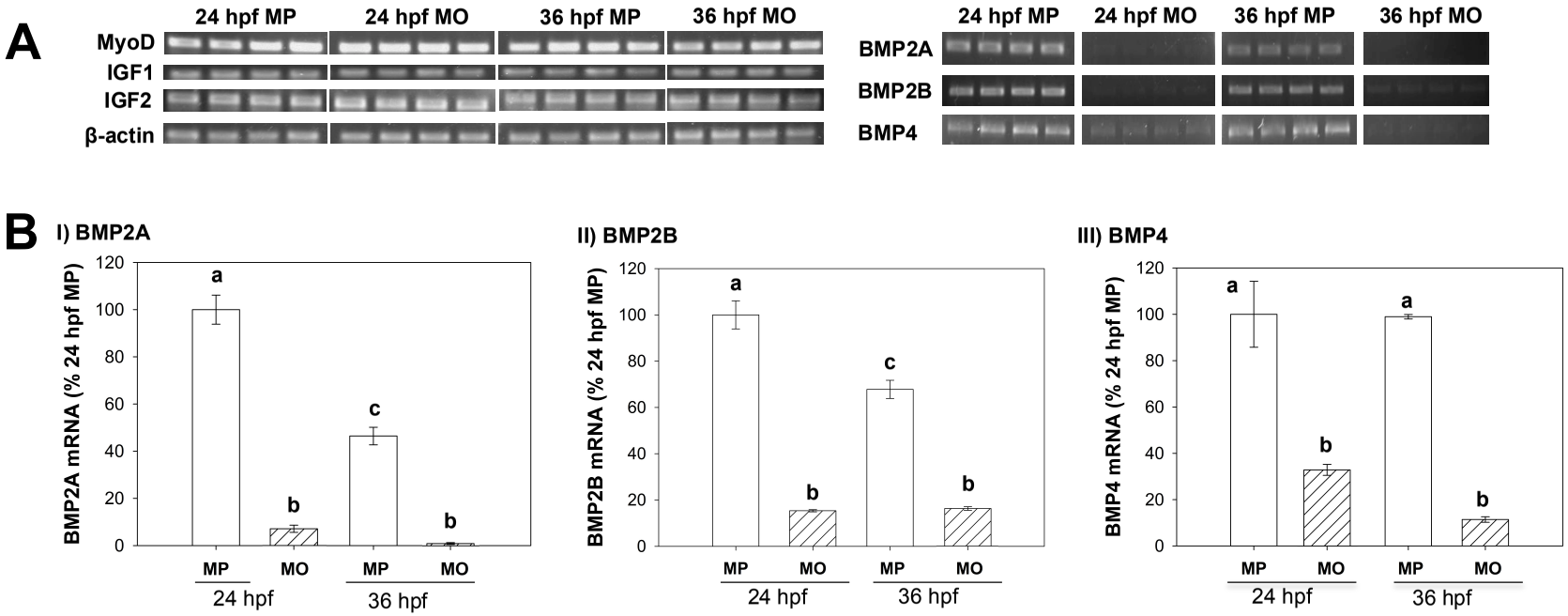
A
24 hpf MP
24 hpf MO
36 hpf MP
36 hpf MO
MyoD
IGF1
IGF2
β-actin
BMP2A
BMP2B
BMP4
B
I) BMP2A
II) BMP2B
III) BMP4
BMP2A mRNA (% 24 hpf MP)
BMP2B mRNA (% 24 hpf MP)
BMP4 mRNA (% 24 hpf MP)
MP
MO
24 hpf
36 hpf

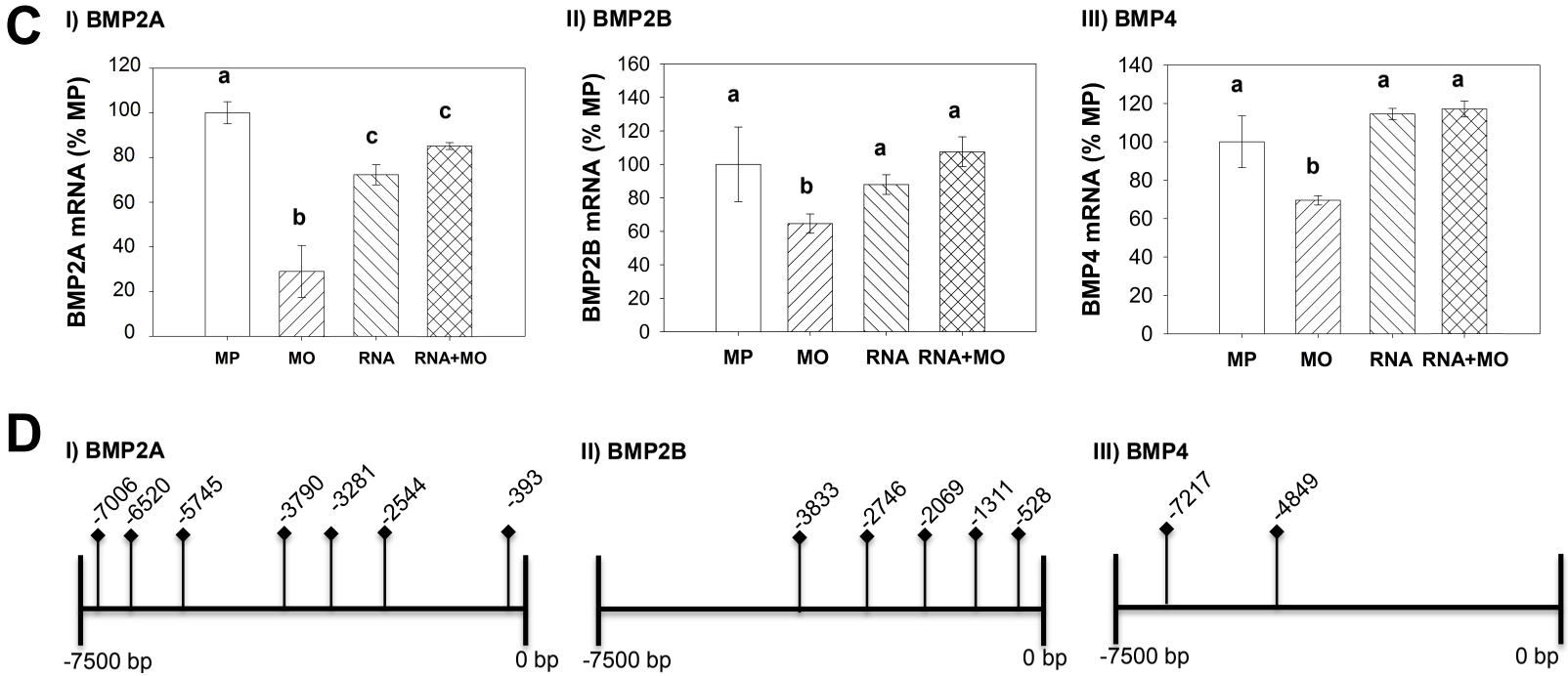
C
I) BMP2A
BMP2A mRNA (% MP)
120
100
80
60
40
20
0
a
b
c
c
MP
MO
RNA
RNA+MO
II) BMP2B
BMP2B mRNA (% MP)
160
140
120
100
80
60
40
20
0
a
b
a
a
MP
MO
RNA
RNA+MO
III) BMP4
BMP4 mRNA (% MP)
140
120
100
80
60
40
20
0
a
b
a
a
MP
MO
RNA
RNA+MO
D
I) BMP2A
-7006
-6520
-5745
-3790
-3281
-2544
-393
-7500 bp
0 bp
II) BMP2B
-3833
-2746
-2069
-1311
-528
-7500 bp
0 bp
III) BMP4
-7217
-4849
-7500 bp
0 bp

Figure 6 – Effects of glucocorticoid receptor knockdown on expression of BMP signaling markers

GR morphants exhibited reduced expression of specific BMP responsive genes, indicating a functional reduction of BMP signaling. mRNA abundance of *eve1* (A), *pax3* (B), and *pax7* (C) in 24 hpf and 36 hpf mispair (MP) and morpholino (MO) embryos as quantified by qPCR. Values shown are mean ± SEM; bars with different letters are statistically different (n=4 pools of 25 embryos, ANOVA, $p<0.05$).

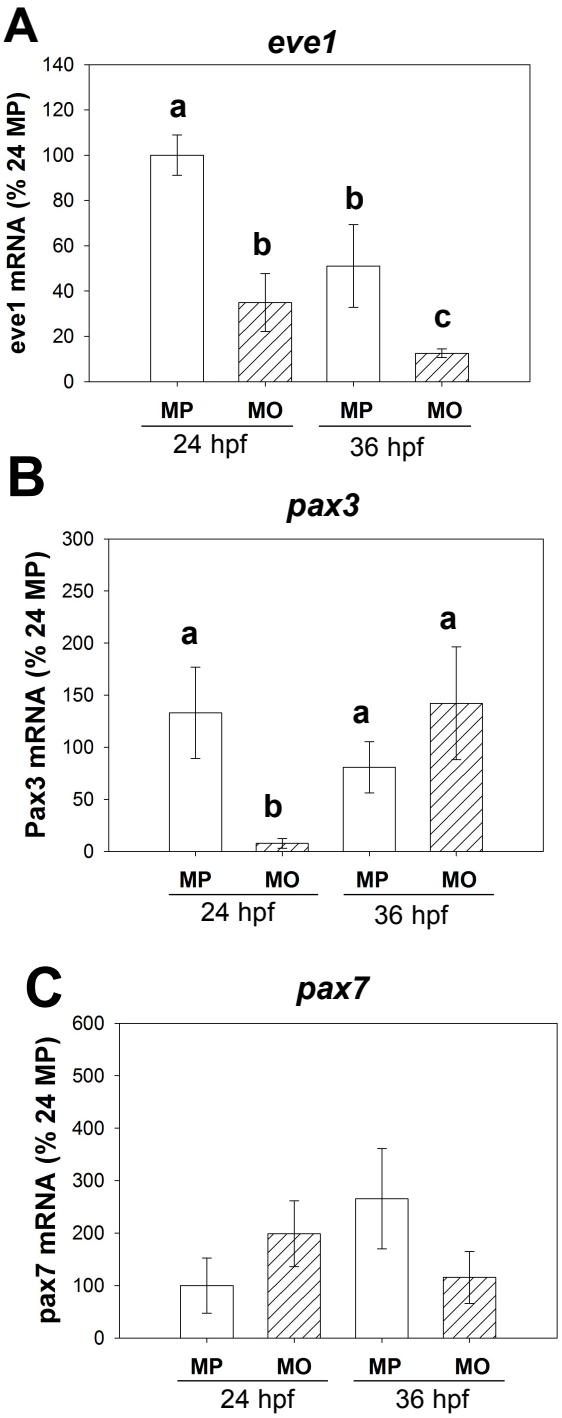
A
eve1
eve1 mRNA (% 24 MP)
140
120
100
80
60
40
20
0
a
b
b
c
MP
MO
MP
MO
24 hpf
36 hpf
B
pax3
Pax3 mRNA (% 24 MP)
300
250
200
150
100
50
0
a
b
a
a
MP
MO
MP
MO
24 hpf
36 hpf
C
pax7
pax7 mRNA (% 24 MP)
600
500
400
300
200
100
0
MP
MO
MP
MO
24 hpf
36 hpf

Figure 7 – Effects of glucocorticoid receptor knockdown on expression of myogenic transcription factors

GR receptor protein knockdown resulted in altered expression of key transcription factors involved in myogenesis at 36 hpf. mRNA abundance of *myod* (A), myogenin (*myog*; B), and myostatin (*mstnb*; C) in 24 hpf and 36 hpf mispair (MP) and morpholino (MO) embryos as measured by qPCR. Values shown are mean ± SEM; bars with different letters are statistically different (n=4 pools of 25 embryos, ANOVA, $p<0.05$).

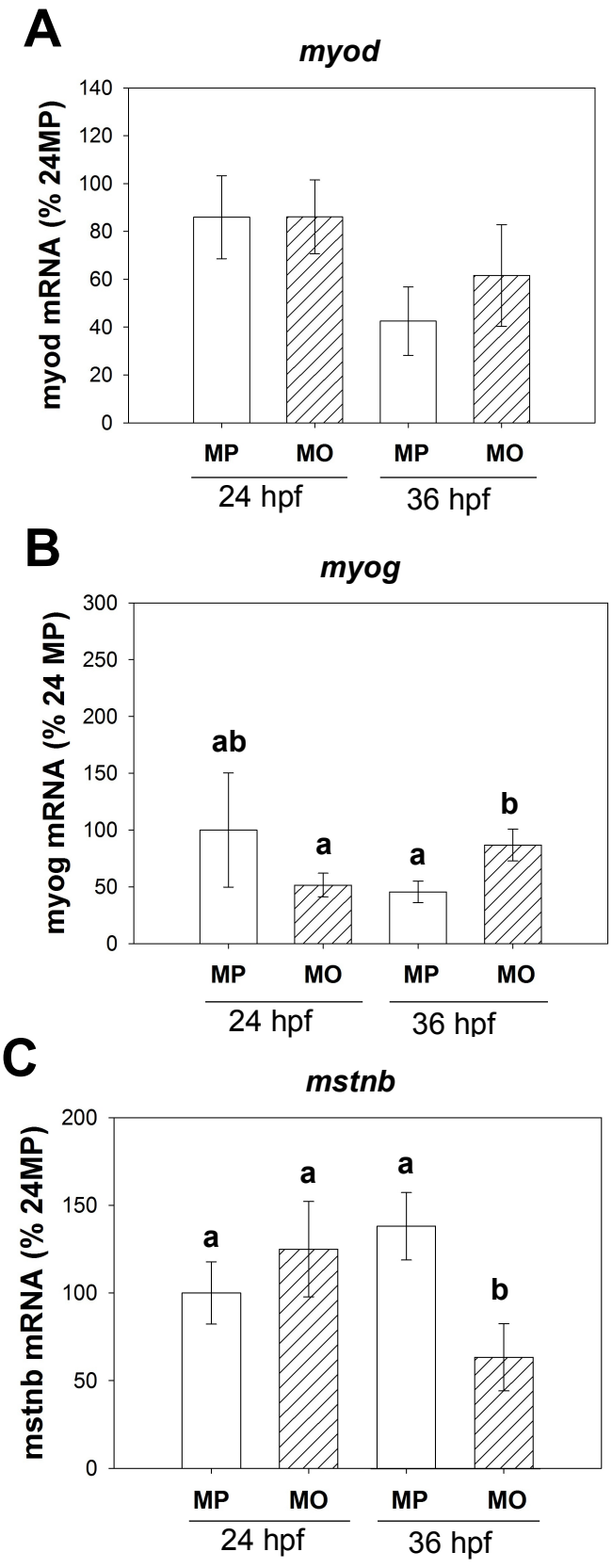
A
myod
myod mRNA (% 24MP)
140
120
100
80
60
40
20
0
MP
MO
MP
MO
24 hpf
36 hpf
B
myog
myog mRNA (% 24 MP)
300
250
200
150
100
50
0
ab
a
a
b
MP
MO
MP
MO
24 hpf
36 hpf
C
mstnb
mstnb mRNA (% 24MP)
200
150
100
50
0
a
a
a
b
MP
MO
MP
MO
24 hpf
36 hpf

Figure 8 – Effects of glucocorticoid receptor knockdown on mRNA abundance of muscle specific proteins

GR morphants exhibited increased mRNA abundance of several muscle-specific proteins. mRNA abundance of slow muscle myosin heavy chain 1 (*smyhc1*; A), fast muscle myosin heavy chain (*myhz2*; B), slow muscle troponin C (*stnnc*; C), and fast muscle troponin I 2a (*tnni2a*; D) in 24 hpf and 36 hpf mispair (MP) and morpholino (MO) embryos as measured by qPCR. Values shown are mean ± SEM; bars with different letters are statistically different (n=4 pools of 25 embryos, ANOVA, $p<0.05$).

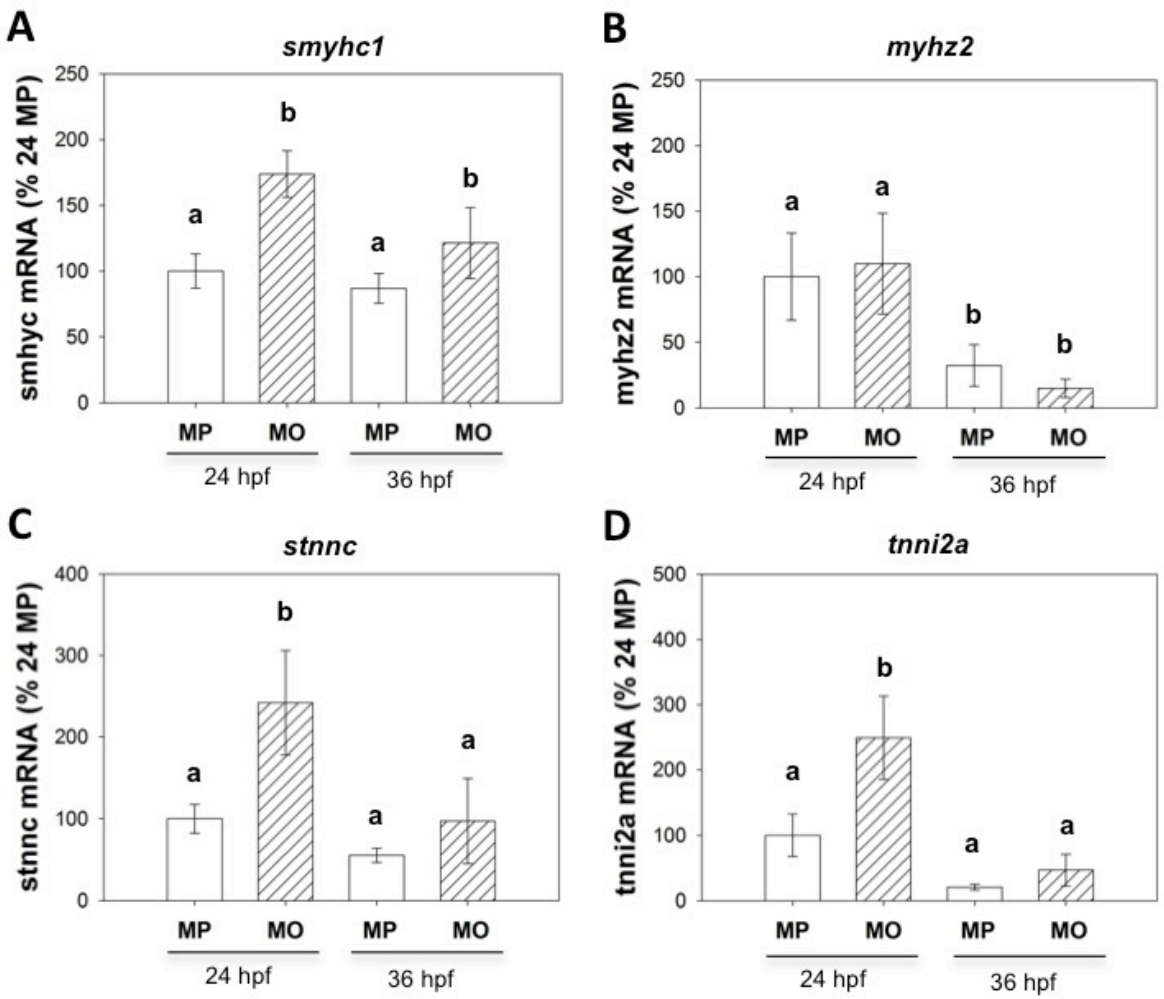
A
smyhc1
smhyc mRNA (% 24 MP)
250
200
150
100
50
0
a
b
a
b
MP
MO
MP
MO
24 hpf
36 hpf
B
myhz2
myhz2 mRNA (% 24 MP)
250
200
150
100
50
0
a
a
b
b
MP
MO
MP
MO
24 hpf
36 hpf
C
stnnc
stnnc mRNA (% 24 MP)
400
300
200
100
0
a
b
a
a
MP
MO
MP
MO
24 hpf
36 hpf
D
tnni2a
tnni2a mRNA (% 24 MP)
500
400
300
200
100
0
a
b
a
a
MP
MO
MP
MO
24 hpf
36 hpf

Figure 9 – GR receptor knockdown and mRNA rescue of disrupted expression of myogenic genes.

Injection of GR mRNA restores the mRNA abundance of key myogenic genes. mRNA abundance of myogenin (*myog*; A) and slow muscle myosin heavy chain (*smyhc1*; B) in mispair (MP), morpholino (MO), RNA-injected (RNA), and RNA and MO co-injected (RNA+MO) 36 hpf embryos. Values shown are mean ± SEM; bars with different letters are statistically different (n=4 pools of 25 embryos, ANOVA, $p<0.05$).

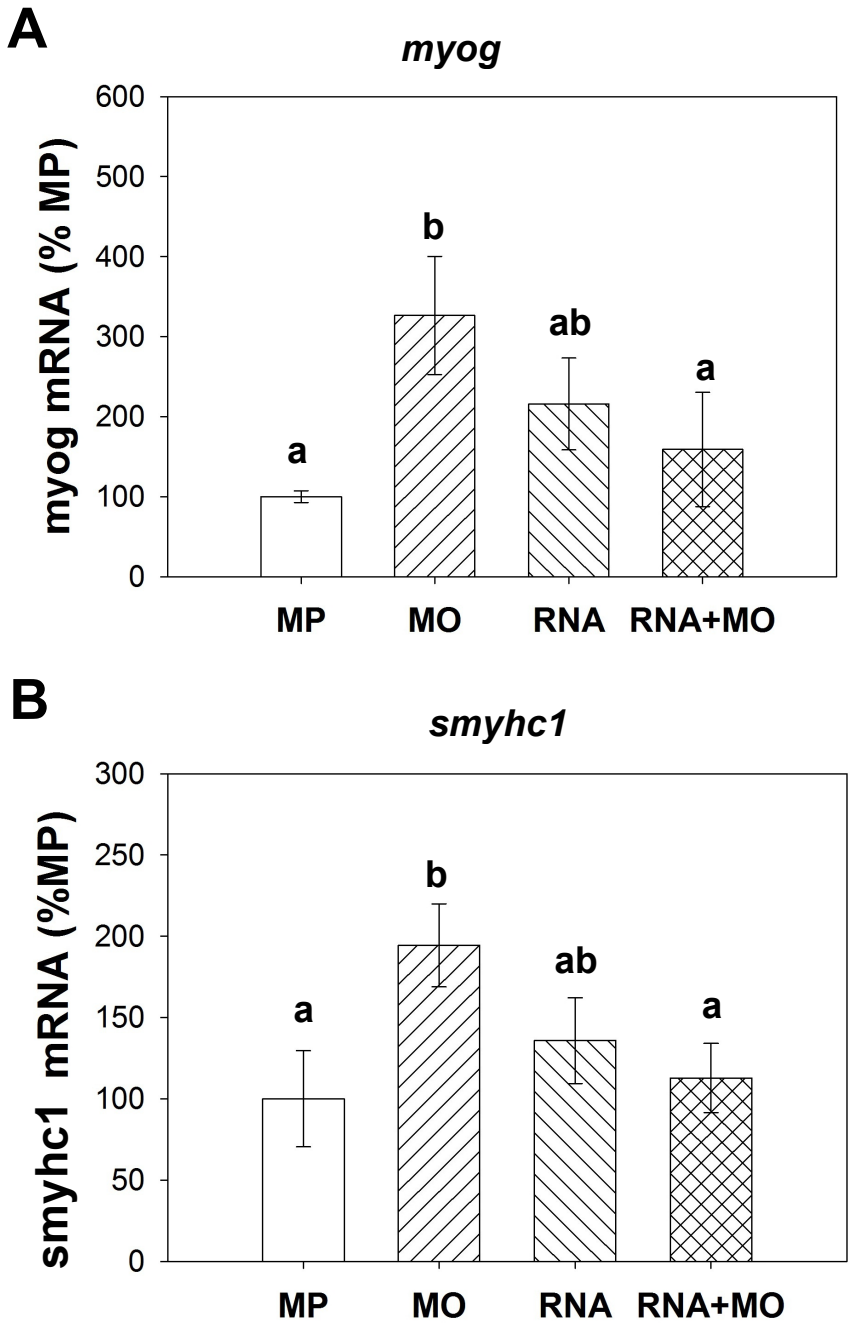
A
myog
myog mRNA (% MP)
600
500
400
300
200
100
0
a
b
ab
a
MP
MO
RNA
RNA+MO
B
smyhc1
smyhc1 mRNA (%MP)
300
250
200
150
100
50
0
a
b
ab
a
MP
MO
RNA
RNA+MO

2.5 Discussion

A novel finding from this study is that GR signaling is playing a key role in mesoderm formation and muscle development in zebrafish. We showed recently that GR gene expression decreases during early embryogenesis in zebrafish (Alsop and Vijayan, 2008; 2009) leading to the proposal that this receptor signaling may be playing a key role in early development. Our results from this study clearly reveal a ubiquitous distribution of maternally derived GR mRNA during the early cleavage stages and is in agreement with a recent study in zebrafish (Pikulkaew et al., 2011). Following the degradation of maternally deposited transcripts, zygotic expression of GR was seen throughout the embryo and GR promoter activation was specifically observed at the somite boundaries, suggesting a role for GR signaling in somite formation. This is further supported by the strong GR gene and protein expression in the somites and developing mesoderm suggesting a morphogenic role for this receptor activation during early development. As cortisol is the primary ligand for GR activation in fish, and this steroid biosynthesis commences only after hatch (Alsop and Vijayan, 2008), we hypothesize that maternal cortisol orchestrates proper mesodermal development and myogenesis in zebrafish.

A role for GR in the developmental regulation of myogenesis was reinforced by our GR knockdown studies that displayed disruptions in somitogenesis and tail deformations. The suppression of GR signaling in the morphant zebrafish was confirmed by the reduced protein expression of this steroid receptor as well as downregulation of *mmp13*, a well established GR-responsive target gene (Hillegass et al., 2007). Our finding is in agreement with a recent study that also showed GR morphants exhibiting abnormal muscle phenotypes in zebrafish (Pikulkaew et al., 2011), suggesting a key role for GR in mesoderm development. The transiently higher expression of GR protein in the tail muscle prior to hatch suggests a key role for GR signaling in early muscle development in zebrafish. Indeed, the 12-36 hpf window prior to hatching, where GR transcripts and protein accumulate throughout the tail, is a critical period in muscle development with muscle cell pioneers being determined from 12 to 24 hpf, and further specification and specialization occurring after 24 hpf (Stickney et al., 2000; Ochi and Westerfield, 2007).

Further support for GR signaling as a key player in the developmental regulation of myogenesis is supported by the changes seen in the expression of important myogenic regulatory factors and muscle-specific genes in GR morphants (Xu et al., 2000; Du et al., 2003; Ochi and Westerfield, 2007). The temporal expression pattern of genes, including myogenin, myostatin, slow myosin heavy chain, fast muscle myosin and slow and fast muscle troponins, suggest time-

specific modulation of molecular events involved in myotomal development by GR signaling. We observed that GR mRNA rescue reversed the changes in expression of myogenin and slow muscle myosin, indicating that these effects are GR-specific, while the mechanisms and downstream regulatory pathways involved remains to be elucidated. Several transcription factors and signaling molecules have been implicated in the developmental regulation of myogenesis (Ochi and Westerfield, 2007), and our results for the first time implicate GR in this process. To this end, IGFs and MyoD are developmentally regulated in zebrafish embryos and critical for cell cycle control and embryo growth (Ochi and Westerfield, 2007; Duan et al., 2010). The absence of any changes in *myod*, *igf1*, and *igf2* expression in GR morphants, despite the presence of two putative GREs upstream of their promoter regions, points to additional control factors involved in the regulation of embryo growth in response to GR signaling.

A key family of morphogens implicated in a variety of developmental processes, including dorsoventral patterning, somitogenesis, mesodermal differentiation, and myogenesis are the BMPs (Reshef et al., 1998; Bubnoff and Cho, 2001; Miyazono et al., 2005; Pyati et al., 2005; Patterson et al., 2010). The suppression of *bmp2a*, *bmp2b*, and *bmp4* prior to hatching in the GR morphant in the present study for the first time underscores a role for GR signaling in the developmental regulation of morphogens in zebrafish. The rescue of morphant phenotype, including the restoration of BMP mRNA abundance, by GR mRNA provides further confirmation that GR signaling modulates developmental expression of BMPs in zebrafish. Furthermore, bioinformatics analysis suggests the presence of putative GRE sites upstream of the BMP genes pointing to a possible direct transcriptional regulation of these morphogens by ligand-activated GR. To our knowledge this is the first study to establish a link between GR signaling and developmental regulation of BMPs in vertebrates, while the mechanism involved remains to be established.

A direct functional role for BMPs in the observed tail deformation and myogenesis in response to GR knockdown was not ascertained in the present study. However, GR morphant phenotype showed morphogenic defects similar to those seen in studies that modulated BMP signaling, including altered somitogenesis (Patterson et al., 2010) and disrupted tail formation (Kishimoto et al., 1997; Pyati et al., 2005; Stickney et al., 2007; Tucker et al., 2008). The mechanisms involved in the developmental regulation of myogenesis by BMPs are not very clear.

For instance, overexpression of BMP increased expression of muscle precursor markers, including *pax3* and *pax7*, and led to a temporal delay in muscle differentiation in zebrafish (Patterson et al., 2010). However, inhibition of BMP signaling did not seem to reverse the effects

seen with overexpression suggesting complex interaction with other myogenic factors in regulating myogenesis (Patterson et al., 2010). The suppression of *eve1*, a BMP-responsive gene involved in mesoderm formation in zebrafish (Seebald and Szeto, 2011), in the GR morphants argues for a role for BMP signaling in orchestrating the mesoderm differentiation associated with GR activation. This was also supported by the reduced expression of *pax3*, but not *pax7*, observed in 24 hpf GR morphants. While the functional significance of these observed gene expressions patterns are not known, we hypothesize that BMPs may be a factor involved in GR-mediated effects on early muscle development and growth. This is increasingly likely given the role played by these morphogens in mesoderm differentiation, including angiogenesis (Tucker et al., 2008; David et al., 2009), myogenesis (Patterson et al., 2010), and organogenesis (Chin et al., 1997; Brand, 2003; Shin et al., 2007; Chung et al., 2008). Consequently, the downregulation of BMPs in the GR morphants may be a key factor leading to embryo mortality seen in GR morphants by 48 hpf. This may include severe disruption of heart function, especially because BMPs have been identified as factors in cardiac cell specification and heart looping (Brand, 2003). This would also account for the increased mortality seen at hatch because prior to that simple diffusion will meet the oxygen demand of the embryos, whereas a functioning heart is critical at hatch (Pelster and Burggren, 1996). We hypothesize that GR is an important developmental regulator, acting upstream of other key developmental factors, including BMPs in zebrafish.

Overall, we have identified GR signaling as a key modulator of mesoderm differentiation and muscle development in zebrafish. The suppression of BMPs and downstream targets involved in myogenesis in the GR morphants leads us to hypothesize that this morphogen is a key player in orchestrating the GR-mediated developmental effects in zebrafish. However, the GR effect on myogenesis may not be limited to just BMP signaling, as several molecular mechanisms are involved in mesoderm formation and muscle development (Ochi and Westerfield, 2007; Chong et al., 2009; Patterson et al., 2010). As cortisol is the primary ligand for GR activation in teleosts (Mommsen et al., 1999), and *de novo* synthesis of this steroid commences only after hatch (Alsop and Vijayan, 2008), we hypothesize that maternal cortisol *via* GR signaling orchestrates the developmental programming of mesoderm differentiation and muscle development. We posit that GR is a key transcription factor acting upstream of multiple important pathways essential for embryogenesis, including BMPs and muscle regulatory transcription factors and muscle-specific proteins. Consequently, any abnormalities in GR signaling, including abnormal cortisol deposition or exposure during this critical developmental window prior to *de novo* cortisol biosynthesis may lead to long-term growth defects, including reduced survival.

2.6 Acknowledgements

This study was supported by the Natural Sciences and Engineering Research Council of Canada discovery grant to MM Vijayan.

Chapter 3

Embryo exposure to elevated cortisol level leads to cardiac performance dysfunction in zebrafish

3.1 Overview

In zebrafish (*Danio rerio*), *de novo* cortisol synthesis commences only after hatching, providing an interesting model to study the effects of maternal stress and abnormal cortisol deposition on embryo development and performance. We hypothesized that elevated cortisol levels during pre-hatch embryogenesis compromise cardiac performance in developing zebrafish. Cortisol was microinjected into one-cell embryos to elevate basal cortisol levels during embryogenesis. Elevated embryo cortisol content increased heart deformities, including pericardial edema and malformed chambers, and lowered resting heartbeat post-hatch. This phenotype coincided with suppression of key cardiac genes, including *nkx2.5,* cardiac myosin light chain 1, cardiac troponin type T2A*,* and calcium transporting ATPase, underpinning a mechanistic link to heart malformation. The attenuation of the heartbeat response to a secondary stressor post-hatch also confirms a functional reduction in cardiac performance. Altogether, high cortisol content during embryogenesis, mimicking increased deposition due to maternal stress, decreases cardiac performance and may reduce zebrafish offspring survival.

3.2 Introduction

Cortisol is the primary circulating corticosteroid in teleosts and it is produced by the steroidogenic cells distributed predominantly around the post-cardinal veins (interrenal tissue) in the head kidney region (Wendelaar Bonga, 1997). A key stimulus for this steroid release is the activation of the hypothalamus-pituitary axis, culminating in the release of adrenocorticotrophic hormone (ACTH) from the pituitary. ACTH binding to its target receptor, the melanocortin 2 receptor (MC2R), activates corticosteroid biosynthesis, leading to elevated circulating levels of this steroid in response to stress (Aluru and Vijayan, 2008; Hontela and Vijayan, 2009). Cortisol has wide-ranging effects on animal physiology and a major role that is evolutionarily conserved is the metabolic adjustments to restore homeostasis in the face of stressor insult (Wendelaar Bonga, 1997; Mommsen et al., 1999). Glucocorticoid effects are mediated via glucocorticoid receptor (GR) and/or mineralocorticoid receptor (MR) activation (Sapolsky et al., 2000), and teleosts express multiple paralogs of these receptors (Bury et al., 2003; Prunet et al., 2006). While the role of MR in cortisol signaling is not very clear in fish, GR signaling is involved in all aspects of animal physiology, including ion regulation, metabolism, immune function and reproduction (Mommsen et al., 1999; Aluru and Vijayan, 2009). The majority of these studies have been carried out in juvenile fish and cell system models, resulting in a paucity of information on the developmental regulation of cortisol in fish. Recent studies using GR gene knockdown with morpholino oligonucleotides points to a key role for signaling by this receptor in zebrafish (*Danio*

rerio) early developmental events, including mesoderm formation (Pikulkaew et al., 2011; Nesan et al., 2012 [Chapter 2]).

In zebrafish, cortisol content during early embryogenesis is of maternal origin as *de novo* synthesis of this steroid commences only after hatch (Alsop and Vijayan, 2008). Also, the ability to increase cortisol levels in response to stress is not active until 3-4 days post fertilization (dpf), as the embryo approaches first feeding (Alsop and Vijayan, 2008; Alderman and Bernier, 2009). Consequently, there is a temporal decrease in maternally deposited cortisol content in the embryos up until hatch in zebrafish (Alsop and Vijayan, 2008). This is also true for other fish species studied, including rainbow trout (*Oncorhynchus mykiss*; [Barry et al., 1995; Auperin and Geslin, 2008]) and common carp (*Cyprinus carpio*; [Stouthart et al., 1998]), leading to the hypothesis that a corticosteroid hyporesponsive period is essential for early development in fish. Indeed, studies have shown that elevated prenatal glucocorticoid exposure disrupts growth and development in animal models (Breuner et al., 2008; Seckl and Meaney, 2004; Kapoor, 2006), including fish (Eriksen et al., 2006), but a clear mechanistic link is missing.

During zebrafish development, the 24 to 48 hours post fertilization (hpf) window is a key period for organogenesis, including heart formation and angiogenesis (Thisse and Zon, 2002; Kimmel et al., 1995). It is also during this time that embryo cortisol content is at its lowest (Alsop & Vijayan, 2008). During this period of cardiac myogenesis there is a marked regulation of structural and functional cardiac muscle proteins, including myosin chains, troponins, and ion transporters (Yelon, 2001; Chen et al., 2008; Hsiao et al., 2003; Ebert et al., 2005). Also, the key cardiac transcription factor, *nkx2.5*, is expressed during this period and it is essential for heart development (Chen and Fishman, 1996) and cardiovascular performance at hatch (Yelon, 2001). Our recent investigation on the role of GR signaling in early embryogenesis indicated a link between GR activation and modulation of bone morphogenetic proteins (BMPs) expression in zebrafish (Nesan et al., 2012 [Chapter 2]). BMPs are key morphogens regulating the expression of genes involved in organogenesis, including heart development (Chin et al., 1997; Chen et al., 1997), providing a potential link between GR-mediated cortisol signaling and cardiac morphogenesis. There have been studies linking cortisol to abnormal heart development and cardiac gene expression in fetal sheep (Lumbers et al., 2005; Reini et al., 2008) and to cardiac hypertrophy in adult salmon (Johansen et al., 2011). However, few studies have examined the role of cortisol in the developmental regulation of cardiac function in fish.

Against this background, we tested the hypothesis that elevated cortisol levels in the embryos, mimicking increased transfer of this steroid from mothers in stressed environments,

may disrupt cardiac development and performance after hatching in zebrafish. The optically transparent zebrafish embryo provides the opportunity to observe cardiac development directly, and zebrafish express only a single GR gene with two splice variants, an unusual characteristic for teleosts, but interestingly similar to humans (Alsop and Vijayan, 2008; Schaaf et al., 2008). Additionally, zebrafish embryos can survive without a functional heart until 4-5 dpf (Pelster and Burggren, 1996), allowing for investigation on heart development and malformations without compromising embryo viability. Taken together, zebrafish is a well-established model for developmental, endocrine, and cardiac research (Chico et al., 2008; Lohr and Hammerschmidt, 2011), providing a uniquely suited test organism for biomedical research on maternal stress effects on development.

We microinjected cortisol into one-cell zebrafish embryos resulting in elevated levels of this steroid compared to the wild-type embryo during pre-hatch embryogenesis. We monitored embryo cortisol content, glucocorticoid receptor gene and protein expressions, and confirmed enhanced GR signaling from cortisol treatment by measuring transcript abundance of a known glucocorticoid-responsive gene (matrix metalloproteinase-13 [*mmp13*]; Hillegass et al., 2007). Cardiac morphogenesis was examined by microscopic observation, as well as by analyzing the transcript abundance of genes encoding key proteins in cardiac development, including *nkx2.5*, cardiac myosin light chain 1 (*cmlc1*), cardiac troponin type T2A (*tnnt2a*), and calcium transporting ATPase (*atp2a2a*). Cardiac performance was assessed by measuring heartbeat at rest and after an acute stressor challenge at 72 hpf.

3.3 Materials and Methods

3.3.1 Zebrafish care

Care and breeding of adult zebrafish and rearing of embryos were performed exactly as described previously (Nesan et al., 2012 [Chapter 2]). Wild-type adult zebrafish were purchased from a commercial source (Big Al's Aquarium Services, Kitchener, ON). The zebrafish care protocol was approved by the animal care committee at the University of Waterloo, and is in accordance with the Canadian Council for Animal Care guidelines.

3.3.2 Cortisol injection

Cortisol (Hydrocortisone; Sigma, St. Louis, MO) stocks were prepared by first diluting in ethanol, then evaporating off the ethanol and reconstituting in sterile water. The final concentrations of the steroid used for embryo injection were 0, 8, 16, and 32 pg/nL. The vehicle for control injections

was prepared exactly the same but without cortisol. Initial trials were performed with each concentration and pools of 25 embryos were frozen at 12, 24, 36, and 48 hpf for measurement of cortisol content. Our preliminary experiment showed that only 32 pg/nL concentration cortisol was able to consistently maintain elevated cortisol content above basal levels compared to control embryos during the early developmental period prior to hatch. Consequently, all experiments were carried out only with this concentration of cortisol. Briefly, one-cell stage embryos were microinjected with 1 nL (~0.5% of total embryo volume) of either vehicle (sterile water) or vehicle containing cortisol (32 pg/nL) using a nitrogen-powered microinjector (Narishige, East Meadow, NY). Embryos were observed at 24, 36, and 48 hpf using an AZ100 microscope and images captured with a DS-Ri1 camera (Nikon, Melville, NY). Embryos (20-25 per sample with a sample size of 3-6 per treatment) were frozen at various time-points for measuring cortisol content and also for molecular and protein analyses.

3.3.3 Embryo morphology

After cortisol injection, embryos were reared until 48 hpf, at which point they were examined and classified into one of four groupings according to the severity of their morphological deformations: “unaffected” - indistinguishable from wild-type; “mild” – visible pericardial edema only; “moderate” - embryos displayed more prominent pericardial edema and visibly malformed heart structures (such as distension or ballooning of the heart chambers); “severe” - embryos showed a ruptured pericardia with no visible/functioning heart structures and mildly deformed curvature. Cortisol-injected embryos did not show a significant increase in mortality during embryogenesis.

3.3.4 Cardiac performance

Control and cortisol-injected larvae were subjected to a standardized physical stressor at 72 hpf, which is the earliest point at which an activated stress response has been shown in zebrafish (Alsop and Vijayan, 2008; Alderman and Bernier, 2009). Only embryos exhibiting the “mild” or “unaffected” cardiac phenotypes were selected for the performance test as the extreme phenotypes displayed irregular heartbeats that were difficult to visualize and quantify. Also, we were interested in assessing whether cortisol effects were evident even in embryos with no visible malformation of cardiac phenotypes. The stressor exposure consisted of placing 100 larvae in a beaker with 80 mL of embryo medium (Westerfield, 2003) and swirling them with a pipette once every second for 60 s. The embryos were maintained at 28.5ºC in an incubator (Fisher Scientific, Ottawa, ON) over the course of the stressor exposure and post-stressor recovery period. After

swirling, individual embryos were transferred to 35mm petri dishes (Fisher Scientific, Ottawa, ON) in embryo medium for heartbeat assessment and maintained in the incubator for the post-stressor period. The heart rates (beats per minute; bpm) of the embryos were counted by viewing under the Nikon AZ100 microscope prior to stressor exposure and at 5, 30, and 60 min post-stressor. The petri dish with a single embryo was removed from the incubator only for the duration of the heartbeat assessment (60s).

3.3.5 Cortisol ELISA

Embryo cortisol concentrations were measured with a commercially available ELISA (Neogen Corp., Lexington, KY) according to the manufacturer's protocol exactly as described previously (Gonçalves et al., 2012).

3.3.6 Gene expression

RNA was extracted and quantified from pools of 48 hpf control and cortisol-injected embryos as described previously (Nesan et al., 2012 [Chapter 2]). 1 µg of RNA was reverse-transcribed with the High Capacity cDNA Reverse Transcription Kit (Applied Biosystems, Carlsbad, CA) to produce a 20 µL mixture according to the manufacturer's protocols.

Real-time quantitative PCR (qPCR) was used to assess gene expression in 36 and 48 hpf control and cortisol-injected embryos. The following genes were measured: *gr*, *mmp13*, *nkx2.5*, *cmlc1*, *tnnt2a*, and *atp2a2a*, and *β-actin*. Primer pair sequences, melting temperatures, and amplicon sizes are included in Table 1. Primer pairs for *gr*, *mmp13*, and*β-actin* have been described and characterized previously (Nesan et al., 2012 [Chapter 2]). Primer pairs for the remaining genes were designed from GenBank sequences: CU019640 (*nkx2.5*); AL845516 (*cmlc1*); AL662880 (*tnnt2a*); CR407563 (*atp2a2a*). qPCR analysis was run in triplicate on an iCycler iQ thermocycler using iQ SYBR Green supermix (BioRad, Hercules, CA) and gene expression was calculated exactly as described previously (Nesan et al., 2012 [Chapter 2]), using *β-actin* as the housekeeping gene (levels of this transcript were consistent across samples).

Table 1: Primers used for qPCR and their amplicon size and melting temperatures (Tm).

Gene	Forward Primer (5'-3')	Reverse Primer (5'-3')	Amplicon Size (bp)	Tm (^{o}C)
atp2a2a	GCAGGTTAGAGCCGTTTCTG	CTGTGCCTTGTGCAATGACT	94	56
cmlc1	CTCCACACTGGGCATACCTT	CTGCACCAGTTCCAGAGACA	159	56
gr	ACAGCTTCTTCCAGCCTCAG	CCGGTGTTCTCCTGTTTGAT	116	60
mmp13	ATGGTGCAAGGCTATCCCAAGAGT	GCCTGTTGTTGGAGCCAAACTCAA	289	60
nkx2.5	TCCCAGCCAAACCATATCTC	GCATCAGAGCTTGGTGAACA	124	55
tnnt2a	CATCCAGCTCCACAATTCCT	GGCGGTTACATGCAAAAGAT	159	56

3.3.7 Protein expression

Pools of 36 and 48 hpf control and cortisol-injected embryos were processed for measurement of protein expression by immunoblotting. Total protein concentration was determined by the bicinchoninic acid method with bovine serum albumin (Sigma, St. Louis, MO) as the standard and 25 μg was loaded onto 8% SDS-PAGE gels for electrophoresis as described previously (Nesan et al., 2012). The GR protein was immunodetected with a polyclonal rabbit anti-zebrafish GR antibody exactly as previously described (Nesan et al., 2012 [Chapter 2]).

3.3.8 Statistical analysis

All data are presented as mean ± standard error of the mean (SEM). Data comparisons for multiple time-points and treatments utilized two-way analysis of variance (ANOVA), while Student's t-test was used for two sample comparisons. Significant interactions with two-way ANOVA were further analyzed using one-way ANOVA for temporal differences (within treatment groups) and Student's t-test for treatment differences at each time point. A Bonferroni *post-hoc* test was used to determine significance for multiple comparisons. All data were normally distributed without need for transformation. All statistical analyses were carried out with the Sigmastat software package (Systat Software, Chicago, IL). A probability value of $p<0.05$ was considered significant.

3.4 Results

3.4.1 Cortisol levels

Cortisol content in newly fertilized embryos was approximately 3.6 pg and this level was significantly reduced at 12 (2.7 pg), 24 (2.0 pg) and 36 hpf (2.2 pg) (Fig. 1). After hatch, embryo cortisol content increased at 48 hpf (3.8 pg) to levels similar to that seen in the newly fertilized embryo but was significantly higher at 72 hpf (Fig. 1). Embryos injected with 32 pg cortisol per embryo displayed elevated steroid content above control embryos at all time points, and did not display the temporal decrease at 12 (3.5 pg), 24 (3.7 pg) and 36 hpf (3.8 pg) that was observed in the control group. The post-hatch cortisol content in the cortisol-injected embryo was significantly higher at 48 and 72 hpf (6.3 pg) compared to the pre-hatch values as well as with the control group (Fig. 1).

Figure 1 – Whole body cortisol content.

One-cell stage embryos were microinjected with either water (control) or cortisol (32 pg/embryo) and sampled at 12, 24, 36, 48 and 72 hpf. 0 hpf measurement was prior to microinjection. All values shown are mean ± standard error of mean [SEM; n=4 pools of 25 embryos]; different letters indicate significant time effects within each treatment group, while the lower and uppercase denotes significant treatment effects (two-way ANOVA, $p<0.05$).

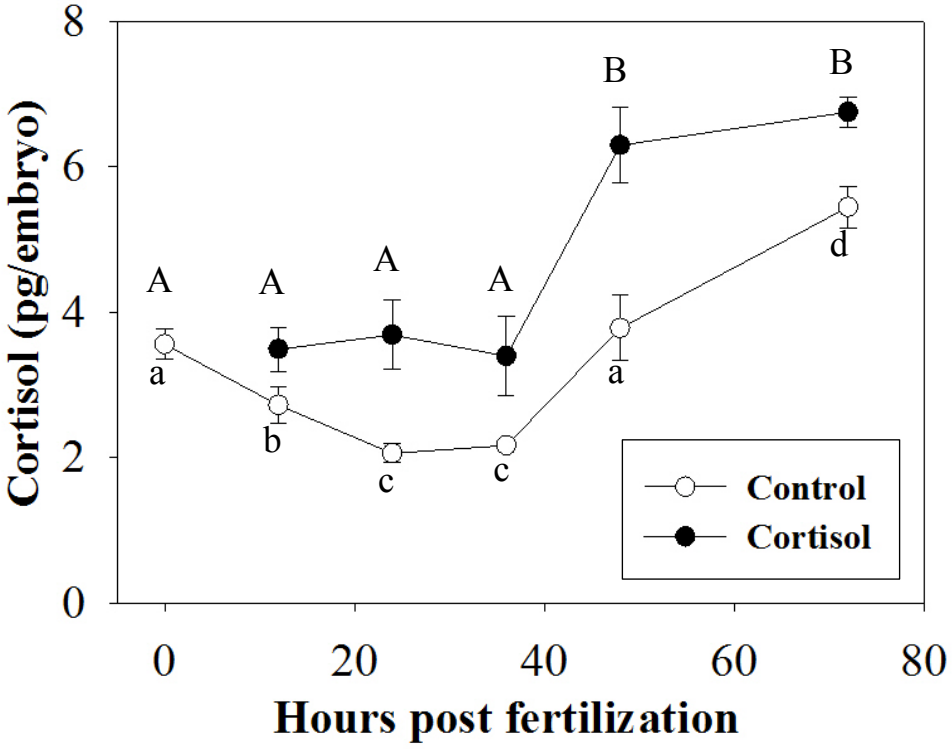
Cortisol (pg/embryo)
Hours post fertilization
0
2
4
6
8
0
20
40
60
80
A
A
A
A
B
B
a
b
c
c
a
d
Control
Cortisol

3.4.2 GR expression and signaling

There was no significant change in GR mRNA abundance (Fig. 2A) or protein expression (Fig. 2B) at 36 or 48 hpf in the cortisol-injected group compared to the control group (Fig. 2A). There was a temporal reduction in GR protein expression (~70%) in both groups at 48 hpf relative to 36 hpf (Fig. 2B). To assess GR signaling we quantified *mmp13*, and the mRNA abundance of this gene was significantly higher in cortisol-injected embryos at both 36 hpf (26 fold increase) and 48 hpf (21 fold increase) compared to controls (Fig. 2C).

Figure 2 – Glucocorticoid receptor (GR) and glucocorticoid responsive gene expressions
One-cell stage embryos were microinjected with either water (control) or cortisol (32 pg/embryo) and sampled at 36 and 48 hpf to measure GR mRNA abundance (A), GR protein expression (B) and *mmp13*, a glucocorticoid responsive gene, mRNA abundance (C). Data is expressed as percentage 36 hpf control. All values shown are mean ± standard error of mean [SEM; n=4-6 pools of 20 embryos for transcripts (A and B) and n=4 pools of 25 embryos for protein (C)]; different letters indicate significant difference (two-way ANOVA, $p<0.05$).

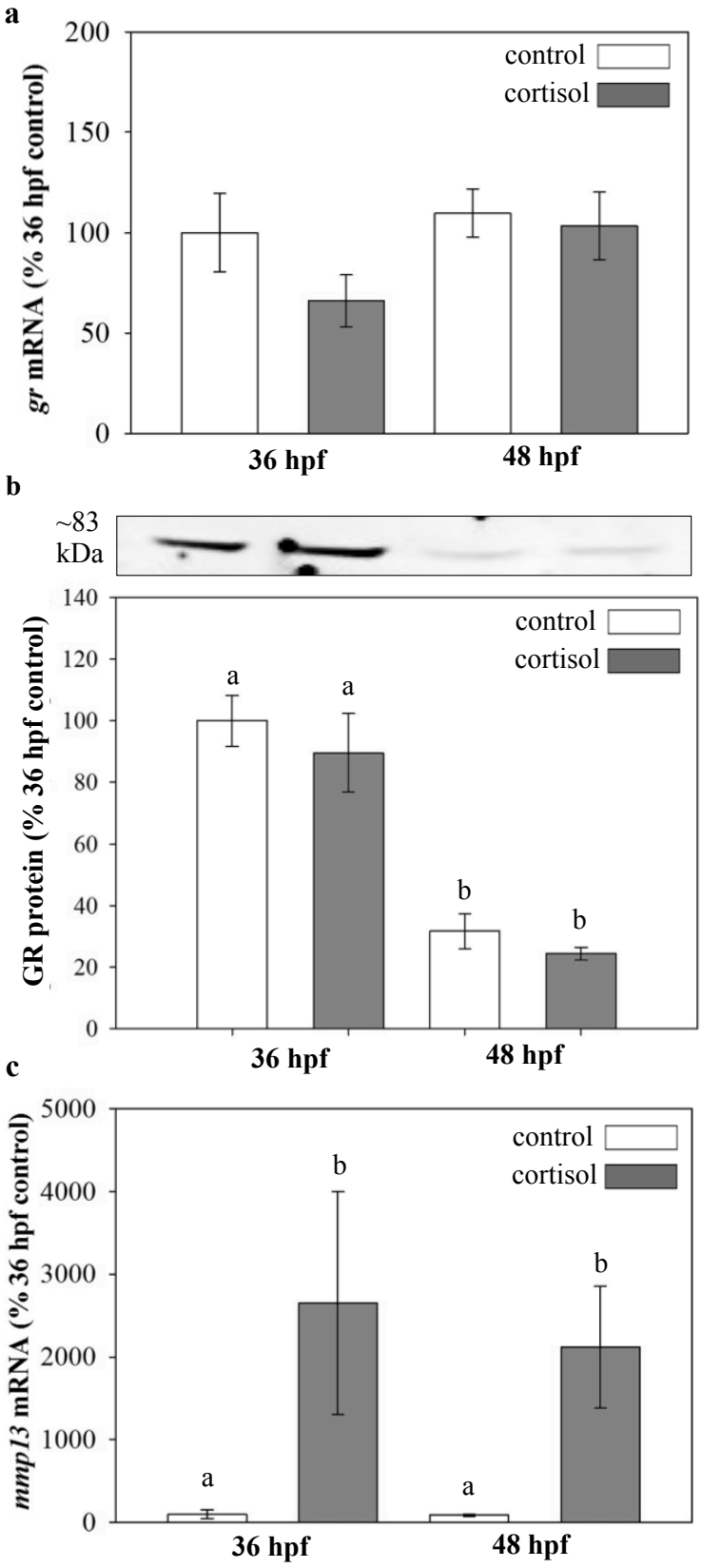
a
200
150
100
50
0
gr mRNA (% 36 hpf control)
control
cortisol
36 hpf
48 hpf
b
~83
kDa
140
120
100
80
60
40
20
0
GR protein (% 36 hpf control)
control
cortisol
a
a
b
b
36 hpf
48 hpf
c
5000
4000
3000
2000
1000
0
mmp13 mRNA (% 36 hpf control)
control
cortisol
a
b
a
b
36 hpf
48 hpf

3.4.3 Cardiac morphogenesis

97% of control embryos were indistinguishable from wild-type embryos throughout development. Injection of 32 pg cortisol/embryo resulted in a range of cardiac phenotypes (Fig. 3). Nearly 51% of embryos treated with cortisol were similar to the control phenotype and were classified as "unaffected" (Fig. 3, first row), while 31% showed a "mild" phenotype (Fig. 3, second row) characterized by pericardial edema, 14% showed a "moderate" phenotype (Fig. 3, third row) consisting of pericardial edema and visibly deformed heart structure (distended or ballooned heart chambers) and 5% were "severe" phenotype (Fig. 3, fourth row) categorized by ruptured pericardia and no visible heartbeat.

Figure 3 – Heart deformity phenotypes

One-cell stage embryos were microinjected with either water (control) or cortisol (32 pg/embryo) and imaged at 48 hpf for morphological deformities. Unaffected embryos (first row) were indistinguishable from wild-type embryos. Mild embryos (second row) displayed pericardial edema only (see arrow); moderate embryos (third row) displayed pericardial edema and malformed heart structures (see arrows); severe embryos (fourth row) exhibited a ruptured pericardium (see arrows) and no heartbeat was ever visible. Percent phenotype from multiple trials are shown as mean ± standard error of mean (SEM) (control: n=16 trials of 37-120 embryos; cortisol: n=14 trials of 53-184 embryos); N.D. - not detectable; * indicates significant difference (Student's t-test, $p<0.05$).

	whole embryo	heart (magnified)	% of control embryos	% of cortisol embryos
unaffected			97 ± 0.4	* 50 ± 1.2
mild			3 ± 0.3	* 31 ± 0.8
moderate		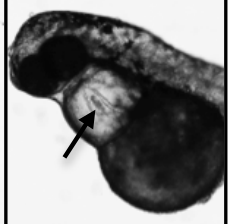	N.D.	* 14 ± 0.6
severe		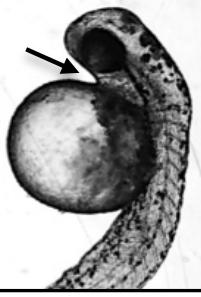	N.D.	* 5 ± 0.7

3.4.4 Marker genes for cardiac development

The observed cardiac deformations were also reflected in disrupted expression of key cardiac genes (Fig. 4). The mRNA abundance of the cardiac transcription factor *nkx2.5* was significantly lower in the cortisol group at 36 hpf (61%) and 48 hpf (72%) compared to the control group (Fig. 4A). Transcription of specific cardiac muscle genes was also suppressed in cortisol-injected embryos relative to control embryos. The mRNA abundances of cardiac myosin light chain 1 (*cmlc1*; Fig. 4B) and cardiac troponin type T2a (*tnnt2a*; Fig. 4C) was significantly reduced at 48 hpf (73% and 66%, respectively), but not at 36 hpf compared to the control group. Also, the mRNA abundance of a cardiac muscle calcium transporter ATPase (*atp2a2a*; Fig. 4D) was significantly lower in the cortisol-injected embryos at both 36 (61%) and 48 hpf (49%) compared to the control embryos.

Figure 4 – mRNA abundance of cardiac genes

One-cell stage embryos were microinjected with either water (control) or cortisol (32 pg/embryo) and sampled at 36 and 48 hpf to quantify the mRNA abundance of *nkx2.5* (A), *cmlc1* (B), *tnnt2a* (C), and *atp2a2a* (D) by qPCR. Data is expressed as percentage 36 hpf control. All values shown are mean ± standard error of mean [SEM; n=4-6 pools of 25 embryos]; different letters indicate significant difference (two-way ANOVA, $p<0.05$).

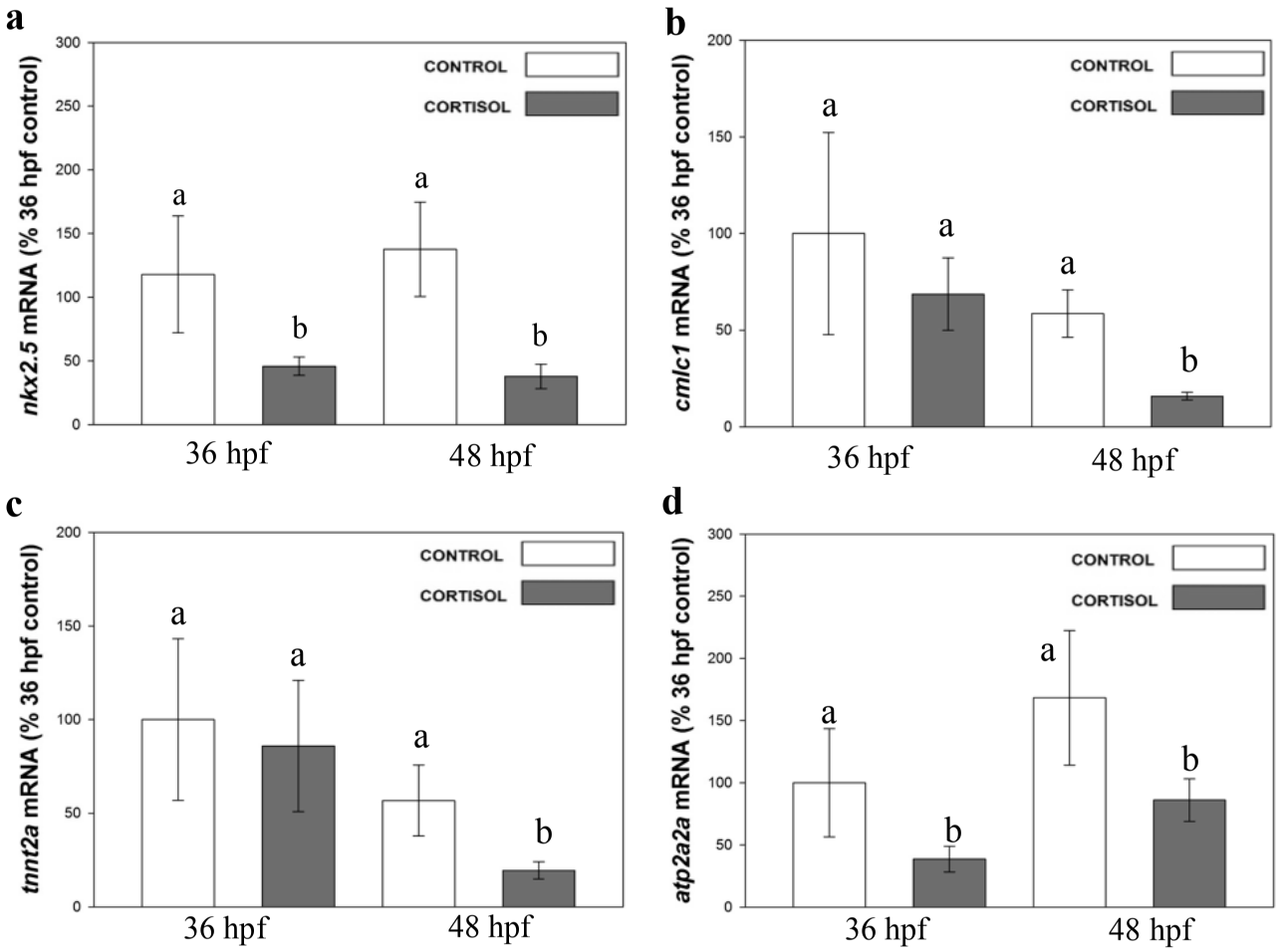
a
nkx2.5 mRNA (% 36 hpf control)
CONTROL
CORTISOL
a
b
a
b
36 hpf
48 hpf
b
cmlc1 mRNA (% 36 hpf control)
a
a
a
b
tnnt2a mRNA (% 36 hpf control)
a
a
a
b
d
atp2a2a mRNA (% 36 hpf control)
a
b
a
b

3.4.5 Cardiac performance

At 72 hpf, control embryos had a heart rate of 160 beats per minute (bpm) (Fig. 5), while embryos injected with 32 pg of cortisol displayed a significantly reduced resting heart rate (149 bpm) (Fig. 5). Subjecting these embryos to an acute physical stressor significantly elevated the control embryo heart rate to 197 bpm by 5 min, after which the rate dropped to 173 bpm at 30 min and was back to the resting levels at 60 min post-stressor exposure (Fig. 5). The cortisol-injected embryos also displayed a transient increase in heart rate in response to stressor exposure, but the magnitude of response was significantly lower than the control group at 5 min (171 bpm), 30 min (157 bpm), and 60 min (151 bpm) post-stressor exposure (Fig. 5).

Figure 5 – Cardiac performance

One-cell stage embryos were microinjected with either water (control) or cortisol (32 pg/embryo) and the heartbeat rate of the larva was measured at 72 hpf either at rest (0 time) or 5, 30, and 60 minutes after an acute stressor exposure. Embryos injected with 32 pg of cortisol at fertilization displayed a disrupted heart rate response to a stressor at 72 hpf. All values shown are mean ± standard error of mean [SEM; n=13-17 embryos, post-stress heart rates were repeated measures]; different letters indicate significant time effects within each treatment group, while the lower and uppercase denotes significant treatment effects (two-way ANOVA, $p<0.05$).

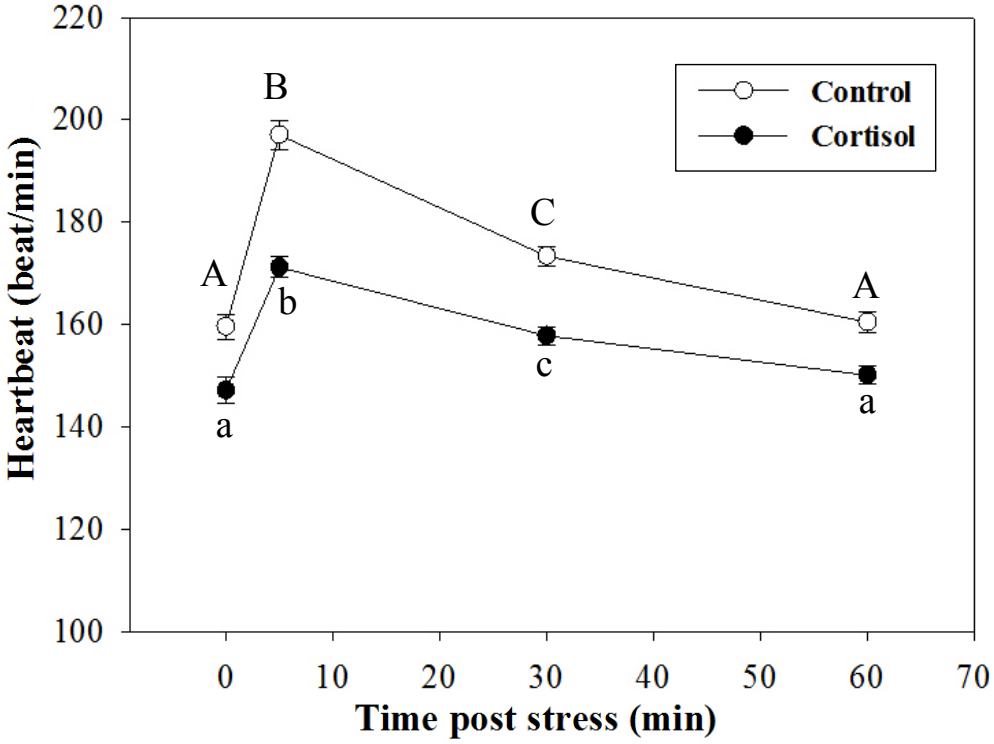
Heartbeat (beat/min)
220
200
180
160
140
120
100
0
10
20
30
40
50
60
70
Time post stress (min)
Control
Cortisol
A
B
C
A
a
b
c
a

3.5 Discussion

The novel finding from this study is that high glucocorticoid exposure during early embryogenesis reduces cardiac performance in zebrafish. Studies have shown that maternal stress and the associated excess prenatal corticosteroid exposure leads to developmental abnormalities in the progeny of vertebrates (Seckl and Meaney, 2004; Eriksen et al., 2006; Kapoor, 2006; Breuner et al., 2008), but there is no clear understanding of the specific pathways that are impacted. Here we demonstrate for the first time that embryonic exposure to elevated cortisol levels involves suppression of genes critical for cardiac morphogenesis in zebrafish, establishing a mechanistic link between maternal stress and compromised fish performance.

Maternal transfer of cortisol to oocytes is well established in the piscine model and recent studies highlight a key role for this steroid deposition in the maternal programming of zebrafish development (Pikulkaew et al., 2011; Nesan et al., 2012 [Chapter 2]). This is because knocking down of glucocorticoid receptor, a key molecule activating cortisol signaling, led to developmental abnormalities and mortality in zebrafish embryos (Pikulkaew et al., 2011; Nesan et al., 2012 [Chapter 2]). However, little is known about post-hatch performance phenotype of embryos exposed to high levels of cortisol during the critical developmental window prior to hatching. Recent studies suggest that maternal stress affects egg characteristics and larval development (McCormick and Nechaev, 2002; Eriksen et al., 2006; Giesing et al., 2011), but this is not consistent among all species (Stratholt et al., 1997) and a clear understanding of how elevated cortisol levels bring about these developmental abnormalities is lacking. In zebrafish and other teleosts, the deposited maternal cortisol levels decrease over time up until hatching after which the *de novo* synthesis of the steroid commences (Alsop and Vijayan, 2008, 2009). This was also confirmed in the present study as cortisol exposure levels dropped during embryogenesis prior to hatching and increased strongly afterwards. Maintaining low cortisol levels during this critical early developmental window is thought to be essential for proper maternal programming of developmental events (Barry et al., 1995; Stouthart et al., 1998; Alsop and Vijayan, 2008; Auperin and Geslin, 2008; Alderman and Bernier, 2009).

We tested this by elevating embryo cortisol levels above basal levels throughout embryogenesis by microinjection of 32 pg of cortisol into the zygote. The temporal changes seen in GR expression during development support our earlier study (Nesan et al., 2012 [Chapter 2]) while prehatch embryo exposure to elevated cortisol levels did not modulate GR expression. However, the upregulation of *mmp13* in the cortisol group confirms enhanced GR activation, as this transcript is glucocorticoid responsive in zebrafish embryos (Hillegass et al., 2007). The

increased early embryonic cortisol stimulation led to clear cardiac phenotypes, including higher incidences of edema, malformed heart chambers, and pericardial rupture. To our knowledge, this is the first study to demonstrate cardiovascular defects in response to embryo exposure to elevated corticosteroid in any animal model. Mammalian studies have suggested cardiovascular dysfunction, including chronic hypertension, due to elevated prenatal glucocorticoids (Seckl and Meaney, 2004). In zebrafish, maternal stressors have been linked with reduced oocyte formation and larval viability (Orn et al., 1998; Carfagnini et al., 2009), but this was not linked to any changes in embryo cortisol content. Our results suggest that increased cortisol deposition and the associated impact on cardiac morphogenesis may be playing a role in this reduced larval viability.

During cardiac development in zebrafish, cardiomyocyte progenitors arise from the lateral plate mesoderm, migrate towards the midline and fuse to form the heart tube, which becomes subdivided into the atrium and the ventricle (Glickman and Yelon, 2002). This process begins post-epiboly and is complete within 24 hpf, as the heart begins to beat sporadically. Involved in this differentiation and fusion process are a number of cardiac transcription factors whose effects are complex and interrelated, including *nkx2.5*, *bmp2b*, and other co-factors (Yelon, 2001). As cardiac tissue develops, cardiac structural genes are upregulated, including myosin chains, troponins, and ion transporters. By 36 hpf, the heart tube begins to bend, positioning the atrium adjacent to the ventricle, and further development of the heart tissue (thickening of the walls, valve development) occurs over the next 12-36 hpf (Glickman and Yelon, 2002). Oxygen delivery via the circulatory system is not critical for embryo survival until 4-5 dpf, as tissue diffusion is sufficient until then (Pelster and Burggren, 1996), but it has been hypothesized that a functional heartbeat and pulsatile blood flow may aid in cardiac tissue maturation and/or angiogenesis (Burggren, 2004). Our results underscore a role for elevated cortisol levels during early embryogenesis in disrupting this developmental regulation of cardiac morphogenesis in zebrafish. The mechanism behind these observed deformations requires further study; however, we have identified some key genes involved in cardiovascular development that are downregulated in cortisol-injected embryos. The cardiac transcription factor *nkx2.5*, which is involved in heart field definition and myofibril development (Chen and Fishman, 1996; Sultana et al., 2008), is suppressed at both 36 and 48 hpf. Knockdown of *nkx2.5* has been shown to cause a variety of cardiac defects in heart chamber formation as well as pericardial edema (Targoff et al., 2008), similar to the phenotype observed in our cortisol-injected embryos. Also, downregulation of *cmlc1* and *tnnt2a* expressions were reported in mutants that display reduced cardiomyocyte differentiation and reduction in *nkx2.5* expression (Reiter et al., 1999; Yelon, 2001), suggesting a role for these transcripts in the disrupted cardiac morphogenesis in response to elevated

embryonic cortisol exposure. The calcium transporter *atp2a2a*, also known as SERCA2, is a key cardiac gene that is essential for contraction (Ebert et al., 2005). Transcript abundance of *atp2a2a* was suppressed in cortisol-injected embryos, and its depletion reduces the heart rate in zebrafish embryos by slowing the restoration of calcium ions in the sarcoplasmic reticulum between contractions (Ebert et al., 2005).

The reduced transcript abundances of these critical genes provide a potential mechanism for the heart defects and the reduced heartbeat observed in larvae exposed to higher cortisol during prehatch embryogenesis. Post-hatch cortisol-injected embryos also exhibited a clear performance dysfunction, displaying an impaired ability to increase heart rate in response to an acute stressor relative to control embryos. Increased heart rate is a well-characterized response to an acute stressor and an essential part of the fight-or-flight response that is mediated by catecholamine signaling (Chrousos and Gold, 1992; Wendelaar Bonga, 1997). A reduction or loss of this ability will compromise the cardiovascular and metabolic adjustments to cope with stress, limiting post-hatch larval viability as a functional heart beat becomes critical for survival (Pelster & Burggren, 1996). Importantly, the performance dysfunction was seen in cortisol-treated embryos without an obvious heart defect phenotype, indicating a functional role for the observed reduction in transcript abundance of key genes involved in cardiac development.

We hypothesize that elevated embryonic cortisol exposure prior to hatch disrupts the developmental programming of cardiac morphogenesis by directly acting on *nkx2.5*. The resulting decrease in cardiomyogenesis, as evidenced by reduced expression of cardiomyocyte markers, may compromise the contractile properties of the heart, with a key factor being decreased expression of *atp2a2a* that disrupts calcium signaling in the heart rhythm. This is supported by the lower basal heart rate at rest, as well as lower heart rate during stressor exposure and recovery in post-hatch embryos that were exposed to higher cortisol levels. Indeed, zebrafish mutants displaying abnormal cardiac phenotypes also exhibit reduced heart rate (Baker et al., 1997; Garrity et al., 2002), associating the slowed heartbeat to heart malformations in the present study. The lowered basal and stress-induced heart rate in our cortisol-injected embryos may be simply due to limited contractile ability as a result of cardiac malformations. However, we cannot rule out the possibility that elevated embryonic cortisol exposure may also affect the heart response to catecholamine stimulation by modulating of β-adrenergic receptors. For instance, knockdown of the β1-adrenergic receptor in zebrafish results in embryos with lowered resting heart rates and a reduced response to stressor stimulation (Steele et al., 2011). The observation that exogenous cortisol treatment of embryos via water exposure led to a higher heart beat in the tropical

damselfish (*Pomacentrus amboinensis*) (McCormick and Nechaev, 2002) suggest that the developmental regulation by this steroid may be species-specific and/or dependent on the timing of exposure. The treatment method in our study, microinjection of cortisol at one-cell stage, mimicked a maternal deposition scenario and underscores a key role for this steroid in programming cardiac development.

In conclusion, maternal stress and the associated elevated cortisol deposition will have a marked effect on embryo heart morphogenesis and performance. Specifically, pre-hatch embryo exposure to elevated glucocorticoid exposure led to defective cardiac phenotype, and reduced cardiac performance in response to an acute stressor. This is the first study to link embryonic exposure to elevated cortisol levels to disruption of genes critical for cardiac development leading to performance defects in any animal model. Taken together, we propose that elevated early embryo cortisol content during the critical window prior to hatch affects developmental programming leading to longer term cardiac dysfunction in zebrafish. This is a novel finding, providing a potential link between maternal stress, and the associated elevated cortisol deposition in eggs, on reduced larval viability in fish. The ecological significance of this finding is the potential for a reduction in fitness and viability of progeny from chronically stressed mothers, leading to population decline in stressful environments.

3.6 Acknowledgement

This study was supported by Natural Sciences and Engineering Research Council of Canada Discovery grant and Discovery Accelerator Supplement to MM Vijayan.

Chapter 4

Knockdown of glucocorticoid receptor protein expression significantly alters global gene expression in developing zebrafish

4.1 Overview

Cortisol is the primary circulating glucocorticoid in teleosts and this steroid's action occurs via activation of the glucocorticoid receptor (GR). In response to stressor exposure, cortisol is released through the coordinated action of the hypothalamic-pituitary-interrenal axis and a major role is in the mobilization of energy stores to reestablish homeostasis. GR transcripts and cortisol are deposited by maternal transfer into the oocyte prior to fertilization. In this study, we utilized the Agilent zebrafish microarray platform to investigate changes in global gene expression in response to morpholino oligonucleotide knockdown of GR at 24 and 36 hours post fertilization (hpf). A total of 1594 and 1002 significantly changed genes were observed at 24 and 36 hpf, respectively. Ingenuity Pathway Analysis software allowed for the functional organization of these genes into important processes and networks. Differences in select gene mRNA abundances observed with microarray were also confirmed by quantitative real-time PCR. Functional analysis of genes that either displayed high-fold changes or were significantly different from mispair controls at both timepoints revealed numerous developmental processes under GR regulation, including neurogenesis, eye development, skeletal and cardiac muscle formation. Together, this study underscores a critical role for glucocorticoid signaling in programming molecular events essential for zebrafish development.

4.2 Introduction

The glucocorticoid receptor (GR) is a key mediator of the vertebrate stress response (Wendelaar Bonga, 1997; Charmandari et al., 2004). It is a cytosolic receptor that, after activation by binding of its primary ligand, cortisol, acts as a transcription factor to modulate gene expression, leading to energy store mobilization to cope with stress (Mommsen et al., 1999; Chrousos, 2006). In teleosts, these actions are coordinated by the initial stressor recognition in the hypothalamus, followed by the release of corticotropin-releasing factor (CRF) that acts on the adenohypophysis, leading to release of adrenocorticotrophic hormone (ACTH) that triggers cortisol release from the interrenal tissue (Wendelaar Bonga, 1997). The effects of GR activation on other systems, including the immune and reproductive systems have been well characterized in a number of different model animals (Nesan and Vijayan, 2012c [Chapter 1]). In teleosts, stressor recognition and a subsequent cortisol response are only present in post-hatch larvae (Nesan and Vijayan, 2012c [Chapter 1]). This inhibition of the stress response during embryogenesis, as assessed by the presence of a stressor-induced increase in circulating cortisol, occurs despite the completed functional development of the stress axis organs, the hypothalamus, the pituitary, and the interrenal tissue (Nesan and Vijayan, 2012c [Chapter 1]).

Recently, studies have revealed novel roles for glucocorticoid signaling in early zebrafish development. GR has been linked with a variety of key developmental factors, including matrix metalloproteinases (MMPs) (Hillegass et al., 2007; 2008; Nesan et al., 2012 [Chapter 2]), bone morphogenetic proteins (BMPs) (Nesan et al., 2012 [Chapter 2]), and myogenic and cardiogenic transcription factors (Nesan et al., 2012 [Chapter 2]; Nesan and Vijayan, 2012a [Chapter 3]). These specific molecular linkages occur alongside significant morphological deformations that result from knockdown of glucocorticoid receptor protein translation (Pikulkaew et al., 2011; Nesan et al., 2012 [Chapter 2]). Perhaps most interestingly, knockdown of maternal GR alters the degradation of maternal mRNA and results in an abnormal transcriptome available for translation after the mid-blastula transition (Pikulkaew et al., 2011). Together, these findings point to a major role for GR in development as a coordinator of a number of important embryogenic pathways.

The linkage of GR signaling to BMP expression indicates a key mechanism by which zygotic corticosteroids may influence embryogenesis. BMPs are a family of developmental morphogens that signal by binding to a number of BMP receptors, causing the activation of the SMAD family of intracellular transcription factors that then translocate into the nucleus to modulate target gene expression (Kondo, 2007; Xiao et al., 2007). BMP signaling has been linked to numerous major developmental events, including dorsoventral patterning, mesodermal patterning, somitogenesis, myogenesis, organogenesis, and craniofacial development (Myers et al., 2002; Willot et al., 2002; Nie et al., 2006; Kondo, 2007; Shin et al., 2007; Xiao et al., 2007; Chung et al., 2008; McCulley et al., 2008; Weber et al., 2008; Patterson et al., 2010; Maurya et al., 2011; Nesan et al., 2012 [Chapter 2]). Three specific BMP genes, *bmp2a*, *bmp2b*, and *bmp4*, are modulated by GR in zebrafish (Nesan et al., 2012 [Chapter 2]).

The period of zebrafish development from 24 to 48 hpf is extremely important for early morphogenesis. This window of time immediately follows the final stages of somitogenesis (Kimmel et al., 1995) and includes the upregulation of muscle progenitors as myogenic differentiation increases significantly (Xu et al., 2000). This is also a critical period of organogenesis, with the brain, pituitary, heart and vasculature, liver, gills, and interrenal tissue undergoing significant development (Kimmel et al., 1995; Brand, 2003; Liu, 2007; Pogoda and Hammerschmidt, 2009). By the end of this 24 h window, the embryo has a functional heartbeat and circulatory system and is ready to hatch (Kimmel et al., 1995), underlining the major developmental events that occur during this time. Previously, we have shown that without GR protein, zebrafish embryos cannot survive beyond the 48 hpf timepoint, indicating that this

receptor signaling may play a role in orchestrating these key developmental events (Nesan et al., 2012 [Chapter 2]).

Given the recent findings that position GR as a key mediator of developmental organization (Nesan and Vijayan, 2012 [Chapter 1]), we tested the hypothesis that key molecular events involved in developmental programming are regulated by GR activation in zebrafish. We specifically sought to identify novel genes and pathways regulated by GR signaling during zebrafish development. To this end we knocked down GR protein translation using morpholino oligonucleotides exactly as described previously (Nesan et al., 2012 [Chapter 2]). A high-density zebrafish microarray was utilized to assess the role of GR signaling on global gene expression pattern within a critical window during early development.

4.3 Materials and Methods

4.3.1 Zebrafish care and breeding

Care and breeding of adult zebrafish was carried out exactly as described previously (Nesan et al., 2012 [Chapter 2]). Adult zebrafish were purchased from a commercial wholesaler (DAP International, Mississauga, ON) and maintained on a 14:10 light dark cycle in an AHAB recirculating system (Aquatic Habitats, Apopka, FL). Zebrafish care protocols were approved by the University of Waterloo Animal Care Committee in accordance with the Canadian Council for Animal Care guidelines.

4.3.2 Morpholino microinjection

A morpholino oligonucleotide (MO) was designed against the start site of translation for the zebrafish glucocorticoid receptor gene, and a 5 base pair mispair oligonucleotide (MP) was designed as a control; both oligonucleotides (Gene Tools, Philomath, OR) have been described and characterized previously (Nesan et al., 2012 [Chapter 2]). Oligonucleotide sequences are as follows (small letters indicate altered bases in mispair control): MO: 5'-CTCCAGTCCTCCTTGATCCATTTTG-3'; MP: 5'-TGcTATgTTTAcTCTCgATACgTG-3'. Morpholino microinjection was performed exactly as described previously (Nesan et al., 2012 [Chapter 2]). Briefly, 1 nL of MO or MP was injected into the yolk of one-cell zebrafish embryos, which were reared in embryo medium (Westerfield, 2007). Each independent sample consisted of a pool of 25 embryos that were flash-frozen at either 24 or 36 hpf. Three replicate pools of each

treatment per timepoint were frozen for microarray analysis, and 5-7 pools of each treatment per timepoint were frozen for qPCR confirmation.

4.3.3 RNA extraction

RNA was extracted from pools of embryos with the RNeasy Mini Kit (Qiagen, Mississauga, ON) with DNAse (Qiagen) treatment to remove genomic DNA contamination. Preliminary RNA quantification was performed via a Nanodrop spectrophotometer (260 nm; Thermo Scientific, Waltham, MA).

4.3.4 Microarray scanning and analysis of resulting data

Microarray analysis was carried out at the Laboratory for Advanced Gene Analysis at the Vancouver Prostate Centre (Vancouver, BC). Quantification and quality analysis of RNA was confirmed by use of the Agilent 2100 Bioanalyzer (Agilent, Santa Clara, CA). Microarray analysis was done on pooled samples from 24 and 36 hpf embryos injected with MP or MO (n=3 pools per timepoint). 200 μg of RNA per sample was used for microarray analysis. Global gene expression in MP and MO samples was analyzed by hybridization to the Zebrafish V2 Gene Expression Microarray (Product ID 019161; Agilent, Santa Clara, CA), after one-colour labeling with the Low Input Quick Amp Labeling Kit (Agilent). Microarrays were scanned with the Agilent DNA Microarray Scanner and quantified with Agilent Feature Extraction 10.5.1.1. Data was normalized using the Agilent GeneSpring 7.3.1 software package by flooring values below 0.05 to 0.05 and normalizing data per chip to a set of positive control genes with raw data above 50 for all samples. The data will be uploaded to the Gene Expression Omnibus (GEO) database run by the National Center for Biotechnology Information (NCBI) for further possible analysis by interested parties. The dataset was restricted to only identified/annotated genes, omitting unidentified or hypothetical gene loci, thereby reducing the number of measured genes per sample to 12261. For genes with multiple oligo spots on the array, fold-changes were calculated and then averaged to yield a single fold-change value for each gene.. The resulting dataset was then subjected to statistical and pathway analyses.

Statistical assessments were carried out using the R Statistical Computing environment (R Foundation, Vienna, Austria). For microarray results, the mean normalized expression was calculated for each gene at each treatment (MP or MO) and timepoint (24 or 36 hpf). These means were then compared within a timepoint using a student's *t*-test, followed by false-discovery rate (FDR) correction using the Benjamini-Hochberg method (Benjamini and Hochberg, 1995). All p-values listed for microarray analysis are FDR-corrected. Data was not

compared between timepoints. The complete lists of statistically significant genes at each timepoint are displayed in the supplemental information, along with each calculated fold-change and p-value (Appendix C, Tables C1, C2). Where required, data from qPCR analysis was log-transformed to ensure normality prior to evaluation via student's *t*-test, no false-discovery rate correction was used for qPCR data. For all comparisons, a value of $p \leq 0.05$ was considered significant. Functional analysis was performed with the Ingenuity Pathway Analysis software package (Ingenuity Systems, Redwood, CA) as well as use of Gene Ontology functional annotations.

4.3.5 Quantitative PCR

Quantitative PCR (qPCR) was used to confirm and explore microarray fold change measurements. Embryos were injected with MO and MP as outlined above, frozen at 36 hpf, and RNA was extracted by use of the Ribozol-chloroform extraction method (Amresco, Solon, OH), following the manufacturer's protocol. After quantification of RNA via Nanodrop spectrophotometer, 1 μg of RNA was reverse transcribed with the High Capacity cDNA Reverse Transcription Kit (Applied Biosystems, Carlsbad, CA), with the Multiscribe recombinant Moloney murine leukemia virus reverse transcriptase, producing a 20 μL mixture according to the manufacturer's protocols. qPCR was performed exactly as described previously (Nesan et al., 2012 [Chapter 2]), using 2.5 μL of cDNA in a 25 μL reaction mixture with iQ SYBR green supermix (Bio-Rad, Hercules, CA) using an iCycler iQ thermocycler (Bio-Rad). The selected genes were generally unrelated, although some are part of related pathways or functions. The selected genes were as follows: the BMP ligand *bmp7a*, the clotting factor *f5*, the orphaned Ftz-F1 receptor homolog *ff1d*, the structural muscle protein *myom1a*, the hormone receptor *mc1r*, and two genes involved with the stress axis and classical glucocorticoid signaling, the ACTH precursor proopiomelanocortin a (*pomca*) and the transport protein responsible for the rate-limiting step in steroidogenesis, the steroidogenic acute regulatory protein (*star*). These genes were selected because their fold-changes were statistically significant and relatively high, as well as being of interest in our exploration of the GR knockdown phenotype. Only one gene was not statistically significant at 36 hpf, *bmp7a*, but it was chosen as it had the largest fold-change of any of the BMP ligands or receptors, and the BMP signaling pathway was considered a key target for qPCR confirmation. Primer sequences, Tm values, and amplicon sizes are provided in Table 1. Transcript abundance was normalized to β-actin as a housekeeping gene as its values did not

change across samples. Normalization was performed using the ΔCT method (Livak and Schmittgen, 2001) as performed previously (Nesan et al., 2012 [Chapter 2]).

Table 1: Details of primer pairs for qPCR, including forward and reverse nucleotide sequences, melting temperatures, and amplicon length.

Gene	Forward primer (5'-3')	Reverse primer (5'-3')	Tm (oC)	Amplicon size (bp)
bmp7a	cagggaagatgcagtggatt	tcggctttggtctcagactt	62	107
f5	cttacaacttcccgactgtc	agttggatgccacagaactg	55	119
ff1d	gggatgatccagagaggaca	cacatcggggttaaagagga	62	108
mc1r	ctcaacagccagcgacataa	caaactgatcaaaccgagca	55	88
myom1a	cacaaccgactcagggaaat	tgcgtggctttactccttct	62	124
pomca	gaagaggaatccgccgaaa	ccagtgggtttaaaggcatctc	60	98
star	tcaaattgtgtgctggcatt	ccaagtgctagctccaggtc	60	121
β-actin	tgtccctgtatgcctctggt	aagtccagacggaggatgg	60	122

4.4 Results

4.4.1 Major trends and characteristics of microarray results

Statistical analysis revealed that 1594 genes were significantly changed between mispair and morpholino-injected embryos at 24 hpf, and 1002 genes were significantly changed at 36 hpf. At 24 hpf, 715 of these genes were downregulated, and 877 were upregulated, while at 36 hpf, 273 genes were downregulated and 729 were upregulated (See Figure 1 and Appendix C, Tables C1, C2). The distribution of genes per range of fold-change at 24 hpf is displayed in Figure 2A. For 36 hpf, the distribution of genes per range of fold-change is displayed in Figure 2B. The 15 genes with the highest and lowest fold-changes for each timepoint are displayed in Tables 2 and 3 along with their p-values, indicating the genes that were most affected by GR knockdown. Among the significantly changed genes at each timepoint, 343 were significantly changed at both 24 hpf and 36 hpf, indicating that these specific GR-modulated genes may be of particular importance in zebrafish development. Of these 343 genes, 275 were upregulated at both time points, 48 were downregulated at both timepoints, and 20 showed opposing changes between the timepoints. These genes are specifically highlighted in Appendix C (Tables C1, C2; green: both upregulated; red: both downregulated: blue: differential). Table 4 lists some genes that were deemed particularly interesting based on pathway analysis and gene ontology characterization of their functional grouping. These genes are organized by their general function, and listed with their fold-changes at each timepoint.

Table 2: Select genes (top ranked based on fold-change) that were significantly upregulated in response to GR knockdown at 24 and 36 hpf, with their respective fold-change values and p-values from statistical comparisons.

24 hpf			36 hpf		
Gene	**Fold Change**	**P-value**	**Gene**	**Fold Change**	**P-value**
esrrd	49.33	0.037	*crygm2b*	45.89	0.049
chad	20.35	0.016	*mip2*	29.42	0.044
mip1	19.25	0.033	*crygm2a*	29.38	0.035
cryba2a	14.72	0.013	*atp2a1l*	25.43	0.045
lim2.4	13.74	0.041	*crygm3*	19.99	0.05
cx44.1	9.96	0.015	*sparcl*	15.23	0.047
xirp2l	8.03	0.038	*grifin*	13.89	0.032
cryba4	7.07	0.05	*crybb1*	13.09	0.045
msn	7.04	0.016	*slc25a4*	13.08	0.041
pvalb5	6.74	0.038	*cryba4*	11.94	0.049
calca	6.71	0.040	*xirp2l*	11.93	0.031
tnnt3b	6.42	0.039	*cryba2a*	11.49	0.034
pvalb4	6.35	0.011	*fabp11b*	10.87	0.05
cpt1b	6.29	0.009	*pfkma*	10.84	0.042
tyrp1b	6.18	0.018	*crygmx*	10.21	0.02

Table 3: Select genes (top ranked based on fold-change) that were significantly downregulated in response to GR knockdown at 24 and 36 hpf, with their respective fold-change values and p-values from statistical comparisons.

24 hpf			36 hpf		
Gene	**Fold Change**	**P-value**	**Gene**	**Fold Change**	**P-value**
cha	0.047	0.026	*lect2l*	0.22	0.046
lect2l	0.057	0.044	*ptgds*	0.24	0.022
tbx16	0.066	0.024	*trac*	0.25	0.006
gfi1.1	0.067	0.029	*gadd45bl*	0.26	0.020
egln3	0.081	0.018	*gnrh2*	0.30	0.041
psme1	0.084	0.040	*oc90*	0.30	0.049
tbx24	0.096	0.027	*flncb*	0.34	0.049
pim1	0.097	0.025	*gpx4a*	0.34	0.045
tbx6	0.098	0.037	*plekhf1*	0.35	0.047
pcdh8	0.104	0.045	*cryaba*	0.35	0.038
ptgs2b	0.104	0.015	*ddb2*	0.36	0.042
cyp24a1l	0.114	0.045	*hdr*	0.36	0.046
ctsc	0.116	0.009	*rspo1*	0.37	0.044
ripply2	0.121	0.042	*optc*	0.37	0.024
cyp11a1	0.125	0.048	*fech*	0.39	0.040

Table 4: Functional grouping (based on Ingenuity Pathway Analysis and Gene Ontology databases) of select genes that were significantly affected by GR knockdown at both 24 and 36 hpf, with their fold-change values at each timepoint.

Functional Grouping	**Subgroupings: Selected Genes (24 hpf fold change, 36 hpf fold change)**
Cardiac and skeletal muscle	Cardiac ATPases: *atp2a1* (1.76, 2.59), *atp2a2a* (0.21, 0.69) Muscle metabolism: *ckmb* (3.03. 2.92), *pfkma* (5.91, 10.91) Structural proteins: *mylk3* (2.7, 3.35), *mylz2* (3.93, 2.19), *mylz3* (3.78, 4.37) *myom1a* (3.2, 2.9), *tmod4* (2.46, 2.10), *tnnc* (2.12, 1.92), *tnnt1* (1.84, 0.41), *tnnt3a* (4.75, 3.97), *tnnt3b* (6.38, 7.12), *ttna* (3.61, 2.23), *ttnb* (1.8, 2.4)
Cell adhesion, extracellular matrix	Cadherins: *cadm2a* (2.69, 2.73), *cadm4* (1.46, 1.68) Claudins: *cldne* (0.54, 0.50), *cldnf* (0.69, 1.61) Collagens: *col1a1* (2.2, 2.68), *col1a2* (1.96, 2.12), *col1a3* (3.19, 3.05), *col6a1* (2.14, 3.05), *col6a2* (2.72, 2.99) Connexins: *cx23* (4.15, 4.41), *cx44.1* (9.96, 2.79) Protocadherins: *pcdh17* (2.18, 1.97), *pcdh1a4* (2.4, 1.37), *pcdh1g18* (2.1, 1.69), *pcdh1gb2* (2.03, 1.84), *pcdh2ac* (1.93, 2.35) Others: *chad* (20.3, 9.65), *itgb1b.2* (3.15, 3.0)
Developmental morphogens	BMP signaling: *smad3b* (2.6, 2.96), *smad7* (0.54, 1.71) Hairy-related proteins: *her3* (0.56, 0.69), *her5* (0.34. 2.77) Others: *agr2* (2.51, 2.13), *gdf11* (1.34, 2.58),
Endocrine systems	Hormones: *avpl* (1.85, 2.75), *calca* (6.71, 2.49), *pyya* (6.15, 9.89) Others: *igfbp3* (1.63, 1.86), *npy1r* (2.54, 2.91), *nr5a1b* (3.18, 3.61)
Neurogenesis	Atonal homologs: *atoh2a* (2.71, 3.74), *atoh2b* (4.94, 3.00) LIM-domain proteins: *ldb3a* (2.2, 3.22), *ldb3b* (2.86, 3.18), *lhx1b* (1.61, 2.64), *lhx6* (3.30, 6.82) Others: *neurod4* (2.28, 3.27), *sox4a* (1.67, 2.732.), *sox9b* (0.39, 1.95)
Organogenesis	*mmp23a* (2.42. 2.57), *pdlim7* (2.69, 2.70), *otpb* (2.73, 2.65)
Vasculature	Clotting factors: *f5* (3.55, 2.72), *f7i* (2.46, 2.17) Others: *ank1* (2.95, 2.87), *vegfab* (1.76, 1.85)

Figure 1 – Numbers of statistically significant genes upregulated and downregulated at 24 and 36 hpf in response to GR knockdown

Of 12261 potential unique genes, the mRNA expression of 1594 were found to be statistically significantly changed at 24 hpf, with 715 downregulated (grey) and 877 upregulated (black). 1002 genes were changed with statistical significance at 36 hpf, of which 273 were downregulated and 729 were upregulated. (n=3 pools of 25 embryos used for microarray analysis, $P \leq 0.05$, students *t*-test with Benjamini-Hochberg false-discovery rate correction).

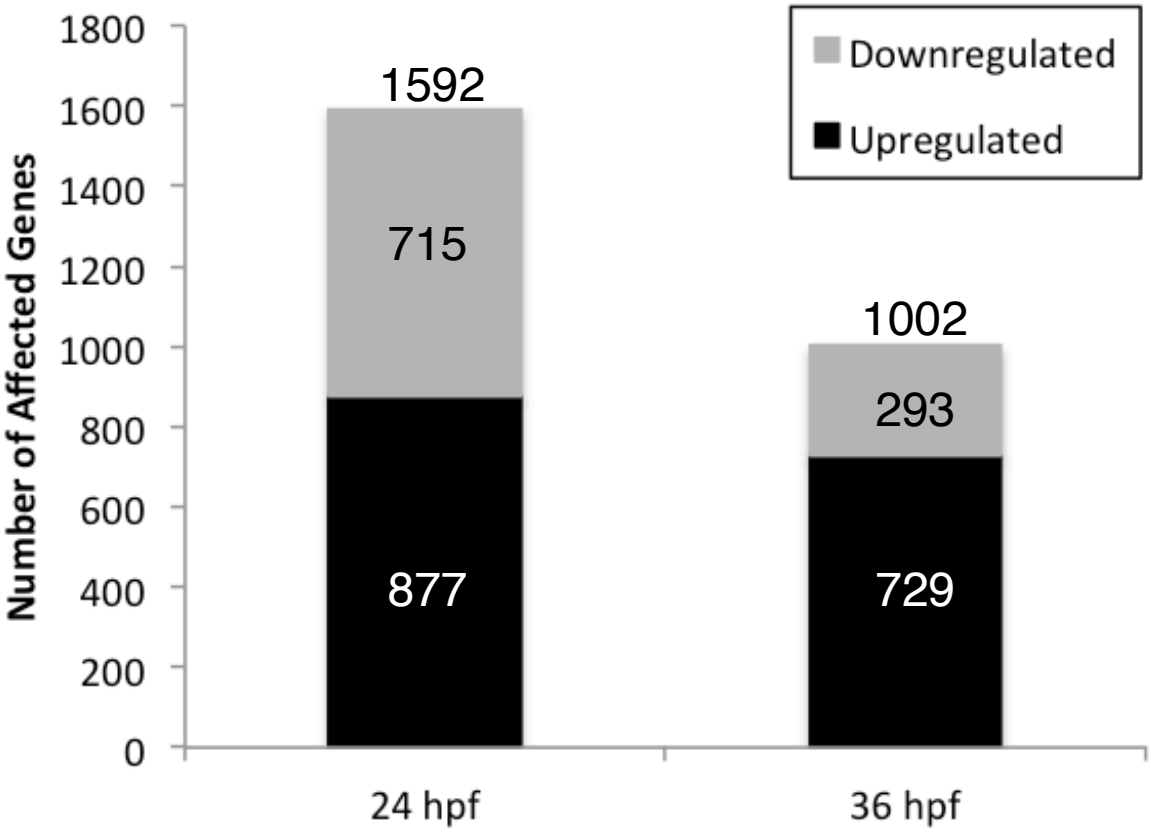
Number of Affected Genes
1800
1600
1400
1200
1000
800
600
400
200
0
1592
715
877
1002
293
729
24 hpf
36 hpf
Downregulated
Upregulated

Figure 2 – Distribution of fold-change for statistically significant genes at 24 and 36 hpf in response to GR knockdown

This figure presents the frequency of genes that were up- or down-regulated at specific fold-change ranges at 24 hpf (A) or 36 hpf (B). In general, there was a relatively normal distribution at 24 hpf, with relatively few genes showing extreme fold changes and a balance between up and downregulation. At 36 hpf, a far greater percentage of genes were upregulated than downregulated, and none showed reduction as severe as at 24 hpf.

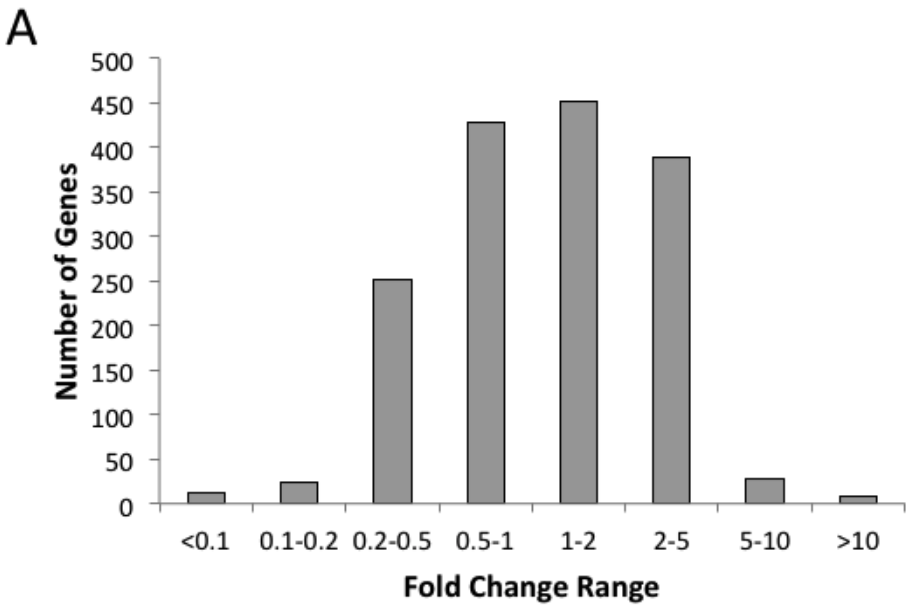
A
500
450
400
350
300
250
200
150
100
50
0
Number of Genes
<0.1
0.1-0.2
0.2-0.5
0.5-1
1-2
2-5
5-10
>10
Fold Change Range

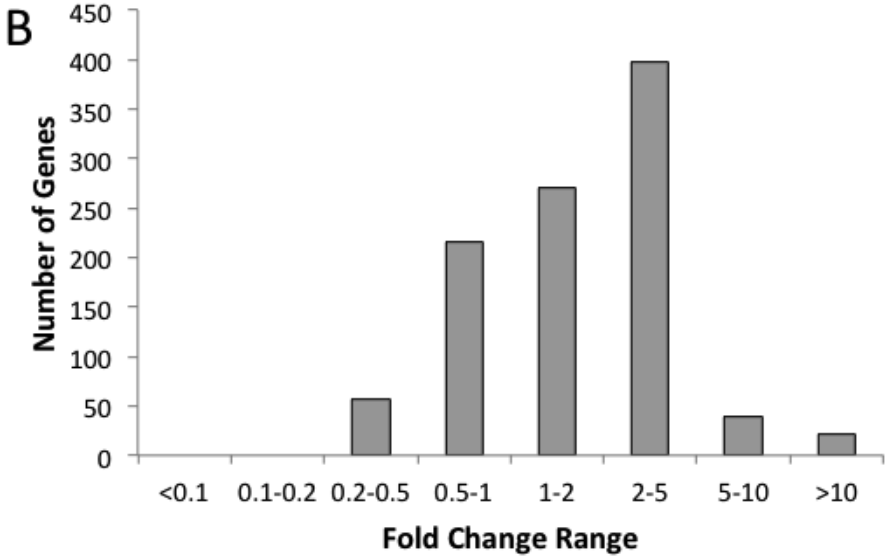
B
450
400
350
300
250
200
150
100
50
0
Number of Genes
<0.1
0.1-0.2
0.2-0.5
0.5-1
1-2
2-5
5-10
>10
Fold Change Range

4.4.2 Results of pathway analysis

Functional analysis using Ingenuity Pathway Analysis revealed networks of genes with known major developmental effects that were affected by GR knockdown. We have selected the top 8 networks, based on the "high score" output obtained with the IPA program reflecting a large number of affected genes in a network, and they were categorized as developmentally relevant (Figure 3). The genes and the relative numbers that were upregulated or downregulated in each network at 24 hpf (Figure 3A) and 36 hpf (Figure 3B) are provided. The genes that are grouped into these networks, their corresponding fold changes, and their IPA scores are listed in Tables 5 (24 hpf) and 6 (36 hpf).

The IPA software also generated pathway networks that show interaction among significantly different genes and are classified according to their function. These networks were used, along with information about the cellular location and the fold change of the genes, to create interactome networks that describe cellular and whole-animal processes that appear to be strongly GR-responsive (Figure 4). At both the 24 and 36 hpf timepoints, the development of the nervous system was identified as the process most strongly disrupted by GR knockdown (Figures 4A and 4B). In addition, we identified other functionally relevant processes that were identified as GR-responsive by the IPA software and that are indicative of the previously characterized GR knockdown phenotype (Nesan et al., 2012 [Chapter 2]). These include transcripts involved in DNA replication and metabolic regulation at 24 hpf (Figure 4C), and cardiovascular development (Figure 4D) and developmental disorders (Figure 4E) at 36 hpf.

Table 5: Gene-regulatory networks that are GR responsive as identified by Ingenuity Pathway Analysis software at 24 hpf and the calculated IPA score (higher scores denote more strongly affected pathways)

Network	**Genes**	**IPA Score**
Nervous system development	*ascl1, calhm2, cbp(family), cdc40, cs, etv4, fev, gad1, hdac, hes6, hes7, hes1, hlx, jag2, klf2, krt8, mapk3, mfng, mpzl2, mpzl3, mtf2, ndrg4, notch2, notch, rab38, smad2, smpx, spry2, tbr1, tbx3, tph2,ubtf, unc5b, zeb1*	45
Cell death	*adh5, aig1, aox1, aplp1, btbd2, dhrs3, DNA-directed DNA polymerase, idh2, igsf21, mthfsd, nae1, piwil1, plk2, pola1, pold2, ppa1, prim1, rab5, ras homolog, rchy1, rho gdi, rprm, sat1, sec61a1, sec61b, spon1, ssr1, tip60, tmbim1, tp63, tp73, tp53bp2, tsc22d1, unc119, xpo7*	41
Endocrine disorders	*adcyap1, adora2a, arid3b, camkv, creb, dcaf13, gmps, grhl1, hnf1a, hnf4a, ins, insulin, isoc2, ldl, me3, mecr, mrps18c, nr4a2, opa3, penk pex12, plekha8, proinsulin, ptpn4, rab3d, rb1, rbks, rsk, runx1, shox, slc25a18, spata6, ssr2, syt11, tmtc4*	40
Cellular assembly & organization	*acat1, arnt2, atpase, bves, calb2, celf2, clstn1, cltc, ctss, entpd2, irx2, irx4, ldl-cholesterol, metap2, mmp, mogat2, myh6, myh7, napg, nsf, plp1, pp1 protein complex group, rab24, s100a4, snap25, snare, snx5, stx1b, stxbp1, syntaxin, syt4, tcfl71, txnrd3, vamp3, zbtb33*	39
Embryonic development	*14-3-3, afmid, arl4a, arntl2, arrb1, box, cbp/p300, cryba2, cryba4, cyp11a1, epas1, gar1,* growth hormone*, gstt1, hcg,* histone h3*,* histone h4*, hmga2, hoxa10, igfbp2, igbp3, importin alpha, kpna2, lef1, maf, mop10, nudt21, pbx1, pno1, sesn1, setd8, shd, tcf7l2, tfap2a, tfap2b*	37
Cardiovascular development	*akap12, asf1a, bcam, c-src, dusp5, egln3, eif3e, figf, gata1, gata4, gata6, gata, gem, hbe1, hedgehog, heyl hmbs, hoxb7, htatip2, jmjd6, klf13, lama6, lamb2, lmo1, lmo2, mucin, os9, parp, pim2, ptpru, secretase gamma, sp8, tal1, tal2, vegf*	35
Skeletal and muscular disorders	*acot7, actn3, alpha actinin, alpha catenin, aph1a, aqp11, arrdc2, c8g, cadherin, cdd2ap, cdh2, cdh4, cdhe/cdhn, chmp4a, col6a1, col6a2, dmrt2, dynamin, egfr, endophilin, fah, g-actin, invs, lim2, matn2, mdh1, parvb, pdcd6ip, pdlim7, pxk, sh3gl2, sparcl1, thbs4, tnnt3*	35
Organ morphology	*alas2, apoa1, ck1, cpn1, creatine kinase, cry2, elastase, fbln1, fgb, fgf13, fgg, fibrin, fibrinogen, gpIIb-IIIa, integrin alpha V beta, mapk, myf5, myf6, myog, nr6a1, pde5a, per1, rgs20, scn4a, setd3, sgcd, sgce, sgcg, six4, slc39a7, sox2-oct4-nanog, stat3-stat3, sucla2, tni, troponin 1*	23

Table 6: Gene-regulatory networks that are GR responsive, identified by Ingenuity Pathway Analysis software at 36 hpf and the calculated IPA score (higher scores denote more strongly affected pathways)

Network	**Genes**	**IPA Score**
Nervous system development	*ap-3, bcl11a, calb2, cirh1a, crabp1, etv1, exoc6, fgf13, foxf1, gfap, ina, irx1, irx2, irx4, isl1, kcnd3, kcnip3, mab21l1, mlph, msi2, mtdh, myo5a, nefl, neurod4, nfkβ (complex), nop14, olig2, pdcd11, pdlim7, pou4f1, prph, rab3c, st9sia2, trim3*	55
Cellular movement	*bmpr2, cofilin, dck, ddx56, dhx16, dhx37, DNA-directed RNA polymerase, eaf1, ebna1bp2, fbl, gtf2f1, hnrnpm, holo RNA polymerase II, med19, mybbp1a, nat10, ncl, nop56, npm1, oc90, p70 56k, pdcd4, pes1, polr1a, polr2b, polr2e, ras, rnr, rrp12, smad1/5/8, srsf1, ssb, trpc1, tsr1, wdr12*	42
Embryonic development	*adrb, barx1, bmp, crmp, dpysl2, dpysl4, dpysl5, fbp2, gck, glud1, gng3, gng12, gpc3, hedgehog, ihh, insm1, jnk, l1cam, meis2, nbl1, neurod1, nkx2-2, pax6, pfkb2, plp1, ppp2c, proinsulin, ptprn2, ptprn, pyy, sec62, sh3gl2, sox2-oct4-nanog, stam2, yes1*	40
Cell-to-cell signaling	*ache, achr, akt, ampa receptor, cacn, cacna1s cacna2d1, cacng2, caveolin, chrna4, cnih2, gnb5, gria2, K channel, l-type calcium channel, magi1, musk, n—type calcium channel, napg, neurod2, nptn, nrxn1, nrxn2, nrxn3, nsf, nxph1, rgs7bp, snap25, snare, sncb, stx1b, stxbp1, syntaxin, vamp1, vamp2*	36
Connective tissue development	*20s proteasome, 26s proteasome, abcc9, amt, arl15, c1qtnf4, cdh10, chemokine, clstn1, dcp1a, dennd4a, dnase1l3, estrogen receptor, gapdh, growth hormone, hsp70, hsp90, kal1, mdm2, mmp24, mmp, nfkbia, nos, nr3c1, onecut1, pax3, pgam1, ret, serinc1, tbx15, tfrc, ubiquitin, wdr3, ywhag, znf326*	33
Cardiovascular development	*acsl4, avp, cdc2, cdkn18, creb, crhbp, cry2, csdc2, cyclin a, cyclin d, cyclin 3, ddx55, e2f, eif6, evx1, exosc8, fancd2, fancl, fdps, gcg, got, hexokinase, map2k1/2, mkrn1, mthfd1, pomc, ppargc1b, rb, rna polymerase II, rngtt, rsk, sod2, stat3-stat3, syt4, xrn2*	27
Skeletal/muscular disorders	*14-3-3, acta1, actn3, aldh3b1, alpha actinin, alpha catenin, calmodulin, camk2a, camk2d, col1a1, col6a1, col6a2, collagen type I, ctnna2,edf1m elavl4, f actin, grin1, hsp27, itpr, kif23, ktn1, lrrtm1, neurod6, pdgf (complex), pp2a, raf, rap1, rgn, smad7, smad, smad2/3-smad4, spectrin, syt9, tpm3*	25
Organ morphology	*Adam17 agr, ampk, bhlhe41, crlf1, dll1, edn1, elmo1, endothelin receptor, gtf3a, hdl, mlc, mphosph10, mstn, myl4, mylpf, myosin, nadph oxidase, notch, pk, plc beta, pp1 protein complex group, pro-inflammatory cytokine, ptf1a, rdx, rem1, rock, scn4a, secretase gamma, slc9a3r1, sp4, tsh, ttn, vam1, vegf*	22

Figure 3 – Functional annotation (using Ingenuity Pathway Analysis software) of genes that were upregulated and downregulated by GR knockdown

Ingenuity pathway analysis software identified prominent developmental pathways that were significantly affected by GR knockdown based on the significantly changed genes at 24 hpf (A) and 36 hpf (B). Each pathway is named and the total number of genes as well as the number of upregulated and downregulated genes is listed (See Tables 5 and 6 for complete list of genes).

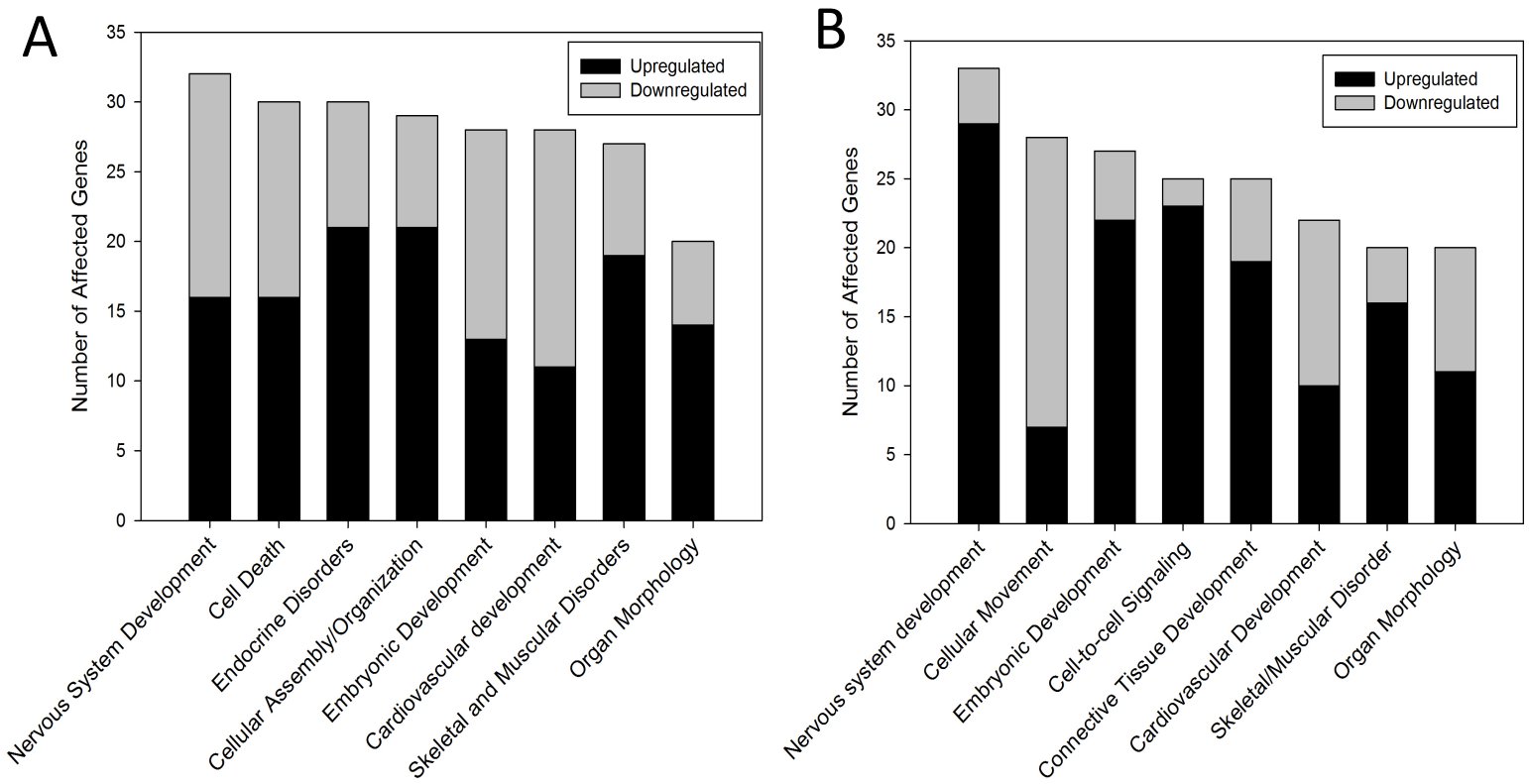
A
Number of Affected Genes
Upregulated
Downregulated
Nervous System Development
Cell Death
Endocrine Disorders
Cellular Assembly/Organization
Embryonic Development
Cardiovascular development
Skeletal and Muscular Disorders
Organ Morphology
B
Number of Affected Genes
Upregulated
Downregulated
Nervous system development
Cellular Movement
Embryonic Development
Cell-to-cell Signaling
Connective Tissue Development
Cardiovascular Development
Skeletal/Muscular Disorder
Organ Morphology

Figure 4 – Interactome networks of select pathways identified as GR responsive by Ingenuity Pathway Analysis software

The IPA software organized and classified genes to identify important networks that were modulated by GR knockdown. These interactome networks detail the regulatory connections between genes as detailed by the connective arrows. The most strongly affected process was nervous system development at both 24 hpf (A) and 36 hpf (B). Other interesting pathways are DNA replication and energy production at 24 hpf (C), cardiovascular development at 36 hpf (D) and developmental disorders at 36 hpf (E). These final 3 pathways each involve a gene that were quantified by qPCR (Figure 4): *f5* (C, E), and *pomca* (D). Single-way arrows indicate one gene regulating another, two-sided arrows indicate co-regulation, looped arrows indicate self-regulation. The shape of each member of the network indicates its cellular location (according to IPA software classifications): Extracellular (diamond); plasma membrane (hexagon); cytosol (square); nucleus (circle); unknown (triangle). The color of each member of the network indicates its mean fold change range: >2 (dark green); 1-2 (light green); unchanged (grey); 0.5-1 (light red), <0.5 (dark red).

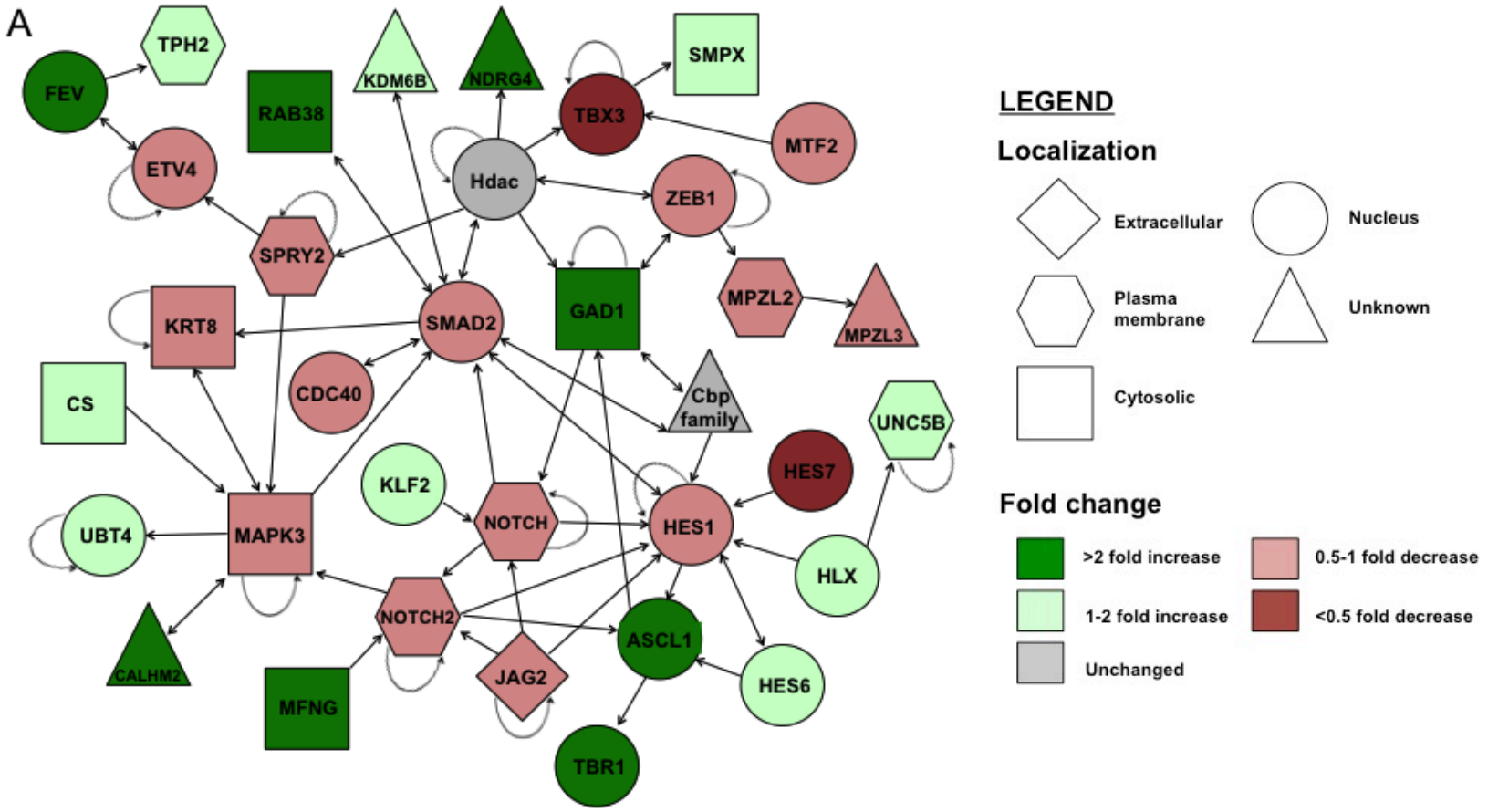
A
TPH2
FEV
RAB38
KDM6B
NDRG4
SMPX
TBX3
MTF2
ETV4
Hdac
ZEB1
SPRY2
MPZL2
MPZL3
KRT8
SMAD2
GAD1
CS
CDC40
Cbp family
UNC5B
HES7
KLF2
NOTCH
HES1
UBT4
MAPK3
HLX
NOTCH2
ASCL1
CALHM2
JAG2
HES6
MFNG
TBR1
LEGEND
Localization
Extracellular
Nucleus
Plasma membrane
Unknown
Cytosolic
Fold change
>2 fold increase
0.5-1 fold decrease
1-2 fold increase
<0.5 fold decrease
Unchanged

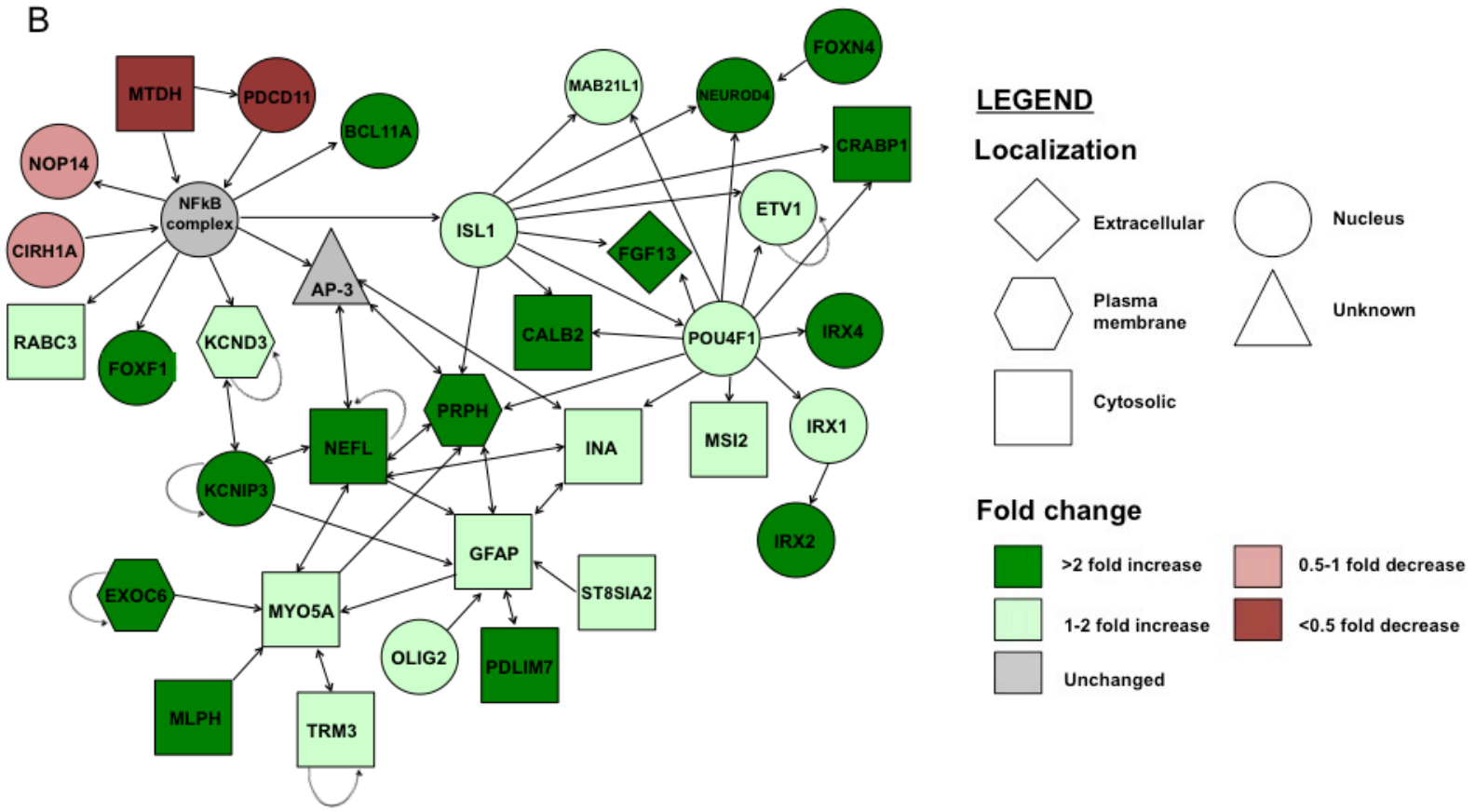
B
MTDH
PDCD11
BCL11A
NOP14
NFkB complex
CIRH1A
RABC3
FOXF1
KCND3
AP-3
ISL1
MAB21L1
NEUROD4
FOXN4
CRABP1
ETV1
FGF13
CALB2
POU4F1
IRX4
IRX1
IRX2
MSI2
PRPH
NEFL
INA
KCNIP3
GFAP
ST8SIA2
EXOC6
MYO5A
OLIG2
PDLIM7
MLPH
TRM3
LEGEND
Localization
Extracellular
Nucleus
Plasma membrane
Unknown
Cytosolic
Fold change
>2 fold increase
0.5-1 fold decrease
1-2 fold increase
<0.5 fold decrease
Unchanged

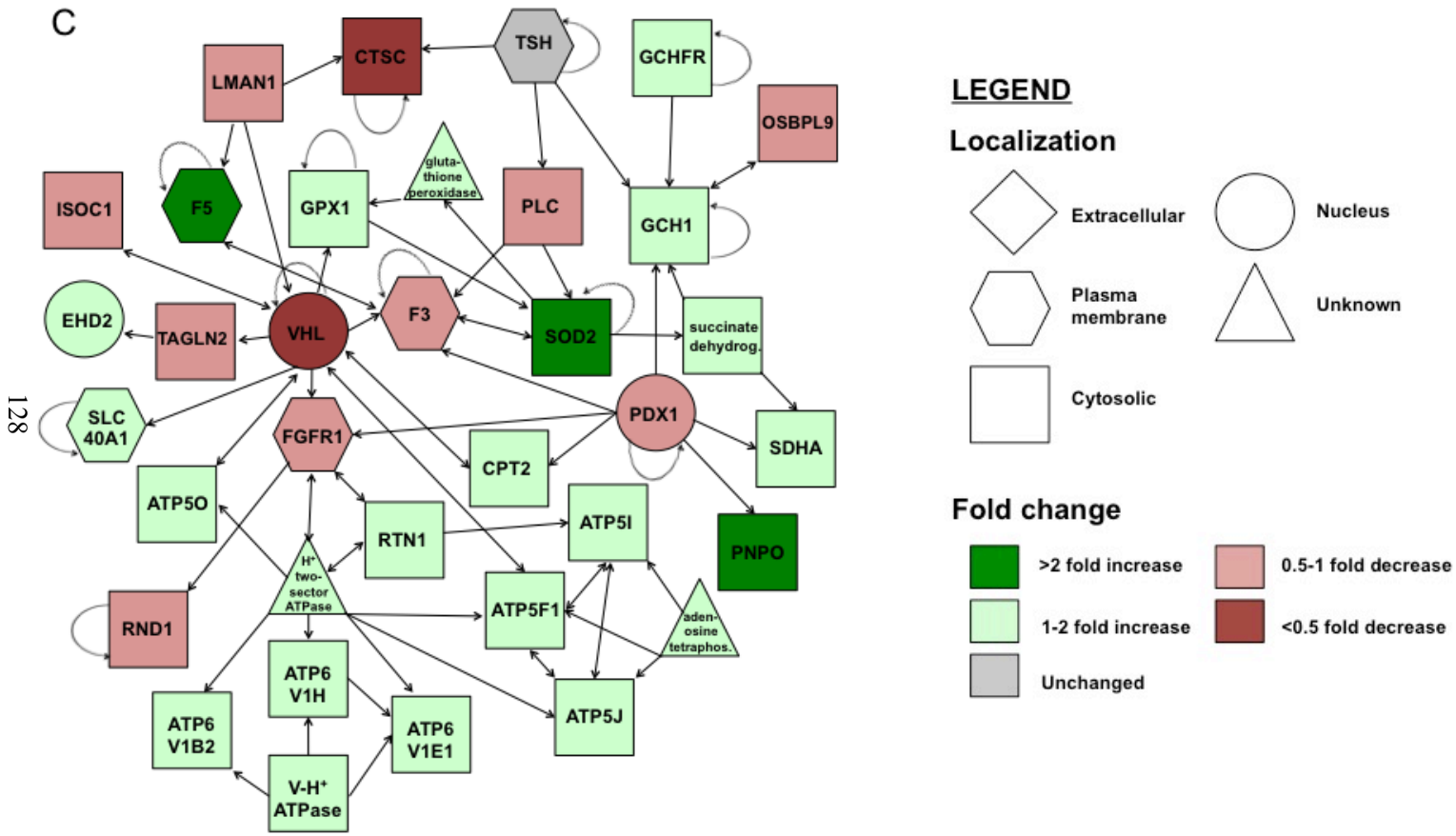
C
LMAN1
CTSC
TSH
GCHFR
OSBPL9
ISOC1
F5
GPX1
gluta-thione peroxidase
PLC
GCH1
EHD2
TAGLN2
VHL
F3
SOD2
succinate dehydrog.
SLC 40A1
FGFR1
PDX1
SDHA
CPT2
ATP5O
RTN1
ATP5I
PNPO
H+ two-sector ATPase
RND1
ATP5F1
aden-osine tetraphos.
ATP6 V1H
ATP6 V1B2
ATP6 V1E1
ATP5J
V-H+ ATPase
LEGEND
Localization
Extracellular
Nucleus
Plasma membrane
Unknown
Cytosolic
Fold change
>2 fold increase
0.5-1 fold decrease
1-2 fold increase
<0.5 fold decrease
Unchanged

D

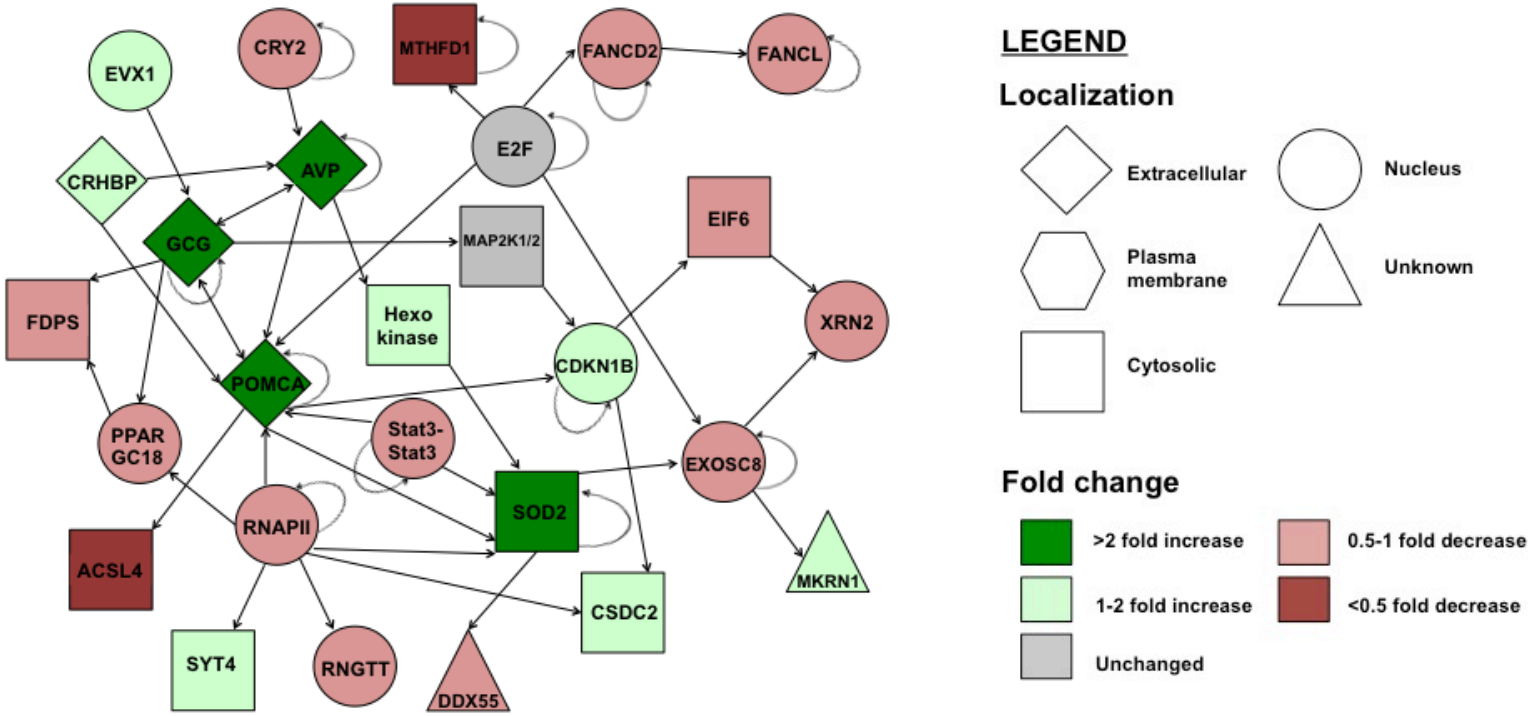
EVX1
CRY2
MTHFD1
FANCD2
FANCL
E2F
CRHBP
AVP
GCG
MAP2K1/2
EIF6
FDPS
Hexo kinase
XRN2
POMCA
CDKN1B
PPAR GC18
Stat3-Stat3
EXOSC8
SOD2
RNAPII
ACSL4
MKRN1
CSDC2
SYT4
RNGTT
DDX55
LEGEND
Localization
Extracellular
Nucleus
Plasma membrane
Unknown
Cytosolic
Fold change
>2 fold increase
0.5-1 fold decrease
1-2 fold increase
<0.5 fold decrease
Unchanged

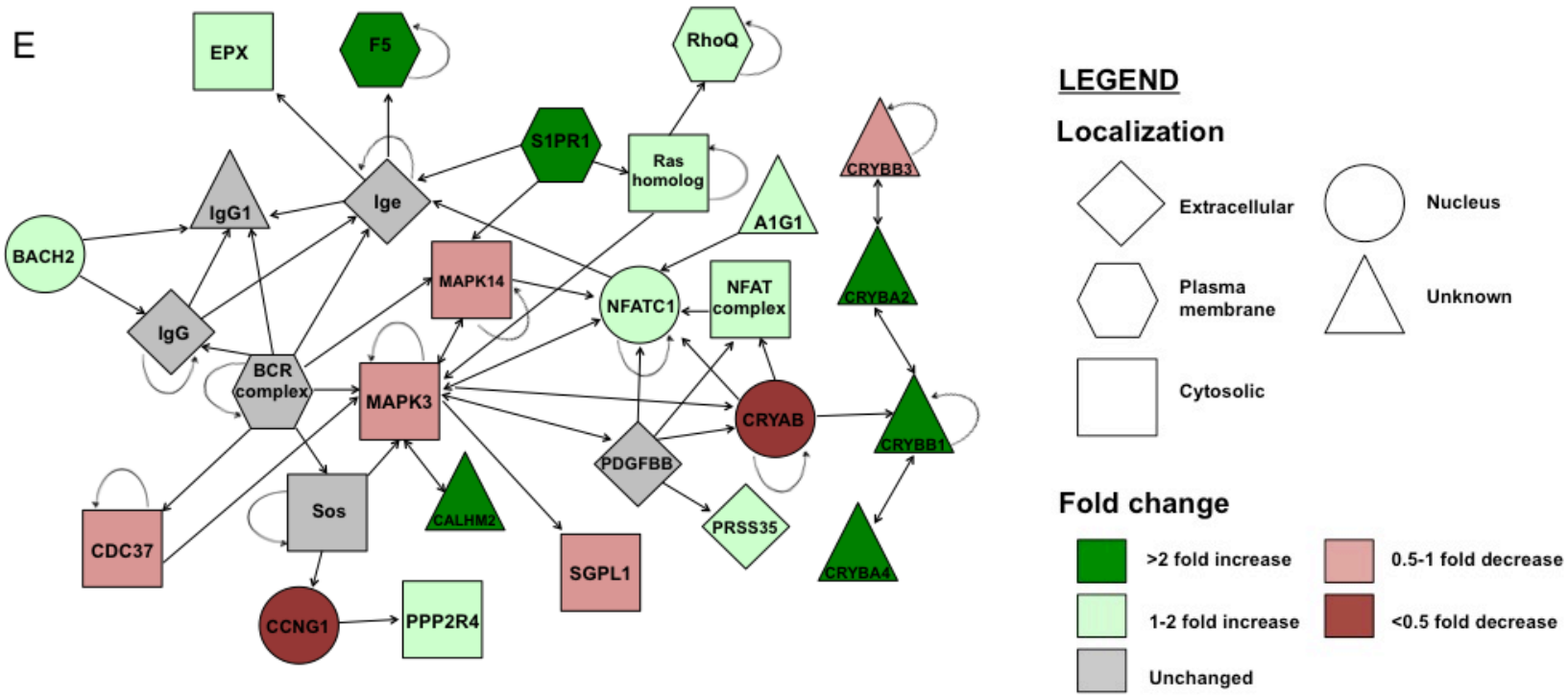
E
EPX
F5
RhoQ
S1PR1
Ras homolog
CRYBB3
IgG1
Ige
A1G1
BACH2
MAPK14
NFATC1
NFAT complex
CRYBA2
IgG
BCR complex
MAPK3
CRYAB
CRYBB1
PDGFBB
Sos
CALHM2
PRSS35
CDC37
SGPL1
CRYBA4
CCNG1
PPP2R4
LEGEND
Localization
Extracellular
Nucleus
Plasma membrane
Unknown
Cytosolic
Fold change
>2 fold increase
0.5-1 fold decrease
1-2 fold increase
<0.5 fold decrease
Unchanged

4.4.3 Confirmation by quantitative PCR

To confirm the reliability of the microarray results, abundance of selected transcripts were quantified using qPCR. Genes were selected that had relatively high fold-changes, which were also deemed of potential interest in understanding the developmental changes observed in GR morphants. These included selected genes from networks identified by IPA software as strongly affected (*f5* - Figures 4C, 4E; *pomca* - Figure 4D), as well genes identified as functionally important in development or which may be involved in the GR knockdown phenotype (*bmp7a*, *ff1d*, *mc1r, myom1a*, *star*). The qPCR analysis of gene expression was in agreement with the microarray findings, with all measured genes showing the same direction of change and similar magnitudes (Table 7, Figure 4) at 36 hpf. In addition, the fold-changes for all 7 genes were statistically significant with qPCR (Figure 4). This included *bmp7a*, which although having a strong reduction in fold-change (0.341), was not statistically significant in the microarray data. Table 7 shows the exact measured fold-changes and p-values for each gene examined, and Figure 4 is a graphical representation of the normalized expression, in arbitrary units.

Table 7: List of genes confirmed using microarray and qPCR with fold-changes and p-values

Gene	36 hpf fold-change (microarray)	P-value (microarray)	36 hpf fold-change (qPCR)	P-value (qPCR)
bmp7a	0.341	0.57	0.13	0.02
f5	1.87	0.038	1.17	0.05
ff1d	3.61	0.046	8.49	0.007
mc1r	3.72	0.04	3.61	0.020
myom1a	2.90	0.044	2.34	0.013
pomca	3.64	0.042	5.99	0.022
star	5.87	0.031	7.05	0.032

Figure 5 – Confirmation of microarray findings by qPCR analysis

qPCR analysis was performed on 7 genes to confirm the transcript abundance seen with the microarray analysis. The selected genes were *bmp7a* (A), *f5* (B), *ff1d* (C), *myom1a* (D), *pomca* (E), *star* (F), *mc1r* (G). Data is presented as mean ± standard error of the mean (normalized to β-actin, SEM; n=5-7 pools of 25 embryos each); * denotes statistical significance (*t*-test, $p<0.05$). (See Table 7 for fold-changes and p-values).

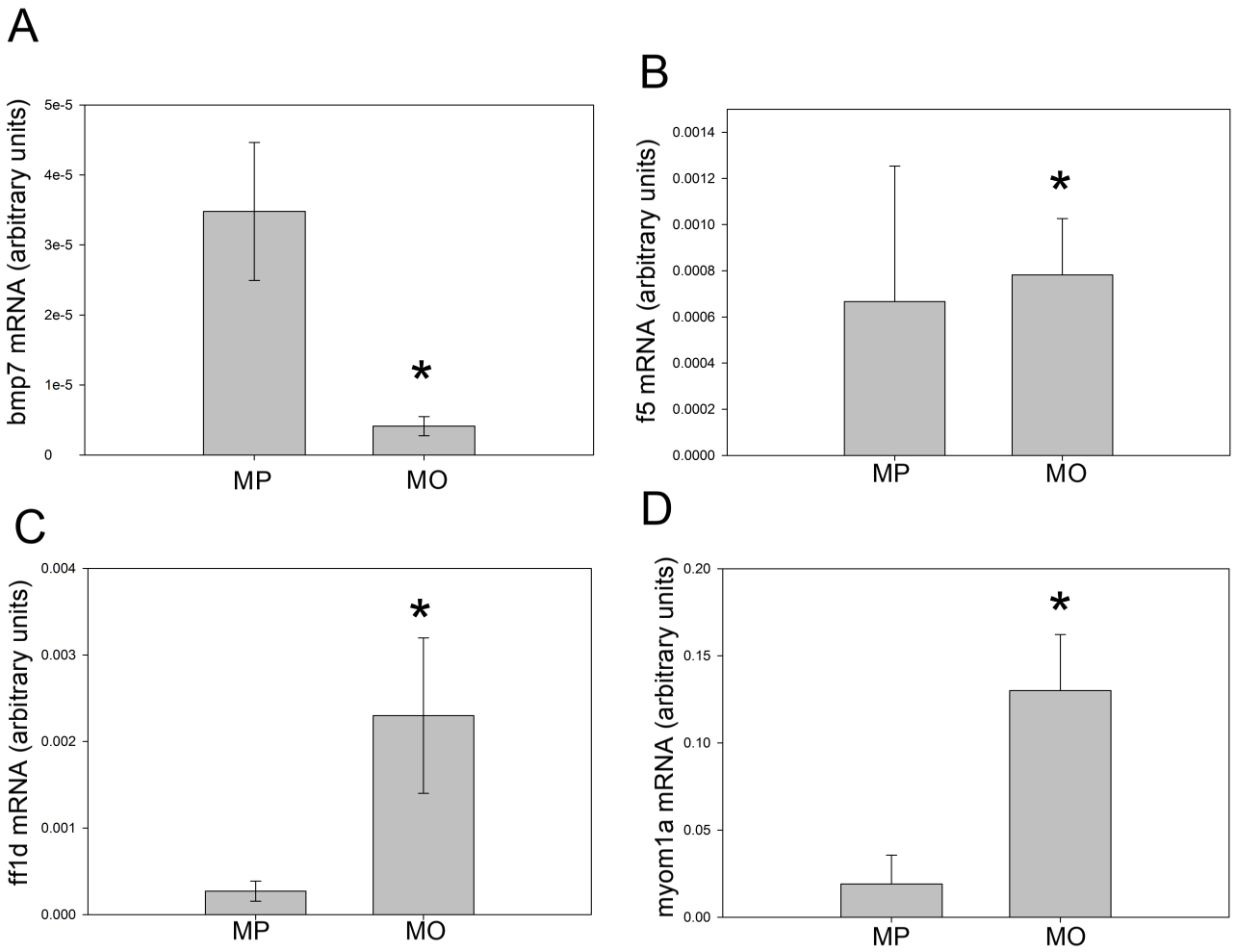
A
bmp7 mRNA (arbitrary units)
5e-5
4e-5
3e-5
2e-5
1e-5
0
*
MP
MO
B
f5 mRNA (arbitrary units)
0.0014
0.0012
0.0010
0.0008
0.0006
0.0004
0.0002
0.0000
*
MP
MO
C
ff1d mRNA (arbitrary units)
0.004
0.003
0.002
0.001
0.000
*
MP
MO
D
myom1a mRNA (arbitrary units)
0.20
0.15
0.10
0.05
0.00
*
MP
MO

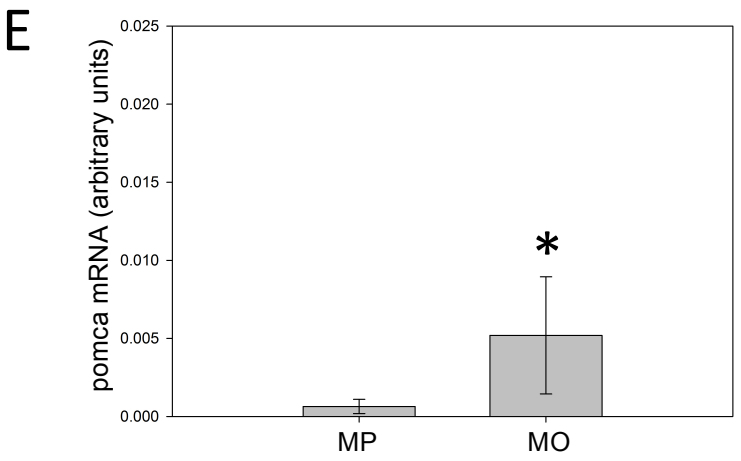
E
pomca mRNA (arbitrary units)
0.025
0.020
0.015
0.010
0.005
0.000
*
MP
MO

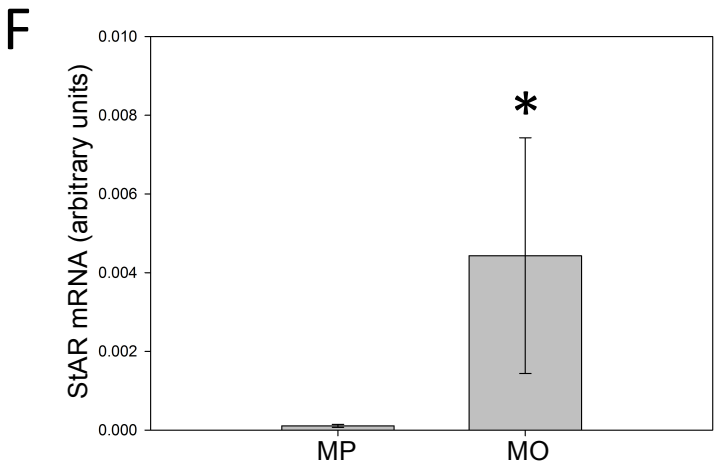
F
StAR mRNA (arbitrary units)
0.010
0.008
0.006
0.004
0.002
0.000
*
MP
MO

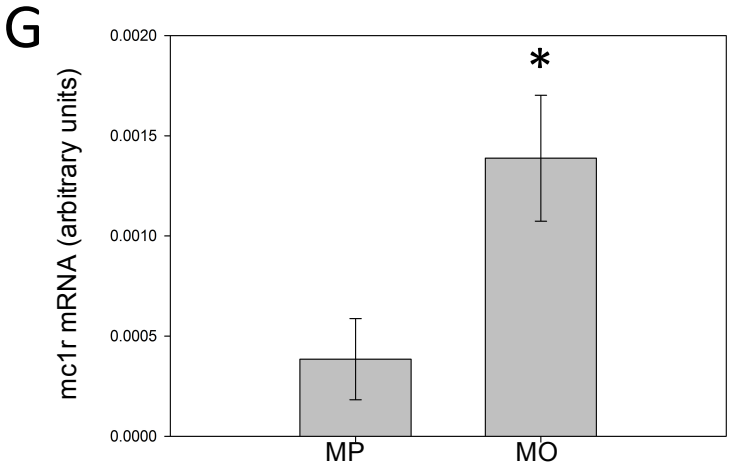
G
mc1r mRNA (arbitrary units)
0.0020
0.0015
0.0010
0.0005
0.0000
*
MP
MO

4.5 Discussion

Through the use of high-density microarray analysis, this study provides some very interesting connections between glucocorticoid receptor signaling and major developmental processes. The findings, further supported by confirmation of selected genes by qPCR, help to explain the developmentally disrupted GR-knockdown phenotype previously established in the literature (Pikulkaew et al., 2011; Nesan et al., 2012 [Chapter 2]). In addition, the sheer volume of changes found and the major developmental actions of the pathways and specific genes involved are a significant contribution to the recent supposition that GR may be a major developmental regulator (Nesan and Vijayan, 2012c [Chapter 1]). Together with a previous study that used a high-density microarray to examine GR-knockdown effects prior to MBT (Pikulkaew et al., 2011), it is becoming increasingly clear that GR actions during embryogenesis are complex but essential for development.

In presenting this data, we have attempted to characterize some large-picture changes that occur in response to GR knockdown at 24 and 36 hpf, and then to examine some specific genes and processes that we find intriguing and worthy of deeper study. It should be noted, as with most high-throughput data studies, that we present only a subset of the findings. In this study, we found that there were far more significantly changed genes at 24 hpf than at 36 hpf, but that within these populations, there was a marked difference in the direction of change. At 24 hpf, the ratio of downregulated to upregulated genes was 45% to 55%, but at 36 hpf, there were far more upregulated genes (73%) than downregulated (27%). This was an unexpected result as it implies that GR could potentially be acting as a suppressor of numerous genes during development or suppressing the actions of some key developmental transcription factors that would otherwise be enhancing gene expression. Previous research has shown downregulation of key metabolic and/or stress-related genes in trout hepatocytes after GR activation (Aluru and Vijayan, 2007), but it is unknown as to whether this effect is conserved in teleosts in general or in the zebrafish specifically. The mechanism of GR-mediated suppression of transcription has been studied in mammalian models and appears to act via monomeric interaction of the ligand-receptor complex with other transcription factors (Lu and Cidlowski, 2006; Bury and Sturm, 2007); however, the extent to which this occurs in teleosts remains unclear.

To attempt to verify the reliability of the fold-changes observed in the microarray analysis we selected 7 genes: *bmp7a*, *f5*, *ff1d*, *mc1r,* for qPCR confirmation (Figure 4). All 7 genes showed the same direction of fold-change and were often quite close in magnitude (Table 7), and all genes were

statistically significant, even in the one case where the microarray result was not (*bmp7a*, despite a large fold-change). This finding indicates that the microarray was an accurate measure of changes in global gene expression and our analysis is likely to be overly conservative in the number of genes we assess as we have mainly limited our observations and discussion to genes that were at or close to statistical significance. It should be noted that these transcripts results allowed us to identify candidate genes for hypothesis testing and for functional characterization using protein expression. Our results cannot confirm whether protein expression would follow the same trend as transcript abundance as we had no access to tools to measure expression of these proteins in zebrafish. Study of changes in protein content of the GR-responsive transcripts described here should be an area of immediate investigation.

4.5.1 Confirmation that the BMP signaling pathway is GR responsive

We have previously indicated that the BMP signaling pathway is suppressed in response to GR knockdown (Nesan et al., 2012 [Chapter 2]), and this may serve to explain some of these inhibitory effects of GR knockdown on global gene expression in zebrafish embryos. BMPs are important developmental morphogens that regulate developmental gene expression via the action of the smad family of intracellular transcription factors (Miyazono et al., 2005). In addition to the previously identified GR-responsive BMP ligands *bmp2a*, *bmp2b*, *bmp4*, in this study we find other members of the BMP signaling pathway that were significantly affected by GR knockdown. The microarray findings identified several novel BMP ligands and receptors that were affected by GR knockdown, including the ligands *bmp3*, *bmp6*, *bmp7a*, and the receptors *bmpr1ab*, and *bmpr1b*. All of these genes were significantly downregulated at 24 hpf (fold-changes and p-values listed in Appendix C), and we further confirmed these findings by quantifying *bmp7a* expression via qPCR (Figure 4A, Table 7). The expression of *bmp7a* showed a large fold-change reduction by microarray analysis, but was not statistically significant; however, qPCR both confirmed the large reduction and was statistically significant as well. It should be noted that in addition to the significantly downregulated genes listed above, all but one of the measured fold-changes for BMP ligands and receptors (17 total genes at two timepoints) showed downregulation, and several were near statistical significance ($p \leq 0.1$), such as *bmp3*, *bmp7b, bmp8,* and *bmper*. The combination of these measures and the finding that the *bmp7a* is significantly reduced when examined via qPCR implies that the reduction in BMP ligand and receptor expression may be more extensive than previously expected. The expression of the intracellular smad genes that transduce signals from BMP receptor binding (Miyazono et al.,

2005) also show a similar trend of suppression. Specific smad genes were significantly downregulated at 24 hpf, such as *smad2* and *smad7*, as well as *smad1*, which was also significantly reduced at 36 hpf. It should be noted that some smad genes were increased by GR knockdown to varying degrees: *smad 3a*, *smad3b*, and *smad7*. However, these genes have been shown to be linked together to repress BMP signal transduction, as *smad3* regulates *smad7*, which has an inhibitory effect on the binding of other smad proteins to DNA (Pogoda and Meyer, 2002; Zhang et al., 2007). Therefore, despite upregulation of some smad genes, our findings remain consistent with a cohesive suppression of the BMP signaling pathway in response to GR knockdown. Together, these results indicate a strong disruption of BMP-mediated functions and BMP-responsive genes. BMP signaling regulates a variety of important developmental processes, including dorsoventral patterning and initial mesodermal differentiation (Nikaido et al., 1997; Pyati et al., 2005), as well as later morphogenic developments such as angiogenesis, myogenesis, and organogenesis (Brand, 2003; Chung et al., 2008; Patterson et al., 2010). These results are striking and intriguing, and the implications for GR control of the BMP pathway naturally lead to questions about the influence of maternally deposited cortisol and glucocorticoid receptor transcripts and proteins at initial fertilization, as BMP signaling is involved in early patterning and developmental cell fate determinations (Nikaido et al., 1997; Tiso et al., 2002).

4.5.2 Novel pathways identified for the GR knockdown phenotype

In addition to confirmation of the reduction in BMP signaling, other previously established aspects of the GR knockdown phenotype were supported by microarray analysis. At both 24 hpf and 36 hpf, the Ingenuity Pathway Analysis (IPA) software identified pathways leading to skeletal/muscular disorders as being severely affected by GR knockdown (Tables 5 and 6). This supports previously published characterizations that displayed disrupted mesoderm formation, somitogenesis, and tail extension in GR morphant embryos (Pikulkaew et al., 2011; Nesan et al., 2012 [Chapter 2]). There were several major muscle proteins among the genes that were significantly changed at both timepoints (Table 4), including myosins (*mylz2*, *mylz3*), troponins (*tnnt1*, *tnnt3a*, *tnnt3b*), titins (*ttna*, *ttnb*), and tropomodulin (*tmod4*). All of these genes were significantly upregulated at both timepoints, further supporting and reinforcing the role of GR as a regulator of myogenesis. Muscle metabolic genes were also affected, such as phosphofructokinase (*pfkma*) and creatine kinase (*ckma*), which were upregulated at both timepoints. Together these results indicate that both muscle differentiation and muscle activity are increased in response to GR knockdown, although the coordination of this

activity remains unclear. Previously we identified myostatin b (*mstnb)* as downregulated in response to GR knockdown (Nesan et al., 2012 [Chapter 2]), but in this study the microarray results for *mstnb* were not conclusive. There were six different oligos for *mstnb*, and while all showed downregulation at 24 hpf, none were statistically significant and only two showed p-values less than 0.1. At 36 hpf, two of the spots showed statistically significant increases (fold changes: 2.6 and 3.36) but the remaining 4 spots showed only small increases or decreases without any statistical significance, making it difficult to assess the reliability of the oligos that displayed increases. The mechanism of GR-mediated myogenesis remains a key area for further study as it is a novel finding only found to date in teleosts and may point to possible conserved mechanisms or areas of interest in the early development of higher vertebrates. Alongside the changes to skeletal muscle genes, we also saw consistent disrupted expression of cardiac muscle structural genes at both timepoints (Table 4), including structural fibre proteins (*mylk3*, *tnnc*), atpases (*atp2a1*, *atp2a2a*), and the cardiac transcription factor *pdlim7* (Camarata et al., 2010). Previously, we have shown that exogenous cortisol administration disrupted zebrafish cardiac development, and identified some key genes that were downregulated in response to increased embryonic cortisol (Nesan and Vijayan, 2012b [Chapter 3]). Our findings in this study point to a complex regulation of cardiac development by glucocorticoid signaling. Most of the genes listed above were upregulated, which is expected if cortisol signaling is an inhibitor of cardiac development as our previous study suggested (Nesan and Vijayan, 2012b [Chapter 3]). However, certain genes were downregulated here in response to GR knockdown, including *atp2a2a*, the calcium ATPase that was shown to also be suppressed by increased cortisol administration, as well as *nkx2.5*, the cardiac transcription factor also previously shown to be reduced in response to increased cortisol, which was also significantly reduced at 24 hpf (Appendix C Table C1, fold change 0.53). The observed changes in these genes were unexpected, and raise some questions as to the mechanisms of cortisol action on cardiogenesis. It is possible that activation of the mineralocorticoid receptor (MR) may be involved in the disrupted cardiogenic effects of increased embryonic cortisol. The function of the zebrafish MR is unknown, but cortisol will bind and activate the receptor *in vitro*, although the extent of *in vivo* action is unclear (Pippal et al., 2011). MR is known to be expressed in mammalian heart tissue and is involved in cardiac muscle hypertrophy (Okoshi et al., 2004), but whether it has any effects on cardiac muscle tissue in zebrafish or other teleosts remains unknown. It should be noted that the GR knockdown phenotype did not display cardiac edema, but there was no observable blood flow in the morphant embryos at any point in development (Nesan and Vijayan, unpublished). It is unclear whether this lack of blood flow was due

to disrupted cardiogenesis or abnormal vascularization, but the microarray results imply that disrupted angiogenesis may also occur in GR morphants. The vascular transcription factor *vegfab* was moderately upregulated at both 24 hpf and 36 hpf (Table 4). Knockdown of *vegfab* inhibits angiogenesis and hematopoiesis (Bahary et al., 2007); however, no studies have tested the effects of overexpression of *vegfab* on the developing zebrafish embryo. Our findings also show a sustained upregulation of two clotting factors, *f5* and *f7i*, presenting a possible mechanism for the lack of blood flow in morphant embryos. If clotting factors are overexpressed, it may impede blood flow or prevent extension of developing vasculature. We further confirmed the upregulation of *f5* by qPCR (Figure 4B). A linkage between VEGF and clotting factors has been established in mammalian models (Nagy et al., 2007) and while VEGF is known to induce hematopoiesis in zebrafish (Liang et al., 2001; Bahary et al., 2007), it is unclear whether it regulates clotting factors for this action. Angiogenesis in the zebrafish embryo is a complex process and there exist numerous subpathways and genes of interest that GR may affect, but the sustained upregulation of *vegfab* implies that glucocorticoid signaling likely plays a role in modulating this critical developmental process, and possibly explains the lack of circulation in GR morphants.

4.5.3 Neurogenesis and eye formation affected by GR knockdown

An unanticipated pathway identified by IPA software was nervous system development, which was ranked as the most strongly affected by GR knockdown (Tables 5 and 6, Figures 5A and 5B). The IPA analysis also determined that the overall quantity of neurons would be increased at 36 hpf. This outcome is reflected in the consistent upregulation of key genes involved in neurogenesis at both observed timepoints (Table 4). These include zebrafish homologs of the classical proneural gene *atonal* from Drosophila (*atoh2a*, *atoh2b*). These two genes are also known as *neurod6a* and *neurod6b*, and a third neurogenic differentiation gene (*neurod4*) was also shown to be upregulated at both timepoints. These genes are expressed in the zebrafish olfactory bulb (Liao et al., 1999; Kuo et al., 2005), and play a role in vertebrate retinal patterning (Bassett and Wallace, 2012), indicating that glucocorticoid signaling may play a role in mediating the formation of sensory apparatus and receptors. Retinal malformation may also occur as a result of the disrupted expression of *sox9b*, which was one of the rare genes that displayed differential changes among the timepoints, as it was downregulated at 24 hpf (Table 4, fold change 0.39) and upregulated at 36 hpf (Table 4, fold change 1.95). Numerous *sox9* targets have been identified, including cartilage and the pectoral fin, but analysis of *sox9* mutants showed a linkage to retinal neurogenesis in zebrafish (Yokoi et al., 2009).

The effects of GR knockdown on genes associated with retinal development is of particular interest as some of the most strongly upregulated genes at each timepoint were lens crystalline proteins (Tables 5; *cryba2a*, *cryba4*, *crygm2a*, *crygm2b*). Initial characterizations of the GR morphants did not indicate any noticeable effects on eye formation (Pikulkaew et al., 2011; Nesan et al., 2012 [Chapter 2]). However, as the morphant embryos were only studied until 48 hpf and were developing at a slower pace (Nesan et al., 2012 [Chapter 2], there may have been changes to lens or retinal formation that were not readily apparent. In zebrafish lens development, crystallins are the most abundant proteins, and are subdivided into three groupings, alpha-, beta-, and gamma-crystallins (Posner et al., 2008). The beta-crystallins, such as *cryba2a* and *cryba4*, are expressed mainly during embryogenesis and gamma-crystallins, such as *crygm2a* and *crygm2b*, are expressed more prominently after embryogenesis in the lens of the juvenile zebrafish (Greiling et al., 2009). Alpha-crystallins tend to dominate in the mature and aging zebrafish lens (Greiling et al., 2009). The only alpha-crystallin to be significantly affected by GR knockdown, *cryaba*, was downregulated at 36 hpf (fold change 0.35). This result implies that lens formation and/or maturation may be a glucocorticoid sensitive process, as cortisol-GR signaling may control the switch from beta/gamma crystalline abundance in development to alpha-crystallin predominance during aging. The reduction of *cryaba* with GR knockdown indicates that it may be under direct glucocorticoid control in zebrafish, a linkage that has already been identified in mammalian cell culture models (Scheier et al., 1996). In mammals, the alpha-crystallins are expressed in various extracellular regions where they act as small heat shock proteins (HSP) to protect cells from damage due to heat and metal stress. Alpha-crystallins do not seem to accumulate outside of the lens in zebrafish (Posner et al., 1999), and although some isoforms appear to be responsive to heat-shock, their localization remains unclear (Elicker and Hutson, 2007). The function of glucocorticoid influence on lens proteins requires further study, to our knowledge there have been no studies linking beta- or gamma-crystallins to the stress response, so GR influence on them may be only for the purposes of lens development. At this stage, the linkage of GR to alpha-crystallins may be either part of the aging process for the lens or for an independent HSP-related action, and presents an intriguing area for future study.

Another key class of neurogenic genes that are affected by GR knockdown are the LIM-domain proteins, three of which (*ldb3a*, *ldb3b*, *lhx1b*), were all significantly up-regulated at both observed timepoints (Table 4) and are all involved in brain development. The two LIM domain binding proteins (*ldb3a* and *ldb3b*), are anterior CNS markers during development (Toyama et al., 1998) and *lhx1b* (also known as *lim6*) is a telencephalon marker (Toyama and Dawid, 1997).

Together, the overexpression of these genes is consistent with the predicted results of the IPA software of increased neuronal development. A second telencephalonic marker, *lhx6*, was also found to be significantly upregulated at 24 hpf (fold change 3.3; Appendix C Table C1), and was very close to a statistically significant increase at 36 hpf (fold change 6.8, p-value 0.053). The only other LIM-domain related gene that was statistically significant at either timepoint, *lhx8*, showed only a modest decrease at 24 hpf (fold change 0.76; Appendix C Table C1). In addition to these telencephalon markers, the hypothalamic marker *otpb* was significantly upregulated at both timepoints. The hypothalamus develops from the diencephalon and *otpb* is necessary for the development of hypothalamic dopaminergic neurons (Blechman et al., 2007; Ryu et al., 2007). Also, *otpb* seems to be specific to only these cells as morpholino knockdown did not disrupt forebrain patterning (Eaton and Glasgow, 2006). The potential involvement of glucocorticoid signaling in patterning the zebrafish hypothalamus is a very interesting finding, as the hypothalamus is the initial organizer for the stress response in vertebrates, recognizing a stressor and beginning the hormone cascade that results in cortisol release from the teleost interrenal cells via the hypothalamic-pituitary-interrenal (HPI) axis (Wendelaar Bonga, 1997; Charmandari et al., 2004). The dopaminergic neurons that are regulated by *otpb* produce the trophic hormones such as corticotropin-releasing hormone (CRH; or corticotropin-releasing factor, CRF, in fish) that will act on the anterior pituitary as part of the stress response and other coordinated endocrine actions (Nesan and Vijayan, 2012c [Chapter 1]). Developmental regulation of the hypothalamus has been previously demonstrated in the ovine model where exogenous developmental glucocorticoids disrupt the stress response in the mature animal by disrupting circulating levels of corticotrophin-releasing hormone (Welberg et al., 2001). The concept of glucocorticoid priming of the stress response is well-described in birds and reptiles, where maternal deposition into the egg is hypothesized as a stress signal that prepares the fetus for adverse conditions (De Fraipont et al., 2000; Hayward and Wingfield, 2004), but whether this occurs in teleosts remains unclear. We also observe the increased expression of other prominent genes associated with the stress response, such as the ACTH precursor *pomca* (Liu et al., 2003; Miller, 2007), and *star*, the cholesterol transport protein involved in the first step of steroidogenesis (Miller, 2007), both of which were also confirmed by qPCR (Figures 4E, 4F, Table 7). Expression of *pomca* was significantly increased at 36 hpf (Table 7) and was close to statistical significance at 24 hpf (fold-change 4.37, p-value 0.068). The expression of *star* displays the same pattern in response to GR knockdown, with a significant increase at 36 hpf (Appendix C Table C2, fold-change 5.87), and a measured increase at 24 hpf that was not statistically significant (fold-change 2.14, p-value 0.117),

but this may be obscured by the conservative nature of microarray analysis. This linkage between embryonic GR, hypothalamic development, and stress axis signaling provides a putative method by which maternal cortisol, which is the sole source of glucocorticoids in the pre-hatch teleost embryo (Alsop and Vijayan, 2008; Nesan and Vijayan, 2012b [Chapter 3]), may regulate HPI axis development and its activity in adult zebrafish. A final indicator that general neurogenesis outside of the brain is also increased by GR knockdown is that expression of *sox4a*, a known mediator of spinal neurogenesis (Gribble et al., 2009), was significantly upregulated at both 24 and 36 hpf. This lends further evidence to the posited action of GR signaling as acting in an inhibitory manner upstream of neurogenesis. It remains unclear as to whether GR action would be directly inhibiting neurogenesis, or whether it may work via intermediate action on other organizing factors. Despite the lack of clarity in the mechanism of action, it appears that key developmental regulators of the telencephalon, the hypothalamus, and possibly other CNS regions, are modulated by GR signaling.

4.5.4 Effects of GR knockdown on endocrine signaling

In addition to the possible disruption of hypothalamic trophic hormone production and homeostasis from increased proliferation to dopaminergic neurons, other hormones and receptors are increased in response to GR knockdown, including arginine vasopressin (*avpl*), which has both osmoregulatory (Nielsen et al., 1995) and complex social actions (Eaton et al., 2008) in mammals, but in fish appears to predominantly act to regulate social behavior in dominant/subordinate relationships (Larson et al., 2006). Interestingly, the previously-mentioned dopaminergic neuron differentiator *otpb*, is also required for development of vasopressin-releasing cells (Eaton et al., 2008). This is an interesting linkage between GR knockdown and increased aggression via modified vasopressin expression in the brain. Numerous species of teleosts are known to adopt dominant/subordinate relationships within populations (Gilmour et al., 2005), and in trout this has been linked to differential activation in the stress response as measured by cortisol release (Pottinger and Carrick, 2001; Overli et al., 2004). Our findings in this study lead us to hypothesize that *otpb*, which is involved in development and differentiation of corticotropin-releasing factor producing dopaminergic neurons and vasopressin-expressing cells (Eaton et al., 2008; Nesan et al., 2012 [Chapter 2]), may be active in the development of this social behavior and regulate the dominant or subordinate status of individual fish. As with previous pathways, with early embryonic GR activation only occurring via maternally deposited cortisol stores, this provides a potential role for the maternal stress state and subsequent possible alterations in cortisol deposition into the oocyte to determine the social status of offspring.

Other hormones, receptors, and endocrine signaling components are also significantly upregulated after GR knockdown, but their effects in the developing embryo are more difficult to assess. Calcitonin (*calca*), the hormone produced by the ultimobranchial bodies associated with the zebrafish thyroid that regulates calcium homeostasis (Porazzi et al., 2009; Lafont et al., 2011), was found to be upregulated at both observed timepoints (Table 4). At this stage it is unclear whether the increased expression of *calca* implies a functionally increased level of calcium sequestration or an increase in the size or productive capacity of the ultimobranchial bodies, or both, but the apparent cross-regulation of other endocrine signaling axes via GR knockdown is a prominent area of future investigation. In addition, we also find genes that are classically involved in feeding and appetite to be upregulated at both timepoints, such as peptide YY (*pyya*), and the NPY receptor *npy1r* (Sundström et al., 2008; Matsuda et al., 2012), both of which were observed to increase at 24 and 36 hpf. The impact of these genes in the pre-hatch, pre-feeding embryo is unclear, but if they are modulated by GR signaling, the post-hatch impact of the previously described GR priming effects on the HPI axis may control feeding patterns. The changes we observed in the hypothalamic dopaminergic neuron marker *otpb*, if it disrupts the stress response, could then affect appetite by changing circulating levels of peptide YY or the expression of the NPY receptor. Finally, we also observed a significant increase in an insulin-like growth factor binding protein (*igfbp3*), which may in part explain the reduction in growth observed in the GR morphants (Nesan et al., 2012 [Chapter 2]). Insulin-like growth factors (IGFs) are produced by the liver and mediate the actions of growth hormone as well as having roles in early developmental patterning of the zebrafish embryo as well as notochord formation (Duan et al., 2003; Eivers et al., 2004; Zou et al., 2009). IGF binding proteins (IGFBPs) chaperone IGFs and can increase their circulating halflife, but also have complex actions as to whether they increase or decrease signaling depending on the IGF member, the tissue type, and other factors (Duan and Xu, 2005). IGFBP3 is the most common binding protein and the majority of IGFs are complexed with at least one IGFBP3 peptide, indicating that an increase in *igfbp3* expression may have a reductive effect on free IGFs available to bind to receptors and act on tissues. This is a potential explanation for the reduced body size that occurred in embryos after GR knockdown (Nesan and Vijayan, 2012b [Chapter 3]), which was reversed by GR mRNA rescue indicating a GR specific effect in developing zebrafish. Additionally, it should be noted that IGFBP3 has effects independent of IGF ligands, including some aspects of skeletal development (Li et al., 2005). Part of IGFBP3 action also results from its antagonizing effects against the BMP signaling pathway (Zhong et al., 2011), and BMP1 inactivates IGFBP3 by proteolytic action (Kim et al., 2011).

While *bmp1* expression was not significantly changed in our microarray analysis, it is of interest that upregulated *igfbp3* will further suppress BMP signaling action by its inhibitory effects. Generally, between overexpression of the key hypothalamic marker *otpb* and these more disparate changes to various hormone and receptors, it appears that endocrine system disruption may be a prominent effect of GR knockdown. This supposition is also supported by the IPA software analysis, which lists disorders of the endocrine system as a major affected pathway based on the genes that were significantly altered at 24 hpf (Table 5).

4.5.5 GR knockdown disrupts expression of cell-adhesion molecules

The final major class of genes that were significantly affected by GR knockdown are those involved in cell-to-cell adhesion and the extracellular matrix. Cell-to-cell signaling, cellular assembly, and connective tissue development were among the major pathways identified as significantly affected by GR protein knockdown by IPA analysis (Tables 5 and 6). Multiple classes of cell adhesion genes showed sustained increases in expression at both timepoints, including cadherins, protocadherins, and numerous collagen fibres (Table 4). Cadherins have a variety of roles in development, mainly involving the movement of cells and tissue sheets during morphogenesis (Halbleib and Nelson, 2006), and the specific cadherins upregulated at both timepoints (*cadm2a* and *cadm4*) are among those involved in nervous system development (Pietri et al., 2008; Hunter et al., 2011). Protocadherins are a major subclass of cadherins, and have a variety of effects in development, with recent research showing prominent protocadherin expression in the nervous system, specifically at synaptic boundaries (Suzuki, 2000; Frank and Kemler, 2002). Multiple variants of protocadherin-1 (*pcdh1a4, pcdh1g18*, *pcdh1gb2*), a protocadherin-2 gene (*pcdh2ac*), and protocadherin-17 (*pcdh17*) were all significantly upregulated at both 24 and 36 hpf (Table 4). The roles of the protocadherin-1 and -2 genes are generally unknown in zebrafish, although there is evidence linking protocadherins in general to zebrafish neurogenesis, as lack of alpha-protocadherins triggers neuronal death (Emond and Jontes, 2008). Studies in mice have implicated protocadherin-1 in multiple developmental processes, including many that overlap with established GR effects from previous studies or what we have inferred from the microarray findings. These pathways include neurogenesis, cardiovascular development, angiogenesis, and organogenesis (Redies et al., 2008), and protocadherin-2 also affects neurogenesis in human fetal models (Pinky, 2004). Protocadherin-17 is the best studied of the affected genes in zebrafish, and interestingly, it is expressed prominently in the eye, and its knockdown results in reduced cell proliferation in the retina (Biswas and Jontes, 2009; Chen et al.,

2012). There is also further evidence for disrupted eye formation in GR morphant embryos, as the two connexin genes that are significantly upregulated at both timepoints, *cx23* and *cx44.1*, are both expressed in the embryonic eye (Cason et al., 2001; Cheng et al., 2003; Iovine et al., 2008). Together, the specific cadherins, protocadherins, and connexins that are upregulated in response to GR knockdown only lend further supporting evidence to our posited role of glucocorticoid signaling in neurogenesis and eye formation. Another prominent group of proteins upregulated by GR knockdown are the extracellular matrix fibril collagens. Three type I collagens (*col1a1*, *col1a2*, *col1a3*) and two type VI collagens (*col6a1*, *col6a2*) displayed sustained significant upregulation in GR morphants at both observed timepoints. The type I collagens tend to be expressed in the developing somites, and then are expressed in high abundance in the dermis tissue (Li et al., 2011) (Thiesse and Thiesse, 2004). It is unclear what the functional significance of the overexpression of these genes may be, but GR morphants did display slowed somitogenesis, and errors in ECM structure and density could contribute to this disruption, as type I collagens form the connective tissue that surrounds developing myotomal regions (Rescan et al., 2005). The upregulation of the type VI collagens appear to be more functionally relevant to the GR morphant phenotype. Knockdown of *col6a1* in zebrafish embryos results in muscle disorders and motor abnormalities (Telfer et al., 2010). In GR morphants, we observed a marked reduction in movement as they approached the normal period of hatching compared to control embryos (Nesan & Vijayan, unpublished), and there is theoretical potential for this to be caused by *col6a1* upregulation. However, this is only supposition at this point and requires further study. Additionally, studies in mice have found congenital heart defects resulting from overexpression of *col6a2*, although this requires the co-overexpression of other molecules (Grossman et al., 2011). No evidence for this kind of effect has been observed in zebrafish, so it remains unclear as to whether type VI collagen overexpression may contribute to the previously described cardiogenic disruptions in GR morphant embryos.

4.5.6 Conclusions

Clearly, from the breadth of this discussion, the microarray analysis of global gene expression in response to GR knockdown has provided a wealth of information and yielded numerous areas that require further investigation. In general, this study provides a number of novel genes, pathways, and processes involved in development that are affected by GR protein expression. We have found multiple major groupings of genes that support and help to explain the previously established GR knockdown phenotype and other effects of modulated GR signaling in the newly fertilized zebrafish

embryo, such as myogenic, cardiovascular, and angiogenic disruption as well as the widespread suppression of BMP signaling molecules and receptors. In addition, we have identified some unexpected developmental pathways that appear to be significantly affected by loss of GR signaling, such as neuronal differentiation, hypothalamic development, and eye formation. Altogether, this study provides strong evidence further supporting the growing consensus that developmental glucocorticoids are important developmental regulators, and that the glucocorticoid receptor is a critical morphogen that modulates a variety of important developmental processes.

4.5.7 Acknowledgement

This study was funded by a Natural Sciences and Engineering Research Council of Canada Discovery grant to MM Vijayan.

Chapter 5

Maternal cortisol is critical for stress axis development in zebrafish

5.1 Overview

Cortisol is the primary circulating glucocorticoid in teleosts. It is released from the interrenal tissue and functions in post-hatch animal to respond to stressor exposure, including energy substrate mobilization. This steroid is secreted by the coordinated activation of the hypothalamic-pituitary-interrenal (HPI) axis, involving the release of corticotropin-releasing-factor from the hypothalamus and adrenocorticotrophic hormone from the anterior pituitary. This stress response is generally highly conserved in vertebrates. There is a growing body of evidence that cortisol signaling, mediated by binding and activation of the glucocorticoid receptor (GR), is critical to the development of the pre-hatch zebrafish embryo. Cortisol synthesis does not begin until hatching in zebrafish, so maternal deposition is the only source of the ligand for early GR activation. In this study, we modulated the amount of embryo cortisol available at fertilization. We increased embryonic cortisol content by injection of exogenous cortisol. Also, we reduced maternal cortisol content by use of a cortisol antibody to sequester the steroid in the yolk. Characterization of the phenotype revealed distinct treatment effects, including mild cardiac edema with cortisol excess and deformed mesoderm and tail structures with cortisol reduction. Also, compared to wild type embryos, excess cortisol led to longer embryos at both 48 and 72 hours post fertilization (hpf), while lower cortisol content resulted in shorter embryo at 48 hpf only. Cortisol antibody embryos also showed impaired straightening of the tail at 72 hpf, remaining curled around the yolk. There was a clear difference in the post-hatch cortisol stress response between the two treatments. Elevated embryo cortisol content completely abolished the stressor-mediated cortisol increase seen in the wildtype zebrafish. The sequestering of maternal cortisol had the opposite effect, displaying a heightened cortisol response to stress. These changes were correlated with altered expression of key HPI axis genes, including *crh, 11β hydroxlase, pomca, star*, which were all downregulated in embryos injected with exogenous cortisol, and upregulated in those that experienced reduced cortisol during embryogenesis. Altogether, maternal cortisol is essential for mesoderm formation and muscle development and dysregulation of embryo cortisol content will lead to abnormal stress axis functioning in zebrafish.

5.2 Introduction

The HPI axis is a coordinated set of organs that sense and respond to stressor insult in teleost fish (Wendelaar Bonga, 1997). The hypothalamus is the site of initial stressor recognition, resulting in the release of corticotrophin-releasing factor (CRF) from dopaminergic neurons (Mommsen et al., 1999; Machluf et al., 2011). CRF acts on the anterior pituitary gland by binding to receptors on cells that

release adrenocorticotrophic hormone (ACTH) into circulation. ACTH binds to the melanocortin 2 receptor (MC2R) expressed on the steroidogenic cells of the interrenal tissue to induce the release of cortisol (Mommsen et al., 1999; Nesan and Vijayan, 2012b [Chapter 1]). The interrenal tissue is analogous to the adrenal gland in higher vertebrates (Liu, 2007) and cortisol is the primary circulating glucocorticoid in fish. Cortisol has a variety of effects in teleosts, but its most well-studied function is to enhance metabolism and mobilize energy stores needed to restore homeostasis (Mommsen et al., 1999).

Recently, studies have described a number of unexpected roles for glucocorticoid signaling in developing zebrafish embryos that are unrelated to the established functions of the HPI axis and the conserved vertebrate stress response (reviewed in Nesan and Vijayan, 2012b [Chapter 1]). Knockdown of GR protein translation in the newly-fertilized zebrafish embryo disrupted multiple developmental processes such as somitogenesis, myogenesis, and reduced overall growth and survival (Pikulkaew et al., 2011; Nesan et al., 2012 [Chapter 2]). Also, exogenous cortisol administration led to disrupted heart formation and the downregulation of key genes involved in cardiac development (Nesan and Vijayan, 2012a [Chapter 3]). Other studies have also linked larval craniofacial development and osmoregulation to glucocorticoid signaling in the zebrafish embryo (Hillegass et al., 2008; Kumai et al., 2012). Altogether, these findings position GR as a major developmental morphogen and key mediator of embryogenesis.

Glucocorticoid receptor transcripts are found in the newly-fertilized embryo, although there is a complete turnover of maternally deposited transcripts just after the mid-blastula transition, and newly produced GR mRNA and protein is widespread in the embryo by 12-24 hpf (Nesan et al., 2012 [Chapter 2]). Cortisol is also maternally deposited into the zebrafish oocyte prior to spawning and fertilization, but it persists in diminishing quantities until *de novo* cortisol synthesis and accumulation begins at approximately 48 hpf and rises dramatically after hatching (Alsop and Vijayan, 2008; Nesan and Vijayan, 2012a [Chapter 3]). This lack of early cortisol synthesis indicates that the identified GR effects, to the extent that they are mediated by classical GR signaling after binding and activation by cortisol, are dependent entirely on the maternal deposition of cortisol prior to fertilization.

The factor limiting cortisol synthesis in the developing zebrafish embryo is unclear. The coordinated response to stress is not inducible in zebrafish until 72 hpf, but the three organs of the HPI axis all begin to differentiate and organize relatively early in embryogenesis (Nesan and Vijayan, 2012b [Chapter 1]). The CRF-producing neurons are fully developed by 36 hpf, and CRF is detectable from

fertilization onwards (Alderman and Bernier, 2009; Machluf et al., 2011; Nesan and Vijayan, 2012b [Chapter 1]), as are the ACTH corticotropes of the anterior pituitary, which are differentiated by ~26 hpf (Liu et al., 2003; Nesan and Vijayan, 2012b [Chapter 1]). While the interrenal tissue is not developmentally mature until post-hatching, it is the chromaffin cells and not the steroidogenic cells that are late to form and migrate to their final position (Nesan and Vijayan, 2012b). Key steroidogenic enzymes, including 11ß-hydroxylase and StAR, are expressed in the embryo by ~28 hpf (Alsop and Vijayan, 2008; Liu, 2007; Nesan and Vijayan, 2012b [Chapter 1]), indicating that the embryo has a functional steroid biosynthesis pathway prior to hatching. With the synthesis and signaling components of the stress axis functionally developed prior to the actual ontogeny of the stress response, there remains a question as to whether HPI axis development or its post-hatch function can be affected by embryonic signals.

The concept of negative feedback in the regulation of stress axis function is well known in a variety of models, as circulating cortisol has been shown to regulate activity of the HPI axis organs in different models, including teleosts (Mommsen et al., 1999; Sathiyaa and Vijayan, 2003; Veillette et al., 2007) and mammals (Bradford et al., 1992; Dallman et al., 1992; Gómez et al., 1998). Numerous studies also link neonatal stress or diminished maternal care with long-term patterning of the stress response (Francis et al., 1996; Caldji et al., 2000; Fish et al., 2004). Additionally, there is established evidence from mammalian models that levels of circulating glucocorticoids during development can affect the functioning of the stress axis in the mature animal, including rats, guinea pigs, and sheep (Kapoor, 2006; Kapoor et al., 2008). Finally, in the fields of bird and reptile physiology, there is research indicating that the deposition of glucocorticoids into the yolk of eggs by the mother may serve as a regulatory signal during development to prepare offspring for potentially stressful conditions (Hayward and Wingfield, 2004; Cadby et al., 2010).

Against this background of extensive information about stress axis development and regulation from a variety of models and the growing body of knowledge regarding the role of glucocorticoid signaling in zebrafish development, we hypothesized that maternally deposited cortisol can regulate HPI axis development in zebrafish embryos. To test this, we used microinjection techniques to alter the levels of cortisol available to the developing zebrafish embryo after fertilization. We used a commercially available cortisol antibody to sequester cortisol in the yolk of embryos, thereby reducing maternal cortisol content for the developing embryos. Also, we microinjected cortisol (as we have done previously, Nesan and Vijayan, 2012a [Chapter 3]) into the yolk of embryos to artificially elevate

cortisol content in the developing embryos. By examining the expression of key genes involved in HPI axis organogenesis and function throughout development as well as assessing the larval stress response, this paper for the first time identifies linkages between maternally deposited cortisol and long-term stress axis programming in zebrafish.

5.3 Materials and Methods

5.3.1 Zebrafish care and breeding

Care and breeding of adult zebrafish was carried out exactly as described previously (Nesan et al., 2012 [Chapter 2]). Adult zebrafish were purchased from a commercial wholesaler (DAP International, Mississauga, ON) and maintained on a 14:10 light-dark cycle in an AHAB recirculating system (Aquatic Habitats, Apopka, FL). Zebrafish care protocols were approved by the University of Waterloo Animal Care Committee in accordance with the Canadian Council for Animal Care guidelines.

5.3.2 Treatment injections

Adult zebrafish were placed in breeding traps (Aquatic Habitats) within system tanks before the onset of the dark period. Single-cell zebrafish embryos were collected from breeding tanks within 30 minutes of light exposure, and cleaned in system water prior to injection. All injections were performed exactly as described previously using a nitrogen-powered microinjector (Narishige, Japan) (Nesan et al., 2012 [Chapter 2]) . The injection treatments were as follows: undiluted cortisol antibody (MP Biomedicals, Solon, OH), previously characterized and used for radioimmunoassay studies (Ings et al., 2012); undiluted commercially available yeast-specific antibody (polyclonal rabbit anti-yeast GCN4, 200 µg/mL; Santa Cruz Biotechnology, Santa Cruz, CA); 32 pg cortisol per egg (prepared and injected exactly as characterized previously, Nesan and Vijayan, 2012a [Chapter 3]); sterile vehicle control (prepared and injected exactly as characterized previously, (Nesan and Vijayan, 2012a [Chapter 3]). GCN4 is a yeast-specific transcriptional activator with no known homolog in zebrafish (Arndt and Fink, 1986). Prior to this study, the anti-GCN4 yeast antibody was titred and characterized to assess whether it affects zebrafish embryogenesis, and no changes in embryogenesis were observed at any point, all embryos at any injection concentration were indistinguishable from wild-type embryos. This antibody was therefore accepted as a useful control against non-specific antibody effects. The vehicle control was prepared exactly as the cortisol solution (dissolving in ethanol, then evaporation and reconstituting in sterile water). In our previous study, we classified a

series of increasingly severe phenotypes for zebrafish embryos injected with 32 pg of cortisol (Nesan and Vijayan, 2012a [Chapter 3]). In this study, only embryos displaying a phenotype without major deformations ("unaffected" or "mild" in the previous study) were used for all quantitative analyses in an attempt to conservatively assess changes arising from modulated cortisol instead of secondary effects of gross malformations in embryogenesis. The injection volume for all treatments was ~1 nL, injected directly into the yolk of the fertilized embryo. After injection, embryos were reared in embryo medium (Westerfield, 2007) and incubated at 28.5 C, with fresh medium at 12 and 36 hpf, exactly as described previously (Nesan et al., 2012 [Chapter 2]). After incubation, pools of embryos were collected at 4, 12, 24, 48, and 72 hpf, flash frozen on dry ice, and subsequently stored at -80C for later analysis of cortisol concentrations and expression of key genes involved in HPI axis function.

5.3.3 Characterization of embryo phenotypes

Embryos from each treatment group were observed throughout development for changes in morphology. Previously, we categorized and characterized a phenotype associated with the injection of exogenous cortisol in one-cell zebrafish embryos and displayed embryos with increasingly severe morphogenic deformations. At 48 hpf and 72 hpf, embryos were observed and bright-field imaged with an AZ-100 dissecting microscope and DS-R1 camera (Nikon, Melville, NY). These images were then used to measure morphometrics in the developing embryos by use of the NIS-Elements software package (Nikon). Embryo growth and extension differences between treatment groups were assessed by two morphometrics: whole embryo length, and head-trunk angle, which were measured exactly as described previously (Nesan et al., 2012 [Chapter 2]).

5.3.4 Stressor exposure

At 72 hpf, larvae from each treatment group were exposed to a physical stressor to assess the functioning of the HPI axis in response to changes in cortisol concentrations in the early embryo. The stress protocol was performed exactly as described previously (Nesan and Vijayan, 2012a [Chapter 3]). Briefly, 100 larvae were placed in an 100 mL beaker containing 80 mL of embryo medium, then swirled with a plastic pipette once per second for 60 s. Embryos were then allowed to recover over a 60 minute period. Pools of 15 larvae were collected prior to stressor exposure, and at 5, 30, and 60 minutes post-stressor. Larvae were then flash-frozen on dry ice and stored at -80C for analysis of cortisol content.

5.3.5 Cortisol extraction and quantification

Cortisol was measured from treated embryos during embryogenesis (24, 48, 72 hpf), as well as from 72 hpf treated embryos that were exposed to a physical stressor (pre-stressor and 5, 30, 60 minute post-stressor). Pools of 25 embryos (24 and 48 hpf) or 15 embryos (72 hpf) were homogenized briefly (15s) with a PowerGen 125 homogenizer (Fisher Scientific, Ottawa, Canada) in 200 uL of 50mM TRIS buffer with added protease inhibitor (Roche, Laval, Canada). Cortisol was then extracted from these embryos using separation with diethyl ether via a modification of the method described previously (Alsop and Vijayan, 2008). Briefly, 1 mL of ether was added to the homogenate, which was then frozen on dry ice to isolate the aqueous phase and allow for decanting. This process was repeated for a total of three extractions and the ether was evaporated off overnight at room temperature. Cortisol quantification was performed via a commercially available colormetric cortisol ELISA (Neogen Corp, Lexington, KY) which has been used and characterized previously (Gonçalves et al., 2012; Nesan and Vijayan, 2012a [Chapter 3]), according to the manufacturer's protocols. Steroid samples were reconstituted in extraction buffer from the ELISA kit.

5.3.6 Gene expression

Expression of genes involved in HPI axis function was measured by real-time quantitative PCR (qPCR) in embryos from each treatment group at 48 hpf, in order to assess changes to the stress response capacity that resulted from modulated embryonic cortisol content. RNA was extracted via the Ribozol-chloroform extraction process (Amresco, Solon, OH) according to the manufacturer's protocols. Extracted RNA was quantified with a Nanodrop Spectrophotometer (Thermo Scientific, Ottawa, Canada). First-strand synthesis of cDNA was carried out via the High Capacity cDNA Reverse Transcription Kit (Applied Biosystems, Carlsbad, CA) with 1 ug of total RNA per sample. qPCR analysis was performed exactly as described previously (Nesan et al., 2012 [Chapter 2]), with samples run in triplicate in an iCycler iQ thermocycler using iQ SYBR green supermix as a fluorophore (both from Biorad, Hercules, CA). The genes measured were: *crh*, *gr*, *mc2r*, *mr*, *pomca*, *star*, and *11β hydroxylase*. Primer pairs, annealing temperatures, amplicon size, and references for previous characterizations of primers (if applicable) are presented in Table 1. Gene expression was quantified as described previously (Nesan et al., 2012 [Chapter 2]) using the $\Delta\Delta C_t$ method (Livak and Schmittgen, 2001) with β-actin as a housekeeping gene (values were similar across all samples).

Table 1 – Primer pair sequences, characteristics, and applicable references used for qPCR

Gene	Forward primer (5'-3')	Reverse Primer (5'-3')	Tm (C)	Amplicon size (bp)	Reference (if applicable)
crh	caccgccgtatgaatgtaga	gaagtactcctcccccaagc	60	118	n/a
gr	acagcttcttccagcctcag	ccggtgttctcctgtttgat	60	116	(Alsop and Vijayan, 2008)
11β hydrox.	tgtgctgaaggtgattctcg	gctcatgcacattctgagga	60	115	(Alsop and Vijayan, 2008)
mc2r	ctccgttctcccttcatctg	attgccggatcaataacagc	60	127	(Alsop and Vijayan, 2008)
mr	cccattgaggaccaaatcac	agtagagcatttgggcgttg	60	106	(Alsop and Vijayan, 2008)
pomca	gaagaggaatccgccgaaa	ccagtgggtttaaaggcatctc	60	107	(Kulkeaw et al., 2011)
star	tcaaattgtgtgctggcatt	ccaagtgctagctccaggtc	60	122	(Alsop and Vijayan, 2008)
β-actin	gtccctgtatgcctctggt	aagtccagacggaggatg	60	120	(Nesan and Vijayan, 2012a)

5.3.7 Statistical analysis

Statistical measures were performed using the Sigmaplot software package. Comparisons were made between cortisol injected and control injected embryos and between cortisol-antibody injected and yeast-antibody injected (control) embryos. Data are presented as mean $\pm$ standard error of the mean (SEM). Statistical comparison of cortisol concentrations during embryogenesis (24, 48, 72 hpf) and after exposure to a physical stressor (0, 5, 30, 60 minutes post stressor) were assessed by two-way ANOVA ($p<0.05$) with a Bonferonni post-hoc test. All other comparisons (early cortisol for antibody confirmation; embryo growth metrics; qPCR analysis) were made using a student's *t*-test ($p<0.05$). Where necessary, data were log-transformed to meet the assumptions of normality and equal variance, while non-transformed data are shown in the figures.

5.4 Results

5.4.1 Confirmation of antibody efficacy

To ensure that the injected cortisol antibody was able to sequester cortisol effectively, embryo cortisol concentration was measured at 4 and 12 hpf via ELISA, with injected cortisol antibody acting to outcompete the antibody utilized in the ELISA. These results are presented in Figure 1. At both 4 hpf (Figure 1A) and 12 hpf (Figure1B) there was a significant reduction (86% and 64%, respectively) in measured cortisol in embryos injected with the cortisol antibody relative to the yeast-specific antibody.

Figure 1 - Confirmation of antibody efficacy

Cortisol content in embryos injected with cortisol antibody (Cort AB) and the yeast-specific antibody (yeast AB) was measured at 4 hpf (A) and 12 hpf (B). At both timepoints, cortisol antibody injected embryos displayed a significant reduction in cortisol content as measured by ELISA, indicating active binding by the injected antibody to sequester cortisol. All data presented is mean ± SEM; * indicates significant differences (n=6 pools of 25 embryos, students t-test, $p<0.05$).

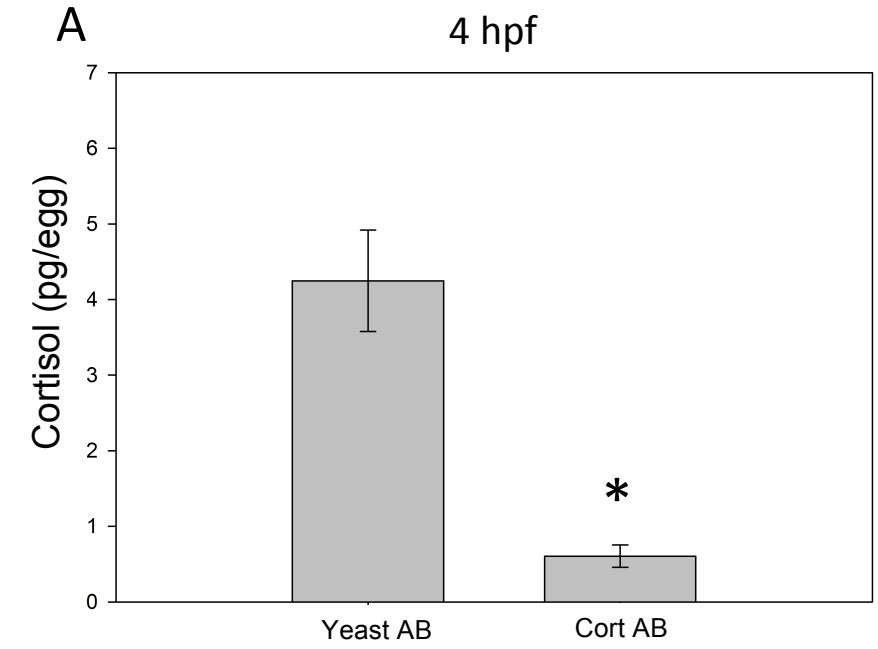
A
4 hpf
Cortisol (pg/egg)
7
6
5
4
3
2
1
0
*
Yeast AB
Cort AB

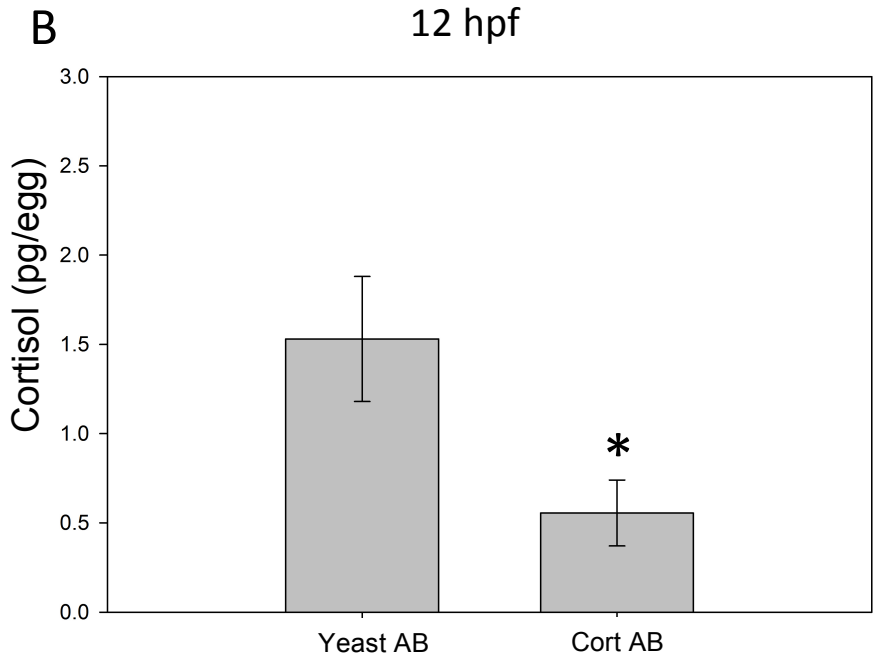
B
12 hpf
Cortisol (pg/egg)
3.0
2.5
2.0
1.5
1.0
0.5
0.0
*
Yeast AB
Cort AB

5.4.2 Observation and characterization of embryo phenotypes

Embryos were observed throughout embryogenesis for gross changes in morphology, and then imaged for further analysis via quantification of growth metrics. Representative embryo images are presented in Figure 2 at 48 hpf (A) and 72 hpf (B). The controls used in the two experiments, the vehicle-only (for cortisol-injection) and the yeast-specific antibody (for cortisol antibody-injection), showed no morphological differences at any point during embryogenesis. Morphological changes were seen with cortisol antibody injection, including moderate tail-kinking and deformed curvature (see arrows). The images presented of the cortisol-injected embryos (Figure 2) are those that showed the previously (Nesan and Vijayan, 2012a) characterized "mild" or "unaffected" phenotypes that exhibited only mild cardiac edema and no other major deformations.

Embryo growth was measured by assessing the length from head to tail at 48 hpf (Figure 3A, B) and 72 hpf (Figure 3C,D). At 48 hpf, there was a significant increase in embryo length in cortisol-injected embryos relative to controls (24% increase, Figure 3A), and this change was even more pronounced at 72 hpf (76% increase, Figure 3C). In cortisol-antibody injected embryos, there was a small decrease in embryo length at 48 hpf (19% reduction, Figure 3B), but no significant change at 72 hpf was observed. In addition to length, the angle between the eye-ear axis and the notochord was measured to assess embryo extension at 72 hpf (Figure 4). There was no change observed in cortisol-injected embryos relative to controls (Figure 4A), but cortisol antibody injected embryos had a significantly increased angle relative to yeast antibody treated embryos (Figure 4B), indicating a pronounced curvature (see Figure 2B).

Figure 2 – Representative images of treated embryos

Embryos injected with 32 pg of cortisol (CORT), vehicle control (CON), cortisol antibody (C-AB), or yeast-specific antibody (Y-AB), were imaged at 48 hpf (A) and 72 hpf (B). Representative images are presented. Cortisol-injected embryos displayed mild cardiac edema (see arrows), and cortisol antibody embryos displayed kinked tails and other disruptions in mesoderm formation (see arrows).

A

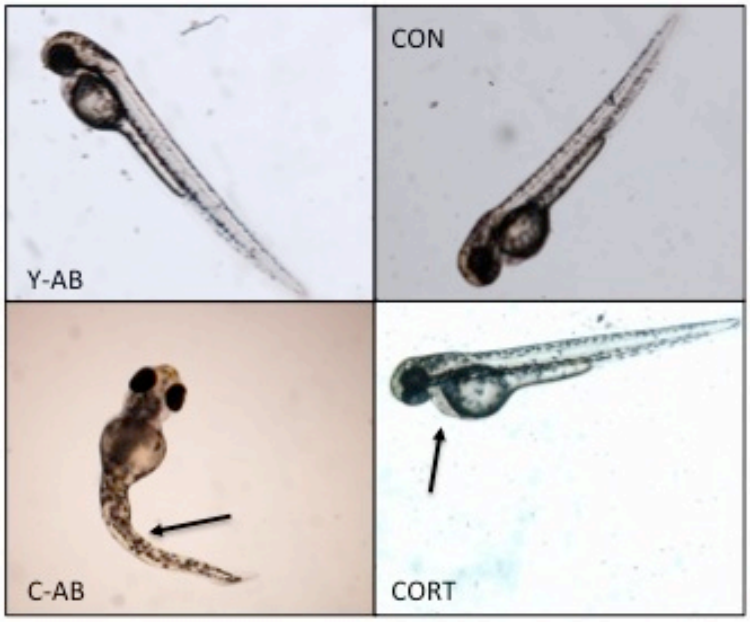

B

Figure 3 – Quantification of embryo length

Embryo growth was measured by the length from the tip of the head to the tail at 48 hpf (A,B) and 72 hpf (C,D) for embryos treated with 32 pg of cortisol or vehicle (A, C) to upregulate cortisol signaling in development, and embryos treated with cortisol antibody or yeast-specific antibody (B,D) to reduce available embryo cortisol content. Cortisol upregulation resulted in increased embryo length at both timepoints, while decreased cortisol signaling reduced embryo length only at 48 hpf. All data presented is mean ± SEM; * indicates significant differences (n=6-7 embryos, students t-test, $p<0.05$).

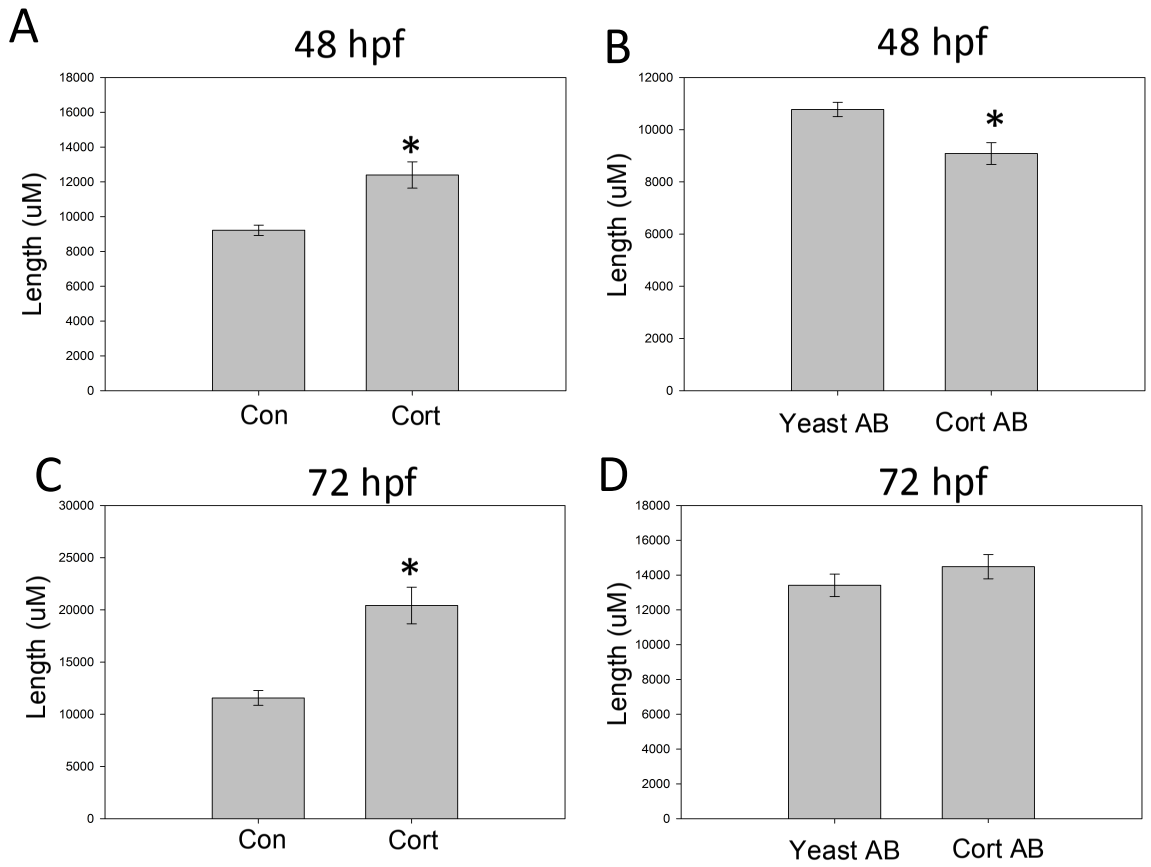
A
48 hpf
Length (uM)
18000
16000
14000
12000
10000
8000
6000
4000
2000
0
*
Con
Cort
B
48 hpf
Length (uM)
12000
10000
8000
6000
4000
2000
0
*
Yeast AB
Cort AB
C
72 hpf
Length (uM)
30000
25000
20000
15000
10000
5000
0
*
Con
Cort
D
72 hpf
Length (uM)
18000
16000
14000
12000
10000
8000
6000
4000
2000
0
Yeast AB
Cort AB

Figure 4 – Quantification of embryo extension

Embryo extension was measured by determining the angle between the ear-eye axis and the notochord in developing embryos at 72 hpf after treatment with either 32 pg of cortisol or vehicle only control (A), or with cortisol or yeast-specific antibody injection (B). Cortisol injection did not result in any change relative to control, but cortisol antibody injected embryos were less extended (indicated by a higher angle which represents a curled embryo). All data presented is mean ± SEM; * indicates significant differences (n=6-7 embryos, students t-test, $p<0.05$).

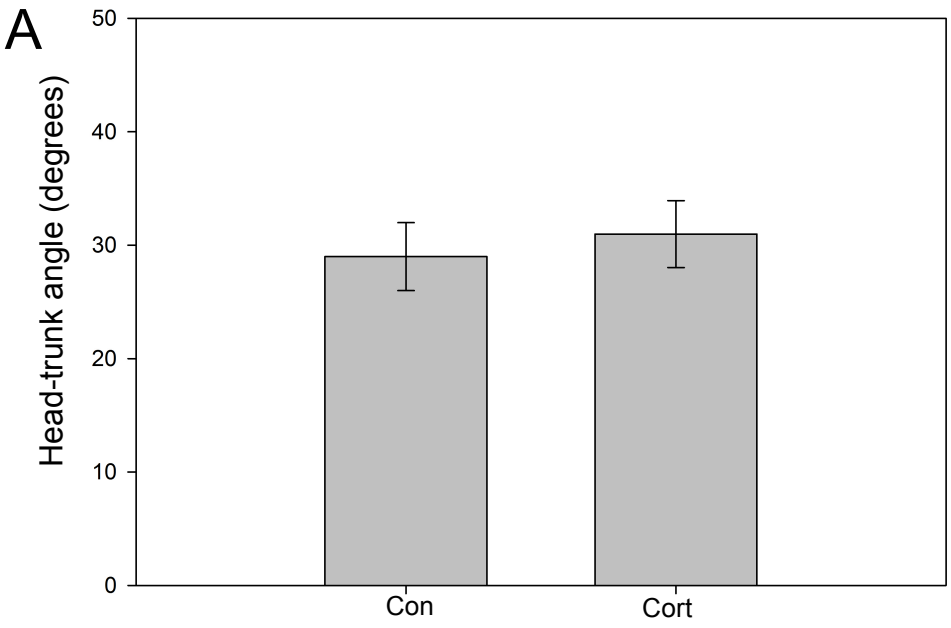
A
Head-trunk angle (degrees)
50
40
30
20
10
0
Con
Cort

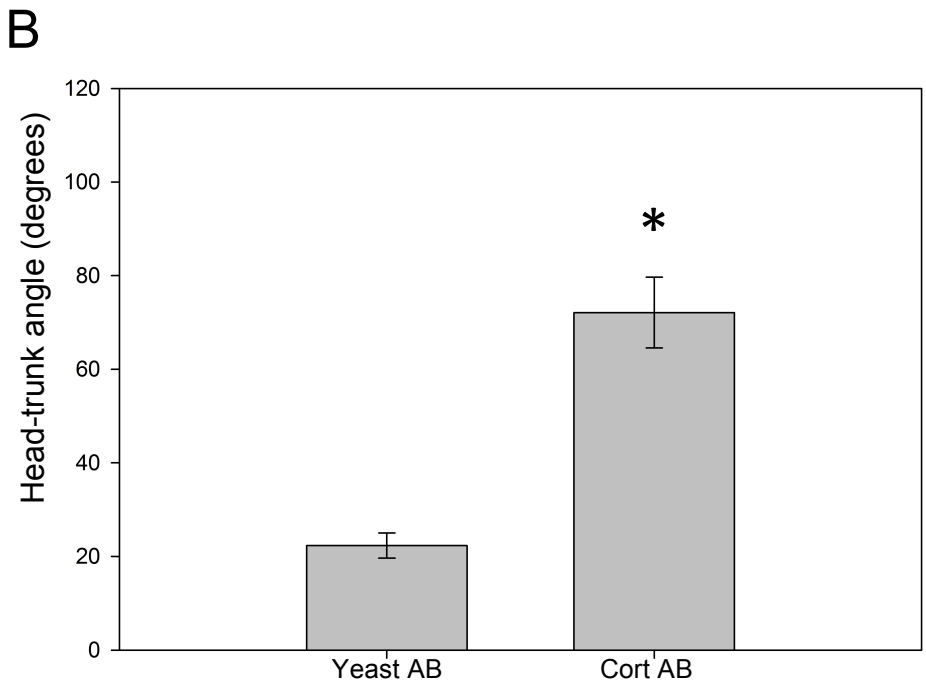
B
Head-trunk angle (degrees)
120
100
80
60
40
20
0
*
Yeast AB
Cort AB

5.4.3 Embryo cortisol concentration throughout development

Exogenous administration of 32 pg of cortisol into the newly-fertilized egg significantly elevated embryo cortisol concentration at all measured developmental timepoints (Figure 5A). At 24 hpf, control-injected embryos had 1.35 pg/egg, compared to 4.83 pg/egg in cortisol-injected embryos. At 48 hpf, control-injected embryos remained relatively constant, containing 1.76 pg/egg, and cortisol-injected embryos did not show a significant increase either at 48 hpf (6.85 pg/egg). Only at 72 hpf was cortisol significantly elevated within each treatment group, with control-embryos containing 5.8 pg/egg and cortisol-injected embryos containing 8.71 pg/egg.

Antibody treatment, which was previously shown to sequester cortisol (Figure 1), also reduced the available cortisol in the embryo at later developmental stages (Figure 5B). At 24 hpf, both the cortisol antibody injected embryos and the yeast antibody injected embryos had quite low cortisol concentrations (0.88 pg/egg and 1.26 pg/egg, respectively), but there was no statistical difference between the values. The result was the same at 48 hpf (1.22 and 1.50 pg/egg, respectively). Again it was only at 72 hpf that there was an observed difference both between the treatment groups and against the earlier timepoints. The cortisol antibody injected embryos had a significantly increased level of cortisol compared to earlier timepoints (3.46 pg/egg), as did the yeast antibody injected embryos (5.79 pg/egg; different letters in Fig. 5B indicate significance within a treatment). Additionally, at 72 hpf, the cortisol antibody injected embryos were significantly lower in cortisol concentration than the yeast antibody injected embryos (Figure 5B).

Figure 5 – Embryo cortisol content of treated embryos during development

ELISA was used to measure cortisol in the developing embryos was measured at 24, 48, and 72 hpf after treatment with either 32 pg of cortisol or vehicle only control (A), or with cortisol or yeast-specific antibody injection (B). Cortisol injection resulted in elevated cortisol content at all times relative to control injection, and both treatments were only significantly elevated at 72 hpf relative to their respective 24 hpf concentrations. All data presented is mean ± SEM; * indicates significant differences (n=4 pools of 15-25 embryos, two-way ANOVA, $p<0.05$).

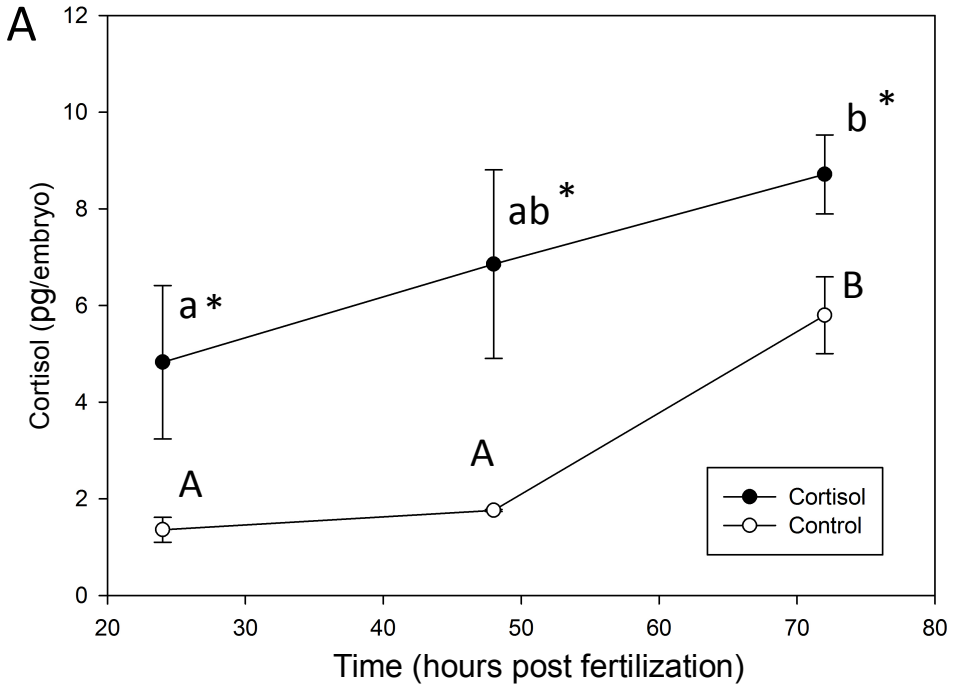
A
Cortisol (pg/embryo)
Time (hours post fertilization)
a *
ab *
b *
A
A
B
Cortisol
Control

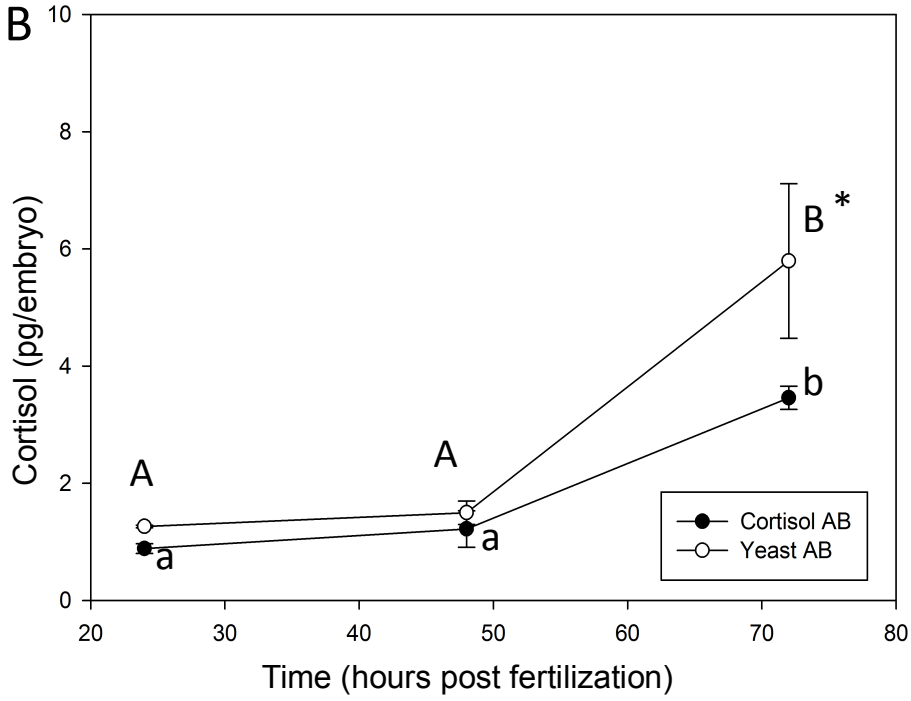
B
Cortisol (pg/embryo)
Time (hours post fertilization)
A
A
a
a
b
B *
Cortisol AB
Yeast AB

5.4.4 Quantifying the response to a physical stressor

The effects of the injected treatments on the stress response were measured by quantifying embryo cortisol concentration during recovery from an acute physical stressor. Cortisol-injected embryos displayed an abrogated stress response relative to control embryos (Figure 6A). Control embryos had an initial cortisol of 6.28 pg/egg, and showed a significant increase at 5 minutes post stressor (11.74 pg/egg), which remained elevated and relatively constant at 30 minutes (11.27 pg/egg) and 60 minutes (11.33 pg/egg) post-stressor. Cortisol-injected embryos had a higher pre-stress cortisol level (8.36 pg/egg) and did not show a stress-induced increase in cortisol at either 5 (9.11 pg/egg) or 30 (9.70 pg/egg) minutes post-stressor, and in fact showed a decrease in cortisol after 60 minutes (6.08 pg/egg).

A reduction in available embryo cortisol, on the other hand, appears to heighten and shorten the stress response (Figure 6B). Yeast antibody injected embryos had an initial cortisol concentration of 5.04 pg/egg, which was not significantly changed at 5 minutes post stressor (6.29 pg/egg), but was elevated at 30 minutes (11.33 pg/egg) post stressor and that level was maintained until 60 minutes (10.03 pg/egg) post-stressor. Cortisol antibody injected embryos had a lower pre-stress cortisol level (3.77 pg/egg) than the yeast antibody injected embryos, as was shown throughout development (Figure 5B). After stressor, cortisol levels increased significantly by 5 minutes (16.09 pg/egg) and remained elevated at 30 minutes (18.14 pg/egg) post-stressor. At both of these timepoints, cortisol antibody injected embryos had significantly higher cortisol content than yeast antibody injected embryos. By 60 minutes post-stressor, the cortisol concentration in the cortisol antibody injected embryos had returned to pre-stress levels (2.66 pg/egg).

Figure 6 – Cortisol response to a physical stressor in treated larvae

ELISA was used to measure changes in cortisol content during recovery from an acute physical stressor in embryos injected with either 32 pg of cortisol or vehicle only control (A), or with cortisol or yeast-specific antibody injection (B). Cortisol injection completely abolished the stress response relative to control embryos, with no observable rise in cortisol concentration at any time point, while control embryos. Cortisol antibody injection accentuated but shortened the stress response in comparison to yeast-specific embryos, with higher cortisol at 5 and 30 minutes post stressor, but a reduced cortisol concentration after 60 minutes. All data presented is mean ± SEM; * indicates significant differences (n=4-6 pools of 15-25 embryos, two-way ANOVA, $p<0.05$).

A

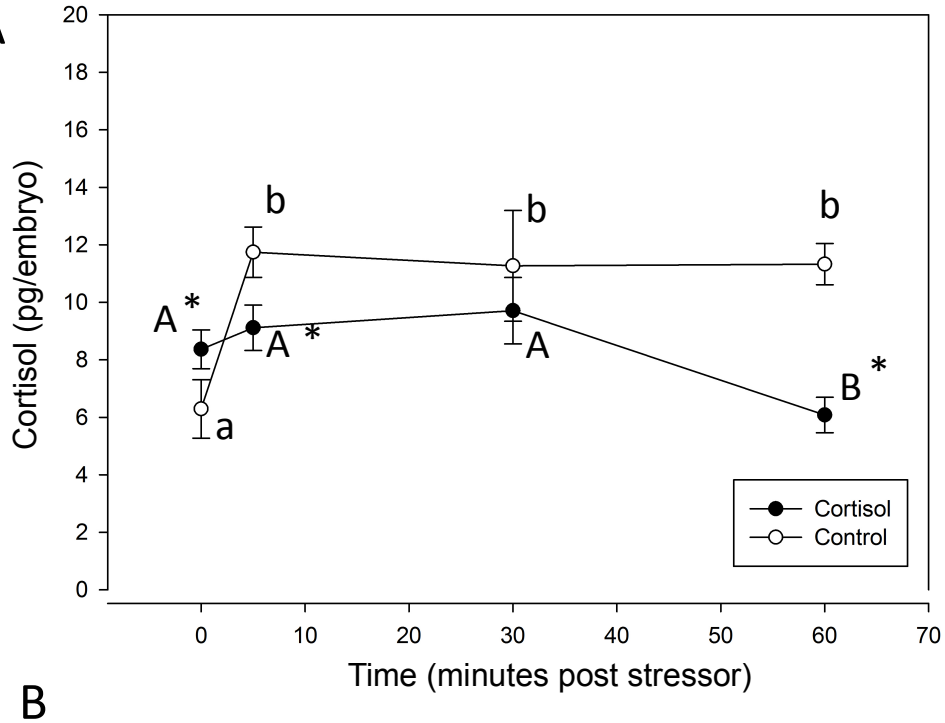
Cortisol (pg/embryo)
Time (minutes post stressor)
Cortisol
Control
A *
a
b
A *
b
A
b
B *

B

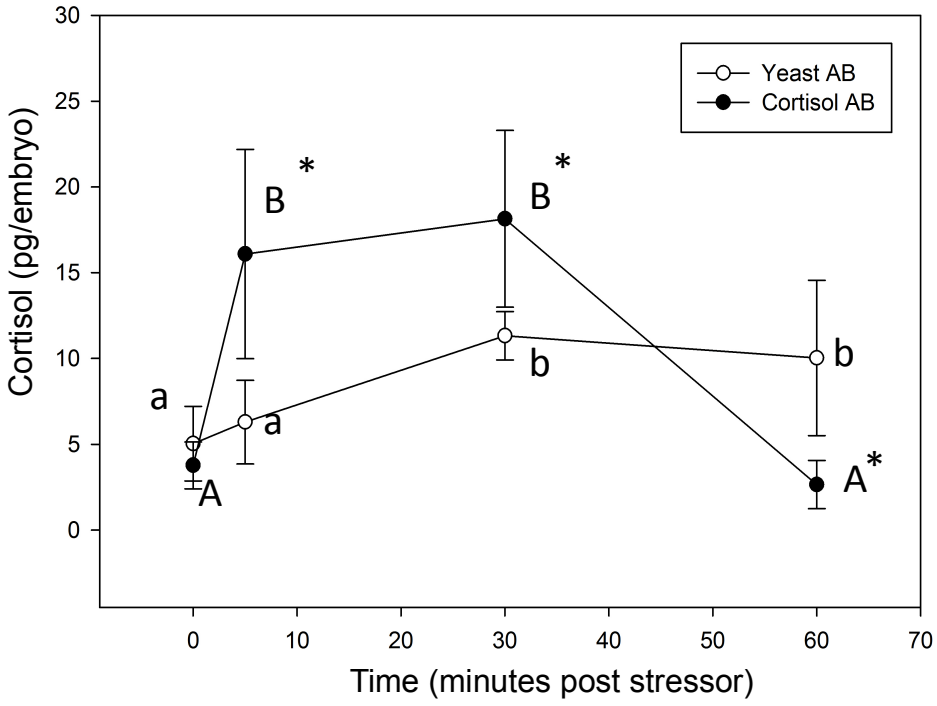
Cortisol (pg/embryo)
Time (minutes post stressor)
Yeast AB
Cortisol AB
a
A
B *
a
B *
b
b
A*

5.4.5 Expression of HPI axis genes

In order to find mechanistic linkages for the disrupted stress response in treated embryos, expression of key genes involved in the function of the HPI axis was measured by qPCR in 48 hpf embryos. These results are displayed in Figure 7, organized by gene: graphs displaying cortisol-injection effects (relative to control embryos) are in the left column; graphs displaying changes from cortisol antibody injection (relative to yeast antibody injected embryos) are on the right.

Expression of a number of HPI genes was significantly changed in cortisol-injected embryos relative to controls. Transcript abundances of *crh* (Figure 7A), *11β-hydroxylase* (Figure 7E). *pomca* (Figure 7K), and *star* (Figure 7M) were all significantly reduced in response to exogenous cortisol administration at 48 hpf. A single gene, *mc2r*, was significantly increased in cortisol-injected embryos relative to controls (Figure 7G). There was no observed change in expression of *gr* (Figure 7C) or *mr* (Figure 7I).

The reduction of cortisol content in the embryo had opposite effects for most of the observed genes. In cortisol antibody injected embryos, the expression of *crh* (Figure 7B), *11β-hydroxylase* (Figure 7F). *pomca* (Figure 7L), and *star* (Figure 7N) were all significantly increased relative to yeast antibody injected embryos. There was also a significant decrease in the expression of *mr* in response to cortisol antibody injection (Figure 7J), but no changes were observed in *gr* (Figure 7D) or *mc2r* (Figure 7H).

Figure 7 – Altered expression of HPI axis genes

Quantitative PCR was used to measure the mRNA abundance of key genes involved in HPI axis function in 48 hpf embryos. Measured genes were: *crh* (A, B), *gr* (C, D), *11B-hydroxylase* (E, F), *mc2r* (G, H), *mr* (I, J), *pomca* (K, L), and *star* (M, N). For all genes, data from embryos injected with either 32 pg of cortisol or vehicle only control are in the left column, and data for embryos with cortisol or yeast-specific antibody injection are in the right column. Expression of *crh, 11B-hydroxylase, pomca,* and *star* were all downregulated as a result of cortisol injection (relative to control embryos), and upregulated after cortisol antibody injection (relative to yeast antibody injected embryos). Expression of *gr* was unchanged by either treatment. Expression of *mr* was downregulated only after cortisol antibody injection, and expression of *mc2r* was upregulated only after cortisol injection. All data presented is mean ± SEM; * indicates significant differences (n=6 pools of 25 embryos, students t-test, $p<0.05$).

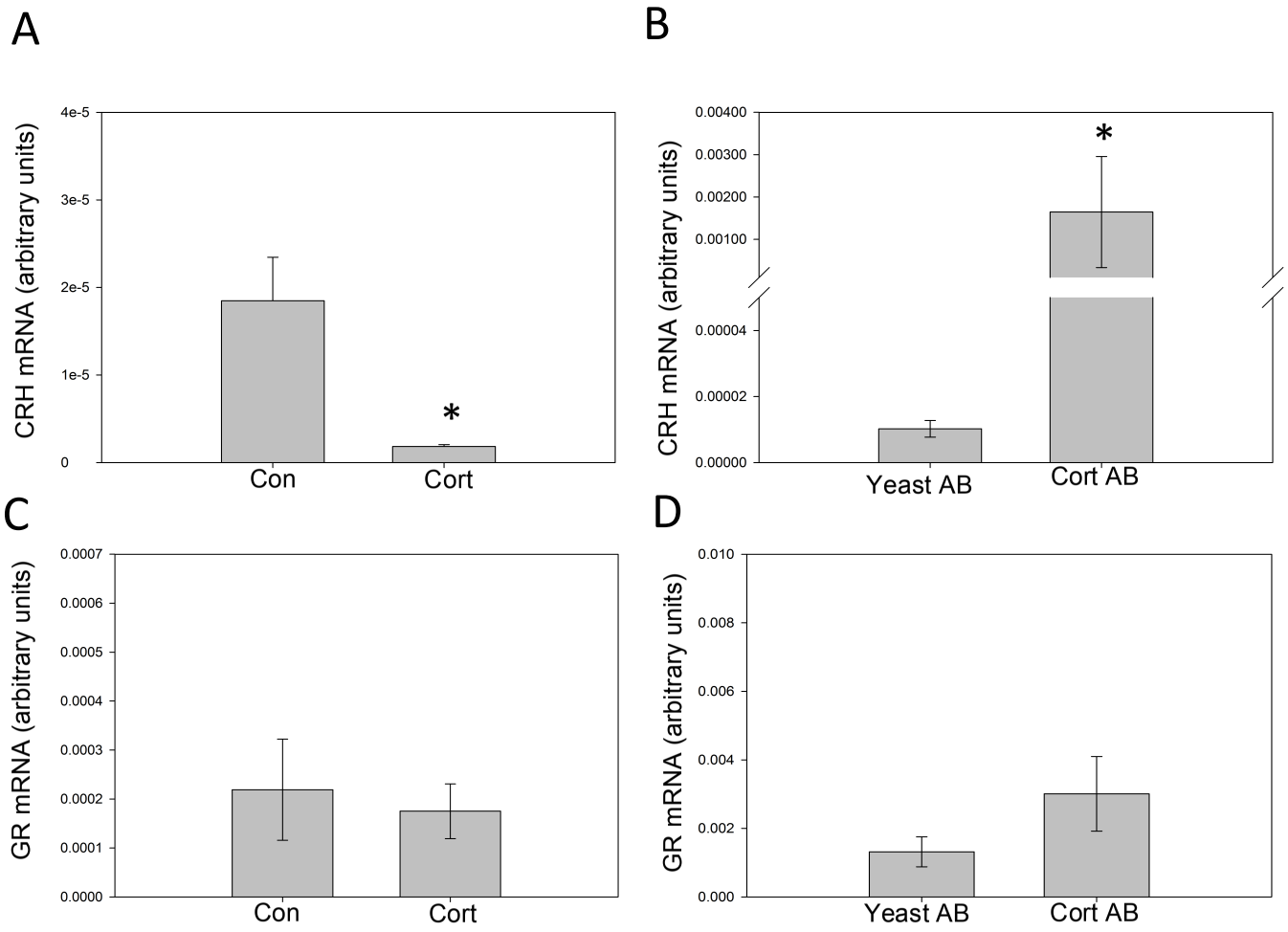
A
CRH mRNA (arbitrary units)
4e-5
3e-5
2e-5
1e-5
0
*
Con
Cort
B
CRH mRNA (arbitrary units)
0.00400
0.00300
0.00200
0.00100
0.00004
0.00002
0.00000
*
Yeast AB
Cort AB
C
GR mRNA (arbitrary units)
0.0007
0.0006
0.0005
0.0004
0.0003
0.0002
0.0001
0.0000
Con
Cort
D
GR mRNA (arbitrary units)
0.010
0.008
0.006
0.004
0.002
0.000
Yeast AB
Cort AB

E
11B-hyd mRNA (arbitrary units)
4e-5
3e-5
2e-5
1e-5
0
Con
Cort
*
F
11B-hyd mRNA (arbitrary units)
0.0006
0.0004
0.0002
0.0000
Yeast AB
Cort AB
*
G
MC2R mRNA (arbitrary units)
7e-5
6e-5
5e-5
4e-5
3e-5
2e-5
1e-5
0
Con
Cort
*
H
MC2R mRNA (arbitrary units)
3.5e-5
3.0e-5
2.5e-5
2.0e-5
1.5e-5
1.0e-5
5.0e-6
0.0
Yeast AB
Cort AB

I
MR mRNA (arbitrary units)
0.0004
0.0003
0.0002
0.0001
0.0000
Con
Cort
J
MR mRNA (arbitrary units)
0.00010
0.00008
0.00006
0.00004
0.00002
0.00000
Yeast AB
Cort AB
*
K
POMCA mRNA (arbitrary units)
0.00030
0.00025
0.00020
0.00015
0.00010
0.00005
0.00000
Con
Cort
*
L
POMCA mRNA (arbitrary units)
0.00012
0.00010
0.00008
0.00006
0.00004
0.00002
0.00000
Yeast AB
Cort AB
*

M
StAR mRNA (arbitrary units)
2.5e-5
2.0e-5
1.5e-5
1.0e-5
5.0e-6
0.0
*
Con
Cort
N
StAR mRNA (arbitrary units)
3.5e-5
3.0e-5
2.5e-5
2.0e-5
1.5e-5
1.0e-5
5.0e-6
0.0
*
Yeast AB
Cort AB

5.5 Discussion

In this study, we describe for the first time some clear linkages between the amount of cortisol available to newly-fertilized zebrafish embryos and the post-larval functioning of the stress axis, and we identify key HPI genes that are under the control of cortisol signaling during early development. Together these results demonstrate that maternally deposited cortisol is functionally relevant in the developing zebrafish embryo and can have significant impacts on the ability to respond to a stressor challenge later in life. These findings point to a putative linkage between the maternal stress state and the offspring phenotype, which has interesting ecological and evolutionary implications for the use of maternally deposited cortisol as a stress-induced signal that may pattern the developing embryo as a preparatory measure.

5.5.1 Characterization and validation of treatments

To investigate the role of maternally deposited cortisol in the fertilized zebrafish embryo, we performed two experiments in parallel. We injected exogenous cortisol into single-cell embryos to mimic increased deposition, and we used a commercially available cortisol antibody to sequester deposited cortisol in the yolk to simulate a reduced deposition load. We have previously characterized and validated the addition of 32 pg of cortisol as sufficient to elevate cortisol content until hatching (Nesan and Vijayan, 2012a [Chapter 3]), and while it is unlikely that this level of deposition can occur in natural conditions, the continued use of this model allows us to further characterize cortisol-responsive processes in development. In this previous study, we showed that 32 pg of cortisol results in upregulation of GR-responsive genes, indicating a functional increase in glucocorticoid signaling.

With the use of the cortisol and yeast-specific antibodies, we took steps to validate their use in this study. First, we saw clear reductions in the frequency and severity of the presented morphological phenotype only with cortisol but not yeast antibody (Figure 2). Furthermore, we found that the cortisol antibody significantly reduced the amount of measurable cortisol in early development (Figure 1), indicating that binding and sequestration are occurring and that it is likely that the amount of cortisol available to the embryo initially after fertilization is drastically different. This is of key importance, as previous research has shown that reduced glucocorticoid signaling (altered by knockdown of GR) results in an altered transcriptome after the mid-blastula transition, implicating cortisol signaling in the degradation of maternal mRNA (Pikulkaew et al., 2011). We also observe that the cortisol antibody shows interesting phenotypic consistencies with previously established GR morphant embryos (Pikulkaew et al., 2011; Nesan et al., 2012 [Chapter 2]), including kinked tails

(Figure 2), reduced growth (Figure 3), and slowed straightening of the tail (Figure 4) during embryogenesis. This indicates that the GR knockdown phenotype is at least partially due to a reduction of glucocorticoid signaling in the embryo as opposed to solely ligand-independent effects. As seen previously (Nesan and Vijayan, 2012a [Chapter 3]), we do not see any changes to embryo extension as a result of increased cortisol signaling in development, but there is a significant increase in growth at both 48 and 72 hpf (Figure 3). This is interesting as we see a decrease in embryo length both in the current study with the administration of cortisol antibody and in morphant embryos after knockdown of GR translation (Nesan et al., 2012 [Chapter 2]). The clear implication is that growth in the developing embryo is glucocorticoid responsive as both increases and decreases in cortisol signaling result in disrupted growth. Previous research in teleosts has shown differing relationships between cortisol and the somatostatic axis (van der Boon et al., 1991). In some cases there is a positive correlation between cortisol and growth hormone expression (Young et al., 1989; Yada et al., 2005), whereas in other situations cortisol inhibits growth (Peterson and Small, 2005; Pierce et al., 2011). To our knowledge, little is known about cortisol action on the growth of the early zebrafish embryo, and this research presents a novel relationship between embryo growth and circulating glucocorticoids.

5.5.2 Developmental cortisol dynamics in our treated embryos

As a preliminary step to assessing the effects of modulated cortisol deposition in the developing embryo, we quantified the basal embryo cortisol levels during development. We have assessed this before for the administration of 32 pg of cortisol (Nesan and Vijayan, 2012a [Chapter 3]) and our results are in general agreement. Our findings in this study also support our previous measurements of ~4 pg/egg of initial cortisol deposition (Alsop and Vijayan, 2008; Nesan and Vijayan, 2012a), indicating that the level of cortisol deposition by unstressed zebrafish mothers appears to be relatively constant. It is unclear to what extent this deposition can vary, although evidence from other teleosts suggests that stressed mothers can deposit an increased amount of steroid (Giesing et al., 2011). During normal zebrafish embryogenesis, cortisol content in the embryo decreases during the pre-hatch period from the initial deposition, with *de novo* synthesis and accumulation becoming significant only after hatching and close to feeding (Alsop and Vijayan, 2008; Nesan and Vijayan, 2012a [Chapter 3]). This pattern was not changed in embryos injected with either the cortisol or yeast-specific antibody, however the cortisol antibody reduced the measured cortisol at 72 hpf. It should be noted that this is expected to be a decrease in the available cortisol that can be measured,

due to sequestration by the antibody, as opposed to a reduction in production or an increase in cortisol turnover. However, as there are multiple feedback levels acting on the HPA in response to cortisol levels (Bradford et al., 1992; Wendelaar Bonga, 1997; Mommsen et al., 1999), there may be a natural reduction in cortisol production or accumulation in response to reduced cortisol deposition at fertilization. It is unclear as to what extent decreased overall embryo cortisol concentration would be functionally relevant at 72 hpf, but a chronic reduction in circulating cortisol can disrupt a variety of functions involving metabolism and other necessary processes (Fries et al., 2005). In humans, hypocortisolism can occur in patients with Addison's disease or other adrenal conditions, and has implications for fatigue, reduced cardiovascular health, and conditions such as fibromyalgia (Heim et al., 2000; Fries et al., 2005; Van Houdenhove et al., 2009).

5.5.3 Reduced embryonic cortisol availability enhances the larval stress response

It is particularly interesting that the sequestration of cortisol and the resulting reduced signaling seems to heighten and sensitize the cortisol response in zebrafish larvae. We observe a stronger, faster, cortisol response in embryos injected with cortisol antibody (Figure 6B). This result coincides with an increased expression of multiple genes involved in HPI axis function at 48 hpf, such as CRH (Figure 7A) and the ACTH precursor POMCA (Figure 7L), which are both necessary for triggering a cortisol response (Wendelaar Bonga, 1997). Two genes involved in steroidogenesis, StAR (Figure 7N), which is involved in initial movement of the steroid precursor cholesterol (Bauer et al., 2000), and 11β hydroxylase (Figure 7F), which is an enzyme involved in the cortisol synthesis pathway (Kawamoto et al., 1992; Alsop and Vijayan, 2008) are also increased in embryos treated with the cortisol antibody. The increased expression of these four genes indicates that these embryos that experienced lowered glucocorticoid signaling in the early embryo have an enhanced HPI signaling and steroid production capacity. It was also observed that mineralocorticoid receptor (MR) expression was decreased in the cortisol antibody treated embryos. MR can bind cortisol *in vitro*, but its exposure to the ligand in live tissues is unclear (Sturm et al., 2005; Pippal et al., 2011), and the overall role of MR in the zebrafish and other teleosts remains to be explored. However, it is interesting that decreased glucocorticoid signaling yields a reduction in MR expression, as it points to potential crosstalk between corticosteroid receptors. This study also reinforces our previous findings from knockdown of GR protein translation, which caused upregulated expression of *pomca* and the hypothalamic marker *otpb* (involved in dopaminergic neuron formation, (Blechman et al., 2007)) at both 24 and 36 hpf (Chapter 4). We observe the same change in *pomca* at 48 hpf and see an increase

in *crh* which would be expected in embryos with increased hypothalamic development. These correlations lend further support to our conclusions that the cortisol antibody administration causes a functional decrease in glucocorticoid signaling, and that this disrupts HPI axis development and function. This indicates that maternal cortisol deposition may be an important signal for patterning the HPI axis development of the embryo.

5.5.4 Exogenous cortisol addition reduces HPI axis stress response capacity

It is particularly interesting that the four genes that were upregulated in cortisol-antibody treated embryos show opposing changes with exogenous cortisol administration. All of the previously mentioned genes, *crh*, *pomca*, *star*, and *11β hydroxylase* were significantly downregulated at 48 hpf in larvae with elevated pre-hatch cortisol (Figures 7A, 7K, 7G and 7M, respectively). In addition, these larvae displayed an abrogated cortisol response after the acute physical stressor (Figure 6A), with no rise in cortisol being evident at any point. This lack of cortisol response is likely to have a large impact on the post-hatch zebrafish, which must begin feeding and competing in environments that are likely to be stressful. The four genes previously mentioned are likely responsible for the inhibited stress response, as cortisol-antibody injected embryos with low expression of *crh* and *pomca* will show reduced activation of the interrenal steroidogenic cells, and the downregulation of *star* and *11β hydroxylase* will reduce the cortisol production capacity of the cells. Altogether, this will result in reduced cortisol production in response to stress in embryos that experience increased developmental glucocorticoid signaling. It should be noted that any effects on the feedback regulation of the HPI axis in our treated zebrafish do not seem to include modulation of GR expression. In other teleosts, GR receptors at different levels of the HPI axis act to feed back and control the axis (Mommsen et al., 1999; Barton, 2002; Alderman et al., 2012), but that was not seen in the current study. Instead, we observed an alteration in expression of *crh, pomca* (produced by the hypothalamus and pituitary, respectively) in both sets of treatment and of *mc2r* (expressed in the interrenals) after upregulation of cortisol signaling, indicating that all three HPI organs may be affected by embryonic cortisol concentration. Together these results provide clues to a mechanistic linkage between embryonic cortisol deposition and HPI axis activity. We posit that glucocorticoid signaling in early development is necessary for proper formation of the hypothalamus, which can then cause long-term programming of the stress axis into maturity.

5.5.5 Potential disruptions to embryo fitness as a result of altered maternal cortisol deposition

The implications for the disrupted HPI axis function on the larval and maturing zebrafish are widespread due to the numerous roles of cortisol in teleosts (Mommsen et al., 1999; Barton, 2002). In addition to the previously mentioned roles in energy metabolism and the implications for growth, cortisol is also a major osmoregulatory hormone in fish (McCormick, 2001). The changes in cortisol responsiveness seen in our study, with cortisol antibody treatment resulting in upregulated cortisol production, and increased cortisol at fertilization having the opposite effect, implies that the ability to respond to a physical stressor may be compromised in these fish as they mature. This may present problems for larvae that are exposed to physically-challenging environments or in the context of predator exposure. In addition, a prominent emerging field in teleost study is the understanding of fish behavioral dynamics. Initial studies in trout and subsequent supporting evidence from other teleost species has linked the magnitude of the cortisol response to stress with aggression, behavior, and the establishment of dominant/subordinate relationships (Pottinger and Carrick, 2001; Gilmour et al., 2005; Barreto et al., 2009; Chang et al., 2012). Social stratification has been observed in zebrafish (Dahlbom et al., 2011), but correlations with stress responsiveness have not been established. However, if the linkage between stress-induced cortisol levels and aggression is conserved in zebrafish, there is interesting potential for maternal stress levels and steroid deposition to pattern the behavior of offspring. This concept of maternal stress hormone deposition as a phenotypic programming molecule for offspring has been established in birds and reptiles, where changes in yolk corticosterone concentration affect the post-hatch animal (De Fraipont et al., 2000; Hayward and Wingfield, 2004; Meylan and Clobert, 2005; Müller et al., 2007; Groothuis and Schwabl, 2008; Love and Williams, 2008). Clearly this is an area of zebrafish development where further exploration is required.

5.5.6 Conclusions

For the first time, our findings provide a linkage between early embryo cortisol content and the post-hatch function of the stress-axis, with measurements altered expression of key HPI genes to provide assessment of HPI organ activity. We also quantify and assess the disrupted cortisol response to stress in embryos that have experienced differential early cortisol signaling, showing that increased cortisol in the embryo suppresses the cortisol response to stress, and that lack of available cortisol at fertilization results in a heightened larval stress response. To our knowledge this is the first instance

in teleosts that maternally deposited cortisol levels have been linked to altered stress axis functioning, but this supports findings from mammalian models. In avian and reptilian models, egg corticosteroid concentration is known to alter the developing phenotype. The actions of the HPI axis in teleosts are complex and fundamental to the survival of the adult animal, underscoring the importance of these novel findings. Together, this study adds further evidence to the growing consensus that glucocorticoid signaling in zebrafish development is critically important to a variety of developmental processes and can have lasting effects in the adult animal.

5.6 Acknowledgement

This study was funded by a Natural Sciences and Engineering Council of Canada Discovery grant to MM Vijayan. We also thank Dr. Bernard Duncker and Darryl Jones for the kind donation of the yeast-specific antibody used in this study.

Chapter 6
General Conclusions

Note: portions of this chapter are reproduced with permission from {Nesan, D., and Vijayan, M.M. 2012. Role of glucocorticoid in developmental programming: Evidence from zebrafish. Gen. Comp. Endocrinol. In press. doi: 10.1016/j.bbr.2011.03.031.}

6.1 Summary of findings

Altogether, the findings from these experiments for the first time underscore a key role for maternal cortisol signaling by glucocorticoid receptor (GR) activation in zebrafish development. The results support the primary hypothesis that maternal cortisol and GR signaling have functional relevance in the early zebrafish embryo.

The first study demonstrated that GR knockdown resulted in a series of deformations and developmental delays in the early embryo, affecting somitogenesis, myogenesis and expression of muscle specific genes, and overall embryo growth and extension, and post-hatch survival (Chapter 2). Perhaps most importantly, GR signaling was shown to disrupt the expression of bone morphogenetic proteins (BMPs), implying a much more prominent role for GR signaling in the developing embryo. These characterized phenotypic changes were rescued with exogenous administration of GR mRNA further supporting our conclusion that the observed changes were GR-specific. This was the first study to demonstrate the importance of GR knockdown to embryo growth and survival and demonstrate the GR responsive nature of specific BMP genes.

This study was followed by exogenous cortisol administration to the newly fertilized embryo, causing disrupted cardiogenesis and yielding a series of phenotypes ranging from mild cardiac edema to complete lack of pericardium and no functional heartbeat (Chapter 3). These changes were linked to altered expression of key cardiogenic genes including the heart field transcription factor *nkx2.5*. In addition to morphogenic malformations of the heart, post-hatch larvae showed a reduced resting heart rate and an inhibited ability to raise heart rate in response to an acute physical stressor. This study provided a definitive linkage between the concentration of cortisol in the developing zebrafish embryo and organogenesis, specifically the development of the heart, and indicated that larval performance will be disrupted by increased zygotic cortisol.

The microarray analysis yielded a wealth of knowledge regarding the effects of GR knockdown at 24 and 36 hpf, measuring over 1000 significantly changed genes at each time point (Chapter 4). These results supported the role of GR in BMP signaling, myogenesis, and cardiogenesis that were presented in the first two chapters, as microarray fold-changes were in agreement with genes measured previously by other methods and helped to explain the previously characterized phenotypes. In addition to this support, the microarray measurements indicated a number of novel pathways and genes that were unexpectedly changed in response to lowered glucocorticoid signaling, including neurogenesis, cell adhesion, eye formation, and hypothalamic-pituitary-interrenal (HPI)

axis formation and function. Together this study displayed the critical role of GR as a developmental regulator that modulates a variety of key pathways in embryogenesis.

The potential role of maternal cortisol signaling in zebrafish HPI axis formation was explored, both in response to increased cortisol in the zygote at fertilization (achieved via exogenous administration as in Chapter 2) and also by reducing cortisol content by sequestering this steroid using antibodies (Chapter 5). In this chapter, glucocorticoid signaling was found to pattern the HPI axis, with significant changes seen in the post-hatch larval ability to increase cortisol levels in response to a physical stressor. Embryos exposed to exogenous cortisol displayed an abrogated stress response, while those that experienced a reduction in available cortisol showed a heightened cortisol peak after a stress challenge. These changes in HPI function were correlated with changes in expression of signaling molecules like *crh*, *11B-hydroxylase*, *pomca*, and *star*. This is the first study to link levels of cortisol in the newly fertilized embryo, which only occur through maternal deposition, to the development and function of the stress axis in post-hatch zebrafish larvae. This is a critical connection between the maternal environment prior to spawning and the resulting offspring phenotype.

Together, these findings add a great deal to the relative paucity of prior knowledge about glucocorticoid signaling in the early zebrafish embryo. The results from this thesis for the first time position GR as a major developmental regulator, acting upstream of key development factors such as BMPs and matrix metalloproteinases, and acting, directly or through intermediates, on a host of developmental events, including maternal mRNA degradation, somitogenesis and myogenesis, cellular migration, cardiogenesis, stress axis development, neurogenesis, eye formation, and craniofacial development (see Figure 1 for a summary). These early GR actions may have lasting effects on developmental programming as the larvae mature, influencing the ability to respond to stressor challenges by compromising osmoregulation or cardiac performance in a manner similar to the established mammalian glucocorticoid programming effects that result in hypertension or other cardiovascular defects.

Figure 1 – Summary of known glucocorticoid-responsive genes and pathways in zebrafish development

The glucocorticoid receptor (GR) is a developmental regulator that affects a variety of genes and pathways, this schematic summarizes the known processes and associated genes during early development in zebrafish (transcription factors are in bold). GR signaling affects myogenesis and modulates myogenic transcription factors and downstream muscle proteins. Specific matrix metalloproteinases (MMPs) have been shown to be GR-responsive which can affect numerous developmental processes associated with extracellular matrix remodeling, and this study has highlighted a variety of other ECM and cell adhesion proteins affected by GR knockdown. Expression of specific bone morphogenetic proteins (BMPs), receptors, and signaling molecules are also modulated by GR signaling and are involved with a variety of major developmental processes. A number of cardiogenic genes and major cardiac muscle proteins are disrupted by increased cortisol signaling, resulting in malformed heart structures and reduced cardiac performance. Osmoregulation has also been shown to be GR-mediated via the ammonia transporter *rhcg1*. Neurogenesis has been shown to be a glucocorticoid responsive process, with a variety of neural transcription factors disrupted and specific hypothalamic markers affected, along with other signaling molecules in the HPI axis response to stress. Finally, GR signaling has been implicated in maternal mRNA degradation at the mid-blastula transition, retina and lens formation, and with overall embryo growth, extension, and survival, but no specific molecular mechanisms have been linked to these effects.

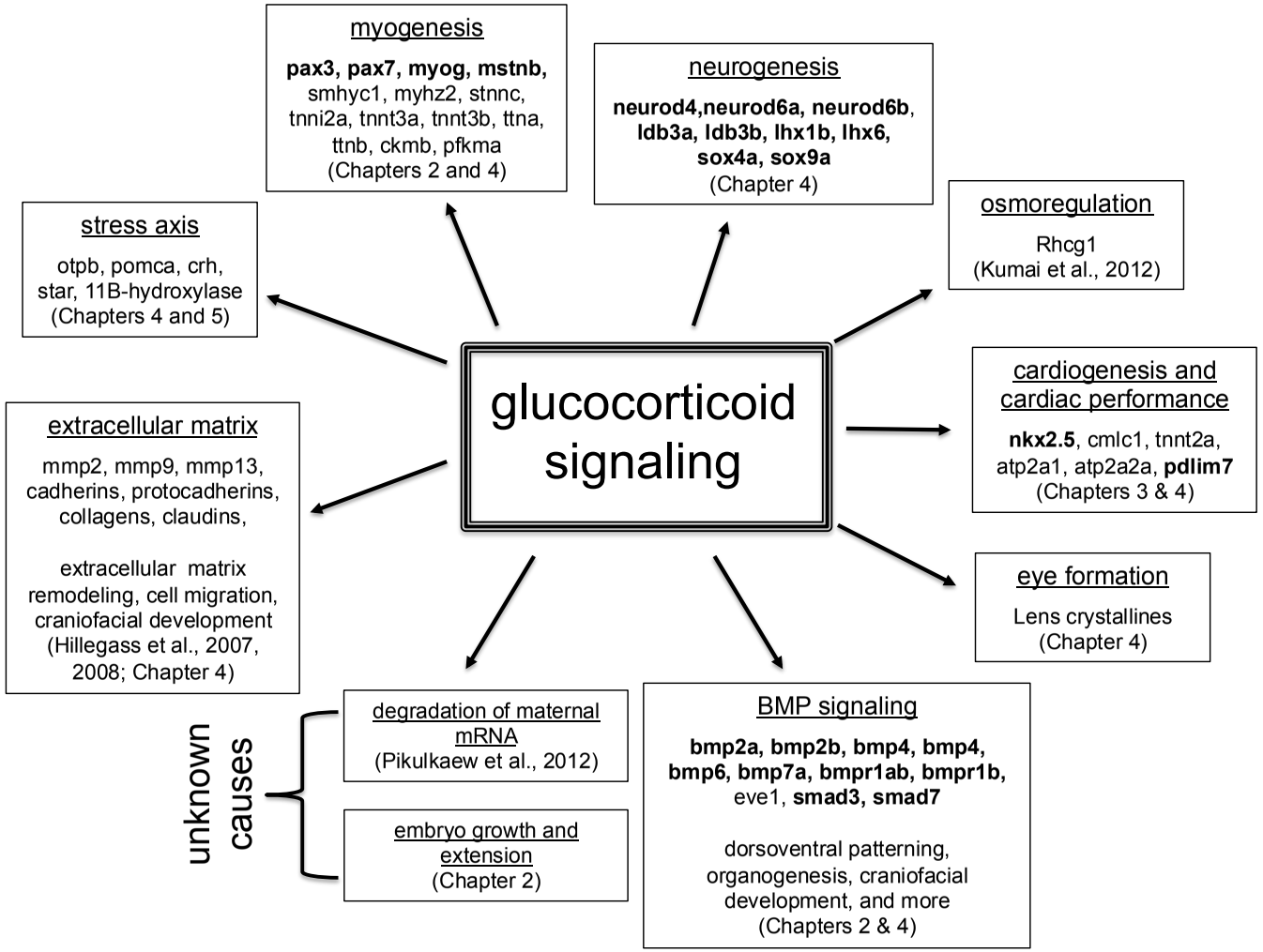
glucocorticoid signaling
myogenesis
pax3, pax7, myog, mstnb, smhyc1, myhz2, stnnc, tnni2a, tnnt3a, tnnt3b, ttna, ttnb, ckmb, pfkma
(Chapters 2 and 4)
neurogenesis
neurod4,neurod6a, neurod6b, ldb3a, ldb3b, lhx1b, lhx6, sox4a, sox9a
(Chapter 4)
stress axis
otpb, pomca, crh, star, 11B-hydroxylase
(Chapters 4 and 5)
osmoregulation
Rhcg1
(Kumai et al., 2012)
extracellular matrix
mmp2, mmp9, mmp13, cadherins, protocadherins, collagens, claudins,
extracellular matrix remodeling, cell migration, craniofacial development
(Hillegass et al., 2007, 2008; Chapter 4)
cardiogenesis and cardiac performance
nkx2.5, cmlc1, tnnt2a, atp2a1, atp2a2a, pdlim7
(Chapters 3 & 4)
eye formation
Lens crystallines
(Chapter 4)
BMP signaling
bmp2a, bmp2b, bmp4, bmp4, bmp6, bmp7a, bmpr1ab, bmpr1b, eve1, smad3, smad7
dorsoventral patterning, organogenesis, craniofacial development, and more
(Chapters 2 & 4)
unknown causes
degradation of maternal mRNA
(Pikulkaew et al., 2012)
embryo growth and extension
(Chapter 2)

6.2 Perspectives and avenues for further research

The findings presented in this thesis provide interesting starting points for research questions in a variety of areas of zebrafish development and physiology. The microarray study alone is likely to contain more novel findings than are presented in Chapter 4. However, there are also questions that stem from the data that have been presented in full. The novel linkages of GR knockdown to increased neurogenesis and di- and tel-encephalon development are an interesting finding. Ascertaining the extent to which these changes occur in the living animal is a critical question remaining in this area, and can apply to a variety of the pathways we have begun to explore in these studies.

Other questions that present themselves involve behavior and the role of maternally deposited cortisol in patterning the phenotype and behavior of the larva and mature animal. It is known that fish populations tend to subdivide into dominant and subordinate individuals that vary in their aggressiveness, feeding patterns, and response to stimuli (Gilmour et al., 2005). A key difference between these subpopulations is that dominant fish have an attenuated cortisol response to stressors (Pottinger and Carrick, 2001; Overli et al., 2004). Given the evidence that prenatal glucocorticoids can modulate the stress response later in life in mammalian (Matthews, 2002; Seckl and Meaney, 2004), avian (Hayward and Wingfield, 2004) and zebrafish (Chapter 5) models, it begs the question whether maternal glucocorticoid deposition into oocytes and the associated changes in brain developmental programming may be playing a role in these social divisions. The zebrafish model provides significant advantages as a model for genetic and behavioural studies and can be used to effectively investigate these questions. The optically clear zebrafish embryos allow for easy visualization of developmental defects, and the speed with which they develop means that behavioral changes at various developmental stages to adulthood can be observed within a few months in this species.

The newfound developmental roles for glucocorticoid action from the zebrafish model, including regulation of morphogens (BMPs, MMPs), cardiogenic, myogenic, and neurogenic transcription factors underscore the role of this steroid in regulating embryogenesis. Understanding the molecular mechanisms of action is critical to unraveling the pathways modulated by cortisol during development. To answer questions of programming, mechanisms of action, and epigenetic effects, the molecular tools available to zebrafish researchers are highly valuable. Forward and reverse genetic techniques are well established, including mutation screens, RNA silencing and

protein knockdown, microarray analysis, and transgenics, along with other molecular and imaging tools (Driever et al., 1994; Jowett, 1999; Rasooly et al., 2003; Teh et al., 2005; McLean and Fetcho, 2008). Next generation sequencing techniques that are now more effective and less cost-prohibitive could also be used to investigate GR effects on the transcriptome at fertilization or around the mid-blastula transition to elucidate GR actions on maternal mRNAs or possible GR-mediated epigenetic effects. These techniques, in combination with the wealth of knowledge of developmental processes that has developed over the last two decades of investigation, makes zebrafish the best possible animal in which to identify the precise mechanisms of cortisol signaling and its effect on development. Promoter characterization and identification of functional glucocorticoid response elements present on target genes of interest may shed light on the mechanisms of action of GR in regulating morphogenesis. Other techniques such as chromatin immunoprecipitation (ChIP) alone or in combination with microarray (ChIP on chip) will be invaluable in revealing novel GR signaling pathways and also assist with establishing the interactome involved in the developmental regulation by glucocorticoids.

A promising area of study is the environmental regulation of long-term phenotypic changes and a key player in this regard is the epigenetic modulation of gene expression during development (Youngson and Whitelaw, 2008; Zhang and Meaney, 2010). GR is a known target for epigenetic regulation (Lillycrop et al., 2007; Oberlander et al., 2008; McGowan et al., 2009), and corticosteroid signaling appears to modulate gene expressions via epigenome modifications (Moritz et al., 2005; Weaver, 2009; Krukowski et al., 2011). These relationships, along with the established effects of GR in the degradation of zebrafish maternal mRNAs (Pikulkaew et al., 2011) suggests that developmental glucocorticoid effects on organogenesis and growth may involve epigenome modifications, but this remains to be tested. The known effects of glucocorticoids on zebrafish organogenesis and the research showing that altered developmental glucocorticoid exposure can modulate the stress response in larval and adult animals (Matthews, 2002; Hayward and Wingfield, 2004; Seckl and Meaney, 2004; Nesan and Vijayan, 2012[Chapter 2]) also leads us to hypothesize that regulation of embryo cortisol levels may be necessary for proper development of the stress axis. The similarity between zebrafish and human GR variants suggest that findings on the functional role of this receptor in zebrafish may provide important clues to the developmental risks and phenotypes associated with fetal stress and/or abnormal prenatal glucocorticoid exposure in humans.

6.3 Conclusions

Stress axis organ ontogeny patterns and the endocrine stress response itself are well conserved throughout vertebrates. Our newfound evidence from zebrafish has identified the primary circulating glucocorticoid, cortisol, and its receptor as a developmental regulator that is critical for embryogenesis, acting upstream of several different developmental processes and pathways. These findings dovetail with established effects of glucocorticoids on mammalian organogenesis and other models. The similarities in vertebrate corticosteroid physiology indicate that the glucocorticoid actions during development may be conserved, providing a mechanistic link between maternal or prenatal stress and developmental abnormalities leading to reduced fitness and survival. The techniques and methodologies that have been developed for use in zebrafish provide an excellent model for understanding the role of fetal glucocorticoid signaling on developmental-endocrine interactions in humans, with important biomedical applications. For the first time, this dissertation presents maternally deposited cortisol and glucocorticoid receptor content as a major developmental morphogen, acting independently of their classically-studied actions in the physiological response to stress. Altogether, this research has spawned a host of novel findings which position glucocorticoid signaling as a key regulator of zebrafish embryogenesis.

Appendix A
Chapter 2 Supplemental Information and Figures

Note: this Appendix contains supplemental information that was published online, reproduced with permission from {Nesan, D., Kamkar, M., Burrows, J., Scott, I.C., Marsden M., and Vijayan, M.M. 2012. Glucocorticoid receptor signaling is essential for mesoderm formation and muscle development in zebrafish. Endocrinology. 153(3), 1288-300.}

Figure A1 – Glucocorticoid receptor-green fluorescent protein (GR-GFP) reporter construct. Schematic display of the construct is presented detailing binding sites and regions of interest within the GR promoter including primer and other putative binding sites (GR2-FR, GR-RV), glucocorticoid response element (GRE), activator protein 1 binding site (AP-1), splicing factor 1 binding site (SP-1), estrogen response element (ERE), and transcription start site (TSS).

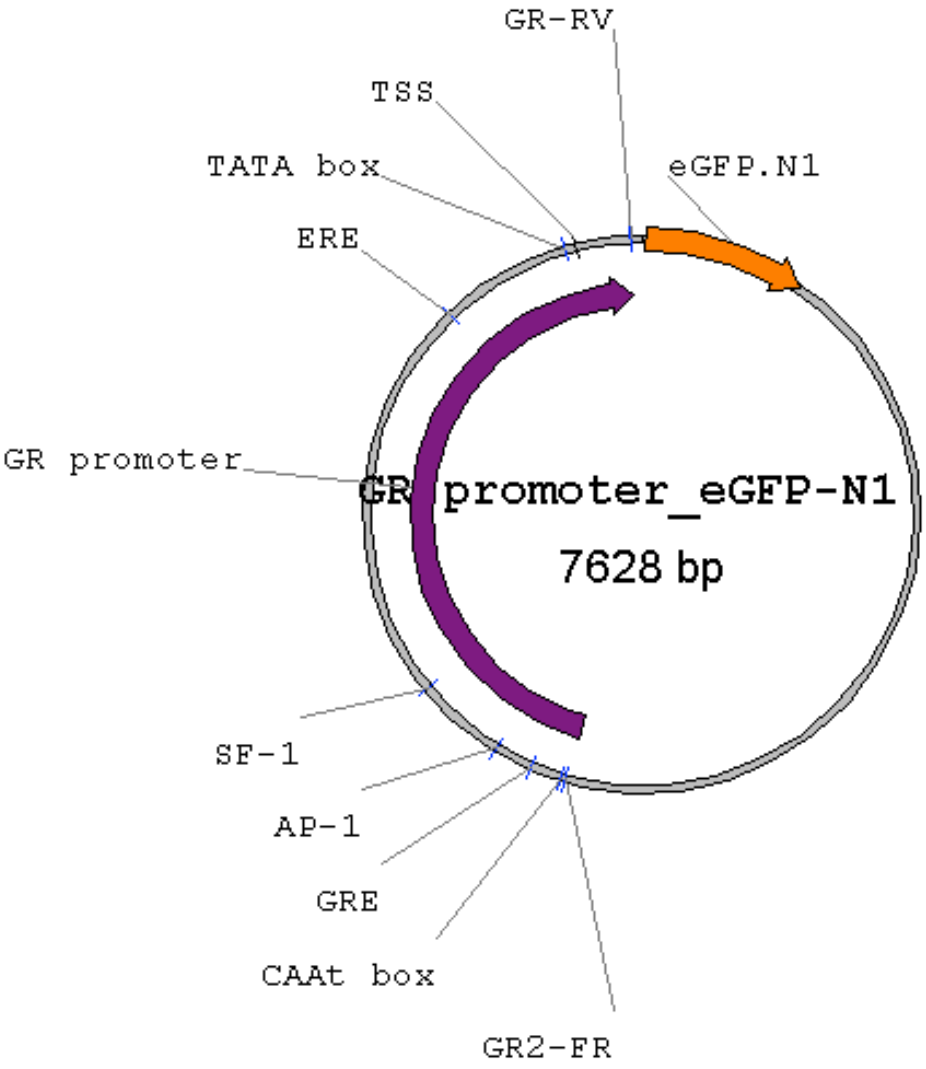
GR-RV
TSS
TATA box
eGFP.N1
ERE
GR promoter
GR promoter_eGFP-N1
7628 bp
SF-1
AP-1
GRE
CAAt box
GR2-FR

Figure A2 – Putative GR promoter sequence
Sequence of putative GR promoter region, complete with specific locations of each putative binding site: glucocorticoid response element (GRE), activator protein 1 binding site (AP-1), splicing factor 1 binding site (SP-1), estrogen response element (ERE), and transcription start site (TSS).

TCGTAAACATGCTTGCTTTGGAGAGGTTGAGATATATCAATAATGATAAATTGGAGATATTAAATAAAACATAGGG

ACAGATATTAGAACACCCTAATGCGTTGGAAGAAATGCAAGCTTAACCAATGACCCCTGTCAAAAACATAGAAAAT

CAAT Box

AAAGATTAAGTGTAATTGATATTCATTCATTCATTTTCTTTTTGGCTTAGTTCCTTTATTAATCCAGAGTCGCCACAG

AATAAACCGCCATTTTATCCAGCGTTTATGCAGCGGATGTCCTTCCAGCTGCAACCCATCTCTGGGAAACATCCATA

GRE

CATACTCATTCACACTCATACACTACGGACAATTTAGTCTAGCCAATTCACCTGTTTTTGGACTGGAGGAAACCGGA

GGAAATCCAAGTAAATGCGGGGAGAACATGCAAAGTCCACACAGAAACGGCAACTGACCCAGCCGAGGCTTGAA

AP-1

CCGGCAACCTTCTTGCTGTGAGGCGACAGCACTACTTATTGCGCCACTGTGTCACCCCTGTAATTGACATACACTAT

TAATAATCTATAATAGATAAATAAAACTATAGTAATATAACAACTTACTTTATTATTACTATTATGAATGCAGTACTT

GACCAGCTAAATTATATTTTGCTTTCATGATCATTTGTCCCTCTGTGTTCTGTTGTTCTGTGTTTTTATGTATCGTGTT

TTATATCTATTATTATTGTATTATATTGTTTTTTCTTCTATATTTTGTTGTAGTTTTATAAAATGCAAAAAGCACAAAA

AACGTTGAAAAAATTAAATTACAGGTGGAACTCAGAGGATGTTAATCAAACAAACAAATGTACTTCACTGACCTTT

CAATTGAATTATTACACTGTAAAATCCAACAGTCAACTTTATCAAATGAAATGAGTGTAGTTAACTCAAAATGTACT

GAAAGTTAATTCTACTCATTTGAAAAGAGTTTTGAACTCAGCGGTAAAGGTAATGAGTTAATTAAATACCTCATTAC

TTCAACTTAAACGGAGTAAGTTCACAGTACTCATATATATATATATATATAATATAGATTAGTTTAACTCAAATGGTT

TGTTGCAATCGGTTTCCTCAAATGGTTTGAGTTGCCTTAACTTACTGGGTTTTACAGTGTATTCCAGCTTGTTAAACC

AAAACTAATTAGTCACGTATGCACTATCACTCATTTCACAACAAATGATTAACATACAGATCACCTTTATATCTACAT

CGCTCTCTCCATAAAAAACTGTCTCAAATAAATTAAAAGTCATTCTGAATAAAAGAATTTATTTGCCTGTGCCAGTT

TTGATTCATCACGGATTATTGTTGCAGTTATAACCGTGTTACTTCTTTATAATGTAGTATGTAGAGTGCAATAAATG

CTATCAGATAAAAAAGAAAGACATAATTCAAGGTGACAACAAGAGTCTCATTTAGTGATTCTAATACATAAAGCTC

ATTAAAAGTGTTTTTTTTTCTTATCTTAAAACAAAAAGCATCCACTAGGTGGAAGTGTTTAGTTGTCACCTACATGTT

TATTTCAGTAATTATCTTCTCTAATGTCATCAATTTAGCTAAACAGCTGAGTCATCACGGAGAAAATGAACACTAGC

TGCCATCTTTAAAACCTGAACCTTCAACAAATAATTTCAATTTACCAATGTAATCATTCATTCAACAATTCTAAACGA

CGGTTAATCTCTTAACCAACATAGTTATTATAGTTATTAATATTTTTACTTGATTTTTAAAATGAATTATTTCCTTTGC

ATTTATTTCATAATAGTTGTCTTTTTTAATATAAATGAAATCTGACATAACAGGCCATTATTTATTTAGTTCTTAACAA

TGAATGAAAGTAAGACATAAAATAAAAGTGTTCACGTTTGTTTTCCTATGGTTTAGTCCCTTTTTTCATCAGGAGTC

ACCACAGCGGAATGAACTGCCAACTTATCTAGCACATGTTTTACACTGCAGCTGCCCTTCCAGCAGCAACCCATTAC

TGAAAACCTCCATACACACTCAAAATTTATCTTTAAAGAACAAACACTCTAAACAACGCTGGTTTGTTTAACTCTAC

ATTTGAGTAAAATGTCAACAAGTTGTGTCCACTATGTACATTACTGGTCAAAAGTTTGGGGTCAGATTTTGTACTTT

TTTTCTTTTTTTTTTTTTTAAGAAAATGATTCTGTTCATCAAGATGGCATTTATTAAATACAAAAAAAATTTTATTGTT

AAATATTTATTAAAAGATTTAATAAATGCTTAGTGGATGTAGTTTGAAATGGAAGTATTACTCCAGTCATTGTTGCT

TTTATTACTATTACTATTAATAATATTAAGAACTGTAATAATTAATATTAGATGATTTCTAAAGGATCATATGACTCT

GAGAACTGGAGTTATAAAACTGAAAATTCATCTTTAAAATCACTGGAATTAATTATTAAATTAAATTATAAAGTACT

TTTGAACAGTTCTTTTATAGTGCAAGAACACTTCACAATTTTAATGTTTGTACTGTATTTTTTATTTAATAAATGTGTC

CTTGGTGAGTGAGAAGCATATTTTAAAACATTTAAAAATCCTACTGACCCCAAACTTCTGACCGGAAGTGTATTTCA

AAGAATTTTCAGGTGGGTTTGACCATATCTTGTATAAACTGATTGTTGTAACAATGCATAAGCTAAATTCTTTGAAA

ERE

CAAACATTACATTCTGAGCTCCGGAGGTTTTAAAAGATTTAAATGTTAACATTTCCTTGCGTTTTACACACTCATAAA

TGTATAATGGAATAATGTTAAATATTTGATCCCACTTTAAACCCAACATTTTGGTTTGTTCACATTTTACAGAAATGT

AGGGTGACGCAAACCATGCGTTGTTTACTTACAAAACCAGCATTAATTCAATAATTCAAATAGTCAAAACAACAAC

AACAACAACAACAACAACAACAACAACAGTTTGATAGGCTATAGATAATGCAACAAACAAAAAAGGGAAATTCTA

ACAAAGACAGTTTGGTTTTATGCATTCTGTCAAAATAATAAACACAAAGCAACAAAGTAATTGCAATTTGTTTGAA

ATATAAACCATAGTATAGCCATTTTTTACTTTTGATTTTCATAATGATCATTGATGCATGAACGAATAATCCTATTTC

AAATTACAAATAAAAGTTTTTGAAAAACTTTCTAAATGTATGTACAAGGGAAATGCATAATAAAAGCAGAGAGAG

TSS*

TATA box

AGAGAGAGAGAGAGAGAGAGAGAGAGAGAGAGAGAGAGAGAGAGGAGGCTGTGTGATTTGT

TTTTATGGTGATATCACCGACTCAGACCCAGATCACACTCTCTCACCCAATGAAGTCACTGTAATAGGAAGCGAGA

TGCAATAACTCTGTACTGCCAATAGGTCGCACTGCATGTTGTAAACAGGGTCGCCGCGGACCTTTCTACTGTAATCT

CCATTTTGAATGTTTTTATGGTTTAGGGTTTTGT

Figure A3 – Fluorescence images of GR promoter activation in developing embryos.
A GR-GFP construct consisting of zebrafish GR promoter region coupled to the GFP coding sequence was injected into embryos (n=9 groups of 40-60 embryos). No fluorescence was detected at 12 hpf (I), but fluorescence was observed at 15 hpf (II) and 18 hpf (III), while a negative control construct lacking the GR promoter region did not fluoresce (IV). Arrows indicate regions of fluorescence.

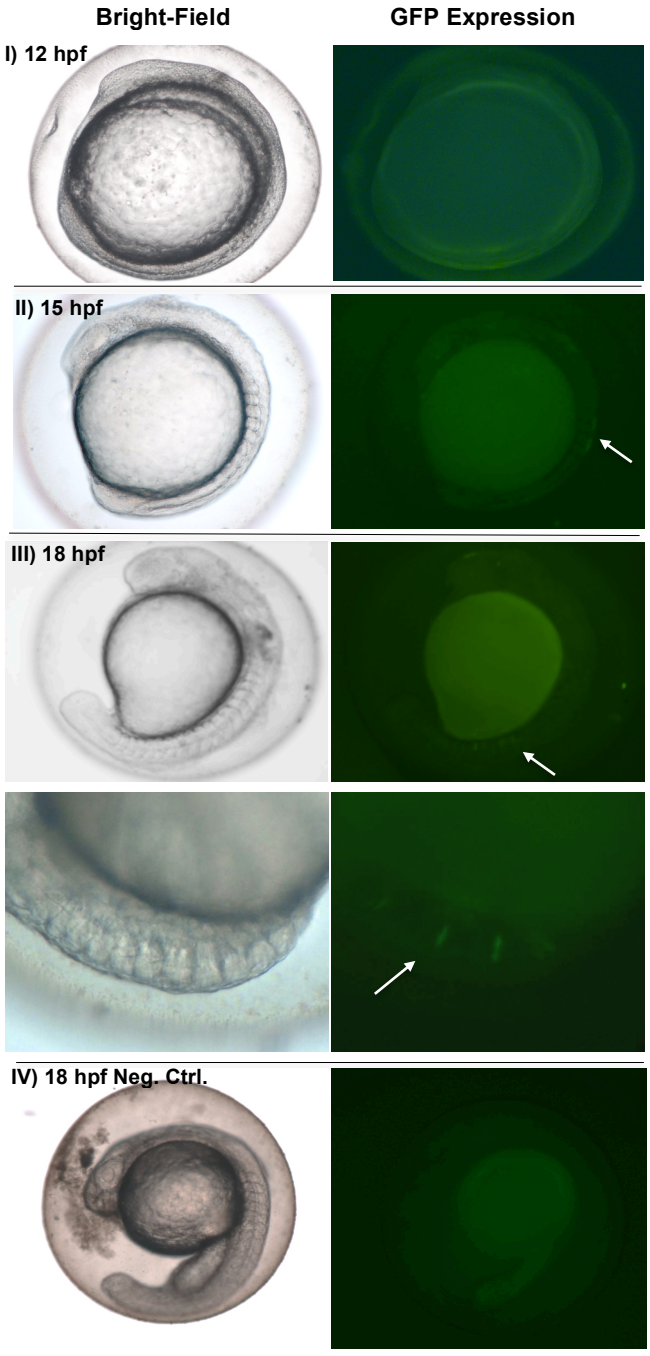
Bright-Field
GFP Expression
I) 12 hpf
II) 15 hpf
III) 18 hpf
IV) 18 hpf Neg. Ctrl.

Figure A4 – Putative non-functional glucocorticoid response elements in MyoD and IGF promoter regions.

Schematics of putative glucocorticoid response elements (GREs; numbered by starting base pair) upstream of MyoD, IGF1, and IGF2.

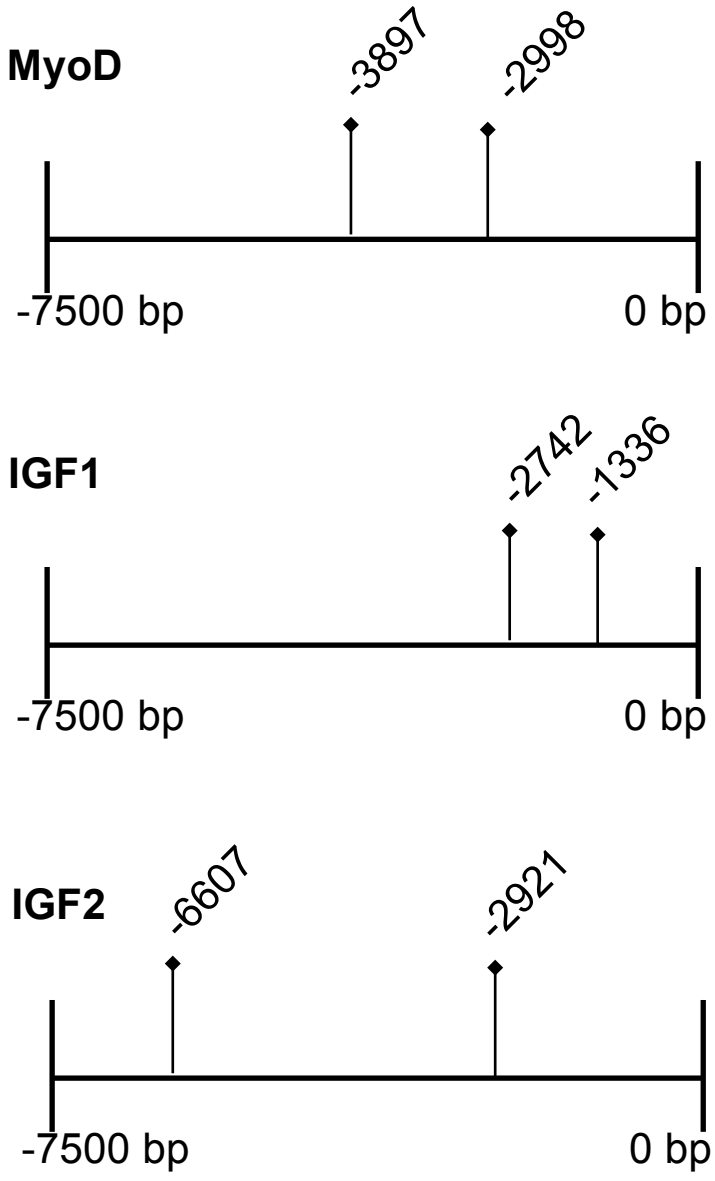
MyoD
-3897
-2998
-7500 bp
0 bp
IGF1
-2742
-1336
-7500 bp
0 bp
IGF2
-6607
-2921
-7500 bp
0 bp

Appendix B
Expanded Methods and Protocols

This appendix contains more detailed protocols for specific methods that are commonly used in this dissertation. As these chapters were written for submission to primary journals, attempts were made to limit the length of each chapter and to refer to published methods where applicable. However, to provide benefit to anyone attempting to repeat or carry on from these studies, this appendix provides more information on specific methods

Zebrafish care and breeding

Adult zebrafish were maintained in an AHAB recirculating system (Aquatic Habitats, Apopka, FL), on a 14h:10h light-dark cycle at ~28 C. For initial studies (Chapter 2), the system was filled with well water from the University of Waterloo main campus supply, however for all remaining studies, the water was made from the addition of 60 mg/L Instant Ocean marine salts (Spectrum Brands), to deionized distilled water. Fish were maintained in 10L tanks at an approximate stocking density of 35 fish per tank. Water in the system was changed at a rate of ~15% per week (40-50L replaced). Ammonia, nitrite, and nitrate concentrations were measured weekly in the system, and pH and temperature were routinely monitored. Fish were fed at least 2 times per day during studies.

During breeding attempts, fish were fed 3 times per day. Breeding was performed by placement of breeding traps (Aquatic Habitats) into the system to minimize handling or transfer stress. Subsets of the fish population were bred randomly 1-2 times per week during each study. Traps were put into the tanks within 60 minutes of the end of the daily light cycle, left overnight, and then removed 30-45 minutes after the start of the subsequent day's light cycle. Eggs were rinsed in system water and cleaned, then transferred to a beaker of embryo medium (Westerfield, 2007) for microinjection and/or incubation. Traps would be returned to the tanks to collect eggs from any subsequent rounds of breeding.

Microinjection protocol

In all experiments in this thesis, we utilize a nitrogen gas powered microinjector (Narishige, Japan) that is able to control the length of time of the injection event and the injection pressure. These measurements, in combination with the use of a microcapillary tube of known internal volume/diameter and an initial quantification of the volume dispensed in a known number of injections, allows us to closely control the amount of treatment injected into the zebrafish embryo. This allows for repeatability and reliability in the presented experiments, which take advantage of the

unique characteristics of the zebrafish embryo that are particularly beneficial when using this technique.

Microinjection needles were made with a PC-10 Dual Stage Micropipette Puller (Narishige), which heated and separated a single microcapillary tube (10uM internal diameter, Sutter Instruments, Novota, CA) into two pieces each with a sealed fine-pointed end. Fine forceps or a sterile razor blade were used to open the sealed end of the needle prior to use. Needle calibration was performed by measuring the injection volume produced by 50-100 injections, by collection in a 1uL capillary tube (Fisher Scientific, Ottawa, ON) and then calculating the volume of a single injection. Injection volume was easily adjusted by varying either the injection pressure or the injection duration on the microinjector to maintain a precise volume. Prior to injection, the cleaned embryos were placed in an injection mold to streamline the procedure. The injection mold was made of 4% agarose in embryo medium, and had grooves to align embryos for speedy injection. On average, hundreds of embryos could be injected within the 30-45 minutes between fertilization and first cleavage. Eggs beyond the two-cell stage were not injected in any study. All injections were carried out at the same time of day. After injection, eggs were transferred to 10 cm petri dishes in embryo medium, and incubated at 28.5 C on a 14h:10h light-dark cycle.

RNA extraction and quantification

Quantification of gene expression is a frequently-used endpoint in this dissertation. In most studies (Chapters 2, 3, 4) RNA was extracted by use of the RNeasy RNA extraction mini-kit with the Qiazol lysis reagent (both from Qiagen, Mississauga, ON), using their protocol for fatty tissues to account for the embryo yolk. In chapter 5, this process was replaced by the use of the Ribozol reagent (Amresco, Soton, OH) and extraction without the use of a kit. Both are very similar processes, based on variations of the phenol-chloroform extraction process, with centrifugation to separate the layers and manual removal of the RNA fraction. Care was taken not to remove any of the thin middle DNA layer, but DNAse treatment was always performed after extraction during or just prior to cDNA synthesis, to prevent genomic contamination. RNA was always quantified by calculation of optical density with a Nanodrop spectrophotometer, measuring 1.5 uL of extracted RNA. RNA was eluted or resolubilized in 20-25 uL of sterile, nuclease-free water in order to maintain high concentrations wherever possible. The absorbance ratios at 260nm/280nm and 230nm/260nm were always observed to ensure a high RNA purity, with 260nm/280nm ratios required to be over 1.8.

Appendix C

Complete List of Significantly Changed Genes from Chapter 4 Microarray Analysis

Data presented in this appendix include the results of statistical testing of microarray analysis fold-changes, as described in Chapter 4, after false discovery correction. Table C1 is all significantly changed genes at 24 hpf, Table C2 is all significantly changed genes at 36 hpf. Calculated fold-changes and p-values are included in the table. Colored text represents a gene that was significantly changed at both 24 and 36 hpf, with the color change indicating that the gene was upregulated at both time points (green text), downregulated (red text), or differentially altered (blue text).

Table C1 – Significantly changed genes at 24 hpf in response to GR knockdown

Gene	Fold Change	P-value
a2bp1	2.235	0.018918
aanat1	0.467	0.017915
aatf	0.602	0.038489
abca1a	0.684	0.041834
abcc9	2.666	0.025931
abcg4b	0.425	0.015937
abhd2b	2.571	0.025968
acad8	1.322	0.021660
acadl	2.257	0.031177
acat1	1.716	0.029248
acat2	1.260	0.019803
accn1	2.148	0.050513
aco2	1.553	0.029248
acot7	1.499	0.011111
acsf2	1.450	0.039732
acta1	1.629	0.030990
actn3a	2.854	0.037196
adcyap1b	2.318	0.014138
add1	1.382	0.041987
adh5	1.240	0.045863
adh8b	1.318	0.049430
adipor1b	0.788	0.046797
adora2aa	0.498	0.034921
adora2ab	0.259	0.030320
adsl	1.303	0.018469
adss	1.795	0.049716
afmid	2.022	0.043103
agr2	2.506	0.047798
agt	0.318	0.050117
ahcy	1.813	0.014456
ahr2	1.499	0.034176
aig1	2.233	0.036903
akap12	0.526	0.031960
alas2	2.161	0.017711
alcam	0.604	0.014755
aldh16a1	1.798	0.027035
aldh18a1	2.273	0.019816

Gene	Fold Change	P-value
aldh7a1	1.724	0.024016
alkbh5	0.401	0.046771
alp	1.987	0.017711
alpi	0.541	0.014138
alx4	1.474	0.036390
amdhd1	3.884	0.016384
amph	2.147	0.027478
angptl2	0.652	0.023632
ank1	2.951	0.017283
ankrd37	0.425	0.035557
anxa11a	0.689	0.037831
anxa13	0.669	0.027768
anxa4	0.207	0.044936
anxa5b	1.925	0.021651
aox1	1.695	0.027537
apc	1.342	0.037465
aph1b	1.707	0.026439
apln	1.637	0.036614
aplnrb	0.466	0.014138
aplp	1.990	0.015977
apoa1	0.348	0.029973
apoea	3.537	0.037436
apoeb	0.587	0.030558
apol1	1.717	0.023632
appb	1.602	0.009609
aqp11	1.681	0.015406
aqp3	5.461	0.025641
arhgef3l	3.657	0.023541
arid3b	0.420	0.046797
arih1l	0.570	0.023632
arl11	1.450	0.026102
arl13b	1.960	0.038572
arl4a	0.623	0.016384
arl4cb	0.784	0.043047
arl4l	0.623	0.023380
arnt2	0.511	0.050264
arntl2	0.360	0.021660
arpc1b	2.663	0.048096
arrb1	1.863	0.040530

Gene	Fold Change	P-value
arrdc2	0.432	0.036472
asb12a	1.428	0.046610
asb5	5.168	0.045683
asb8	1.436	0.041446
ascl1a	2.009	0.017296
ascl1b	3.182	0.013268
asf1b	1.532	0.043752
aspdh	1.868	0.046610
asph	0.589	0.019803
aspn	2.052	0.043731
atad4a	1.850	0.034606
atl1	1.446	0.038905
atl3	0.548	0.047394
atoh2a	2.706	0.049189
atoh2b	4.936	0.014755
atp1a1	0.646	0.023541
atp1a1a.2	2.785	0.017081
atp1a1a.4	0.521	0.027478
atp1a1b	2.021	0.027478
atp1a3a	1.877	0.045960
atp1b1b	2.712	0.009574
atp1b3b	1.623	0.047798
atp2a1	1.764	0.014755
atp2a2a	0.211	0.043599
atp2b1a	0.521	0.039732
atp2b1b	0.414	0.033794
atp5f1	1.383	0.014755
atp5i	1.460	0.037831
atp5j	2.520	0.031549
atp5o	1.235	0.025693
atp6v1b2	1.708	0.038572
atp6v1e1	1.269	0.023541
atp6v1h	1.349	0.039732
avpl	1.847	0.029321
b3gnt5	2.468	0.027300
b3gnt7	0.226	0.043599
barhl1.1	2.874	0.012309
bbox1	0.199	0.017296
bcam	0.342	0.049141

Gene	Fold Change	P-value
bcl11a	2.704	0.019803
bcl2l	0.395	0.009320
bcl9l	0.516	0.049863
bhmt	0.374	0.031834
bik	0.509	0.034173
bin1	2.174	0.015977
bin2a	1.903	0.044019
birc2	0.810	0.030990
birc5a	1.542	0.035436
blvrb	2.335	0.049570
bmp4	0.563	0.015821
bmp6	0.440	0.015406
bmp7a	0.288	0.025641
bmpr1ab	0.374	0.041871
bmpr1b	0.454	0.035855
bnip3l	0.510	0.043733
boka	0.740	0.038489
bpnt1	3.784	0.027300
brn1.2	1.440	0.030901
brunol5	2.122	0.017915
bsg	0.612	0.033951
btbd2	1.853	0.019803
btbd6	1.671	0.027664
bxdc1	0.541	0.039949
bzw1b	0.704	0.030914
c1qtnf5	2.257	0.021660
c6orf115	1.921	0.043103
c8g	1.990	0.046371
ca15a	2.449	0.040993
ca2	1.579	0.039949
ca8	0.538	0.033951
cacna1s	2.654	0.020489
cacnb2b	0.563	0.049769
cacnb4b	2.303	0.050237
cacng2	2.512	0.021660
cacng2b	2.979	0.014755
cadm2a	2.690	0.026439
cadm4	1.458	0.039918
calb2l	2.325	0.014755

Gene	Fold Change	P-value
calca	6.711	0.040419
calhm2	2.660	0.020880
calm3a	2.465	0.014755
camk2a	3.702	0.025610
camk2d2	2.462	0.027478
camkv	2.156	0.049812
capg	2.033	0.009609
capn9	0.728	0.030758
caprin1b	0.728	0.013925
casp2	1.301	0.043265
cast	0.562	0.041159
casz1	2.020	0.038054
cat	2.082	0.027478
cav3	2.348	0.026439
cbln1	2.223	0.021014
cbln4	2.235	0.021651
cbx3b	1.753	0.011111
ccl1	0.491	0.029248
ccng2	0.468	0.014755
ccnt2	0.525	0.043407
cd2apl	0.718	0.047859
cdc40	0.720	0.039082
cdca8	1.404	0.031578
cdh1	0.606	0.036472
cdh2	0.502	0.038572
cdh4	4.957	0.014755
cdk2	1.843	0.014138
cdk5	1.457	0.014755
cdk5r2	3.196	0.015720
ch25h	0.093	0.038489
cha	0.047	0.026439
chad	20.346	0.016033
chaf1b	1.995	0.021660
chat	1.391	0.049430
chchd3	1.796	0.048096
chchd7	1.833	0.012827
chka	0.500	0.050239
chmp4b	1.225	0.049863
chrm2a	2.543	0.009609

Gene	Fold Change	P-value
chrne	2.980	0.014755
chst1	1.968	0.034652
ciita	0.254	0.048096
cited3	0.550	0.023878
cki	0.646	0.035882
ckmb	3.034	0.050281
ckmt1	0.363	0.046610
cldnc	0.275	0.015406
cldne	0.541	0.042824
cldnf	0.686	0.050249
clgn	1.468	0.034606
clstn1	1.943	0.017711
cltcb	1.496	0.025693
clu	1.432	0.038211
cmya5l	4.043	0.013226
cnot10	1.379	0.032414
cnot6	0.706	0.040970
cog8	2.061	0.030901
col15a1	0.299	0.009320
col18a1	0.610	0.040023
col1a1	2.196	0.026588
col1a2	1.960	0.017843
col1a3	3.180	0.018797
col28a1a	1.750	0.026439
col4a4	1.584	0.027300
col6a1	2.146	0.048096
col6a2	2.720	0.033311
col7a1l	0.564	0.036157
col9a2	1.323	0.049812
colm	1.551	0.049770
copg2	0.738	0.049222
coro1a	2.615	0.050403
coro1b	1.450	0.047161
cox17	1.972	0.042150
cox7a2	1.297	0.029961
cplx2	2.732	0.021634
cpn1	0.679	0.030501
cpox	0.627	0.045331
cpsf5	0.923	0.043047

Gene	Fold Change	P-value
cpt1b	6.290	0.009320
cpt2	1.846	0.025610
crabp2b	0.412	0.014755
crfb8	0.569	0.027300
crispld1	4.249	0.009414
crsp6	0.679	0.030501
crtap	0.694	0.011111
cry1b	0.546	0.029248
cry3	0.562	0.040958
cry4	0.589	0.023541
cryba1b	13.454	0.014138
cryba2a	9.402	0.013226
cryba4	7.075	0.049812
crygn1	0.362	0.038572
cs	1.563	0.046610
csdc2	1.894	0.026300
csf1b	4.339	0.045683
csnk1e	1.982	0.021660
cspg5	1.593	0.015805
ctgf	0.651	0.035952
ctnnb1	0.799	0.030901
ctsc	0.117	0.009320
ctsh	0.419	0.017915
ctssb.1	0.321	0.017711
ctsz	1.598	0.033873
cugbp2	1.901	0.013925
cul4a	0.734	0.032879
cul5	1.457	0.032723
cwf19l2	0.742	0.050403
cx23	4.160	0.017711
cx33.8	2.005	0.014755
cx36.7	0.429	0.014755
cx39.9	3.262	0.021660
cx44.1	9.961	0.014878
cxcr4a	0.567	0.032723
cxcr4b	0.570	0.030901
cyb5r2	0.616	0.015821
cyb5r3	1.403	0.026439
cygb1	2.064	0.033244

Gene	Fold Change	P-value
cyp11a1	0.125	0.048167
cyp17a1	1.873	0.019739
cyp24a1l	0.122	0.009609
cyp2j27	1.599	0.046610
cyp51	0.561	0.046771
cyth1	0.660	0.021014
d2hgdh	0.740	0.046977
dab1	1.533	0.027300
dao.2	1.702	0.028164
daxx	0.848	0.026632
dbx1a	1.525	0.038572
dci	1.627	0.030030
dct	4.506	0.025951
dctn2	1.366	0.031683
ddx54	0.513	0.029105
defbl1	6.171	0.014755
depdc6	1.636	0.031563
desm	1.461	0.050232
dgat1	2.284	0.046610
dhfr	1.646	0.046681
dhrs3a	0.527	0.034176
dhrs3a	0.525	0.032414
dia1	1.351	0.023541
diras1	2.465	0.038266
dlc	0.628	0.035665
dldh	1.228	0.045286
dlg1	0.679	0.043954
dlg2	1.527	0.031056
dlx5a	0.856	0.037831
dmrt2a	0.317	0.018469
dmrt3a	2.450	0.045226
dnaja1l	2.079	0.044064
dnase1l3l	0.407	0.045760
dnm1l	2.131	0.038572
dpyd	2.546	0.009320
dpysl3	1.799	0.016847
dpysl5a	1.734	0.029852
dpysl5b	1.924	0.023676
drd2a	1.473	0.042304

Gene	Fold Change	P-value
dtna	1.930	0.025727
duox1	1.728	0.025538
dusp5	0.425	0.027478
dync1li1	1.970	0.015720
ebi3	3.220	0.049716
echs1	2.037	0.014755
ecm2	2.270	0.046807
ef1	0.637	0.022269
efcab4a	0.465	0.034176
efemp2	0.360	0.030758
efna3b	1.582	0.040526
efna5a	0.670	0.014755
efnb2b	0.580	0.048596
egfl7	0.594	0.043445
egfr	0.519	0.021660
egln3	0.081	0.017863
egr2b	0.176	0.009320
ehd2	1.625	0.046797
ehhadh	2.140	0.019960
ehmt1a	1.426	0.027300
eif3ea	0.626	0.046610
eif3m	0.667	0.045863
eif3s2	0.845	0.037831
eif6	0.667	0.049448
ek1	1.873	0.030501
elavl4	2.188	0.044973
elmod2	1.842	0.039082
elovl7a	0.578	0.025136
emx3	0.759	0.039171
eng1a	3.308	0.023632
eng1b	2.010	0.038572
enkur	0.745	0.021660
eno1	0.674	0.027478
eno2	2.166	0.022408
enpp6	1.545	0.029105
entpd2a.1	2.408	0.047394
eomesa	2.157	0.013451
eomesb	1.389	0.046771
epas1	2.561	0.037465

Gene	Fold Change	P-value
erf	0.610	0.027599
esr2b	0.426	0.046797
esrp1	0.545	0.037430
esrrd	49.326	0.036903
etfa	1.377	0.038905
evlb	2.107	0.014755
eya4	1.880	0.011735
f	2.506	0.014138
f3a	0.500	0.014755
f5	3.559	0.019925
f7i	2.462	0.014755
faah2a	2.305	0.013602
fabp2	0.615	0.026036
fabp3	1.581	0.015982
fabp7b	3.272	0.010347
fah	2.558	0.044480
fam134a	0.765	0.020559
fam46b	0.126	0.030990
fam91a1	1.517	0.033944
farp2	0.653	0.020422
fbln1	0.378	0.034945
fbln4	0.306	0.017763
fbp2	3.103	0.019602
fbxl2	0.627	0.043047
fbxo25	1.415	0.048478
fbxo3	1.506	0.023541
fev	2.317	0.033216
fez1	2.607	0.014755
fga	4.825	0.003518
fgb	3.628	0.022269
fgd	1.323	0.034173
fgf13	2.325	0.031553
fgf13l	1.788	0.027970
fgf17	0.183	0.011111
fgf2	0.463	0.045032
fgf24	0.461	0.019803
fgf8a	0.414	0.020153
fgfr1a	0.609	0.011111
fgfr1b	0.348	0.028980

Gene	Fold Change	P-value
fgfrl1a	0.458	0.037436
fgg	3.612	0.046610
fhl3	0.598	0.025136
fhla	0.447	0.038198
fibin	0.581	0.041590
figf	1.668	0.046610
figla	0.247	0.019960
fign	0.669	0.050403
fkbp11	0.413	0.037465
fkbp3	1.401	0.037900
fkbp4	1.673	0.027792
flt4	0.669	0.029248
fn1b	0.178	0.046524
foxa1	0.706	0.021660
foxa3	0.568	0.038352
foxb1.1	0.598	0.024681
foxc1b	0.452	0.018986
foxd5	0.235	0.027300
foxg1	1.326	0.014755
foxk1	0.611	0.022269
foxl2	0.401	0.027478
foxn4	2.572	0.014755
foxp1a	0.312	0.020665
fstb	2.270	0.021660
ftr67	0.484	0.041590
ftr78	0.399	0.039909
ftr79	0.293	0.050239
furina	0.401	0.042024
fut9	0.453	0.022799
fyna	1.500	0.047537
fzd3l	0.640	0.027300
g12	0.335	0.036903
gad1	5.437	0.009609
gad2	2.071	0.020829
gadd45b	0.221	0.017542
gata1	0.504	0.045372
gata2b	2.502	0.039949
gata4	0.366	0.029105
gata6	0.356	0.014755

Gene	Fold Change	P-value
gats	0.479	0.033164
gba2	0.739	0.044557
gbp	0.355	0.037006
gbx2	0.621	0.044932
gc3	2.691	0.013226
gch2	3.940	0.014755
gchfr	1.631	0.038905
gdf11	1.343	0.049292
gem	0.648	0.031722
gfi1.1	0.067	0.028718
gfpt1	0.438	0.045683
ghrb	1.399	0.038054
glb1l	1.781	0.015977
glcea	2.421	0.029248
gle1l	2.419	0.030501
glod4	1.609	0.028846
glra4a	2.072	0.049716
glula	0.550	0.031960
gmpr	1.606	0.015223
gmps	1.906	0.046610
gnai2l	0.759	0.033951
gnai3	0.739	0.043047
gnao1b	1.697	0.043663
gnat2	1.845	0.030990
gnav1	0.519	0.023068
gngt1	3.268	0.038605
gnsb	0.480	0.032870
golga5	0.556	0.015173
gopc	0.705	0.046610
gorasp2	0.859	0.050239
got1	1.574	0.027300
gpd1	0.522	0.030320
gpd1b	1.750	0.049086
gpib	5.472	0.033311
gpm6aa	2.579	0.009320
gpm6ab	1.804	0.050513
gpr133	0.494	0.023803
gpr143	1.570	0.036903
gpr177	0.556	0.045918

Gene	Fold Change	P-value
gpr27	1.540	0.023781
gprc5c	0.563	0.046695
gpsm2	1.724	0.011111
gpx1a	1.429	0.038572
gpx4a	0.555	0.047798
grb10	0.531	0.040023
grem2	1.931	0.029574
grhl1	0.405	0.050594
gria2a	2.111	0.029105
gria2b	3.904	0.029248
gria4b	1.446	0.027478
grin1a	3.514	0.046797
grna	1.991	0.026187
grnas	1.243	0.030501
grtp1a	2.079	0.044936
gspt1	1.911	0.025136
gstt1a	2.164	0.009320
gtpbp4	0.596	0.038572
gygl	2.254	0.027478
h1fx	0.390	0.032713
hadhb	1.691	0.050911
hand2	0.557	0.040166
hao1	3.186	0.043690
hapln1a	2.040	0.036921
hapln1b	0.314	0.027478
hbae1	2.178	0.026632
hbae3	2.306	0.009609
hbbe3	1.703	0.025136
hcrt	4.575	0.030758
heatr1	0.624	0.027478
her1	0.140	0.009609
her12	1.129	0.043599
her13	2.105	0.014138
her2	1.800	0.015178
her3	0.560	0.049156
her5	0.340	0.017711
her6	0.483	0.018469
hey1	0.528	0.023781
heyl	2.180	0.049430

Gene	Fold Change	P-value
hhatla	3.099	0.014138
hhatlb	2.175	0.011111
hhex	0.370	0.043954
hhip	0.777	0.033951
hibadhb	1.546	0.026439
hif1al2	4.268	0.025641
hint2	1.349	0.049812
hirip5	0.725	0.044932
hkdc1	0.373	0.048596
hlx1	2.241	0.023322
hmbsb	1.488	0.039909
hmox1	0.445	0.030758
hmx4	1.618	0.039560
hn1	2.189	0.030501
hnf1a	0.485	0.026439
hnf4a	0.317	0.036614
homer1	3.619	0.011492
hoxa10b	0.542	0.013186
hoxa11a	0.444	0.035079
hoxa13b	0.368	0.011111
hoxa2b	0.771	0.042304
hoxa9a	0.680	0.014755
hoxa9b	0.492	0.012913
hoxb10a	0.549	0.030758
hoxb1a	0.282	0.011111
hoxb7a	0.398	0.018918
hoxb9a	0.602	0.048385
hoxc10a	0.595	0.013226
hoxc3a	0.428	0.032870
hoxc6a	0.533	0.017081
hoxc6b	0.740	0.014755
hoxc8a	0.589	0.033216
hoxd10a	0.659	0.038947
hoxd12a	0.339	0.013186
hprt1l	1.744	0.015465
hsd17b10	1.716	0.025693
hsd17b2	0.305	0.014755
hsf2	0.802	0.026439
hsp90ab1	0.834	0.046274

Gene	Fold Change	P-value
hspa12b	1.823	0.011111
hspb6	2.053	0.041501
hspb9	1.848	0.041590
htatip2	2.234	0.009609
hyou1	0.681	0.050638
icn	1.607	0.032981
idh2	1.336	0.019960
idh3g	0.571	0.030491
ift46	2.272	0.011111
igf2bp2a	1.367	0.047394
igfbp1a	0.358	0.025136
igfbp2a	1.884	0.031598
igfbp3	1.638	0.049189
igfbp5b	3.473	0.014755
ighm	4.828	0.027478
igsf21a	2.008	0.019960
il15l	0.590	0.049905
il17c	0.490	0.030901
il17d	1.406	0.038352
il17rd	0.317	0.014138
il1rapl1a	2.067	0.017081
ilk	0.836	0.038905
inadl	0.610	0.030501
ing5a	0.680	0.049696
inhbaa	0.443	0.030758
ins	2.256	0.044936
insb	0.329	0.047394
insig1	0.286	0.029469
invs	0.446	0.025641
ip6k2	1.797	0.021357
irak3	0.520	0.044480
irx2a	2.248	0.041829
irx4a	2.758	0.014138
irx6a	2.413	0.030262
irx7	0.218	0.019651
isl2a	0.526	0.014755
islr2	2.904	0.023068
isoc1	0.675	0.031834
isoc2	2.398	0.049770

Gene	Fold Change	P-value
itgb1b.2	3.151	0.017843
itgb4	1.818	0.033601
itih2	0.457	0.014755
itm2bb	0.515	0.045918
itpk1	0.406	0.027478
ivd	1.796	0.023803
ivns1abpa	0.604	0.013602
jag2	0.591	0.039431
jagn1b	0.742	0.045331
jmjd6	0.231	0.025753
jph2	2.163	0.036614
junbl	0.389	0.014755
kbtbd8	1.525	0.049448
kcnd3	1.512	0.046681
kcnip3	0.433	0.017081
kcnip3l	3.320	0.029852
kcnip3l	1.961	0.043663
kctd6	1.340	0.043047
kctd7	1.778	0.000083
kdm6b	1.733	0.031183
kdr	0.410	0.032723
keap1a	1.680	0.017081
kif3c	2.537	0.043599
kif5a	2.130	0.042038
klf13l	1.624	0.041046
klf2b	1.522	0.032881
klf4	0.422	0.037913
klf7	1.367	0.035293
klhdc6	5.852	0.016413
klhl31	2.011	0.026439
kpna2	1.526	0.030758
krcp	1.269	0.035344
krt1-19d	2.178	0.011449
krt8	0.679	0.027478
lama5	0.474	0.038947
lamb1	0.330	0.016556
lamb2	2.251	0.046797
lamb4	2.357	0.015977
ldb3a	2.200	0.030758

Gene	Fold Change	P-value
ldb3b	2.864	0.014755
ldhb	1.348	0.023632
ldhd	1.879	0.019960
ldlrap1a	1.663	0.041348
ldlrap1b	0.415	0.026439
lect2l	0.057	0.044019
lef1	0.374	0.031183
lgals1l2	1.802	0.027478
lhx1b	1.614	0.042024
lhx6	3.309	0.049350
lim2.4	13.737	0.041070
lingo1b	3.036	0.026632
lipf	1.354	0.025752
lman1	0.683	0.015582
lmf2	1.640	0.025727
lmo1	1.432	0.011111
lmo2	0.369	0.024306
lmx1b.2	0.611	0.014755
lnx2a	2.144	0.021660
loxl5b	0.311	0.026187
lratb	0.580	0.020047
lrrc4a	2.559	0.046977
lrrc50	0.629	0.046610
lrrc8a	0.739	0.043642
lrrn1	2.587	0.027300
lrrtm1	2.080	0.009728
lrrtm2	2.205	0.038054
lsrl	0.753	0.027664
lyricl	0.633	0.049349
mab21l1	2.989	0.014755
maf	1.926	0.019970
mafba	0.491	0.030491
mafg2	1.714	0.039225
man2a1	0.458	0.021357
map1b	2.224	0.029248
map1lc3b	0.615	0.030901
map3k5	0.686	0.029105
mapk14a	0.567	0.050856
mapk3	0.531	0.024864

Gene	Fold Change	P-value
mapk4	1.519	0.043599
mark1	2.440	0.031699
marveld2b	0.443	0.027478
matn3a	2.064	0.020422
matn4	2.767	0.015977
mc5ra	4.606	0.009320
mcl1b	0.231	0.021660
mdh1a	1.607	0.046681
mdh1b	2.942	0.009320
mdka	1.394	0.027478
mdm2	0.319	0.031183
me1	1.478	0.037831
me2	1.845	0.014138
me3	2.194	0.036903
mecr	1.363	0.027035
meox1	0.276	0.027478
mespb	0.173	0.045657
metap2l	1.718	0.037373
mfap1	0.845	0.049189
mfng	2.444	0.014755
mfsd2b	1.615	0.025968
mgll	0.631	0.037903
mhc1uba	0.296	0.049189
mif	1.728	0.030262
mip1	19.248	0.032881
mitfa	2.741	0.025727
mkln1	1.642	0.023999
mknk2b	0.178	0.014755
mkrn1	1.325	0.049430
mllt3	0.288	0.036614
mlphb	3.028	0.019970
mmp23a	2.423	0.050560
mobkl1a	1.287	0.033216
mogat2	0.515	0.043773
moxd1	1.323	0.041501
mpeg1	3.179	0.030841
mpp1	0.549	0.026632
mpp5a	0.639	0.014755
mpzl2	0.702	0.021357

Gene	Fold Change	P-value
mpzl3	0.511	0.023632
mrps18c	1.276	0.046681
mrps31	2.308	0.048167
msi2a	0.667	0.049375
msn	7.040	0.015805
msxb	0.492	0.015977
mtch2	1.239	0.042849
mterfd1	0.513	0.043773
mtf2	0.502	0.042038
mthfsd	1.501	0.015406
mtmr8	0.678	0.026102
murc	3.260	0.011492
mut	1.208	0.046610
mxa	0.308	0.014138
mxd3	1.554	0.036921
mxra8a	1.807	0.041590
mybl2	1.318	0.019803
mybpc3	3.584	0.015406
myf5	0.150	0.035004
myf6	2.390	0.019970
myh11	0.273	0.014755
myh6	1.913	0.038181
mylk3	2.706	0.035079
mylz2	3.930	0.014138
mylz3	3.789	0.014755
myo15l1	0.279	0.014755
myoc	0.477	0.026439
myog	0.534	0.038605
myom1a	3.206	0.048905
myoz2	2.344	0.025610
mypt2	0.751	0.046775
nadk	0.686	0.044936
nae1	1.501	0.028212
nalcn	2.041	0.037961
napgl	0.520	0.030501
narf	0.623	0.038572
nbas	1.389	0.038572
nccrp1	1.752	0.049430
ncoa3	0.606	0.049812

Gene	Fold Change	P-value
ND5	1.825	0.023541
ndel1a	1.788	0.038905
ndrg1	0.282	0.013065
ndrg4	2.068	0.046722
ndufa10	1.433	0.035785
ndufab1	1.397	0.025968
ndufb5	1.311	0.038489
nefl	3.201	0.020422
nefm	2.974	0.020422
negr1	1.457	0.031329
net1	0.642	0.017863
neurod4	2.279	0.017081
nf2a	0.676	0.015937
nfe2l3	1.600	0.030030
ngf	0.559	0.027478
nipsnap1	0.302	0.043954
nitr3a	3.417	0.028846
nkx1.2la	0.513	0.032190
nkx1.2lb	4.125	0.039082
nkx2.5	0.542	0.021660
nlcam	0.537	0.016033
nme2l	0.247	0.031183
nmnat2	1.780	0.030501
nog1	0.477	0.036614
nola1	0.699	0.039954
nom1	0.667	0.035595
nop10	0.600	0.025727
nos2b	2.314	0.019697
notch1a	0.544	0.023781
notch2	0.696	0.025641
nots	0.736	0.017843
nox1	0.099	0.044737
npb	2.131	0.011735
nphs2	0.808	0.043047
npl	0.557	0.043861
npsnl	2.241	0.037831
npy1r	2.541	0.045991
nr1h5	1.563	0.044737
nr2f1a	1.937	0.039175

Gene	Fold Change	P-value
nr2f1b	2.322	0.027904
nr4a2a	1.394	0.043165
nr5a1b	3.181	0.046139
nr6a1a	0.233	0.034021
nrarpb	2.415	0.043047
nrg1	0.439	0.043731
nrp1a	0.538	0.015982
nrp2b	0.522	0.049189
nrxn1b	2.882	0.037196
nrxn3b	2.412	0.040154
nsf	2.940	0.014755
ntd5	0.518	0.031863
nubpl	0.875	0.048527
nudt15	0.440	0.025693
nudt4	1.299	0.015406
numbl	0.400	0.018972
nup133	1.270	0.044936
nvl	0.705	0.048679
nxph1	1.909	0.040146
oat	4.751	0.010347
oclna	0.683	0.041496
oep	0.335	0.014138
ogt.2	1.369	0.023376
olfm1b	3.003	0.013925
olfml3	1.653	0.036903
onecut1	2.481	0.019803
opa3	1.464	0.049939
or125-2	1.257	0.031856
os9	1.399	0.041590
osbpl9	0.743	0.023781
otpb	2.726	0.050911
otx1	0.684	0.030841
otx1l	0.526	0.035344
oxsr1b	0.527	0.014755
p2rx3b	1.813	0.029264
p2rx5	2.328	0.043676
p4ha1	0.241	0.029720
p4ha2	0.235	0.027478
pabpc1b	1.570	0.028846

Gene	Fold Change	P-value
paics	0.454	0.023541
pak1	0.647	0.017711
paqr3b	1.511	0.034176
paqr8	0.657	0.028320
pard3	0.729	0.039889
park7	2.212	0.042160
parp12b	1.300	0.014755
parvb	1.600	0.050667
pax2a	0.641	0.029574
pax9	1.697	0.033873
pbk	1.374	0.046555
pbp	1.666	0.012299
pbx1a	1.614	0.027599
pcbd1	1.371	0.037196
pcdh17	2.182	0.023541
pcdh1a4	2.405	0.031140
pcdh1g18	2.061	0.030518
pcdh1gb2	2.031	0.035947
pcdh2ac	1.930	0.013451
pcdh8	0.104	0.044533
pcm1	1.669	0.049769
pcmt	2.271	0.018972
pcsk1nl	3.268	0.014138
pcyt1bb	0.530	0.015977
pdcd6ip	1.324	0.009609
pde5a	1.736	0.014983
pdgfra	0.715	0.021756
pdlim7	2.694	0.014138
pdzk1ip1l	2.521	0.030030
pea3	0.451	0.034276
peli2	0.532	0.019486
penkl	2.930	0.016384
per1b	0.389	0.030501
pex12	1.480	0.031863
pfkfb1	0.604	0.021014
pfkfb2	2.009	0.027300
pfkfb3	0.137	0.012839
pfkfb4	0.566	0.013451
pfkfb4l	0.639	0.017711

Gene	Fold Change	P-value
pfkma	5.920	0.047859
pfn2	1.274	0.030171
pgam1a	0.403	0.025582
pgam1b	1.501	0.029264
pgd	1.559	0.043954
pglyrp2	0.657	0.009703
phactr2	1.337	0.038351
phax	1.574	0.014755
phlda3	0.318	0.048478
pigp	3.020	0.017843
pik3c3	1.628	0.049189
pik3r3	1.726	0.046344
pim1	0.097	0.025136
piwil1	0.528	0.027922
pla2g12b	0.692	0.025538
pla2g15	0.753	0.032723
plcd1b	0.773	0.016384
plcxd3	2.014	0.025136
plekha8	1.592	0.044341
plk2	0.548	0.014755
plod1a	0.507	0.009609
plp1a	2.821	0.030901
plxna4	1.592	0.049430
plxnd1	0.652	0.043599
pno1	0.688	0.028857
pnpo	3.410	0.042820
pnx	0.266	0.048096
pola1	1.470	0.027300
pold2	1.496	0.027300
polr1e	0.707	0.039175
polr2c	1.669	0.013925
pomgnt1	1.251	0.043773
popdc1	2.494	0.029248
popdc3	4.245	0.046695
pou12	1.427	0.019370
pou3f3b	1.725	0.028718
pp	0.488	0.050577
ppa1	1.712	0.039162
ppcdc	1.735	0.046274

Gene	Fold Change	P-value
ppib	1.142	0.031183
ppm1k	1.304	0.045331
ppp1cc	1.485	0.050856
ppp2r4	1.283	0.050239
prcp	2.240	0.029973
prdm1a	0.450	0.019388
prdm1b	0.208	0.047394
prdx6	2.909	0.032881
prickle1a	0.152	0.037831
prickle1b	0.518	0.014755
prim1	1.648	0.036903
prkar2ab	1.967	0.042786
prkch	0.399	0.044064
prl	3.767	0.042677
prlrb	0.358	0.014755
prnprs3	1.848	0.014755
prox1	1.491	0.038947
prph	2.007	0.013226
prss35	3.970	0.049086
prtga	0.660	0.046610
psap	0.701	0.030501
pskh1	1.574	0.018972
psmb9b	0.197	0.016384
psme1	0.084	0.040023
ptgisl	0.553	0.022563
ptgs1	0.370	0.033996
ptgs2b	0.104	0.014755
pth2	5.652	0.013925
ptpn4	0.661	0.033996
ptprk	0.469	0.021660
ptpru	0.630	0.042431
ptrf	2.043	0.027478
purb	2.028	0.041446
pvalb1	5.177	0.027478
pvalb2	4.830	0.038905
pvalb4	4.403	0.023781
pvalb5	6.742	0.038489
pvrl2l	0.478	0.049716
pxk	0.645	0.013925

Gene	Fold Change	P-value
pyya	6.151	0.042958
qdpra	2.161	0.041774
rab14	1.750	0.015821
rab24	0.877	0.047798
rab38	2.826	0.009320
rab39b	2.022	0.014138
rab3c	1.574	0.038489
rab3d	1.380	0.014755
rab6b	1.949	0.021014
rac2	1.522	0.025693
racgap1	0.764	0.043047
rad23b	0.430	0.038905
rarga	0.469	0.014755
rb1	1.335	0.042842
rbb4	1.407	0.044973
rbks	1.842	0.015406
rbp1a	1.519	0.025727
rbp4	4.338	0.036614
rbpms2	0.505	0.021660
rchy1	0.759	0.037066
rcl1	0.583	0.022563
rcv1	0.358	0.027792
rd3	1.396	0.042024
rdh5	3.266	0.043165
rel	0.404	0.034176
rfx2	0.476	0.025641
rfx4	0.379	0.038905
rgl1	0.511	0.027734
rgs17	2.506	0.014138
rgs20	1.845	0.039137
rgs4	0.250	0.011111
rgs7bpb	1.623	0.047321
rhag	3.123	0.003761
rhbg	0.350	0.015406
rhogc	1.204	0.039280
rhoub	0.496	0.043645
ripply1	0.151	0.042038
ripply2	0.122	0.041590
rnaseka	0.802	0.046371

Gene	Fold Change	P-value
rnd1l	0.495	0.014138
rnd3a	0.622	0.025693
rnf11	0.636	0.032623
rnf14	1.279	0.025727
rnf17	0.740	0.029248
rnf24	0.439	0.015406
rnls	1.514	0.030841
rorab	2.240	0.047981
rpl10a	0.770	0.047798
rpl28l	0.804	0.050203
rpl4	0.787	0.025641
rpl8	0.759	0.039732
rprm	0.258	0.033996
rps24	1.512	0.035028
rqcd1	2.080	0.025727
rrbp1	0.771	0.030901
rrm1	1.415	0.048096
rtf1	1.499	0.049769
rtn1a	1.861	0.014755
rtn1b	2.252	0.040600
rtn2b	3.292	0.034652
rtn4a	1.590	0.043861
rtn4rl1	1.468	0.032779
rundc3b	0.282	0.027599
runx1	0.343	0.023312
runx3	0.343	0.047798
rxraa	0.614	0.042615
ryr1a	1.370	0.036222
s100a10a	0.442	0.035004
s100a10b	1.636	0.041921
s100u	0.683	0.017915
s1pr1	1.978	0.017296
sall1a	1.960	0.027404
sall4	0.393	0.035806
sap30l	1.155	0.045598
sat1	1.792	0.036157
scn4ab	3.359	0.029248
scn4ba	2.827	0.015406
scpp8	0.620	0.043676

Gene	Fold Change	P-value
sdad1	0.637	0.040043
sdcbp	0.624	0.031863
sdha	1.527	0.021660
sdr16c5	2.091	0.014755
sec14l1	0.686	0.049189
sec61al2	0.547	0.023541
sec61b	0.541	0.045321
sema3fb	0.525	0.014755
sepn1	0.717	0.046977
sept4b	0.392	0.019917
sept9a	0.659	0.050577
serac1	1.803	0.035028
serf2	1.242	0.034208
serhl	2.840	0.023878
serinc1	0.716	0.036157
sesn1	0.532	0.021651
setd3	1.474	0.024006
setd8a	0.865	0.023541
setmar	2.357	0.030758
sfrs7	1.817	0.046977
sgcd	2.631	0.023541
sgce	1.771	0.046771
sgcg	2.572	0.043191
sgk1	0.502	0.038572
sh3bp5	0.657	0.024941
sh3gl2	1.481	0.044064
shd	0.572	0.025727
shmt1	0.518	0.038489
shox	2.075	0.043773
shox2	2.892	0.027300
silva	2.744	0.012650
silvb	4.092	0.014138
six4.2	0.681	0.043191
six6b	2.540	0.038544
skap1	0.554	0.041590
slc10a1	2.837	0.049863
slc10a4	2.396	0.046797
slc12a2	1.516	0.030320
slc16a12b	1.433	0.039606

Gene	Fold Change	P-value
slc17a6l	3.073	0.021014
slc1a2	2.014	0.023165
slc1a3	1.323	0.038198
slc20a1a	1.625	0.050207
slc25a22	1.945	0.028402
slc25a25	2.030	0.030901
slc25a28	1.426	0.038947
slc25a3	0.670	0.048096
slc25a36b	0.440	0.027379
slc25a4	5.194	0.033573
slc25a46	1.646	0.030501
slc25a5	0.751	0.017542
slc26a5	0.614	0.038947
slc2a15a	4.284	0.009320
slc2a15b	2.744	0.012309
slc31a1	0.379	0.014755
slc34a2aas	1.528	0.040096
slc34a2b	0.527	0.031863
slc37a4	0.568	0.036390
slc38a3	0.527	0.017542
slc38a4	2.039	0.045321
slc38a7	0.557	0.031799
slc39a6	0.791	0.043047
slc39a7	1.355	0.039338
slc40a1	3.283	0.050513
slc46a1	0.712	0.025727
slc4a1	2.800	0.017711
slc4a1b	1.658	0.029264
slc4a4b	1.574	0.047798
slc5a11	1.708	0.027478
slc5a9	2.076	0.017863
slc6a5	3.471	0.015982
slc7a7	1.666	0.046681
slc8a3	1.566	0.046797
slc9a3r2	0.767	0.036390
smad2	0.606	0.040600
smad3b	2.601	0.014755
smad7	0.550	0.014755
smo	0.701	0.016384

Gene	Fold Change	P-value
smpx	1.528	0.049769
smyd1a	2.814	0.014755
smyd2b	1.936	0.030501
smyd3	0.714	0.036614
snai1a	0.340	0.042677
snai1b	0.172	0.049423
snap25a	2.380	0.030990
snap25b	3.535	0.019960
sncb	1.909	0.027478
sncga	2.162	0.033601
sncgb	2.203	0.009320
snd1	0.431	0.011111
snx5	1.292	0.035693
sod2	2.760	0.012299
sox11a	1.454	0.037831
sox21b	1.645	0.046435
sox4a	1.674	0.050390
sox7	0.408	0.027537
sox9b	0.388	0.030320
sp5	0.631	0.017711
sp5l	0.312	0.020422
sp7	0.327	0.043668
sp8	0.584	0.021660
sp8l	0.801	0.038947
sp9	0.575	0.013268
spam1	3.967	0.046610
sparcl	2.482	0.044064
spata6	1.384	0.038528
spcs3	0.745	0.045331
spi1	0.546	0.036908
spon1a	2.368	0.046681
sprn	4.612	0.015223
spry2	0.674	0.028846
spry4	0.514	0.009320
spsb4a	0.607	0.036529
sptb	2.449	0.036614
src	0.533	0.014755
srl	1.800	0.015545
srp68	0.747	0.042820

Gene	Fold Change	P-value
ssbp3	0.555	0.046899
ssr1	0.413	0.046610
ssr2	0.582	0.028980
st13	1.343	0.039247
st6galnac5	1.918	0.037831
st8sia1	1.539	0.044936
st8sia7.1	0.355	0.030990
stac3	2.688	0.014755
stap2b	0.261	0.043663
stard10	0.554	0.043599
stat1a	0.495	0.021660
stm	0.456	0.021651
stmn1b	2.799	0.049189
stmn2a	2.003	0.031863
stmn2b	1.839	0.014138
stnnc	2.090	0.028846
stom	0.700	0.043047
strada	1.514	0.021660
stx11b.1	0.516	0.046888
stxbp1	2.178	0.014755
sub1	1.405	0.044019
sucla2	1.697	0.019970
suclg1	1.367	0.023781
sulf1	0.654	0.033164
sulf2	1.738	0.030758
sult1st4	3.736	0.031203
sult1st6	2.605	0.027875
sult2st1	0.677	0.037831
suv39h1a	1.425	0.036921
syn2a	2.136	0.017711
syn2b	2.589	0.025641
syngr3	1.906	0.017296
syntaxin1b	1.953	0.031863
syt1	1.572	0.011111
syt11a	1.777	0.028320
syt12	2.177	0.047798
syt4	1.951	0.014138
tac1	2.125	0.015977
taf1b	0.660	0.027300

Gene	Fold Change	P-value
tagln2	0.533	0.023068
tal1	0.402	0.035028
tal2	2.335	0.023541
tbc1d7	0.664	0.035028
tbr1	2.291	0.023084
tbx15	1.764	0.009320
tbx16	0.066	0.024006
tbx24	0.096	0.027478
tbx2a	0.605	0.023781
tbx3b	0.463	0.003518
tbx6	0.098	0.036614
tcf7l1a	0.558	0.013925
tcf7l2	1.510	0.046797
tead1	0.242	0.029973
tekt2	1.758	0.048096
tfa	0.596	0.043047
tfap2a	0.718	0.026588
tfap2b	1.766	0.041590
tfap2c	0.655	0.045331
tfap2e	3.459	0.009320
tfcp2l1	1.620	0.042849
tfdp1	0.748	0.023541
tfdp2	1.717	0.019033
tfip11	0.794	0.015982
tgm2	3.054	0.015406
thbs1	2.271	0.027537
thbs3b	0.534	0.049793
thbs4b	0.683	0.040267
them2	1.790	0.004320
thoc5	0.591	0.025641
tie1	0.669	0.033316
tigarb	0.622	0.049169
tjp2b	0.768	0.029973
tm9sf3	0.794	0.039175
tmbim1	0.392	0.042155
tmem110l	0.736	0.014755
tmem115	0.714	0.039082
tmem150	0.551	0.030990
tmem178	2.229	0.020047

Gene	Fold Change	P-value
tmem57a	1.367	0.045260
tmem59l	1.923	0.031863
tmod4	2.466	0.026187
tmprss13a	1.855	0.019960
tmprss4a	0.629	0.038605
tmsb	2.396	0.013925
tmtc3	0.652	0.043047
tmtc4	1.775	0.030501
tnc	1.976	0.043047
tnfsf10l2	1.926	0.036207
tnks	0.607	0.014755
tnnc	2.129	0.021081
tnnt1	1.842	0.050177
tnnt3a	4.749	0.028320
tnnt3b	6.382	0.047350
tnr	1.607	0.028846
tnrc5	1.643	0.025529
tnw	3.710	0.011785
tomm20	0.641	0.025968
tor2a	0.782	0.026632
tp53bp2	0.693	0.040023
tp63	0.495	0.031183
tp73	0.693	0.030501
tph2	1.606	0.049430
tpm3	1.698	0.046681
tpm4	0.725	0.027728
traf3	0.217	0.049716
traf4b	1.493	0.038489
tram1	0.616	0.036614
trim71	0.397	0.028846
trpc4apa	0.807	0.028320
trpc5	1.468	0.035947
trpn1	2.188	0.038947
trpv6	2.149	0.023659
tsc22d2	0.467	0.011735
tspan15	0.491	0.043477
tspan7b	1.904	0.031553
ttc25	0.683	0.034909
ttna	3.607	0.015720

Gene	Fold Change	P-value
ttnb	1.804	0.046835
ttpa	0.760	0.035344
tuba1	3.065	0.025968
tuba2	2.350	0.017081
twf2	3.363	0.012753
twistnb	0.457	0.024016
txnip	0.424	0.011111
txnrd1	2.027	0.027038
tyms	1.521	0.029105
tyrp1b	6.180	0.018469
tyw3	0.734	0.046797
uap1	0.669	0.043540
ube2r2	1.502	0.027173
ube2w	0.672	0.024306
ubn2	0.740	0.022269
ubtf	1.520	0.030758
ubtfl	1.917	0.046610
uchl3	1.719	0.027478
ulk1	2.334	0.014138
unc119.1	0.745	0.014755
unc119.2	1.575	0.049863
unc5b	0.539	0.046771
uncx4.1	0.373	0.038572
unk	0.431	0.020223
upk3l	1.951	0.015406
uso1	0.623	0.040419
usp16	0.833	0.037436
usp25	0.786	0.049863
uvrag	0.616	0.027191
vamp3	0.796	0.050048
vat1	2.140	0.027537
vcanb	1.976	0.024681
vcl	1.803	0.013268
vdac3	1.664	0.050594
vegfab	1.761	0.038834
vgll2b	0.547	0.015173
vhl	0.434	0.027300
vmhc	0.729	0.013065
vsx1	1.901	0.014755

Gene	Fold Change	P-value
vtnb	5.096	0.033601
wdsof1	0.630	0.014755
wif1	0.680	0.042150
wnt16	0.650	0.044936
wnt2b	0.276	0.011324
wnt4a	0.597	0.015406
wnt5b	0.495	0.016384
xdh	2.761	0.029248
xirp2	2.470	0.014339
xirp2l	8.025	0.038211
xpo7	0.819	0.030758
ypel1	0.250	0.040170
ypel3	0.469	0.049442
ywhae2	0.600	0.040043
ywhag1	1.874	0.020422
ywhah	1.154	0.047659
ywhaqa	0.631	0.037831
zbtb33	1.750	0.044936
zc3h15	1.624	0.046797
zcchc9	0.711	0.038874
zfand1	1.425	0.041446
zfand5a	0.540	0.023781
zfhx1	0.528	0.049812
zfyve21	0.696	0.014755
znf503	0.555	0.046775
znf536	2.069	0.009320
znf598	1.313	0.045244
znf703	0.621	0.039732
znfl1	0.376	0.043663
znrd1	0.728	0.041442
znrf1	2.194	0.024016

Table C2 – Significantly changed genes at 36 hpf in response to GR knockdown

Gene	Fold Change	P-value
a2bp1	1.904	0.020380
aanat2	0.601	0.040592
aatf	0.590	0.038630
abat	0.786	0.040365
abcc9	3.522	0.049154
abcd3b	0.645	0.044795
abhd2a	0.762	0.043023
acadl	2.723	0.041818
acat1	1.983	0.041292
accn2a	2.385	0.041795
accn2c	1.809	0.044245
ache	2.211	0.049497
acsl4a	0.607	0.035106
acsl4l	0.461	0.040956
acss1	0.549	0.032396
acta1b	3.130	0.032631
actn3a	2.852	0.034461
ada	2.820	0.041377
adam10b	1.279	0.044997
adam17a	0.880	0.045768
adcyap1b	2.551	0.028907
adi1	0.688	0.047397
adipor1b	0.785	0.046466
adssl1	2.639	0.043463
agpat4	0.737	0.050355
agr2	2.127	0.045159
agxtl	1.837	0.044997
ahr2	1.654	0.041795
ahrrb	2.616	0.044795
aig1	2.750	0.043387
alas1	0.569	0.031970
aldh2b	1.926	0.045514
aldh3d1	0.615	0.046829
allc	4.029	0.044121
amph	2.053	0.044004
amt	0.696	0.048422
ank1	2.872	0.035106

Gene	Fold Change	P-value
aox1	2.182	0.039477
apba1	1.410	0.044795
aplp	2.797	0.032396
apoea	3.179	0.032396
appb	1.756	0.032974
arhgef7b	1.253	0.048823
arl15b	1.336	0.028477
arl6ip4	0.561	0.050828
arl6ip5	0.439	0.048823
arpc1b	2.436	0.039705
asb16	2.225	0.041050
asb8	1.653	0.045514
ascl1a	2.276	0.044245
ascl1b	2.843	0.046598
aspdh	2.778	0.040365
atad4b	0.483	0.046320
atl1	1.790	0.048598
atoh2a	3.744	0.034461
atoh2b	3.008	0.048598
atp2a1	2.591	0.041818
atp2a1l	25.433	0.044997
atp2a2a	0.693	0.035106
atp2b3a	2.537	0.034461
atp6v1b2	2.247	0.032396
avpl	2.752	0.050266
b3gat2	1.751	0.046083
bach2	1.806	0.035106
barhl1.1	2.819	0.035106
barx1	3.155	0.044795
bcl11a	5.987	0.044121
bdnf	2.006	0.041795
bhlhb3l	0.576	0.045159
bmpr2b	1.756	0.032396
bod1	1.165	0.050828
brpf1	1.355	0.044936
brunol5	2.403	0.050266
c1d	0.690	0.035106
c1qtnf4	2.422	0.032396
c6	0.526	0.046751

Gene	Fold Change	P-value
ca14	8.968	0.049517
ca2	2.205	0.046751
cabp1	2.744	0.034163
cacna1s	2.172	0.045133
cacna2d1a	1.770	0.045514
cacnb2b	0.425	0.039705
cacnb4b	2.798	0.047676
cacng2	2.316	0.032396
cacng2b	2.116	0.040296
cad	0.663	0.044245
cadm2a	2.735	0.045761
cadm3	2.241	0.046822
cadm4	1.685	0.032919
calb2	2.560	0.041795
calb2l	3.645	0.024975
calca	2.496	0.050346
calhm2	2.596	0.044245
calm1b	1.537	0.047563
calrl	0.726	0.043387
camk2a	2.368	0.046235
camk2d2	3.115	0.031433
camkv	2.579	0.044245
camsap1	1.951	0.039705
cant1b	0.546	0.035106
caprin1a	1.237	0.043800
caspb	6.239	0.039669
cblb	1.837	0.035106
cbln1	3.338	0.033095
cbln2b	1.798	0.049186
cbln4	2.006	0.024975
cbx1b	2.351	0.034163
cbx4	1.189	0.048823
ccbl1	1.765	0.034163
ccdc85al	2.494	0.031970
ccl-c11b	2.133	0.044997
ccng1	0.566	0.049154
cd9	1.250	0.040832
cdc14aa	0.732	0.032396
cdc37	0.810	0.047397

Gene	Fold Change	P-value
cdh10	1.806	0.047397
cdk5r2	3.220	0.039477
cdkn1b	1.213	0.045159
chad	9.655	0.050206
chchd3	1.762	0.049236
chordc1	0.716	0.032974
chrna4	1.839	0.047920
chst1	2.146	0.049154
cirh1a	0.549	0.044004
ciz1	1.170	0.049154
ckma	3.325	0.040832
ckmb	2.923	0.041795
clasp2	1.576	0.035106
clcn7	0.794	0.047397
cldn19	2.540	0.037957
cldnb	0.493	0.041795
cldne	0.499	0.044245
cldnf	1.614	0.047563
clstn1	1.614	0.047563
cmlc1	0.523	0.040832
cnih2	4.204	0.021690
cntn1b	4.417	0.035106
col1a1	2.684	0.043905
col1a2	2.127	0.044083
col1a2	1.501	0.048422
col1a3	3.105	0.048598
col1a3	3.105	0.048598
col6a1	3.053	0.034461
col6a1	3.053	0.034461
col6a2	2.988	0.044795
col6a2	2.988	0.044795
colm	3.557	0.034461
colm	3.557	0.034461
coro1b	1.875	0.038630
coro1b	1.875	0.038630
cplx2	2.472	0.040832
cpt1b	3.835	0.044245
cpt1b	4.143	0.045159
cpvl	0.783	0.049691

Gene	Fold Change	P-value
crabp1a	2.007	0.048823
crabp1b	2.232	0.034461
crfb1	1.749	0.045159
crhbp	1.434	0.039477
crip2	0.418	0.044900
crispld1	3.028	0.047563
crlf1a	0.665	0.037484
cry3	0.611	0.046320
cryaba	0.353	0.037660
cryba1b	7.381	0.024975
cryba2a	8.994	0.040296
cryba4	9.623	0.020380
crybb1	13.092	0.042308
crybb3	0.818	0.050266
crygm2a	29.380	0.035106
crygm2b	45.889	0.048823
crygm3	19.986	0.049517
crygmx	10.219	0.020380
crygn2	8.704	0.039477
csdc2	2.792	0.039705
csf1b	3.004	0.046822
csmd2	2.013	0.024975
csnk1e	1.834	0.048294
cspg5	1.702	0.044245
ctnna2	3.090	0.047887
ctsba	0.577	0.045003
ctssa	4.286	0.032396
cugbp1	0.685	0.048422
cugbp2	2.212	0.045003
cul3	1.186	0.048598
cx23	3.177	0.043800
cx43.4	0.519	0.047920
cx44.1	2.787	0.050126
cygb1	0.415	0.041818
cygb2	2.360	0.039705
cyp19a1b	1.504	0.048598
cyp1b1	3.484	0.041795
cyp2j27	2.084	0.040956
cyp2x12	1.813	0.048823

Gene	Fold Change	P-value
cyp4v2	2.609	0.039750
dab1	2.363	0.047563
dbx1a	1.988	0.045768
dck	1.738	0.045133
dclk1	1.974	0.040956
dclk2	1.677	0.040331
dcp1a	1.358	0.050525
dct	3.512	0.039705
ddb2	0.360	0.041795
ddc	2.840	0.040296
ddx18	0.570	0.046320
ddx51	0.410	0.044083
ddx55	0.700	0.050870
ddx56	0.593	0.048528
def	0.658	0.048823
defbl1	6.124	0.039477
dennd4a	0.869	0.047397
dgat1	2.544	0.040365
dhdhl	0.637	0.049497
dhrs11a	0.735	0.039681
dhx16	0.756	0.044245
dhx37	0.590	0.048422
dio2	2.788	0.044795
diras1	3.251	0.037660
dixdc1	1.713	0.046320
dkc1	0.561	0.044795
dla	2.062	0.037952
dlb	2.108	0.044245
dlc	1.451	0.050355
dld	1.857	0.020380
dlx4a	2.657	0.044795
dlx6a	1.649	0.048422
dnase1l3l	12.346	0.050266
dnmt4	0.623	0.044245
dnttip2	0.622	0.041779
dpp6b	2.220	0.022280
dpyd	1.516	0.049038
dpysl2	1.680	0.040296
dpysl4	1.810	0.049517

Gene	Fold Change	P-value
dpysl5b	1.778	0.047887
drd2a	1.610	0.022397
drd4a	1.590	0.021690
dtnb	1.791	0.039669
dusp5	0.459	0.045133
dynlt3	1.378	0.046215
eaf1	1.306	0.034163
eapp	0.762	0.041795
ebna1bp2l	0.536	0.040296
edf1	0.673	0.046751
edn1	0.798	0.049038
ednrb1	2.170	0.045159
efcab7	1.294	0.045514
eif2b3	0.571	0.044083
eif6	0.686	0.043800
ek1	1.885	0.044795
elavl4	2.587	0.050355
elmo1	1.501	0.040832
elovl4	1.452	0.048598
elovl6	2.029	0.041795
emilin1a	1.451	0.032396
eno2	1.603	0.042308
eno3	2.000	0.031433
enpp6	2.229	0.041292
eomesa	1.661	0.049154
epyc	5.508	0.024975
ercc2	0.755	0.044795
etv1	1.786	0.047233
evi1	1.679	0.044900
evla	1.518	0.040956
evlb	2.565	0.039705
evx1	1.976	0.037957
exoc6	2.022	0.049154
exosc8	0.613	0.032974
eya4	1.582	0.034163
f5	2.728	0.049691
f7i	2.167	0.042787
fabp11b	10.868	0.049517
fabp7a	4.000	0.046235

Gene	Fold Change	P-value
fah	2.312	0.043967
fam70a	6.040	0.035106
fancd2	0.840	0.040832
fancl	0.755	0.032396
fbl	0.655	0.037957
fbln1	0.486	0.049517
fbp1a	1.462	0.046829
fbp2	4.126	0.020380
fdps	0.790	0.043463
fech	0.392	0.039692
fez1	3.566	0.036240
fgf13l	2.427	0.020380
fgf6a	2.432	0.049154
fgl2	1.184	0.049517
fhl	1.674	0.044795
fkbp1b	1.883	0.032396
flncb	0.337	0.048823
foxf1	2.268	0.045768
foxn4	4.716	0.044245
foxq1	0.659	0.048422
frem3	0.748	0.049038
fstb	0.657	0.050266
ftr29	0.706	0.044795
ftr79	0.658	0.050355
fxyd6	5.856	0.032396
fyna	2.188	0.039705
gabra1	3.145	0.039477
gabrb2	2.521	0.039705
gad1	3.826	0.046320
gad2	4.133	0.039477
gadd45a	0.550	0.037957
gadd45bl	0.256	0.020380
gapdh	1.737	0.035106
gart	0.553	0.035106
gbgt1l3	2.374	0.050243
gcga	2.149	0.039669
gck	1.624	0.040956
gcm2	0.651	0.044795
gdf11	2.584	0.050870

Gene	Fold Change	P-value
gefiltin	2.587	0.035106
gfap	1.390	0.041795
ggt1	3.559	0.032396
glra1	9.846	0.039705
glra3	2.274	0.050243
glud1b	2.060	0.048963
glula	0.421	0.040956
gmfb	0.620	0.045842
gnai3	0.671	0.040592
gnao1a	1.852	0.037957
gnb5	2.204	0.046829
gng12	0.802	0.044245
gng2	1.619	0.040296
gng3	2.254	0.040592
gng7	1.555	0.049855
gnrh2	0.299	0.040832
gpc3	1.603	0.040467
gpib	2.732	0.043463
gpm6aa	3.168	0.040296
gpm6ab	2.210	0.035106
gpr177	0.642	0.043463
gpr27	2.518	0.040832
gpx4a	0.339	0.045003
grhl1	0.509	0.035106
gria2a	3.666	0.048422
gria2b	3.247	0.035106
grifin	13.894	0.032396
grin1b	8.644	0.044795
gtf2f1	0.850	0.024975
gtf3aa	0.542	0.034461
guca1e	0.617	0.045768
gys1	2.626	0.046744
hccsa	0.618	0.029813
hdac9b	0.531	0.044795
hdr	0.363	0.046320
heca	1.965	0.040592
helt	2.507	0.041377
her13	2.887	0.031433
her3	0.686	0.050159

Gene	Fold Change	P-value
her4.2	2.180	0.044121
her5	2.766	0.045514
her8.2	4.583	0.032974
hes5	1.487	0.039477
hhatla	3.008	0.032396
hlx1	3.008	0.032396
hlxb9la	1.570	0.048988
hmx3	1.732	0.049691
hnrnpa0	0.712	0.020380
hnrnpa3	1.430	0.049038
hnrnpm	1.338	0.042308
homer1	2.222	0.050870
hpca	1.741	0.047299
hs6st2	0.621	0.046822
hsd17b3	0.770	0.044083
hspb3	5.547	0.034163
ier5	1.147	0.041818
ifng1-2	0.519	0.025317
igfbp3	1.862	0.046761
igsf21a	2.015	0.040296
ihha	0.628	0.041795
il15	1.636	0.046829
ing5b	0.610	0.039813
insl5b	1.988	0.044245
insm1a	2.846	0.034163
irge4	0.706	0.034163
irgf3	0.547	0.047858
irx1a	1.536	0.039669
irx2a	2.773	0.035995
irx4a	3.478	0.050870
isl1	1.783	0.038292
islr2	3.392	0.039477
isoc2	2.165	0.041795
itgb1b.2	2.999	0.042261
itgb3b	2.395	0.039477
itm1	1.234	0.045443
itm2ca	1.983	0.046320
jph2	3.784	0.047233
kal1a	1.831	0.046235

Gene	Fold Change	P-value
kat2b	3.014	0.024975
kcnd3	1.896	0.020380
kcnip3	2.521	0.022236
kcnip3l	2.310	0.020380
kdm6b	1.796	0.044245
kidins220b	1.610	0.039553
kif23	2.063	0.048823
kif3c	4.195	0.037957
kif5a	2.361	0.032974
klf13l	1.969	0.044245
klf2b	1.187	0.024975
klhdc6	5.948	0.039705
klhl6	2.053	0.042542
kmo	2.080	0.042308
kpna4	0.890	0.048823
kri1l	0.618	0.040832
krt15	3.340	0.045514
ktn1	1.183	0.035106
lbx1b	2.645	0.035106
ldb3a	3.224	0.032396
ldb3b	3.184	0.046822
lect2l	0.218	0.046215
lhx1b	2.642	0.046744
lhx6	6.826	0.050346
lhx9	2.559	0.036776
lim2.3	10.201	0.044245
lim2.4	9.430	0.050206
lin37	0.761	0.041795
lin7a	3.198	0.041779
lingo1b	2.714	0.035106
lmbr1l	0.639	0.034145
lmbrd2b	1.993	0.035106
lmo1	2.009	0.035106
lmo3	2.495	0.040832
lnx2a	2.830	0.039705
lonp2	0.603	0.050266
lox	1.861	0.047397
lrit1	2.437	0.040721
lrrc4a	2.466	0.044245

Gene	Fold Change	P-value
lrrc4c	2.373	0.044121
lrrc50	0.670	0.041292
lrrn1	1.938	0.049154
lrrtm1	2.447	0.043463
lrrtm2	2.518	0.024063
lyricl	0.532	0.035106
lyz	3.283	0.041795
mab21l1	1.587	0.046456
magi1	1.333	0.048598
mak16	0.461	0.039705
map1b	1.427	0.044795
mapk10	2.487	0.020380
mapk14a	0.729	0.046320
mapk3	0.746	0.035106
mapk4	2.039	0.048422
matn3a	3.241	0.020380
mc1r	3.728	0.039705
mcoln1	2.164	0.044083
mdm2	0.355	0.044795
me1	2.462	0.020380
med19b	0.786	0.048598
megf11	3.573	0.024975
meis2.1	2.005	0.024975
meis2.2	1.566	0.044795
mif4gda	0.735	0.045003
mip1	7.800	0.020380
mip2	29.418	0.043905
mkrn1	2.374	0.044795
mlphb	2.695	0.040956
mmp23a	2.572	0.047459
mmp23al	3.089	0.039477
mmp24	3.464	0.032396
mogat2	0.637	0.044083
mphosph10	0.564	0.041818
mpp1	0.720	0.049193
mpp2b	2.003	0.024975
mpx	3.588	0.038630
msi2b	1.324	0.034461
msn	4.675	0.035106

Gene	Fold Change	P-value
mstn	3.365	0.022236
mtap	0.664	0.043905
mthfd1	0.494	0.048294
mthfsd	0.629	0.041795
mtmr7b	1.643	0.048636
mus81	0.742	0.050266
musk	0.626	0.044900
mxa	0.623	0.047227
mxra8b	4.855	0.044245
mybbp1a	0.495	0.032396
mycbp2	1.431	0.046235
mylk3	3.352	0.040832
mylz2	3.412	0.034461
mylz3	4.369	0.034461
myo3a	1.938	0.040832
myo5a	1.806	0.032974
myom1a	2.902	0.044121
nadl1.2	2.006	0.048422
nalcn	2.000	0.044245
nap1l4b	1.604	0.049517
napg	2.658	0.034461
nat10	0.504	0.044900
nat5	0.871	0.044795
nbr1	1.536	0.020380
ncald	1.407	0.046250
ncl	0.510	0.034461
ndel1b	0.463	0.034461
ndor1	1.858	0.047563
ndpkz2	4.298	0.028962
ndrg4	5.340	0.035106
nefl	4.733	0.034461
nenf	0.688	0.035106
neurod	1.699	0.034145
neurod2	4.673	0.044083
neurod4	3.266	0.037952
nfatc1	1.642	0.044245
nfkbiab	0.689	0.044795
ngdn	0.486	0.034461
nhlh2	2.637	0.043800

Gene	Fold Change	P-value
nkx1.2lb	3.887	0.031083
nkx2.2a	1.440	0.034461
nkx6.3	2.915	0.032396
nlgn4b	1.786	0.040956
nmbr	0.560	0.041795
nmnat2	2.455	0.034461
noc3l	0.642	0.028962
nod2	1.582	0.041818
nola1	0.604	0.047397
nom1	0.715	0.054707
nop10	0.643	0.046829
nop14	0.686	0.050355
nop56	0.570	0.032919
npm1	0.448	0.040832
nppa	6.808	0.020380
npsnl	3.493	0.032396
nptn	2.120	0.043800
npy	0.509	0.041818
npy1r	2.905	0.050035
nr2f1a	1.974	0.050702
nr3c1	3.851	0.035106
nr5a1b	3.606	0.044795
nrarpb	1.607	0.032396
nrxn1b	4.848	0.048528
nrxn2a	2.551	0.041818
nrxn2b	2.668	0.032921
nrxn3b	2.699	0.032974
nsf	2.502	0.044795
nsun2	0.601	0.049154
nupr1	1.874	0.045003
nxph1	2.857	0.040832
oc90	0.308	0.039477
oca2	2.326	0.034461
ociad2	1.289	0.049154
olfm1a	1.991	0.047098
olfm1b	2.505	0.035106
olfm3	2.766	0.020380
olfml3	2.708	0.032974
olig2	1.509	0.047563

Gene	Fold Change	P-value
omp	2.322	0.035106
onecut1	2.290	0.037952
oprl	2.899	0.048766
optc	0.372	0.047397
or120-1	2.151	0.039705
or130-1	2.779	0.043463
otpb	2.646	0.046320
p2rx3a	0.524	0.048422
pax3a	1.523	0.044795
pax6a	1.323	0.044368
pbx3b	2.923	0.034461
pcdh17	1.968	0.044795
pcdh1a4	2.846	0.028477
pcdh1g18	1.689	0.053460
pcdh1g3	1.629	0.038670
pcdh1gb2	1.838	0.044795
pcdh2ac	2.351	0.020380
pcolce2b	0.485	0.046822
pcp4a	2.838	0.037957
pcp4b	3.882	0.040956
pcp4l1	1.819	0.050738
pcsk1nl	2.046	0.048823
pdcd11	0.571	0.041795
pdcd4b	1.862	0.043463
pde6c	0.485	0.020380
pde6g	5.530	0.032631
pdgfrl	3.642	0.049363
pdlim5	2.288	0.050355
pdlim7	2.700	0.032396
penk	2.742	0.034504
pes	0.535	0.044083
pfkfb2	2.292	0.035106
pfkma	10.841	0.041795
pgam1b	2.018	0.040832
phkg2	1.348	0.035106
pion	0.579	0.050870
pisd	1.197	0.049154
pla1a	1.185	0.044245
plekhf1	0.348	0.046751

Gene	Fold Change	P-value
plekho1	1.512	0.041795
plp1a	2.545	0.044083
plxna4	2.200	0.049497
pofut2	0.834	0.041818
polr1a	0.613	0.041292
polr2b	0.687	0.044795
polr2e	0.754	0.041818
pomca	3.643	0.042542
pou3f3b	1.737	0.033081
pou47	1.483	0.044245
pou4f1	1.814	0.044245
ppan	0.527	0.032396
ppargc1b	0.691	0.048422
ppig	0.599	0.041795
ppox	0.580	0.043967
ppp2r4	1.447	0.041104
pppde2a	2.003	0.030693
prg4	0.498	0.044855
prkcsh	1.301	0.050870
prph	2.647	0.040956
prss35	2.393	0.041377
ptf1a	4.169	0.035106
ptgds	0.242	0.022236
pth1a	2.774	0.031970
ptprn	2.533	0.036240
ptprn2	1.591	0.035106
pufa	0.419	0.039692
pus7	0.580	0.041795
pvalb1	4.616	0.040832
pvalb2	3.490	0.045514
pvalb4	6.632	0.044083
pvalb5	6.739	0.049517
pvalb6	2.336	0.039692
pwp2h	0.618	0.046215
pycrl	0.878	0.039477
pyya	9.890	0.034461
qtrtd1	0.550	0.039669
rab11fip4b	0.557	0.048294
rab36	0.796	0.044795

Gene	Fold Change	P-value
rab39b	2.756	0.044083
rab3a	1.473	0.034461
rab3b	3.199	0.049038
rab3c	1.433	0.042542
rab40c	2.056	0.044121
rab6b	1.724	0.034461
ralgps1	2.320	0.032396
raly	1.893	0.040832
rbm41	1.236	0.044663
rcl1	0.500	0.054437
rdh11	0.520	0.032396
rdh8	0.557	0.040832
rel	0.444	0.043967
rem1	1.810	0.034461
renbp	0.436	0.034461
ret1	1.360	0.049497
rgn	0.612	0.050355
rgs12	1.857	0.044245
rgs17	1.651	0.046315
rgs7bpa	2.990	0.045768
rgs7bpb	2.162	0.039705
rhag	2.108	0.043967
rhoq	1.484	0.046320
rnasekb	1.596	0.050828
rnf103	1.235	0.046751
rngtt	0.825	0.048823
rnpc3	0.722	0.049038
rnu3ip2	0.535	0.025317
rogdi	1.740	0.032396
rorb	2.963	0.040296
rpia	0.486	0.022236
rpl7l1	0.592	0.050349
rprml	1.934	0.042308
rrbp1	0.543	0.034163
rrp12	0.570	0.037957
rspo1	0.366	0.044245
rtn1a	1.920	0.044795
rtn1b	2.475	0.037957
rtn2b	3.559	0.044245

Gene	Fold Change	P-value
rybpa	1.802	0.047563
s1pr1	2.207	0.046320
sarm1	2.432	0.034461
scn1ba	1.952	0.046215
scn2b	3.248	0.030590
scn4aa	0.540	0.047887
scn4ab	2.924	0.045768
scn4ba	4.888	0.035106
scn8ab	1.756	0.039477
scpep1	0.614	0.042308
scrn3	2.303	0.048422
sdad1	0.521	0.041818
sec62	0.656	0.039477
sept5a	1.664	0.048294
serinc1	1.246	0.050266
setdb2	0.724	0.037964
setx	0.699	0.049154
sfrs1	1.254	0.050266
sgcg	2.164	0.050017
sgk1	0.617	0.044795
sgpl1	0.757	0.050266
sh3gl2	1.792	0.034461
silva	2.849	0.038297
silvb	4.408	0.040365
sim2	2.300	0.020380
slc17a6	2.135	0.043463
slc17a6l	2.621	0.040365
slc1a2	2.927	0.049517
slc24a5	2.516	0.047397
slc25a32b	0.740	0.045514
slc25a4	13.082	0.041377
slc26a1	0.496	0.032631
slc2a15a	2.539	0.037138
slc30a7	0.822	0.039669
slc32a1	2.406	0.037957
slc38a7	0.607	0.045003
slc6a11	0.536	0.050058
slc7a4	1.283	0.040365
slc9a3r2	0.631	0.035106

Gene	Fold Change	P-value
slitrk4	4.148	0.046320
smad3a	1.388	0.050355
smad3b	2.967	0.040832
smad7	1.711	0.045768
smarce1	1.151	0.049691
snai3	0.570	0.040296
snap25a	1.818	0.040956
snap25b	2.143	0.032396
sncb	2.117	0.044997
snrnp48	0.779	0.049154
snw1	0.786	0.042542
snx10a	0.502	0.040832
snx25	2.033	0.035155
sod2	3.062	0.046829
sox11b	2.429	0.044795
sox4a	2.736	0.040592
sox9b	1.946	0.035106
sp4	1.295	0.044245
spam1	2.357	0.048422
sparcl	15.226	0.046822
spon1a	1.848	0.045159
spon1b	1.568	0.031433
sprn	7.113	0.035106
srfl	0.536	0.035106
ssb	0.535	0.044795
sst1	2.649	0.045768
st6gal1	2.458	0.034461
st8sia2	1.812	0.044121
stac3	2.962	0.049691
stam2	0.701	0.048963
stap2a	2.465	0.044997
star	5.874	0.031433
stat3	0.629	0.020380
stmn1b	2.451	0.045768
stmn2a	2.891	0.044795
stmn2b	1.725	0.049038
stxbp1	1.744	0.034504
sult1st4	2.133	0.050266
sult6b1	0.620	0.045768

Gene	Fold Change	P-value
syk	1.347	0.044795
syn2a	2.727	0.035106
syn2b	2.148	0.035775
synbl	2.220	0.045514
syne1a	1.488	0.040956
syngr1	2.079	0.040832
synpr	4.087	0.020380
syntaxin1b	1.785	0.047563
sypb	1.878	0.042308
syt1	2.232	0.043967
syt11a	1.766	0.040956
syt12	1.598	0.032919
syt4	1.674	0.042308
syt9b	1.718	0.044795
syvn1	1.318	0.044795
tal2	2.406	0.042308
tas1r2.1	0.624	0.035106
tbc1d22a	1.427	0.039705
tbx15	2.088	0.040956
tcf7l2	2.169	0.048422
tdh	1.372	0.044245
tef	0.406	0.041795
tfap2e	2.578	0.047558
tfr1a	0.620	0.049996
tgfbi	1.756	0.037952
th	1.819	0.034461
thop1	5.653	0.044083
tln2	1.344	0.041795
tlr5b	0.610	0.045081
tmem16c	0.654	0.048316
tmem195	1.775	0.039705
tmem22	1.763	0.045003
tmem59l	2.895	0.034461
tmod4	2.099	0.046822
tmsb	1.965	0.048422
tnnt1	0.410	0.050386
tnnt3a	3.970	0.033095
tnnt3b	7.127	0.020380
tnr	1.895	0.043463

Gene	Fold Change	P-value
tnw	3.810	0.031083
tpi1a	2.633	0.048963
tpm3	0.809	0.036889
tpma	2.693	0.045159
tpp1	0.586	0.049497
tprg1l	1.505	0.047563
trac	0.245	0.005627
trh	0.505	0.040592
trim36	1.873	0.040956
trim3b	1.380	0.038218
trim9	1.868	0.044795
trmt5	0.659	0.040592
trnau1ap	0.709	0.046215
trnau1apl	0.744	0.044245
trpc1	1.517	0.048598
trpn1	2.292	0.048823
tspan13	1.820	0.044795
tsr1	0.683	0.045443
ttna	2.231	0.034163
ttnb	2.403	0.050176
tuba2	3.147	0.036240
tuba7l	1.908	0.044997
tyrp1b	3.786	0.041795
ube2q1	1.153	0.049691
uhrf1bp1l	1.343	0.041377
urod	0.455	0.048316
utp6	0.590	0.046315
vamp1	3.215	0.031433
vamp2	2.364	0.020380
vax1	1.215	0.045555
vegfab	1.843	0.050188
vldlr	1.900	0.049691
vps4a	1.268	0.034461
vtnb	1.621	0.034461
wdr12	0.634	0.044795
wdr3	0.577	0.031433
wdr46	0.616	0.049517
wdr55	0.594	0.028477
wdsof1	0.675	0.032974

Gene	Fold Change	P-value
wnt4b	2.506	0.039692
wrb	1.410	0.045761
xdh	3.207	0.040832
xirp2l	5.246	0.048823
xk	1.832	0.048785
xkr6	2.153	0.040721
xrn2	0.664	0.043877
yes1	0.684	0.048422
yipf1	0.583	0.040721
ywhag2	1.697	0.041292
zbtb2b	0.795	0.046751
zcchc17	0.695	0.043967
zcchc24	0.804	0.046822
zfpm2a	1.423	0.047563
zfpm2b	2.173	0.048422
zmiz1	1.741	0.049517
znf259	0.630	0.044795
znf277	0.733	0.039705
znf326	2.215	0.041795
znf593	0.573	0.020380
znrd1	0.623	0.039477
znrf1	2.431	0.039669
zranb2	1.334	0.040956
zswim6	2.214	0.044121

Publication Permissions

This section contains the permission agreements for republication of published chapters from the appropriate journal associations, where necessary.

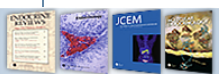

Confirmation - Free

The Endocrine Society
8401 Connecticut Avenue, Suite 900
Chevy Chase, MD 20815-5817
Telephone: 301-941-0200
Fax: 301-941-0259
www.endo-society.org
TIN Number: 73-0531256

This printable page is your letter granting copyright permission. A copy of this page will be sent to you via email for your records.

Form was submitted by: dnesan@gmail.com

Original author to publish in a Dissertation.

Date: November 17, 2012
Reference Number:

Name: Dinushan Nesan
Organization: University of Waterloo
Department:
Address: 200 University Ave W
B1-181
City, State and Postal Code: Waterloo, Ontario N2L 3G1
Country: Canada
Phone: 5198070615
Fax:
Email: dnesan@gmail.com

Journal: Endocrinology
Author Name: D Nesan
Title: Glucocorticoid Receptor Signaling Is Essential for Mesoderm Formation and Muscle Development in Zebrafish
Year: 2012
Volume: 153
Page Range: 1288-1300
Figure Reproduction:
Figure Number(s): Figure 1, Figure 2, Figure 3, Figure 4, Figure 5, Figure 6, Figure 7, Figure 8, Figure 9, Table 1
Where will the figures appear:
- Dissertation

- Title: The Role of Glucocorticoid Receptor Signaling in Zebrafish Development

The Endocrine Society grants permission to reproduce tables/figures Figure 1, Figure 2, Figure 3, Figure 4, Figure 5, Figure 6, Figure 7, Figure 8, Figure 9 and Table 1 from the selected article stated above contingent upon the following conditions: 1) That you give proper credit to the author(s) and to include in your citation, the title of journal, title of article, volume, issue number, date, and page numbers. 2) That you include the statement *Copyright 2012, The Endocrine Society*. Please understand that permission is granted for one-time use only. Permission must be requested separately for future editions, revisions, translations, derivative works, and promotional pieces.

Title: Journal Publications Coordinator
Date: November 17, 2012

Order Completed

Thank you very much for your order.

This is a License Agreement between Dinu Nesan ("You") and Elsevier ("Elsevier"). The license consists of your order details, the terms and conditions provided by Elsevier, and the payment terms and conditions.

Get the printable license.

License Number	3031690646945
License date	Nov 17, 2012
Licensed content publisher	Elsevier
Licensed content publication	Molecular and Cellular Endocrinology
Licensed content title	Embryo exposure to elevated cortisol level leads to cardiac performance dysfunction in zebrafish
Licensed content author	Dinushan Nesan,Mathilakath M. Vijayan
Licensed content date	5 November 2012
Licensed content volume number	363
Licensed content issue number	1–2
Number of pages	7
Type of Use	reuse in a thesis/dissertation
Portion	full article
Format	both print and electronic
Are you the author of this Elsevier article?	Yes
Will you be translating?	No
Order reference number	
Title of your thesis/dissertation	The Role of Glucocorticoid Receptor Signaling in Zebrafish Development
Expected completion date	Jan 2013
Estimated size (number of pages)	200
Elsevier VAT number	GB 494 6272 12
Permissions price	0.00 USD
VAT/Local Sales Tax	0.0 USD
Total	0.00 USD

References

Chapter 1

Abraham, E., Palevitch, O., Gothilf, Y., and Zohar, Y. (2009). The zebrafish as a model system for forebrain GnRH neuronal development. General and Comparative Endocrinology *164*, 151–160.

Abrams, E.W., and Mullins, M.C. (2009). Early zebrafish development: It's in the maternal genes. Current Opinion in Genetics & Development *19*, 396–403.

Adcock, I.M. (2001). Glucocorticoid-regulated transcription factors. Pulm Pharmacol Ther *14*, 211–219.

Alderman, S., and Bernier, N. (2009). Ontogeny of the corticotropin-releasing factor system in zebrafish. General and Comparative Endocrinology *164*, 61–69.

Aleström, P., Holter, J.L., and Nourizadeh-Lillabadi, R. (2006). Zebrafish in functional genomics and aquatic biomedicine. Trends Biotechnol. *24*, 15–21.

Ali, S., Champagne, D.L., Spaink, H.P., and Richardson, M.K. (2011). Zebrafish embryos and larvae: A new generation of disease models and drug screens. Birth Defect Res C *93*, 115–133.

Alsop, D., and Vijayan, M. (2008). Development of the corticosteroid stress axis and receptor expression in zebrafish. American Journal of Physiology- Regulatory, Integrative and Comparative Physiology *294*, R711.

Alsop, D., and Vijayan, M. (2009). Molecular programming of the corticosteroid stress axis during zebrafish development. Comparative Biochemistry and Physiology Part a: Physiology *153*, 49–54.

Altmann, C.R., and Brivanlou, A.H. (2001). Neural patterning in the vertebrate embryo. Int. Rev. Cytol. *203*, 447–482.

Aluru, N., and Vijayan, M. (2009). Stress transcriptomics in fish: A role for genomic cortisol signaling. General and Comparative Endocrinology *164*, 142–150.

Aluru, N., and Vijayan, M.M. (2007). Hepatic transcriptome response to glucocorticoid receptor activation in rainbow trout. Physiological Genomics *31*, 483–491.

Åberg Andersson, M., Silva, P.I.M., Steffensen, J.F., and Höglund, E. (2011). Effects of maternal stress coping style on offspring characteristics in rainbow trout (Oncorhynchus mykiss). Hormones and Behavior *60*, 699–705.

Ballard, P., and Ballard, R. (1974). Cytoplasmic receptor for glucocorticoids in lung of the human fetus and neonate. Journal of Clinical Investigation *53*, 477.

Bamberger, C.M., Bamberger, A.M., de Castro, M., and Chrousos, G.P. (1995). Glucocorticoid receptor beta, a potential endogenous inhibitor of glucocorticoid action in humans. J. Clin. Invest. *95*, 2435–2441.

Baram, T.Z., and Lerner, S.P. (1991). Ontogeny of corticotropin releasing hormone gene expression eak peak of m in rat hypothalamus--comparison with somatostatin. Int. J. Dev. Neurosci. *9*, 473–478.

Barry, T.P., Malison, J.A., Held, J.A., and Parrish, J.J. (1995). Ontogeny of the cortisol stress response in larval rainbow trout. General and Comparative Endocrinology *97*, 57–65.

Barton, B.A. (2002). Stress in fishes: a diversity of responses with particular reference to changes in circulating corticosteroids. Integrative and Comparative Biology *42*, 517–525.

Barut, B.A., and Zon, L.I. (2000). Realizing the potential of zebrafish as a model for human disease. Physiological Genomics *2*, 49–51.

Bauer, M.E. (2005). Stress, glucocorticoids and ageing of the immune system. Stress *8*, 69–83.

Berman, J.N., Kanki, J.P., and Look, A.T. (2005). Zebrafish as a model for myelopoiesis during embryogenesis. Exp. Hematol. *33*, 997–1006.

Bernier, N.J., and Peter, R.E. (2001). The hypothalamic-pituitary-interrenal axis and the control of food intake in teleost fish. Comparative Biochemistry and Physiology Part B: Biochemistry and Molecular Biology *129*, 639–644.

Blechman, J., Borodovsky, N., Eisenberg, M., Nabel-Rosen, H., Grimm, J., and Levkowitz, G. (2007). Specification of hypothalamic neurons by dual regulation of the homeodomain protein Orthopedia. Development *134*, 4417–4426.

Boden, S., McCuaig, K., Hair, G., Racine, M., Titus, L., Wozney, J., and Nanes, M. (1996). Differential effects and glucocorticoid potentiation of bone morphogenetic protein action during rat osteoblast differentiation in vitro. Endocrinology *137*, 3401.

Bolt, R.J., van Weissenbruch, M.M., Lafeber, H.N., and Delemarre-van de Waal, H.A. (2001). Glucocorticoids and lung development in the fetus and preterm infant. Pediatr. Pulmonol. *32*, 76–91.

Boonstra, R. (2005). Equipped for life: the adaptive role of the stress axis in male mammals. Journal of Mammalogy *86*, 236–247.

Borell, von, E., Dobson, H., and Prunier, A. (2007). Stress, behaviour and reproductive performance in female cattle and pigs. Hormones and Behavior *52*, 130–138.

Bourque, C., and Houvras, Y. (2011). Hooked on zebrafish: insights into development and cancer of endocrine tissues. Endocr. Relat. Cancer *18*, R149–R164.

Brand, T. (2003). Heart development: molecular insights into cardiac specification and early morphogenesis. Developmental Biology *258*, 1–19.

Briggs, J.P. (2002). The zebrafish: a new model organism for integrative physiology. American Journal of Physiology- Regulatory, Integrative and Comparative Physiology *282*, R3–R9.

Bubnoff, von, A., and Cho, K.W. (2001). Intracellular BMP signaling regulation in vertebrates: pathway or network? Developmental Biology *239*, 1–14.

Burnstein, K., and Cidlowski, J. (1989). Regulation of gene expression by glucocorticoids. Annu. Rev. Physiol. *51*, 683–699.

Bury, N., and Sturm, A. (2007). Evolution of the corticosteroid receptor signalling pathway in fish. General and Comparative Endocrinology *153*, 47–56.

Carvalho, L., and Heisenberg, C.-P. (2010). The yolk syncytial layer in early zebrafish development. Trends in Cell Biology *20*, 586–592.

Celsi, G., Wang, Z.M., Akusjärvi, G., and Aperia, A. (1993). Sensitive Periods for Glucocorticoids' Regulation of Na+, K+-ATPase mRNA in the Developing Lung and Kidney. Pediatr Res *33*, 5–9.

Chai, C., and Chan, W.K. (2000). Developmental expression of a novel Ftz-F1 homologue, ff1b (NR5A4), in the zebrafish Danio rerio. Mechanisms of Development *91*, 421–426.

Chai, C., Liu, Y., and Chan, W.K. (2003). Ff1b is required for the development of steroidogenic component of the zebrafish interrenal organ. Developmental Biology *260*, 226–244.

Chapman, S.C., Sawitzke, A.L., Campbell, D.S., and Schoenwolf, G.C. (2005). A three-dimensional atlas of pituitary gland development in the zebrafish. J. Comp. Neurol. *487*, 428–440.

Charmandari, E., Kino, T., and Chrousos, G.P. (2004a). Glucocorticoids and their actions: an introduction. Annals of the New York Academy of Sciences *1024*, 1–8.

Charmandari, E., Tsigos, C., and Chrousos, G. (2004b). Endocrinology of the stress response1. Annu. Rev. Physiol.

Chatelain, A., Dupouy, J., and Dubois, M. (1979). Ontogenesis of cells producing polypeptide hormones (ACTH, MSH, LPH, GH, prolactin) in the fetal hypophysis of the rat: influence of the hypothalamus. Cell Tissue Res *196*, 409–427.

Chen, J.N., and Fishman, M.C. (1996). Zebrafish tinman homolog demarcates the heart field and initiates myocardial differentiation. Development *122*, 3809–3816.

Chen, S., and Kimelman, D. (2000). The role of the yolk syncytial layer in germ layer patterning in zebrafish. Development *127*, 4681–4689.

Chico, T.J.A., Ingham, P.W., and Crossman, D.C. (2008). Modeling cardiovascular disease in the zebrafish. Trends in Cardiovascular Medicine *18*, 150–155.

Childs, S., Chen, J.-N., Garrity, D.M., and Fishman, M.C. (2002). Patterning of angiogenesis in the zebrafish embryo. Development *129*, 973–982.

Chong, S.W., Korzh, V., and Jiang, Y.J. (2009). Myogenesis and molecules - insights from zebrafish Danio rerio. Journal of Fish Biology *74*, 1693–1755.

Chrousos, G. (2006). Stressors, stress, and neuroendocrine integration of the adaptive response: The 1997 Hans Selye Memorial Lecture. Annals of the New York Academy of Sciences *851*, 311–335.

Chrousos, G.P. (2000). The HPA axis and the stress response. Endocr. Res. *26*, 513–514.

Chrousos, G.P., and Gold, P.W. (1992). The concepts of stress and stress system disorders. Overview of physical and behavioral homeostasis. Jama *267*, 1244–1252.

Chung, W., Shin, C., and Stainier, D. (2008). Bmp2 signaling regulates the hepatic versus pancreatic fate decision. Developmental Cell *15*, 738–748.

Cole, T., Myles, K., Purton, J., Brereton, P., Solomon, N., Godfrey, D., and Funder, J. (2001). GRKO mice express an aberrant dexamethasone-binding glucocorticoid receptor, but are profoundly glucocorticoid resistant. Molecular and Cellular Endocrinology *173*, 193–202.

Dale, J.K., Vesque, C., Lints, T.J., Sampath, T.K., Furley, A., Dodd, J., and Placzek, M. (1997). Cooperation of BMP7 and SHH in the induction of forebrain ventral midline cells by prechordal mesoderm. Cell *90*, 257–269.

Dallman, M., Akana, S., Scribner, K., Bradbury, M., Walker, C., Strack, A., and Cascio, C. (1992). Stress, feedback and facilitation in the hypothalamo-pituitary-adrenal axis. Journal of Neuroendocrinology *4*, 517–526.

David, L., Feige, J., and Bailly, S. (2009). Emerging role of bone morphogenetic proteins in angiogenesis. Cytokine & Growth Factor Reviews *20*, 203–212.

De Fraipont, M., Clobert, J., John, H., and Meylan, S. (2000). Increased pre‐natal maternal corticosterone promotes philopatry of offspring in common lizards Lacerta vivipara. Journal of Animal Ecology *69*, 404–413.

de Jesus, E.G., Hirano, T., and Inui, Y. (1991). Changes in cortisol and thyroid hormone concentrations during early development and metamorphosis in the Japanese flounder, Paralichthys olivaceus. General and Comparative Endocrinology *82*, 369–376.

de Kloet, E., Joëls, M., and Holsboer, F. (2005). Stress and the brain: from adaptation to disease. Nature Reviews Neuroscience *6*, 463–475.

de Robertis, E.M., Larrain, J., Oelgeschläger, M., and Wessely, O. (2000). The establishment of Spemann's organizer and patterning of the vertebrate embryo. Nat Rev Genet *1*, 171.

Del Giacco, L., Pistocchi, A., Cotelli, F., Fortunato, A.E., and Sordino, P. (2008). A peek inside the neurosecretory brain through Orthopedia lenses. Dev. Dyn. *237*, 2295–2303.

Del Giacco, L., Sordino, P., Pistocchi, A., Andreakis, N., Tarallo, R., Di Benedetto, B., and Cotelli, F. (2006). Differential regulation of the zebrafish orthopedia 1 gene during fate determination of diencephalic neurons. BMC Developmental Biology *6*, 50.

Denver, R.J. (2009). Structural and functional evolution of vertebrate neuroendocrine stress systems. Annals of the New York Academy of Sciences *1163*, 1–16.

Denver, R.J., Glennemeier, K.A., and Boorse, G.C. (2002). Endocrinology of complex life cycles: amphibians. Hormones, Brain and Behavior *2*, 469–513.

Dick, A., Meier, A., and Hammerschmidt, M. (1999). Smad1 and Smad5 have distinct roles during dorsoventral patterning of the zebrafish embryo. Dev. Dyn. *216*, 285–298.

Djouadi, F., Bastin, J., Kelly, D.P., and Merlet-Benichou, C. (1996). Transcriptional regulation by glucocorticoids of mitochondrial oxidative enzyme genes in the developing rat kidney. Biochem. J. *315 (Pt 2)*, 555–562.

Dohms, J.E., and Metz, A. (1991). Stress--mechanisms of immunosuppression. Veterinary Immunology and Immunopathology *30*, 89–109.

Dooley, K., and Zon, L.I. (2000). Zebrafish: a model system for the study of human disease. Current Opinion in Genetics & Development *10*, 252–256.

Drake, A.J., Walker, B.R., and Seckl, J.R. (2005). Intergenerational consequences of fetal programming by in utero exposure to glucocorticoids in rats. American Journal of Physiology-Regulatory, Integrative and Comparative Physiology *288*, R34–R38.

Driever, W., Stemple, D., Schier, A., and Solnica-Krezel, L. (1994). Zebrafish: genetic tools for studying vertebrate development. Trends in Genetics *10*, 152–159.

Dutta, S., Dietrich, J.-E., Aspöck, G., Burdine, R.D., Schier, A., Westerfield, M., and Varga, Z.M. (2005). pitx3 defines an equivalence domain for lens and anterior pituitary placode. Development *132*, 1579–1590.

Edwards, C., Burt, D., McIntyre, M.A., de Kloet, E.R., Stewart, P.M., Brett, L., Sutanto, W.S., and Monder, C. (1988). Localisation of 11β-hydroxysteroid dehydrogenase—tissue specific protector of the mineralocorticoid receptor. Lancet *332*, 986–989.

Eisen, J. (1996). Zebrafish make a big splash. Cell *87*, 969–977.

Eisen, J.S., and Smith, J.C. (2008). Controlling morpholino experiments: don't stop making antisense. Development *135*, 1735–1743.

Ekker, S.C., Ungar, A.R., Greenstein, P., Kessler, von, D.P., Porter, J.A., Moon, R.T., and Beachy, P.A. (1995). Patterning activities of vertebrate hedgehog proteins in the developing eye and brain. Curr. Biol. *5*, 944–955.

Ellis, T., Yildiz, H.Y., López-Olmeda, J., Spedicato, M.T., Tort, L., Overli, O., and Martins, C.I.M. (2012). Cortisol and finfish welfare. Fish Physiology and Biochemistry 1–26.

Eriksen, M.S., Espmark, Å., Braastad, B.O., Salte, R., and Bakken, M. (2007). Long-term effects of maternal cortisol exposure and mild hyperthermia during embryogeny on survival, growth and morphological anomalies in farmed Atlantic salmon Salmo salar offspring. Journal of Fish Biology *70*, 462–473.

Feist, G., and Schreck, C.B. (2001). Ontogeny of the stress response in chinook salmon, Oncorhynchus tshawytscha*. Fish Physiology and Biochemistry *25*, 31–40.

Field, H., Ober, E., Roeser, T., and Stainier, D. (2003). Formation of the digestive system in zebrafish. I. Liver morphogenesis. Developmental Biology *253*, 279–290.

Friedrich, R., Jacobson, G., and Zhu, P. (2010). Circuit Neuroscience in Zebrafish. Current Biology.

Fuentes, R., and Fernández, J. (2010). Ooplasmic segregation in the zebrafish zygote and early embryo: Pattern of ooplasmic movements and transport pathways. Dev. Dyn. *239*, 2172–2189.

Funder, J. (1997). Glucocorticoid and mineralocorticoid receptors: biology and clinical relevance. Annual Review of Medicine *48*, 231–240.

Funder, J.W. (1993). Mineralocorticoids, glucocorticoids, receptors and response elements. Science *259*, 1132–1133.

Furthauer, M. (2004). Fgf signalling controls the dorsoventral patterning of the zebrafish embryo. Development *131*, 2853–2864.

Gerlai, R. (2003). Zebra fish: an uncharted behavior genetic model. Behav. Genet. *33*, 461–468.

Gesina, E., Tronche, F., Herrera, P., Duchene, B., Tales, W., Czernichow, P., and Breant, B. (2004). Dissecting the role of glucocorticoids on pancreas development. Diabetes *53*, 2322–2329.

Giesing, E.R., Suski, C.D., Warner, R.E., and Bell, A.M. (2011). Female sticklebacks transfer information via eggs: effects of maternal experience with predators on offspring. Proc. Biol. Sci. *278*, 1753–1759.

Giraldez, A., Mishima, Y., Rihel, J., Grocock, R., van Dongen, S., Inoue, K., Enright, A., and Schier, A. (2006). Zebrafish MiR-430 promotes deadenylation and clearance of maternal mRNAs. Science *312*, 75.

Glasgow, E., Karavanov, A.A., and Dawid, I.B. (1997). Neuronal and neuroendocrine expression of lim3, a LIM class homeobox gene, is altered in mutant zebrafish with axial signaling defects. Developmental Biology *192*, 405–419.

Glickman, N., and Yelon, D. (2002). Cardiac development in zebrafish: coordination of form and function. Seminars in Cell & Developmental Biology *13*, 507–513.

Glickman, N.S., Kimmel, C.B., Jones, M.A., and Adams, R.J. (2003). Shaping the zebrafish notochord. Development *130*, 873–887.

Greenberg, N. (1990). Behavioural endocrinology of physiological stress in a lizard. J. Exp. Zool. *256*, 170–173.

Grunwald, D., and Eisen, J. (2002). Headwaters of the zebrafish—emergence of a new model vertebrate. Nat Rev Genet *3*, 717–724.

Hammerschmidt, M., and Mullins, M. (2002). Dorsoventral patterning in the zebrafish: bone morphogenetic proteins and beyond. Results and Problems in Cell Differentiation *40*, 72–95.

Harvey, S., and Hall, T. Hormones and stress in birds: activation of the hypothalamo-pituitary-adrenal axis. Prog Clin Biol Res *342*, 453–460.

Hayward, L., and Wingfield, J. (2004). Maternal corticosterone is transferred to avian yolk and may alter offspring growth and adult phenotype. General and Comparative Endocrinology *135*, 365–371.

Heasman, J. (2002). Morpholino Oligos: Making Sense of Antisense? Developmental Biology *243*, 209–214.

Heikkila, M., Peltoketo, H., Leppäluoto, J., Ilves, M., Vuolteenaho, O., and Vainio, S. (2002). Wnt-4 deficiency alters mouse adrenal cortex function, reducing aldosterone production. Endocrinology *143*, 4358–4365.

Heitzer, M.D., Wolf, I.M., Sanchez, E.R., Witchel, S.F., and Defranco, D.B. (2007). Glucocorticoid receptor physiology. Reviews in Endocrine & Metabolic Disorders *8*, 321–330.

Herzog, W., Sonntag, C., Hardt, von der, S., Roehl, H.H., Varga, Z.M., and Hammerschmidt, M. (2004a). Fgf3 signaling from the ventral diencephalon is required for early specification and subsequent survival of the zebrafish adenohypophysis. Development *131*, 3681–3692.

Herzog, W., Sonntag, C., Walderich, B., Odenthal, J., Maischein, H.-M., and Hammerschmidt, M. (2004b). Genetic analysis of adenohypophysis formation in zebrafish. Mol. Endocrinol. *18*, 1185–1195.

Herzog, W., Zeng, X., Lele, Z., Sonntag, C., Ting, J.W., Chang, C.Y., and Hammerschmidt, M. (2003). Adenohypophysis formation in the zebrafish and its dependence on sonic hedgehog. Developmental Biology *254*, 36–49.

Hess, L. (2006). Corticosteroid synthesis and metabolism in birds. Seminars in Avian and Exotic Pet Medicine *11*, 65–70.

Hillegass, J., Villano, C., Cooper, K., and White, L. (2007). Matrix metalloproteinase-13 is required for zebra fish (Danio rerio) development and is a target for glucocorticoids. Toxicological Sciences *100*, 168.

Hillegass, J., Villano, C., Cooper, K., and White, L. (2008). Glucocorticoids alter craniofacial development and increase expression and activity of matrix metalloproteinases in developing zebrafish (Danio rerio). Toxicological Sciences.

Ho, R.K. (1992). Cell movements and cell fate during zebrafish gastrulation. Dev. Suppl. 65–73.

Howley, C., and Ho, R.K. (2000). mRNA localization patterns in zebrafish oocytes. Mechanisms of Development *92*, 305–309.

Hsu, H.J., Lin, G., and Chung, B. (2003). Parallel early development of zebrafish interrenal glands and pronephros: differential control by wt1 and ff1b. Development *130*, 2107–2116.

Huang, W.L., Beazley, L.D., Quinlivan, J.A., Evans, S.F., Newnham, J.P., and Dunlop, S.A. (1999). Effect of corticosteroids on brain growth in fetal sheep. Obstet Gynecol *94*, 213–218.

Huang, W.L., Harper, C.G., Evans, S.F., Newnham, J.P., and Dunlop, S.A. (2001). Repeated prenatal corticosteroid administration delays astrocyte and capillary tight junction maturation in fetal sheep. Int. J. Dev. Neurosci. *19*, 487–493.

Hwang, P.P., and Wu, S.M. (1993). Role of cortisol in hypoosmoregulation in larvae of the tilapia (Oreochromis mossambicus). General and Comparative Endocrinology *92*, 318–324.

Ishimoto, H., and Jaffe, R.B. (2011). Development and function of the human fetal adrenal cortex: a key component in the feto-placental unit. Endocrine Reviews *32*, 317–355.

Jenkins, S.A., and Porter, T.E. (2004). Ontogeny of the hypothalamo–pituitary–adrenocortical axis in the chicken embryo: a review. Domestic Animal Endocrinology *26*, 267–275.

Jentoft, S., Held, J.A., Malison, J.A., and Barry, T.P. (2002). Ontogeny of the cortisol stress response in yellow perch (Perca flavescens). Fish Physiology and Biochemistry *26*, 371–378.

Jeong, J.Y., Einhorn, Z., Mercurio, S., Lee, S., Lau, B., Mione, M., Wilson, S.W., and Guo, S. (2006). Neurogenin1 is a determinant of zebrafish basal forebrain dopaminergic neurons and is regulated by the conserved zinc finger protein Tof/Fezl. Proc. Natl. Acad. Sci. U.S.a. *103*, 5143–5148.

Johnson, E.O., Kamilaris, T.C., Chrousos, G.P., and Gold, P.W. (1992). Mechanisms of stress: a dynamic overview of hormonal and behavioral homeostasis. Neuroscience & Biobehavioral Reviews *16*, 115–130.

Johnson, R.L., Laufer, E., Riddle, R.D., and Tabin, C. (1994). Ectopic expression of Sonic hedgehog alters dorsal-ventral patterning of somites. Cell *79*, 1165–1173.

Kane, D., and Kimmel, C. (1993). The zebrafish midblastula transition. Development *119*, 447.

Kapsimali, M. (2004). Inhibition of Wnt/Axin/ -catenin pathway activity promotes ventral CNS midline tissue to adopt hypothalamic rather than floorplate identity. Development *131*, 5923–5933.

Keegan, C.E., Herman, J.P., Karolyi, I.J., O'Shea, K.S., Camper, S.A., and Seasholtz, A.F. (1994). Differential expression of corticotropin-releasing hormone in developing mouse embryos and adult brain. Endocrinology *134*, 2547–2555.

Kimmel, C., Ballard, W., Kimmel, S., Ullmann, B., and Schilling, T. (1995). Stages of embryonic development of the zebrafish. Dev. Dyn. *203*, 253–310.

Kimmel, C.B. (1989). Genetics and early development of zebrafish. Trends in Genetics *5*, 283–288.

Kimmel, C.B., and Law, R.D. (1985a). Cell lineage of zebrafish blastomeres. I. Cleavage pattern and cytoplasmic bridges between cells. Developmental Biology *108*, 78–85.

Kimmel, C.B., and Law, R.D. (1985b). Cell lineage of zebrafish blastomeres. II. Formation of the yolk syncytial layer. Developmental Biology *108*, 86–93.

Kimmel, C.B., and Warga, R.M. (1987). Cell lineages generating axial muscle in the zebrafish embryo. Nature *327*, 234–237.

Kimmel, C.B., Warga, R.M., and Schilling, T.F. (1990). Origin and organization of the zebrafish fate map. Development *108*, 581–594.

Kino, T., Manoli, I., Kelkar, S., Wang, Y., Su, Y.A., and Chrousos, G.P. (2009). Glucocorticoid receptor (GR) beta has intrinsic, GRalpha-independent transcriptional activity. Biochemical and Biophysical Research Communications *381*, 671–675.

Kishimoto, Y., Lee, K., Zon, L., Hammerschmidt, M., and Schulte-Merker, S. (1997). The molecular nature of zebrafish swirl: BMP2 function is essential during early dorsoventral patterning. Development *124*, 4457.

Kyrou, I., and Tsigos, C. (2009). Stress hormones: physiological stress and regulation of metabolism. Current Opinion in Pharmacology *9*, 787–793.

Lance, V. (1990). Stress in Reptiles. Prog Clin Biol Res *342*, 461–466.

Langdown, M.L., Holness, M.J., and Sugden, M.C. (2003). Effects of prenatal glucocorticoid exposure on cardiac calreticulin and calsequestrin protein expression during early development and in adulthood. Biochem. J. *371*, 61–69.

Lawrence, C. (2007). The husbandry of zebrafish (Danio rerio): a review. Aquaculture *269*, 1–20.

Leatherland, J.F., Li, M., and Barkataki, S. (2010). Stressors, glucocorticoids and ovarian function in teleosts. Journal of Fish Biology *76*, 86–111.

Lee, J.E., Wu, S.F., Goering, L.M., and Dorsky, R.I. (2006). Canonical Wnt signaling through Lef1 is required for hypothalamic neurogenesis. Development *133*, 4451–4461.

Lele, Z., and Krone, P.H. (1996). The zebrafish as a model system in developmental, toxicological and transgenic research. Biotechnol. Adv. *14*, 57–72.

Levine, S. (2001). Primary social relationships influence the development of the hypothalamic-pituitary-adrenal axis in the rat. Physiology & Behavior *73*, 255–260.

Li, M., Bureau, D.P., King, W.A., and Leatherland, J.F. (2010). The actions of in ovo cortisol on egg fertility, embryo development and the expression of growth-related genes in rainbow trout embryos, and the growth performance of juveniles. Mol. Reprod. Dev. *77*, 922–931.

Li, Q., Frank, M., Thisse, C.I., Thisse, B.V., and Uitto, J. (2011). Zebrafish: a model system to study heritable skin diseases. J. Invest. Dermatol. *131*, 565–571.

Liggins, G.C. (1994). The role of cortisol in preparing the fetus for birth. Reproduction Fertility and Development *6*, 141–150.

Lin, Y.-Y. (2012). Muscle diseases in the zebrafish. Neuromuscul. Disord. *22*, 673–684.

Liu, N.-A., Huang, H., Yang, Z., Herzog, W., Hammerschmidt, M., Lin, S., and Melmed, S. (2003a). Pituitary corticotroph ontogeny and regulation in transgenic zebrafish. Mol. Endocrinol. *17*, 959–966.

Liu, Y. (2007). Interrenal Organogenesis in the Zebrafish Model. Organogenesis *3*, 44.

Liu, Y.W., Gao, W., Teh, H.L., Tan, J.H., and Chan, W.K. (2003b). Prox1 is a novel coregulator of Ff1b and is involved in the embryonic development of the zebra fish interrenal primordium. Molecular and Cellular Biology *23*, 7243–7255.

Löhr, H., and Hammerschmidt, M. (2011). Zebrafish in Endocrine Systems: Recent Advances and Implications for Human Disease. Annu. Rev. Physiol. *73*, 183–211.

Lumbers, E.R., Boyce, A.C., Joulianos, G., Kumarasamy, V., Barner, E., Segar, J.L., and Burrell, J.H. (2005). Effects of cortisol on cardiac myocytes and on expression of cardiac genes in fetal sheep. American Journal of Physiology- Regulatory, Integrative and Comparative Physiology *288*, R567–R574.

Machluf, Y., Gutnick, A., and Levkowitz, G. (2011). Development of the zebrafish hypothalamus. Annals of the New York Academy of Sciences *1220*, 93–105.

Maier, E., Nord, H., Hofsten, von, J., and Gunhaga, L. (2011). A Balance of BMP and Notch Activity Regulates Neurogenesis and Olfactory Nerve Formation. PLoS One *6*, e17379.

Majumdar, A.P., and Nielsen, H. (1985). Influence of glucocorticoids on prenatal development of the gut and pancreas in rats. Scand. J. Gastroenterol. *20*, 65–71.

Mallo, M., Wellik, D.M., and Deschamps, J. (2010). Hox genes and regional patterning of the vertebrate body plan. Developmental Biology *344*, 7–15.

Marlow, F.L., and Mullins, M.C. (2008). Bucky ball functions in Balbiani body assembly and animal-vegetal polarity in the oocyte and follicle cell layer in zebrafish. Developmental Biology *321*, 40–50.

Maroto, M., Bone, R.A., and Dale, J.K. (2012). Somitogenesis. Development *139*, 2453–2456.

Martin, L.B., and Rubenstein, D.R. (2008). Stress hormones in tropical birds: patterns and future directions. Ornitologia Neotropical *19*, 207–218.

Mathieu, J., Barth, A., Rosa, F.M., Wilson, S.W., and Peyriéras, N. (2002). Distinct and cooperative roles for Nodal and Hedgehog signals during hypothalamic development. Development *129*, 3055–3065.

Matthews, S.G. (2002). Early programming of the hypothalamo-pituitary-adrenal axis. Trends in Endocrinology & Metabolism *13*, 373–380.

Maxwell, S.R., Moots, R.J., and Kendall, M.J. (1994). Corticosteroids: do they damage the cardiovascular system? Postgrad Med J *70*, 863–870.

Mccormick, M. (1999). Experimental test of the effect of maternal hormones on larval quality of a coral reef fish. Oecologia *118*, 412–422.

McCormick, M.I. (1998). Behaviorally induced maternal stress in a fish influences progeny quality by a hormonal mechanism. Ecology *79*, 1873–1883.

McCormick, S. (2001). Endocrine control of osmoregulation in teleost fish. Integrative and Comparative Biology *41*, 781.

McCulley, D., Kang, J., Martin, J., and Black, B. (2008). BMP4 is required in the anterior heart field and its derivatives for endocardial cushion remodeling, outflow tract septation, and semilunar valve development. Dev. Dyn. *237*, 3200–3209.

McGonnell, I.M., and Fowkes, R.C. (2006). Fishing for gene function--endocrine modelling in the zebrafish. J. Endocrinol. *189*, 425–439.

Mescher, E., Platzker, A., Ballard, P., Kitterman, J., Clements, J., and Tooley, W. (1975). Ontogeny of tracheal fluid, pulmonary surfactant, and plasma corticoids in the fetal lamb. Journal of Applied Physiology *39*, 1017.

Meyer, A., and van de Peer, Y. (2005). From 2R to 3R: evidence for a fish-specific genome duplication (FSGD). Bioessays *27*, 937–945.

Milla, S., Wang, N., Mandiki, S.N.M., and Kestemont, P. (2009). Corticosteroids: Friends or foes of teleost fish reproduction? Comparative Biochemistry and Physiology, Part A *153*, 242–251.

Mitani, F., Mukai, K., Miyamoto, H., Suematsu, M., and Ishimura, Y. (1999). Development of functional zonation in the rat adrenal cortex. Endocrinology *140*, 3342–3353.

Miyazono, K., Maeda, S., and Imamura, T. (2005). BMP receptor signaling: transcriptional targets, regulation of signals, and signaling cross-talk. Cytokine & Growth Factor Reviews *16*, 251–263.

Mommsen, T., Vijayan, M., and Moon, T. (1999). Cortisol in teleosts: dynamics, mechanisms of action, and metabolic regulation. Reviews in Fish Biology and Fisheries *9*, 211–268.

Montero, J.A. (2005). Shield formation at the onset of zebrafish gastrulation. Development *132*, 1187–1198.

Moore, I.T., and Jessop, T.S. (2003). Stress, reproduction, and adrenocortical modulation in amphibians and reptiles. Hormones and Behavior *43*, 39–47.

Mormede, P., Foury, A., Barat, P., Corcuff, J.-B., Terenina, E., Marissal-Arvy, N., and Moisan, M.-P. (2011). Molecular genetics of hypothalamic-pituitary-adrenal axis activity and function. Annals of the New York Academy of Sciences *1220*, 127–136.

Mueller, T., and Wullimann, M.F. (2003). Anatomy of neurogenesis in the early zebrafish brain. Brain Res. Dev. Brain Res. *140*, 137–155.

Mueller, T., and Wullimann, M.F. (2005). Atlas of early zebrafish brain development: a tool for molecular neurogenetics (Amsterdam: Elsevier).

Nasevicius, A., and Ekker, S. (2000). Effective targeted gene “knockdown”in zebrafish. Nature Genetics *26*, 216–220.

Nechaev, I., Dikhnich, A., Kostin, V., and Romanenko, V. (2006). Dynamics of cortisol and the development of the glucocorticoid function in the early ontogenesis of Atlantic salmon Salmo salar. Journal of Ichthyology *46*, 328–341.

Nica, G., Herzog, W., Sonntag, C., and Hammerschmidt, M. (2004). Zebrafish pit1 mutants lack three pituitary cell types and develop severe dwarfism. Mol. Endocrinol. *18*, 1196–1209.

Nica, G., Herzog, W., Sonntag, C., Nowak, M., Schwarz, H., Zapata, A.G., and Hammerschmidt, M. (2006). Eya1 is required for lineage-specific differentiation, but not for cell survival in the zebrafish adenohypophysis. Developmental Biology *292*, 189–204.

Nicolaides, N., Galata, Z., Kino, T., Chrousos, G., and Charmandari, E. (2010). The human glucocorticoid receptor: Molecular basis of biologic function. Steroids *75*, 1–12.

Nie, X., Luukko, K., and Kettunen, P. (2006). BMP signalling in craniofacial development. Int. J. Dev. Biol. *50*.

Nikaido, M., Tada, M., Saji, T., and Ueno, N. (1997). Conservation of BMP signaling in zebrafish mesoderm patterning. Mechanisms of Development *61*, 75–88.

O'Connor, T.M., O'Halloran, D.J., and Shanahan, F. (2000). The stress response and the hypothalamic-pituitary-adrenal axis: from molecule to melancholia. Qjm *93*, 323–333.

Ottaviani, E., and Franceschi, C. (1996). The neuroimmunology of stress from invertebrates to man. Progress in Neurobiology *48*, 421–440.

Padgett, D.A., and Glaser, R. (2003). How stress influences the immune response. Trends in Immunology *24*, 444–448.

Pankhurst, N.W. (2011). The endocrinology of stress in fish: An environmental perspective. General and Comparative Endocrinology *170*, 265–275.

Pascual-Le Tallec, L., and Lombes, M. (2005). The mineralocorticoid receptor: a journey exploring its diversity and specificity of action. Molecular Endocrinology *19*, 2211.

Patterson, S., Bird, N., and Devoto, S. (2010). BMP regulation of myogenesis in zebrafish. Dev. Dyn. *239*, 806–817.

Pelegri, F. (2003). Maternal factors in zebrafish development. Dev. Dyn. *228*, 535–554.

Pepels, P.P.L.M., and Balm, P.H.M. (2004). Ontogeny of corticotropin-releasing factor and of hypothalamic–pituitary–interrenal axis responsiveness to stress in tilapia (Oreochromis mossambicus; Teleostei). General and Comparative Endocrinology *139*, 251–265.

Pierce, R., Mariencheck, W., Sandefur, S., Crouch, E., and Parks, W. (1995). Glucocorticoids upregulate tropoelastin expression during late stages of fetal lung development. American Journal of Physiology- Lung Cellular and Molecular Physiology *268*, 491.

Pikulkaew, S., de Nadai, A., and Belvedere, P. (2009). Expression analysis of steroid hormone receptor mRNAs during zebrafish embryogenesis. General and Comparative Endocrinology *165*, 215–220.

Pippal, J.B., Cheung, C.M.I., Yao, Y.-Z., Brennan, F.E., and Fuller, P.J. (2011). Characterization of the zebrafish (Danio rerio) mineralocorticoid receptor. Molecular and Cellular Endocrinology *332*, 58–66.

Pogoda, H.-M., and Hammerschmidt, M. (2007). Molecular genetics of pituitary development in zebrafish. Seminars in Cell & Developmental Biology *18*, 543–558.

Pogoda, H.-M., and Hammerschmidt, M. (2009). How to make a teleost adenohypophysis: molecular pathways of pituitary development in zebrafish. Molecular and Cellular Endocrinology *312*, 2–13.

Pogoda, H.-M., Hardt, von der, S., Herzog, W., Kramer, C., Schwarz, H., and Hammerschmidt, M. (2006). The proneural gene ascl1a is required for endocrine differentiation and cell survival in the zebrafish adenohypophysis. Development *133*, 1079–1089.

Prunet, P., Cairns, M.T., Winberg, S., and Pottinger, T.G. (2008). Functional genomics of stress responses in fish. Reviews in Fisheries Science *16*, 157–166.

Prunet, P., Sturm, A., and Milla, S. (2006). Multiple corticosteroid receptors in fish: from old ideas to new concepts. General and Comparative Endocrinology *147*, 17–23.

Rall, L., Pictet, R., Githens, S., and Rutter, W. (1977). Glucocorticoids modulate the in vitro development of the embryonic rat pancreas. Journal of Cell Biology *75*, 398.

Rebagliati, M.R., Toyama, R., Fricke, C., Haffter, P., and Dawid, I.B. (1998). Zebrafish nodal-related genes are implicated in axial patterning and establishing left-right asymmetry. Developmental Biology *199*, 261–272.

Reeder, D.A.M., and Kramer, K.M. (2005). Stress in free-ranging mammals: integrating physiology, ecology, and natural history. Journal of Mammalogy *86*, 225–235.

Rehan, V.K. (1996). Antenatal steroids: miracle drug for preemies. Indian J Pediatr *63*, 599–608.

Rollins-Smith, L.A. (2001). Neuroendocrine-immune system interactions in amphibians: implications for understanding global amphibian declines. Immunol. Res. *23*, 273–280.

Rozario, T., and DeSimone, D. (2009). The extracellular matrix in development and morphogenesis: A dynamic view. Developmental Biology.

Russek-Blum, N., Gutnick, A., Nabel-Rosen, H., Blechman, J., Staudt, N., Dorsky, R.I., Houart, C., and Levkowitz, G. (2008). Dopaminergic neuronal cluster size is determined during early forebrain patterning. Development *135*, 3401–3413.

Russek-Blum, N., Nabel-Rosen, H., and Levkowitz, G. (2009). High resolution fate map of the zebrafish diencephalon. Dev. Dyn. *238*, 1827–1835.

Saito, S., Tachibana, T., Choi, Y.-H., Denbow, D.M., and Furuse, M. (2005). ICV CRF and isolation stress differentially enhance plasma corticosterone concentrations in layer- and meat-type neonatal chicks. Comparative Biochemistry and Physiology, Part A *141*, 305–309.

Sampath-Kumar, R., Byers, R., Munro, A., and Lam, T. (1995). Profile of cortisol during the ontogeny of the Asian seabass, Lates calcarifer. Aquaculture *132*, 349–359.

Sangild, P., Westrom, B., Fowden, A., and Silver, M. (1994). Developmental regulation of the porcine exocrine pancreas by glucocorticoids. Journal of Pediatric Gastroenterology and Nutrition *19*, 204.

Sapolsky, R., Romero, L., and Munck, A. (2000). How do glucocorticoids influence stress responses? Integrating permissive, suppressive, stimulatory, and preparative actions. Endocrine Reviews *21*, 55.

Savage, J.J., Yaden, B.C., Kiratipranon, P., and Rhodes, S.J. (2003). Transcriptional control during mammalian anterior pituitary development. Gene *319*, 1–19.

Sbrogna, J.L., Barresi, M.J.F., and Karlstrom, R.O. (2003). Multiple roles for Hedgehog signaling in zebrafish pituitary development. Developmental Biology *254*, 19–35.

Schaaf, M., Champagne, D., van Laanen, I., van Wijk, D., Meijer, A., Meijer, O., Spaink, H., and Richardson, M. (2008). Discovery of a functional glucocorticoid receptor {beta}-isoform in zebrafish. Endocrinology *149*, 1591.

Schaaf, M., Chatzopoulou, A., and Spaink, H. (2009). The zebrafish as a model system for glucocorticoid receptor research. Comparative Biochemistry and Physiology Part a: Physiology.

Schaaf, M.J.M., and Cidlowski, J.A. (2002). Molecular mechanisms of glucocorticoid action and resistance. The Journal of Steroid Biochemistry and Molecular Biology *83*, 37–48.

Schaeffer, C., Diab-Assef, M., Plateroti, M., Laurent-Huck, F., Reimund, J.M., Kedinger, M., and Foltzer-Jourdainne, C. (2000). Cytokine gene expression during postnatal small intestinal development: regulation by glucocorticoids. Gut *47*, 192–198.

Schier, A.F. (2001). Axis formation and patterning in zebrafish. Current Opinion in Genetics & Development *11*, 393–404.

Schmidt, M., Enthoven, L., van der Mark, M., Levine, S., de Kloet, E.R., and Oitzl, M.S. (2003). The postnatal development of the hypothalamic–pituitary–adrenal axis in the mouse. International Journal of Developmental Neuroscience *21*, 125–132.

Schmidt, T., and Litwack, G. (1982). Activation of the glucocorticoid-receptor complex. Physiological Reviews *62*, 1131–1192.

Schoneveld, O., Gaemers, I., and Lamers, W. (2004). Mechanisms of glucocorticoid signalling. Biochimica Et Biophysica Acta (BBA)-Gene Structure and Expression *1680*, 114–128.

Schoonheim, P., Chatzopoulou, A., and Schaaf, M. (2010). The zebrafish as an in vivo model system for glucocorticoid resistance. Steroids.

Schreck, C.B. (2010). Stress and fish reproduction: the roles of allostasis and hormesis. General and Comparative Endocrinology *165*, 549–556.

Schreck, C.B., Contreras-Sanchez, W., and Fitzpatrick, M.S. (2001). Effects of stress on fish reproduction, gamete quality, and progeny* 1. Aquaculture *197*, 3–24.

Schroter, C., Herrgen, L., Cardona, A., Brouhard, G., Feldman, B., and Oates, A. (2008). Dynamics of zebrafish somitogenesis. Dev. Dyn. *237*, 545.

Seckl, J. (2001). Glucocorticoid programming of the fetus; adult phenotypes and molecular mechanisms. Molecular and Cellular Endocrinology *185*, 61–71.

Seckl, J.R., and Meaney, M.J. (2004). Glucocorticoid Programming. Annals of the New York Academy of Sciences *1032*, 63–84.

Segner, H. (2009). Zebrafish (Danio rerio) as a model organism for investigating endocrine disruption. Comparative Biochemistry and Physiology, Part C *149*, 187–195.

Shalhoub, V., Conlon, D., Stein, G.S., Lian, J.B., Tassinari, M., Quinn, C., and Partridge, N. (1992). Glucocorticoids promote development of the osteoblast phenotype by selectively modulating expression of cell growth and differentiation associated genes. J. Cell. Biochem. *50*, 425–440.

Sheng, H.Z. (1997). Multistep Control of Pituitary Organogenesis. Science *278*, 1809–1812.

Shin, D., Shin, C., Tucker, J., Ober, E., Rentzsch, F., Poss, K., Hammerschmidt, M., Mullins, M., and Stainier, D. (2007). Bmp and Fgf signaling are essential for liver specification in zebrafish. Development *134*, 2041.

Shine, R., and Downes, S.J. (1999). Can pregnant lizards adjust their offspring phenotypes to environmental conditions? Oecologia *119*, 1–8.

Siegel, H. (1980). Physiological stress in birds. Bioscience 529–534.

Sloman, K.A. (2010). Exposure of ova to cortisol pre-fertilisation affects subsequent behaviour and physiology of brown trout. Hormones and Behavior *58*, 433–439.

Smith, S.M., and Vale, W.W. (2006). The role of the hypothalamic-pituitary-adrenal axis in neuroendocrine responses to stress. Dialogues Clin Neurosci *8*, 383–395.

Solnica-Krezel, L., and Driever, W. (1994). Microtubule arrays of the zebrafish yolk cell: organization and function during epiboly. Development *120*, 2443–2455.

Stainier, D., and Fishman, M. (1994). The zebrafish as a model system to study cardiovascular development. Trends in Cardiovascular Medicine *4*, 207–212.

Steenbergen, P.J., Richardson, M.K., and Champagne, D.L. (2011). The use of the zebrafish model in stress research. Prog. Neuropsychopharmacol. Biol. Psychiatry *35*, 1432–1451.

Stickney, H., Barresi, M., and Devoto, S. (2000). Somite development in zebrafish. Dev. Dyn. *219*, 287–303.

Stouthart, A., Lucassen, E., van Strien, F., Balm, P., Lock, R., and Wendelaar Bonga, S. (1998). Stress responsiveness of the pituitary-interrenal axis during early life stages of common carp (Cyprinus carpio). Journal of Endocrinology *157*, 127.

Stratholt, M., Donaldson, E., and Liley, N. (1997). Stress induced elevation of plasma cortisol in adult female coho salmon (Oncorhynchus kisutch), is reflected in egg cortisol content, but does not appear to affect early development. Aquaculture *158*, 141–153.

Sturm, A., Bury, N., Dengreville, L., (null), Flouriot, G., (null), and Prunet, P. (2005). 11-deoxycorticosterone is a potent agonist of the rainbow trout (Oncorhynchus mykiss) mineralocorticoid receptor. Endocrinology *146*, 47.

Summers, C.H. (2002). Social interaction over time, implications for stress responsiveness. Integrative and Comparative Biology *42*, 591–599.

Summers, C.H., Watt, M.J., Ling, T.L., Forster, G.L., Carpenter, R.E., Korzan, W.J., Lukkes, J.L., and Overli, O. (2005). Glucocorticoid interaction with aggression in non-mammalian vertebrates: reciprocal action. Eur. J. Pharmacol. *526*, 21–35.

Summerton, J., and Weller, D. (1997). Morpholino antisense oligomers: design, preparation, and properties. Antisense and Nucleic Acid Drug Development *7*, 187–196.

Sylva, M., Li, V.S.W., Buffing, A.A.A., van Es, J.H., van den Born, M., van der Velden, S., Gunst, Q., Koolstra, J.H., Moorman, A.F.M., Clevers, H., et al. (2011). The BMP antagonist follistatin-like 1 is required for skeletal and lung organogenesis. PLoS One *6*, e22616.

Tetsuka, M. (2007). Actions of glucocorticoid and their regulatory mechanisms in the ovary. Animal Science Journal *78*, 112–120.

Thakore, J.H., and Dinan, T.G. (1994). Growth hormone secretion: the role of glucocorticoids. Life Sciences *55*, 1083–1099.

Tilbrook, A., Turner, A., and Clarke, I. (2000). Effects of stress on reproduction in non-rodent mammals: the role of glucocorticoids and sex differences. Rev. Reprod. *5*, 105–113.

To, T., Hahner, S., Nica, G., Rohr, K., Hammerschmidt, M., Winkler, C., and Allolio, B. (2007). Pituitary-interrenal interaction in zebrafish interrenal organ development. Molecular Endocrinology *21*, 472.

Tort, L. (2011). Stress and immune modulation in fish. Dev. Comp. Immunol. *35*, 1366–1375.

Tort, L., and Teles, M. The Endocrine Response to Stress-A Comparative View.

Traver, D., Herbomel, P., Patton, E.E., Murphey, R.D., Yoder, J.A., Litman, G.W., Catic, A., Amemia, C.T., Zon, L.I., and Trede, N.S. (2003). The Zebrafish as a Model Organism to Study Development of the Immune System. In Advances in Immunology, (Elsevier), pp. 254–330.

Tsigos, C., and Chrousos, G.P. (2002). Hypothalamic-pituitary-adrenal axis, neuroendocrine factors and stress. Journal of Psychosomatic Research *53*, 865–871.

van der Boon, J., van den Thillart, G., and Addink, A. (1991). The effects of cortisol administration on intermediary metabolism in teleost fish. Comparative Biochemistry and Physiology Part a: Physiology *100*, 47–53.

van Weerd, J., and Komen, J. (1998). The effects of chronic stress on growth in fish: a critical appraisal. Comparative Biochemistry and Physiology Part a: Physiology *120*, 107–112.

Vatine, G., Vallone, D., Gothilf, Y., and Foulkes, N.S. (2011). Itâ€™s time to swim! Zebrafish and the circadian clock. FEBS Letters *585*, 1485–1494.

Vijayan, M., Prunet, P., and Boone, A.N. (2005). Xenobiotic Impact on Corticosteroid Signaling. Biochemistry and Molecular Biology of Fishes *6*, 365–394.

Vrekoussis, T., Kalantaridou, S.N., Mastorakos, G., Zoumakis, E., Makrigiannakis, A., Syrrou, M., Lavasidis, L.G., Relakis, K., and Chrousos, G.P. (2010). The role of stress in female reproduction and pregnancy: an update. Annals of the New York Academy of Sciences *1205*, 69–75.

Wada, H. (2008). Glucocorticoids: Mediators of vertebrate ontogenetic transitions. General and Comparative Endocrinology *156*, 441–453.

Wada, H., Ghysen, A., Satou, C., and Higashijima, S. (2010). Dermal morphogenesis controls lateral line patterning during postembryonic development of teleost fish. Developmental Biology.

Wagner, D.O., Sieber, C., Bhushan, R., Börgermann, J.H., Graf, D., and Knaus, P. (2010). BMPs: from bone to body morphogenetic proteins. Sci Signal *3*, mr1.

Walker, B.R. (2007). Glucocorticoids and cardiovascular disease. Eur. J. Endocrinol. *157*, 545–559.

Wallace, K.N., Akhter, S., Smith, E.M., Lorent, K., and Pack, M. (2005). Intestinal growth and differentiation in zebrafish. Mechanisms of Development *122*, 157–173.

Walsh, D.W., Godson, C., Brazil, D.P., and Martin, F. (2010). Extracellular BMP-antagonist regulation in development and disease: tied up in knots. Trends in Cell Biology *20*, 244–256.

Wang, W., and Lufkin, T. (2000). The murine Otp homeobox gene plays an essential role in the specification of neuronal cell lineages in the developing hypothalamus. Developmental Biology *227*, 432–449.

Wang, Z.M., Yasui, M., and Celsi, G. (1994). Glucocorticoids regulate the transcription of Na(+)-K(+)-ATPase genes in the infant rat kidney. Am. J. Physiol. *267*, C450–C455.

Webster, J.C., Jewell, C.M., Bodwell, J.E., Munck, A., Sar, M., and Cidlowski, J.A. (1997). Mouse glucocorticoid receptor phosphorylation status influences multiple functions of the receptor protein. J Biol Chem *272*, 9287–9293.

Welberg, L.A., and Seckl, J.R. (2001). Prenatal stress, glucocorticoids and the programming of the brain. Journal of Neuroendocrinology *13*, 113–128.

Welberg, L.A., Seckl, J.R., and Holmes, M.C. (2001). Prenatal glucocorticoid programming of brain corticosteroid receptors and corticotrophin-releasing hormone: possible implications for behaviour. Neuroscience *104*, 71–79.

Wendelaar Bonga, S. (1997). The stress response in fish. Physiological Reviews *77*, 591–626.

Westerfield, M. (2007). The Zebrafish Book (Eugene, Oregon: University of Oregon Press).

Weyts, F., Cohen, N., Flik, G., and Verburg-van Kemenade, B. (1999). Interactions between the immune system and the hypothalamo-pituitary-interrenal axis in fish. Fish & Shellfish Immunology *9*, 1–20.

Wingfield, J.C., and Sapolsky, R.M. (2003). Reproduction and resistance to stress: when and how. Journal of Neuroendocrinology *15*, 711–724.

Wolkowitz, O., Burke, H., Epel, E., and Reus, V. (2009). Glucocorticoids: Mood, Memory, and Mechanisms. Annals of the New York Academy of Sciences *1179*, 19–40.

Yanagita, M. (2005). BMP antagonists: their roles in development and involvement in pathophysiology. Cytokine & Growth Factor Reviews *16*, 309–317.

Yang, K. (1997). Placental 11 beta-hydroxysteroid dehydrogenase: barrier to maternal glucocorticoids. Rev. Reprod. *2*, 129–132.

Yin, C., Ciruna, B., and Solnica-Krezel, L. (2009). Chapter 7 - Convergence and Extension Movements During Vertebrate Gastrulation (Elsevier Inc.).

Yoong, S., O'Connell, B., Soanes, A., Crowhurst, M., Lieschke, G., and Ward, A. (2007). Characterization of the zebrafish matrix metalloproteinase 9 gene and its developmental expression pattern. Gene Expression Patterns *7*, 39–46.

Yudt, M., and Cidlowski, J. (2002). The glucocorticoid receptor: coding a diversity of proteins and responses through a single gene. Molecular Endocrinology *16*, 1719.

ZFIN Staff (2006). Curation of Ensemble Database.

Zhang, J., Bai, S., Zhang, X., Nagase, H., and Sarras, M. (2003). The expression of gelatinase A (MMP-2) is required for normal development of zebrafish embryos. Development Genes and Evolution *213*, 456–463.

Zhang, S., Fei, T., Zhang, L., Zhang, R., Chen, F., Ning, Y., Han, Y., Feng, X.-H., Meng, A., and Chen, Y.-G. (2007). Smad7 antagonizes transforming growth factor beta signaling in the nucleus by interfering with functional Smad-DNA complex formation. Molecular and Cellular Biology *27*, 4488–4499.

Zhao, Y., Yang, Z., Phelan, J.K., Wheeler, D.A., Lin, S., and McCabe, E.R.B. (2006). Zebrafish dax1 is required for development of the interrenal organ, the adrenal cortex equivalent. Mol. Endocrinol. *20*, 2630–2640.

Zhou, J., and Cidlowski, J.A. (2005). The human glucocorticoid receptor: one gene, multiple proteins and diverse responses. Steroids *70*, 407–417.

Zon, L.I., and Peterson, R.T. (2005). In vivo drug discovery in the zebrafish. Nat Rev Drug Discov *4*, 35–44.

CHAPTER 2

Alsop, D., and Vijayan, M. (2008). Development of the corticosteroid stress axis and receptor expression in zebrafish. American Journal of Physiology- Regulatory, Integrative and Comparative Physiology *294*, R711.

Alsop, D., and Vijayan, M. (2009). Molecular programming of the corticosteroid stress axis during zebrafish development. Comparative Biochemistry and Physiology Part a: Physiology *153*, 49–54.

Aluru, N., Leatherland, J., and Vijayan, M. (2010). Bisphenol A in Oocytes Leads to Growth Suppression and Altered Stress Performance in Juvenile Rainbow Trout. PLoS One *5*, e10741.

Boone, A.N., and Vijayan, M.M. (2002). Constitutive heat shock protein 70 (HSC70) expression in rainbow trout hepatocytes: effect of heat shock and heavy metal exposure. Comparative Biochemistry and Physiology, Part C *132*, 223–233.

Brand, T. (2003). Heart development: molecular insights into cardiac specification and early morphogenesis. Developmental Biology *258*, 1–19.

Bubnoff, von, A., and Cho, K.W. (2001). Intracellular BMP signaling regulation in vertebrates: pathway or network? Developmental Biology *239*, 1–14.

Chin, A., Chen, J., and Weinberg, E. (1997). Bone morphogenetic protein-4 expression characterizes inductive boundaries in organs of developing zebrafish. Development Genes and Evolution *207*, 107–114.

Chong, S.W., Korzh, V., and Jiang, Y.J. (2009). Myogenesis and molecules - insights from zebrafish Danio rerio. Journal of Fish Biology *74*, 1693–1755.

Chung, W., Shin, C., and Stainier, D. (2008). Bmp2 signaling regulates the hepatic versus pancreatic fate decision. Developmental Cell *15*, 738–748.

Cole, T., Myles, K., Purton, J., Brereton, P., Solomon, N., Godfrey, D., and Funder, J. (2001). GRKO mice express an aberrant dexamethasone-binding glucocorticoid receptor, but are profoundly glucocorticoid resistant. Molecular and Cellular Endocrinology *173*, 193–202.

David, L., Feige, J., and Bailly, S. (2009). Emerging role of bone morphogenetic proteins in angiogenesis. Cytokine & Growth Factor Reviews *20*, 203–212.

Du, S., Gao, J., and Anyangwe, V. (2003). Muscle-specific expression of myogenin in zebrafish embryos is controlled by multiple regulatory elements in the promoter. Comparative Biochemistry and Physiology Part B: Biochemistry and Molecular Biology *134*, 123–134.

Duan, C., Ren, H., and Gao, S. (2010). Insulin-like growth factors (IGFs), IGF receptors, and IGF-binding proteins: Roles in skeletal muscle growth and differentiation. General and Comparative Endocrinology.

Hillegass, J., Villano, C., Cooper, K., and White, L. (2007). Matrix metalloproteinase-13 is required for zebra fish (Danio rerio) development and is a target for glucocorticoids. Toxicological Sciences *100*, 168.

Kishimoto, Y., Lee, K., Zon, L., Hammerschmidt, M., and Schulte-Merker, S. (1997). The molecular nature of zebrafish swirl: BMP2 function is essential during early dorsoventral patterning. Development *124*, 4457.

Liggins, G.C. (1994). The role of cortisol in preparing the fetus for birth. Reproduction Fertility and Development *6*, 141–150.

Little, S.C., and Mullins, M.C. (2006). Extracellular modulation of BMP activity in patterning the dorsoventral axis. Birth Defect Res C *78*, 224–242.

Livak, K., and Schmittgen, T. (2001). Analysis of relative gene expression data using real-time quantitative PCR and the 2-[Delta][Delta] CT method. Methods *25*, 402–408.

Miyazono, K., Maeda, S., and Imamura, T. (2005). BMP receptor signaling: transcriptional targets, regulation of signals, and signaling cross-talk. Cytokine & Growth Factor Reviews *16*, 251–263.

Mommsen, T., Vijayan, M., and Moon, T. (1999). Cortisol in teleosts: dynamics, mechanisms of action, and metabolic regulation. Reviews in Fish Biology and Fisheries *9*, 211–268.

Nikaido, M., Tada, M., Saji, T., and Ueno, N. (1997). Conservation of BMP signaling in zebrafish mesoderm patterning. Mechanisms of Development *61*, 75–88.

Ochi, H., and Westerfield, M. (2007). Signaling networks that regulate muscle development: lessons from zebrafish. Development Growth and Differentiation *49*, 1.

Palstra, A.P., Tudorache, C., Rovira, M., Brittijn, S.A., Burgerhout, E., van den Thillart, G.E.E.J.M., Spaink, H.P., and Planas, J.V. (2010). Establishing Zebrafish as a Novel Exercise Model:

Swimming Economy, Swimming-Enhanced Growth and Muscle Growth Marker Gene Expression. PLoS One *5*, e14483.

Patterson, S., Bird, N., and Devoto, S. (2010). BMP regulation of myogenesis in zebrafish. Dev. Dyn. *239*, 806–817.

Pelster, B., and Burggren, W. (1996). Disruption of hemoglobin oxygen transport does not impact oxygen-dependent physiological processes in developing embryos of zebra fish (Danio rerio). Circulation Research *79*, 358.

Pikulkaew, S., Benato, F., Celeghin, A., Zucal, C., Skobo, T., Colombo, L., and Valle, L.D. (2011). The knockdown of maternal glucocorticoid receptor mRNA alters embryo development in zebrafish. Dev. Dyn. *240*, 874–889.

Pyati, U., Webb, A., and Kimelman, D. (2005). Transgenic zebrafish reveal stage-specific roles for Bmp signaling in ventral and posterior mesoderm development. Development *132*, 2333.

Reshef, R., Maroto, M., and Lassar, A. (1998). Regulation of dorsal somitic cell fates: BMPs and Noggin control the timing and pattern of myogenic regulator expression. Genes & Development *12*, 290.

Sapolsky, R., Romero, L., and Munck, A. (2000). How do glucocorticoids influence stress responses? Integrating permissive, suppressive, stimulatory, and preparative actions. Endocrine Reviews *21*, 55.

Schaaf, M., Champagne, D., van Laanen, I., van Wijk, D., Meijer, A., Meijer, O., Spaink, H., and Richardson, M. (2008). Discovery of a functional glucocorticoid receptor {beta}-isoform in zebrafish. Endocrinology *149*, 1591.

Schoonheim, P., Chatzopoulou, A., and Schaaf, M. (2010). The zebrafish as an in vivo model system for glucocorticoid resistance. Steroids.

Seebald, J.L., and Szeto, D.P. (2011). Zebrafish eve1 regulates the lateral and ventral fates of mesodermal progenitor cells at the onset of gastrulation. Developmental Biology *349*, 78–89.

Shin, D., Shin, C., Tucker, J., Ober, E., Rentzsch, F., Poss, K., Hammerschmidt, M., Mullins, M., and Stainier, D. (2007). Bmp and Fgf signaling are essential for liver specification in zebrafish. Development *134*, 2041.

Stickney, H., Barresi, M., and Devoto, S. (2000). Somite development in zebrafish. Dev. Dyn. *219*, 287–303.

Stickney, H., Imai, Y., Draper, B., Moens, C., and Talbot, W. (2007). Zebrafish bmp4 functions during late gastrulation to specify ventroposterior cell fates. Developmental Biology *310*, 71–84.

Thisse, C., and Thisse, B. (2008). High-resolution in situ hybridization to whole-mount zebrafish embryos. Nat Protoc *3*, 59–69.

Tucker, J., Mintzer, K., and Mullins, M. (2008). The BMP signaling gradient patterns dorsoventral tissues in a temporally progressive manner along the anteroposterior axis. Developmental Cell *14*, 108–119.

Ward, A.M.V. (2004). Fetal Programming of the Hypothalamic-Pituitary-Adrenal (HPA) Axis: Low Birth Weight and Central HPA Regulation. Journal of Clinical Endocrinology & Metabolism *89*, 1227–1233.

Westerfield, M. (2007). The Zebrafish Book (Eugene, Oregon: University of Oregon Press).

Xu, Y., He, J., Wang, X., Lim, T., and Gong, Z. (2000). Asynchronous activation of 10 muscle-specific protein (MSP) genes during zebrafish somitogenesis. Dev. Dyn. *219*, 201–215.

CHAPTER 3

Alderman, S., Bernier, N., 2009. Ontogeny of the corticotropin-releasing factor system in zebrafish. Gen. Comp. Endocrinol. 164, 61–69.

Alsop, D., Vijayan, M.M., 2008. Development of the corticosteroid stress axis and receptor expression in zebrafish. Am. J. Physiol. Regul. Integr. Comp. Physiol. 294, R711-719.

Alsop, D., Vijayan, M.M., 2009. Molecular programming of the corticosteroid stress axis during zebrafish development. Comp. Biochem. Physiol. A Mol. Integr. Physiol. 153, 49–54.

Aluru, N., Vijayan, M.M., 2009. Stress transcriptomics in fish: A role for genomic cortisol signaling. Gen. Comp. Endocrinol. 164, 142–150.

Aluru, N., Vijayan, M.M., 2008. Molecular Characterization, Tissue-Specific Expression, and Regulation of Melanocortin 2 Receptor in Rainbow Trout. Endocrinology 149, 4577–4588.

Auperin, B., Geslin, M., 2008. Plasma cortisol response to stress in juvenile rainbow trout is influenced by their life history during early development and by egg cortisol content. Gen. Comp. Endocrinol. 158, 234–239.

Baker, K., Warren, K.S., Yellen, G., Fishman, M.C., 1997. Defective "pacemaker" current (I_h) in a zebrafish mutant with a slow heart rate. Proc. Natl. Acad. Sci. U.S.A. 94, 4554-4559.

Barry, T.P., Malison, J.A., Held, J.A., Parrish, J.J., 1995. Ontogeny of the cortisol stress response in larval rainbow trout. Gen. Comp. Endocrinol. 97, 57–65.

Breuner, C.W., Patterson, S.H., Hahn, T.P., 2008. In search of relationships between the acute adrenocortical response and fitness. Gen. Comp. Endocrinol. 157, 288–295.

Burggren, W., 2004. What is the purpose of the embryonic heart beat? Or how facts can ultimately prevail over physiological dogma. Physiol. Biochem. Zool. 77, 333–345.

Bury, N.R., Sturm, A., Le Rouzic, P., Lethimonier, C., Ducouret, B., Guiguen, Y., Robinson-Rechavi, M., Laudet, V., Rafestin-Oblin, M.E., Prunet, P., 2003. Evidence for two distinct functional glucocorticoid receptors in teleost fish. J. Mole. Endocrinol. 31, 141–156.

Carfagnini, A.G., Rodd, F.H., Jeffers, K.B., Bruce, A.E.E., 2009. The effects of habitat complexity on aggression and fecundity in zebrafish (Danio rerio). Environ. Biol. Fishes 86, 403–409.

Chen, J.N., Fishman, M.C., 1996. Zebrafish tinman homolog demarcates the heart field and initiates myocardial differentiation. Development 122, 3809–3816.

Chen, J.N., van Eeden, F.J.M., Warren K.S., Chin, A., Nusslein-Volhard, C., Haffter, P., Fishman, M.C., 1997. Left-right pattern of cardiac BMP4 may drive asymmetry of the heart in zebrafish. Development 124, 4373-4382.

Chen, Z., Huang, W., Dahme, T., Rottbauer, W., Ackerman, M.J., Xu, X., 2008. Depletion of zebrafish essential and regulatory myosin light chains reduces cardiac function through distinct mechanisms. Cardiovasc. Res. 79, 97–108.

Chico, T.J.A., Ingham, P.W., Crossman, D.C., 2008. Modeling cardiovascular disease in the zebrafish. Trends Cardiovasc. Med. 18, 150-155.

Chin, A.J., Chen, J.N., Weinberg, E.S., 1997. Bone morphogenetic protein-4 expression characterizes inductive boundaries in organs of developing zebrafish. Dev. Genes Evol. 207, 107-114.

Chrousos, G.P., Gold, P.W., 1992. The concepts of stress and stress system disorders - overview of physical and behavioral homeostasis. JAMA 267, 1244-1252.

Ebert, A.M., Hume, G.L., Warren, K.S., Cook, N.P., Burns, C.G., Mohideen, M.A., Siegal, G., Yelon, D., Fishman, M.C., Garrity, D.M., 2005. Calcium extrusion is critical for cardiac morphogenesis and rhythm in embryonic zebrafish hearts. Proc. Natl. Acad. Sci. U.S.A. 102, 17705–17710.

Eriksen, M., Bakken, M., Espmark, Å., Braastad, B., Salte, R., 2006. Prespawning stress in farmed Atlantic salmon Salmo salar: maternal cortisol exposure and hyperthermia during embryonic development affect offspring survival, growth and incidence of malformations. J.Fish Biol. 69, 114–129.

Garrity, D.M., Childs, S., Fishman, M.C., 2002. The heartstrings mutation in zebrafish causes heart/fin Tbx5 deficiency syndrome. Development 129, 4635-4645.

Giesing, E.R., Suski, C.D., Warner, R.E., Bell, A.M., 2011. Female sticklebacks transfer information via eggs: effects of maternal experience with predators on offspring. Proc. Biol. Sci. 278, 1753–1759.

Glickman, N., Yelon, D., 2002. Cardiac development in zebrafish: coordination of form and function. Sem. Cell Dev. Biol. 13, 507–513.

Gonçalves, A.F., Páscoa, I., Neves, J.V., Coimbra, J., Vijayan, M.M., Rodrigues, P., Wilson, J.M., 2012. The inhibitory effect of environmental ammonia on Danio rerio LPS induced acute phase response. Dev. Comp. Immunol. 36, 279–288.

Hillegass, J., Villano, C., Cooper, K., White, L., 2007. Matrix metalloproteinase-13 is required for zebra fish (Danio rerio) development and is a target for glucocorticoids. Toxicol. Sci. 100, 168-179.

Hontela, A., Vijayan, M.M., 2008. Adrenocortical toxicology in fishes, in: Harvey, P.W., Everett, D., Springall, C. (Eds.), Adrenal Toxicology. Taylor and Francis, Florida, pp. 233–256.

Hsiao, C.-D., Tsai, W.-Y., Horng, L.-S., Tsai, H.-J., 2003. Molecular structure and developmental expression of three muscle-type troponin T genes in zebrafish. Dev. Dyn. 227, 266–279.

Johansen, I.B., Lunde, I.G., Rosjo, H., Christensen, G., Nilsson, G.E., Bakken, M., Overli, O., 2011. Cortisol response to stress is associated with myocardial remodeling in salmonid fishes. J. Exp. Biol. 214, 1313-1321.

Kapoor, A., 2006. Fetal Programming of Hypothalamo-Pituitary-Adrenal (HPA) Function: Prenatal Stress and Glucocorticoids. J. Physiol. 572, 31-44.

Kimmel, C., Ballard, W., Kimmel, S., Ullmann, B., Schilling, T., 1995. Stages of embryonic development of the zebrafish. Dev. Dyn. 203, 253–310.

Lohr, H., Hammerschmidt, M., 2011. Zebrafish in endocrine systems: recent advances and implications for human disease. Annu. Rev. Physiol. 72, 183-211.

Lumbers, E.R., Boyce, A.C., Joulianos, G., Kumarasamy, V., Barner, E., Segar, J.L., and Burrell, J.H., 2004. Effects of cortisol on cardiac myocytes and on expression of cardiac genes in fetal sheep. Am. J. Physiol. Regul. Integr. Comp. Physiol. 288, R567-R574.

Mccormick, M.I., Nechaev, I.G., 2002. Influence of cortisol on developmental rhythms during embryogenesis in a tropical damselfish. J. Exp. Zool. 293, 456-466.

Mommsen, T.P., Vijayan, M.M., Moon, T.W., 1999. Cortisol in teleosts: dynamics, mechanisms of action, and metabolic regulation. Rev. Fish Biol. Fish. 9, 211–268.

Nesan, D., Kamkar, M., Burrows, J., Scott, I.C., Marsden, M., Vijayan, M.M., 2012. Glucocorticoid Receptor Signaling Is Essential for Mesoderm Formation and Muscle Development in Zebrafish. Endocrinology 153, 1288-1300.

Orn, S., Andersson, P.L., Förlin, L., Tysklind, M., Norrgren, L., 1998. The impact on reproduction of an orally administered mixture of selected PCBs in zebrafish (Danio rerio). Arch. Environ. Contam. Toxicol. 35, 52–57.

Pelster, B., Burggren, W., 1996. Disruption of hemoglobin oxygen transport does not impact oxygen-dependent physiological processes in developing embryos of zebra fish (Danio rerio). Circ. Res. 79, 358-362.

Pikulkaew, S., Benato, F., Celeghin, A., Zucal, C., Skobo, T., Colombo, L., Valle, L.D., 2011. The knockdown of maternal glucocorticoid receptor mRNA alters embryo development in zebrafish. Dev. Dyn. 240, 874–889.

Prunet, P., Sturm, A., Milla, S., 2006. Multiple corticosteroid receptors in fish: from old ideas to new concepts. Gen. Comp. Endocrinol. 147, 17–23.

Reini, S.A., Dutta, G., Wood, C.E., Keller-Wood, M., 2008. Cardiac corticosteroid receptors mediate the enlargement of the ovine fetal heart induced by chronic increases in maternal cortisol. J. Endocrinol. 198, 419-427.

Reiter, J.F., Alexander, J., Rodaway, A., Yelon, D., Patient, R., Holder, N., Stainier, D.Y., 1999. Gata5 is required for the development of the heart and endoderm in zebrafish. Genes Dev. 13, 2983–2995.

Sapolsky, R., Romero, L., Munck, A., 2000. How do glucocorticoids influence stress responses? Integrating permissive, suppressive, stimulatory, and preparative actions. Endocr. Rev. 21, 55-89.

Schaaf, M.J.M., Champagne, D., van Laanen, I.H.C., van Wijk, D.C.W.A., Meijer, A.H., Meijer, O.C., Spaink, H.P., Richardson, M.K., 2008. Discovery of a functional glucocorticoid receptor ß-isoform in zebrafish. Endocrinology 149, 1591-1599.

Seckl, J.R., Meaney, M.J., 2004. Glucocorticoid Programming. Ann. N.Y. Acad. Sci. 1032, 63–84.

Steele, S.L., Yang, X., Debiais-Thibaud, M., Schwerte, T., Pelster, B., Ekker, M., Tiberi, M., Perry, S.F., 2011. In vivo and in vitro assessment of cardiac -adrenergic receptors in larval zebrafish (Danio rerio). J. Exp. Biol. 214, 1445–1457.

Stouthart, A., Lucassen, E., van Strien, F., Balm, P., Lock, R., Wendelaar Bonga, S., 1998. Stress responsiveness of the pituitary-interrenal axis during early life stages of common carp (Cyprinus carpio). J Endocrinol. 157, 127-137.

Stratholt, M.L., Donaldson, E.M., Liley, N.R., 1997. Stress induced elevation of plasma cortisol in adult female coho salmon (Oncorhynchus kisutch), is reflected in egg cortisol content, but does not appear to affect early development. Aquaculture 158, 141-153.

Sultana, N., Nag, K., Hoshijima, K., Laird, D.W., Kawakami, A., Hirose, S., 2008. Zebrafish early cardiac connexin, Cx36.7/Ecx, regulates myofibril orientation and heart morphogenesis by establishing Nkx2.5 expression. Proc. Natl. Acad. Sci. U.S.A. 105, 4763–4768.

Targoff, K.L., Schell, T., Yelon, D., 2008. Nkx genes regulate heart tube extension and exert differential effects on ventricular and atrial cell number. Dev. Biol. 322, 314–321.

Thisse, C., Zon, L., 2002. Organogenesis--heart and blood formation from the zebrafish point of view. Science 295, 457-462.

Wendelaar Bonga, S., 1997. The stress response in fish. Physiol. Rev. 77, 591–626.

Westerfield, M., 2007. The zebrafish book. A guide for the laboratory use of zebrafish (Danio rerio), fifth ed. University of Oregon Press, Eugene, OR.

Yelon, D., 2001. Cardiac patterning and morphogenesis in zebrafish. Dev. Dyn. 222, 552–563.

CHAPTER 4

Alsop, D., and Vijayan, M. (2008). Development of the corticosteroid stress axis and receptor expression in zebrafish. American Journal of Physiology- Regulatory, Integrative and Comparative Physiology *294*, R711.

Aluru, N., and Vijayan, M.M. (2007). Hepatic transcriptome response to glucocorticoid receptor activation in rainbow trout. Physiological Genomics *31*, 483–491.

Bahary, N., Goishi, K., Stuckenholz, C., Weber, G., LeBlanc, J., Schafer, C.A., Berman, S.S., Klagsbrun, M., and Zon, L.I. (2007). Duplicate VegfA genes and orthologues of the KDR receptor tyrosine kinase family mediate vascular development in the zebrafish. Blood *110*, 3627–3636.

Bassett, E.A., and Wallace, V.A. (2012). Cell fate determination in the vertebrate retina. Trends Neurosci. *35*, 565–573.

Benjamini, Y., and Hochberg, Y. (1995). Controlling the false discovery rate: a practical and powerful approach to multiple testing. Journal of the Royal Statistical Society. Series B (Methodological) 289–300.

Biswas, S., and Jontes, J.D. (2009). Cloning and characterization of zebrafish protocadherin–17. Development Genes and Evolution *219*, 265–271.

Blechman, J., Borodovsky, N., Eisenberg, M., Nabel-Rosen, H., Grimm, J., and Levkowitz, G. (2007). Specification of hypothalamic neurons by dual regulation of the homeodomain protein Orthopedia. Development *134*, 4417–4426.

Brand, T. (2003). Heart development: molecular insights into cardiac specification and early morphogenesis. Developmental Biology *258*, 1–19.

Bury, N., and Sturm, A. (2007). Evolution of the corticosteroid receptor signalling pathway in fish. General and Comparative Endocrinology *153*, 47–56.

Cason, N., White, T.W., Cheng, S., Goodenough, D.A., and Valdimarsson, G. (2001). Molecular cloning, expression analysis, and functional characterization of connexin44.1: a zebrafish lens gap junction protein. Dev. Dyn. *221*, 238–247.

Camarata, T., Krcmery, J. Snyder, D., Park, S., Topczewski, J., and Simon, H.G. (2010). Pdlim7 (LMP4) regulation of Tbx5 specifies zebrafish atrio-ventricular boundary and valve formation. Developmental Biology, *337*, 233-245.

Charmandari, E., Tsigos, C., and Chrousos, G. (2004). Endocrinology of the stress response1. Annu. Rev. Physiol.

Chen, Y., Londraville, R., Brickner, S., El-Shaar, L., Fankhauser, K., Dearth, C., Fulton, L., Sochacka, A., Bhattarai, S., Marrs, J.A., et al. (2012). Protocadherin-17 function in zebrafish retinal development. Dev Neurobiol in press.

Cheng, S., Christie, T., and Valdimarsson, G. (2003). Expression of connexin48.5, connexin44.1, and connexin43 during zebrafish (Danio rerio) lens development. Dev. Dyn. *228*, 709–715.

Chrousos, G. (2006). Stressors, stress, and neuroendocrine integration of the adaptive response: The 1997 Hans Selye Memorial Lecture. Annals of the New York Academy of Sciences *851*, 311–335.

Chung, W., Shin, C., and Stainier, D. (2008). Bmp2 signaling regulates the hepatic versus pancreatic fate decision. Developmental Cell *15*, 738–748.

De Fraipont, M., Clobert, J., John, H., and Meylan, S. (2000). Increased pre‐natal maternal corticosterone promotes philopatry of offspring in common lizards Lacerta vivipara. Journal of Animal Ecology *69*, 404–413.

Duan, C., and Xu, Q. (2005). Roles of insulin-like growth factor (IGF) binding proteins in regulating IGF actions. General and Comparative Endocrinology *142*, 44–52.

Duan, C., Ding, J., Schlueter, P.J., Li, Y., Zhang, J., and TL, R. (2003). A zebrafish view of the insulin-like growth factor (IGF) signaling pathway. Acta Zoologica Sinica *4*, 000.

Eaton, J.L., and Glasgow, E. (2006). Zebrafish orthopedia (otp) is required for isotocin cell development. Development Genes and Evolution *217*, 149–158.

Eaton, J.L., Holmqvist, B., and Glasgow, E. (2008). Ontogeny of vasotocin-expressing cells in zebrafish: Selective requirement for the transcriptional regulators orthopediaand single-minded 1in the preoptic area. Dev. Dyn. *237*, 995–1005.

Eivers, E., Mccarthy, K., Glynn, C., Nolan, C.M., and Byrnes, L. (2004). Insulin-like growth factor (IGF) signalling is required for early dorso-anterior development of the zebrafish embryo. Int. J. Dev. Biol. *48*, 1131–1140.

Elicker, K.S., and Hutson, L.D. (2007). Genome-wide analysis and expression profiling of the small heat shock proteins in zebrafish. Gene *403*, 60–69.

Emond, M.R., and Jontes, J.D. (2008). Inhibition of protocadherin-α function results in neuronal death in the developing zebrafish. Developmental Biology *321*, 175–187.

Frank, M., and Kemler, R. (2002). Protocadherins. Current Opinion in Cell Biology *14*, 557–562.

Gilmour, K.M., Dibattista, J.D., and Thomas, J.B. (2005). Physiological causes and consequences of social status in salmonid fish. Integrative and Comparative Biology *45*, 263–273.

Greiling, T.M.S., Houck, S.A., and Clark, J.I. (2009). The zebrafish lens proteome during development and aging. Mol. Vis. *15*, 2313–2325.

Gribble, S.L., Kim, H.-S., Bonner, J., Wang, X., and Dorsky, R.I. (2009). Tcf3 inhibits spinal cord neurogenesis by regulating sox4a expression. Development *136*, 781–789.

Grossman, T.R., Gamliel, A., Wessells, R.J., Taghli-Lamallem, O., Jepsen, K., Ocorr, K., Korenberg, J.R., Peterson, K.L., Rosenfeld, M.G., Bodmer, R., et al. (2011). Over-Expression of DSCAM and COL6A2 Cooperatively Generates Congenital Heart Defects. PLoS Genetics *7*, e1002344.

Halbleib, J.M., and Nelson, W.J. (2006). Cadherins in development: cell adhesion, sorting, and tissue morphogenesis. Genes & Development *20*, 3199–3214.

Hayward, L., and Wingfield, J. (2004). Maternal corticosterone is transferred to avian yolk and may alter offspring growth and adult phenotype. General and Comparative Endocrinology *135*, 365–371.

Hillegass, J., Villano, C., Cooper, K., and White, L. (2007). Matrix metalloproteinase-13 is required for zebra fish (Danio rerio) development and is a target for glucocorticoids. Toxicological Sciences *100*, 168.

Hillegass, J., Villano, C., Cooper, K., and White, L. (2008). Glucocorticoids alter craniofacial development and increase expression and activity of matrix metalloproteinases in developing zebrafish (Danio rerio). Toxicological Sciences.

Hunter, P.R., Nikolaou, N., Odermatt, B., Williams, P.R., Drescher, U., and Meyer, M.P. (2011). Localization of Cadm2a and Cadm3 proteins during development of the zebrafish nervous system. J. Comp. Neurol. *519*, 2252–2270.

Iovine, M.K., Gumpert, A.M., Falk, M.M., and Mendelson, T.C. (2008). Cx23, a connexin with only four extracellular-loop cysteines, forms functional gap junction channels and hemichannels. FEBS Letters *582*, 165–170.

Kim, B., Huang, G., Ho, W.B., and Greenspan, D.S. (2011). Bone morphogenetic protein-1 processes insulin-like growth factor-binding protein 3. J Biol Chem *286*, 29014–29025.

Kimmel, C., Ballard, W., Kimmel, S., Ullmann, B., and Schilling, T. (1995). Stages of embryonic development of the zebrafish. Dev. Dyn. *203*, 253–310.

Kondo, M. (2007). Bone morphogenetic proteins in the early development of zebrafish. Febs J. *274*, 2960–2967.

Kuo, M.-W., Lou, S.-W., Postlethwait, J., and Chung, B.-C. (2005). Chromosomal Organization, Evolutionary Relationship, and Expression of Zebrafish GnRH Family Members. Journal of Biomedical Science *12*, 629–639.

Lafont, A.-G., Wang, Y.-F., Chen, G.-D., Liao, B.-K., Tseng, Y.-C., Huang, C.-J., and Hwang, P.-P. (2011). Involvement of calcitonin and its receptor in the control of calcium-regulating genes and calcium homeostasis in zebrafish (Danio rerio). Journal of Bone and Mineral Research *26*, 1072–1083.

Larson, E.T., O'Malley, D.M., and Melloni, R.H., Jr. (2006). Aggression and vasotocin are associated with dominant–subordinate relationships in zebrafish. Behavioural Brain Research *167*, 94–102.

Li, Q., Frank, M., Thisse, C.I., Thisse, B.V., and Uitto, J. (2011). Zebrafish: a model system to study heritable skin diseases. J. Invest. Dermatol. *131*, 565–571.

Li, Y., Xiang, J., and Duan, C. (2005). Insulin-like growth factor-binding protein-3 plays an important role in regulating pharyngeal skeleton and inner ear formation and differentiation. J Biol Chem *280*, 3613–3620.

Liang, D., Chang, J., Chin, A., Smith, A., Kelly, C., Weinberg, E., and Ge, R. (2001). The role of vascular endothelial growth factor (VEGF) in vasculogenesis, angiogenesis, and hematopoiesis in zebrafish development. Mechanisms of Development *108*, 29–43.

Liao, J., He, J., Yan, T., Korzh, V., and Gong, Z. (1999). A class of neuroD-related basic helix-loop-helix transcription factors expressed in developing central nervous system in zebrafish. DNA and Cell Biology *18*, 333–344.

Liu, N.-A., Huang, H., Yang, Z., Herzog, W., Hammerschmidt, M., Lin, S., and Melmed, S. (2003). Pituitary corticotroph ontogeny and regulation in transgenic zebrafish. Mol. Endocrinol. *17*, 959–966.

Liu, Y. (2007). Interrenal Organogenesis in the Zebrafish Model. Organogenesis *3*, 44.

Livak, K., and Schmittgen, T. (2001). Analysis of relative gene expression data using real-time quantitative PCR and the 2-[Delta][Delta] CT method. Methods *25*, 402–408.

Lu, N.Z., and Cidlowski, J.A. (2006). Glucocorticoid receptor isoforms generate transcription specificity. Trends in Cell Biology *16*, 301–307.

Matsuda, K., Sakashita, A., Yokobori, E., and Azuma, M. (2012). Neuroendocrine control of feeding behavior and psychomotor activity by neuropeptide Y in fish. Neuropeptides 1–9.

Maurya, A.K., Tan, H., Souren, M., Wang, X., Wittbrodt, J., and Ingham, P.W. (2011). Integration of Hedgehog and BMP signalling by the engrailed2a gene in the zebrafish myotome. Development *138*, 755–765.

McCulley, D., Kang, J., Martin, J., and Black, B. (2008). BMP4 is required in the anterior heart field and its derivatives for endocardial cushion remodeling, outflow tract septation, and semilunar valve development. Dev. Dyn. *237*, 3200–3209.

Miller, W. (2007). StAR search--what we know about how the steroidogenic acute regulatory protein mediates mitochondrial cholesterol import. Molecular Endocrinology *21*, 589.

Miyazono, K., Maeda, S., and Imamura, T. (2005). BMP receptor signaling: transcriptional targets, regulation of signals, and signaling cross-talk. Cytokine & Growth Factor Reviews *16*, 251–263.

Mommsen, T., Vijayan, M., and Moon, T. (1999). Cortisol in teleosts: dynamics, mechanisms of action, and metabolic regulation. Reviews in Fish Biology and Fisheries *9*, 211–268.

Myers, D.C., Sepich, D.S., and Solnica-Krezel, L. (2002). Bmp activity gradient regulates convergent extension during zebrafish gastrulation. Developmental Biology *243*, 81–98.

Nagy, J.A., Dvorak, A.M., and Dvorak, H.F. (2007). VEGF-A and the Induction of Pathological Angiogenesis. Annu. Rev. Pathol. Mech. Dis. *2*, 251–275.

Nesan, D., and Vijayan, M.M. (2012a). Embryo exposure to elevated cortisol level leads to cardiac performance dysfunction in zebrafish. Molecular and Cellular Endocrinology 1–31.

Nesan, D., and Vijayan, M.M. (2012b). Embryo exposure to elevated cortisol level leads to cardiac performance dysfunction in zebrafish. Molecular and Cellular Endocrinology *363*, 85–91.

Nesan, D., and Vijayan, M.M. (2012c). Role of glucocorticoid in developmental programming: Evidence from zebrafish. General and Comparative Endocrinology 1–10.

Nesan, D., Kamkar, M., Burrows, J., Scott, I.C., Marsden, M., and Vijayan, M.M. (2012). Glucocorticoid receptor signaling is essential for mesoderm formation and muscle development in zebrafish. Endocrinology *153*, 1288–1300.

Nie, X., Luukko, K., and Kettunen, P. (2006). BMP signalling in craniofacial development. Int. J. Dev. Biol. *50*.

Nielsen, S., Chou, C.L., Marples, D., Christensen, E.I., Kishore, B.K., and Knepper, M.A. (1995). Vasopressin increases water permeability of kidney collecting duct by inducing translocation of aquaporin-CD water channels to plasma membrane. Proc. Natl. Acad. Sci. U.S.a. *92*, 1013–1017.

Nikaido, M., Tada, M., Saji, T., and Ueno, N. (1997). Conservation of BMP signaling in zebrafish mesoderm patterning. Mechanisms of Development *61*, 75–88.

Okoshi, M.P., Yan, X., Okoshi, K., Nakayama, M., Schuldt, A.J.T., O'Connell, T.D., Simpson, P.C., and Lorell, B.H. (2004). Aldosterone directly stimulates cardiac myocyte hypertrophy. Journal of Cardiac Failure *10*, 511–518.

Overli, O., Korzan, W.J., Höglund, E., Winberg, S., Bollig, H., Watt, M., Forster, G.L., Barton, B.A., ØVerli, E., Renner, K.J., et al. (2004). Stress coping style predicts aggression and social dominance in rainbow trout. Hormones and Behavior *45*, 235–241.

Patterson, S., Bird, N., and Devoto, S. (2010). BMP regulation of myogenesis in zebrafish. Dev. Dyn. *239*, 806–817.

Pietri, T., Easley-Neal, C., Wilson, C., and Washbourne, P. (2008). Six cadm/ synCAMgenes are expressed in the nervous system of developing zebrafish. Dev. Dyn. *237*, 233–246.

Pikulkaew, S., Benato, F., Celeghin, A., Zucal, C., Skobo, T., Colombo, L., and Valle, L.D. (2011). The knockdown of maternal glucocorticoid receptor mRNA alters embryo development in zebrafish. Dev. Dyn. *240*, 874–889.

Pinky (2004). Studies on protocadherin-2 expression in the human fetal central nervous system. 1–9.

Pippal, J.B., Cheung, C.M.I., Yao, Y.-Z., Brennan, F.E., and Fuller, P.J. (2011). Characterization of the zebrafish (Danio rerio) mineralocorticoid receptor. Molecular and Cellular Endocrinology *332*, 58–66.

Pogoda, H.-M., and Hammerschmidt, M. (2009). How to make a teleost adenohypophysis: molecular pathways of pituitary development in zebrafish. Molecular and Cellular Endocrinology *312*, 2–13.

Pogoda, H.-M., and Meyer, D. (2002). Zebrafish Smad7 is regulated by Smad3 and BMP signals. Dev. Dyn. *224*, 334–349.

Porazzi, P., Calebiro, D., Benato, F., Tiso, N., and Persani, L. (2009). Thyroid gland development and function in the zebrafish model. Molecular and Cellular Endocrinology *312*, 14–23.

Posner, M., Hawke, M., Lacava, C., Prince, C.J., Bellanco, N.R., and Corbin, R.W. (2008). A proteome map of the zebrafish (Danio rerio) lens reveals similarities between zebrafish and mammalian crystallin expression. Mol. Vis. *14*, 806–814.

Posner, M., Kantorow, M., and Horwitz, J. (1999). Cloning, sequencing and differential expression of αB-crystallin in the zebrafish, Danio rerio. Biochimica Et Biophysica Acta (BBA)-Gene Structure and Expression *1447*, 271–277.

Pottinger, T.G., and Carrick, T.R. (2001). Stress responsiveness affects dominant-subordinate relationships in rainbow trout. Hormones and Behavior *40*, 419–427.

Pyati, U., Webb, A., and Kimelman, D. (2005). Transgenic zebrafish reveal stage-specific roles for Bmp signaling in ventral and posterior mesoderm development. Development *132*, 2333.

Redies, C., Heyder, J., Kohoutek, T., Staes, K., and Van Roy, F. (2008). Expression of protocadherin-1 (Pcdh1) during mouse development. Dev. Dyn. *237*, 2496–2505.

Rescan, P.Y., Ralliere, C., Chauvigné, F., and Cauty, C. (2005). Expression patterns of collagen I (α1) encoding gene and muscle-specific genes reveal that the lateral domain of the fish somite forms a connective tissue surrounding the myotome. Dev. Dyn. *233*, 605–611.

Ryu, S., Mahler, J., Acampora, D., Holzschuh, J., Erhardt, S., Omodei, D., Simeone, A., and Driever, W. (2007). Orthopedia Homeodomain Protein Is Essential for Diencephalic Dopaminergic Neuron Development. Current Biology *17*, 873–880.

Scheier, B., Foletti, A., Stark, G., Aoyama, A., Döbbeling, U., Rusconi, S., and Klemenz, R. (1996). Glucocorticoids regulate the expression of the stressprotein alpha B-crystallin. Molecular and Cellular Endocrinology *123*, 187–198.

Shin, D., Shin, C., Tucker, J., Ober, E., Rentzsch, F., Poss, K., Hammerschmidt, M., Mullins, M., and Stainier, D. (2007). Bmp and Fgf signaling are essential for liver specification in zebrafish. Development *134*, 2041.

Sundström, G., Larsson, T.A., Brenner, S., Venkatesh, B., and Larhammar, D. (2008). Evolution of the neuropeptide Y family: New genes by chromosome duplications in early vertebrates and in teleost fishes. General and Comparative Endocrinology *155*, 705–716.

Suzuki, S. (2000). Recent Progress in Protocadherin Research. Exp. Cell Res. *261*, 13–18.

Telfer, W.R., Busta, A.S., Bonnemann, C.G., Feldman, E.L., and Dowling, J.J. (2010). Zebrafish models of collagen VI-related myopathies. Human Molecular Genetics *19*, 2433–2444.

Tiso, N., Filippi, A., Pauls, S., Bortolussi, M., and Argenton, F. (2002). BMP signalling regulates anteroposterior endoderm patterning in zebrafish. Mechanisms of Development *118*, 29–37.

Toyama, R., Kobayashi, M., Tomita, T., and Dawid, I.B. (1998). Expression of LIM-domain binding protein (ldb) genes during zebrafish embryogenesis. Mechanisms of Development *71*, 197–200.

Toyama, R., and Dawid, I.B. (1997). lim6, a novel LIM homeobox gene in the zebrafish: Comparison of its expression pattern with lim1. Developmental Dynamics *209*, 406-417.

Weber, S., Taylor, J., Winyard, P., Baker, K., Sullivan-Brown, J., Schild, R., Knuppel, T., Zurowska, A., Caldas-Alfonso, A., and Litwin, M. (2008). SIX2 and BMP4 mutations associate with anomalous kidney development. Journal of the American Society of Nephrology *19*, 891.

Welberg, L.A., Seckl, J.R., and Holmes, M.C. (2001). Prenatal glucocorticoid programming of brain corticosteroid receptors and corticotrophin-releasing hormone: possible implications for behaviour. Neuroscience *104*, 71–79.

Wendelaar Bonga, S. (1997). The stress response in fish. Physiological Reviews *77*, 591–626.

Westerfield, M. (2007). The Zebrafish Book (Eugene, Oregon: University of Oregon Press).

Willot, V., Mathieu, J., Lu, Y., Schmid, B., Sidi, S., Yan, Y.-L., Postlethwait, J.H., Mullins, M., Rosa, F., and Peyriéras, N. (2002). Cooperative action of ADMP- and BMP-mediated pathways in regulating cell fates in the zebrafish gastrula. Developmental Biology *241*, 59–78.

Xiao, Y.-T., Xiang, L.-X., and Shao, J.-Z. (2007). Bone morphogenetic protein. Biochemical and Biophysical Research Communications *362*, 550–553.

Xu, Y., He, J., Wang, X., Lim, T., and Gong, Z. (2000). Asynchronous activation of 10 muscle-specific protein (MSP) genes during zebrafish somitogenesis. Dev. Dyn. *219*, 201–215.

Yokoi, H., Yan, Y.-L., Miller, M.R., BreMiller, R.A., Catchen, J.M., Johnson, E.A., and Postlethwait, J.H. (2009). Expression profiling of zebrafish sox9 mutants reveals that Sox9 is required for retinal differentiation. Developmental Biology *329*, 1–15.

Zhang, S., Fei, T., Zhang, L., Zhang, R., Chen, F., Ning, Y., Han, Y., Feng, X.-H., Meng, A., and Chen, Y.-G. (2007). Smad7 antagonizes transforming growth factor beta signaling in the nucleus by interfering with functional Smad-DNA complex formation. Molecular and Cellular Biology *27*, 4488–4499.

Zhong, Y., Lu, L., Zhou, J., Li, Y., Liu, Y., Clemmons, D.R., and Duan, C. (2011). IGF binding protein 3 exerts its ligand-independent action by antagonizing BMP in zebrafish embryos. Journal of Cell Science *124*, 1925–1935.

Zou, S., Kamei, H., Modi, Z., and Duan, C. (2009). Zebrafish IGF Genes: Gene Duplication, Conservation and Divergence, and Novel Roles in Midline and Notochord Development. PLoS One *4*, e7026.

CHAPTER 5

Alderman, S., and Bernier, N. (2009). Ontogeny of the corticotropin-releasing factor system in zebrafish. General and Comparative Endocrinology *164*, 61–69.

Alderman, S.L., McGuire, A., Bernier, N.J., and Vijayan, M.M. (2012). Central and peripheral glucocorticoid receptors are involved in the plasma cortisol response to an acute stressor in rainbow trout. General and Comparative Endocrinology *176*, 79–85.

Alsop, D., and Vijayan, M. (2008). Development of the corticosteroid stress axis and receptor expression in zebrafish. American Journal of Physiology- Regulatory, Integrative and Comparative Physiology *294*, R711.

Arndt, K., and Fink, G.R. (1986). GCN4 protein, a positive transcription factor in yeast, binds general control promoters at all 5“ TGACTC 3” sequences. Proc. Natl. Acad. Sci. U.S.a. *83*, 8516–8520.

Barreto, R.E., Volpato, G.L., de Brito Faturi, C., Giaquinto, P.C., de Freitas, E.G., and de Castilho, M.F. (2009). Aggressive behaviour traits predict physiological stress responses in Nile tilapia (Oreochromis niloticus). Marine and Freshwater Behaviour and Physiology *42*, 109–118.

Barton, B.A. (2002). Stress in fishes: a diversity of responses with particular reference to changes in circulating corticosteroids. Integrative and Comparative Biology *42*, 517–525.

Bauer, M.P., Bridgham, J.T., Langenau, D.M., Johnson, A.L., and Goetz, F.W. (2000). Conservation of steroidogenic acute regulatory (StAR) protein structure and expression in vertebrates. Molecular and Cellular Endocrinology *168*, 119–125.

Blechman, J., Borodovsky, N., Eisenberg, M., Nabel-Rosen, H., Grimm, J., and Levkowitz, G. (2007). Specification of hypothalamic neurons by dual regulation of the homeodomain protein Orthopedia. Development *134*, 4417–4426.

Bradford, C.S., Fitzpatrick, M.S., and Schreck, C.B. (1992). Evidence for ultra-short-loop feedback in ACTH-induced interrenal steroidogenesis in coho salmon: acute self-suppression of cortisol secretion in vitro. General and Comparative Endocrinology *87*, 292–299.

Cadby, C.D., Jones, S.M., and Wapstra, E. (2010). Are increased concentrations of maternal corticosterone adaptive to offspring? A test using a placentotrophic lizard. Functional Ecology *24*, 409–416.

Caldji, C., Diorio, J., and Meaney, M.J. (2000). Variations in maternal care in infancy regulate the development of stress reactivity. Biological Psychiatry *48*, 1164–1174.

Chang, C., Li, C.Y., Earley, R.L., and Hsu, Y. (2012). Aggression and Related Behavioral Traits: The Impact of Winning and Losing and the Role of Hormones. Integrative and Comparative Biology *52*, 801–813.

Dahlbom, S.J., Lagman, D., Lundstedt-Enkel, K., Sundström, L.F., and Winberg, S. (2011). Boldness predicts social status in zebrafish (Danio rerio). PLoS One *6*, e23565.

Dallman, M., Akana, S., Scribner, K., Bradbury, M., Walker, C., Strack, A., and Cascio, C. (1992). Stress, feedback and facilitation in the hypothalamo-pituitary-adrenal axis. Journal of Neuroendocrinology *4*, 517–526.

De Fraipont, M., Clobert, J., John, H., and Meylan, S. (2000). Increased pre‐natal maternal corticosterone promotes philopatry of offspring in common lizards Lacerta vivipara. Journal of Animal Ecology *69*, 404–413.

FISH, E.W., SHAHROKH, D., BAGOT, R., CALDJI, C., BREDY, T., Szyf, M., and Meaney, M.J. (2004). Epigenetic programming of stress responses through variations in maternal care. Annals of the New York Academy of Sciences *1036*, 167–180.

Francis, D., Diorio, J., LaPlante, P., Weaver, S., Seckl, J.R., and Meaney, M.J. (1996). The role of early environmental events in regulating neuroendocrine development. Moms, pups, stress, and glucocorticoid receptors. Annals of the New York Academy of Sciences *794*, 136–152.

Fries, E., Hesse, J., Hellhammer, J., and Hellhammer, D.H. (2005). A new view on hypocortisolism. Psychoneuroendocrinology *30*, 1010–1016.

Giesing, E.R., Suski, C.D., Warner, R.E., and Bell, A.M. (2011). Female sticklebacks transfer information via eggs: effects of maternal experience with predators on offspring. Proc. Biol. Sci. *278*, 1753–1759.

Gilmour, K.M., Dibattista, J.D., and Thomas, J.B. (2005). Physiological causes and consequences of social status in salmonid fish. Integrative and Comparative Biology *45*, 263–273.

Gonçalves, A.F., Páscoa, I., Neves, J.V., Coimbra, J., Vijayan, M.M., Rodrigues, P., and Wilson, J.M. (2012). The inhibitory effect of environmental ammonia on Danio rerio LPS induced acute phase response. Dev. Comp. Immunol. *36*, 279–288.

Gómez, F., de Kloet, E.R., and Armario, A. (1998). Glucocorticoid negative feedback on the HPA axis in five inbred rat strains. Am. J. Physiol. *274*, R420–R427.

Groothuis, T.G.G., and Schwabl, H. (2008). Hormone-mediated maternal effects in birds: mechanisms matter but what do we know of them? Philosophical Transactions of the Royal Society B: Biological Sciences *363*, 1647–1661.

Hayward, L., and Wingfield, J. (2004). Maternal corticosterone is transferred to avian yolk and may alter offspring growth and adult phenotype. General and Comparative Endocrinology *135*, 365–371.

Heim, C., Ehlert, U., and Hellhammer, D.H. (2000). The potential role of hypocortisolism in the pathophysiology of stress-related bodily disorders. Psychoneuroendocrinology *25*, 1–35.

Hillegass, J., Villano, C., Cooper, K., and White, L. (2008). Glucocorticoids alter craniofacial development and increase expression and activity of matrix metalloproteinases in developing zebrafish (Danio rerio). Toxicological Sciences.

Ings, J.S., Vijayan, M.M., and Servos, M.R. (2012). Tissue-specific metabolic changes in response to an acute handling disturbance in juvenile rainbow trout exposed to municipal wastewater effluent. Aquatic Toxicology *108*, 53–59.

Kapoor, A. (2006). Fetal Programming of Hypothalamo-Pituitary-Adrenal (HPA) Function: Prenatal Stress and Glucocorticoids. The Journal of Physiology.

Kapoor, A., Petropoulos, S., and Matthews, S.G. (2008). Fetal programming of hypothalamic-pituitary-adrenal (HPA) axis function and behavior by synthetic glucocorticoids. Brain Research Reviews *57*, 586–595.

Kawamoto, T., Mitsuuchi, Y., Toda, K., Yokoyama, Y., Miyahara, K., Miura, S., Ohnishi, T., Ichikawa, Y., Nakao, K., and Imura, H. (1992). Role of steroid 11 beta-hydroxylase and steroid 18-hydroxylase in the biosynthesis of glucocorticoids and mineralocorticoids in humans. Proc. Natl. Acad. Sci. U.S.a. *89*, 1458–1462.

Kulkeaw, K., Ishitani, T., Kanemaru, T., Ivanovski, O., Nakagawa, M., Mizuochi, C., Horio, Y., and Sugiyama, D. (2011). Cold exposure down-regulates zebrafish pigmentation. Genes to Cells *16*, 358–367.

Kumai, Y., Nesan, D., Vijayan, M.M., and Perry, S.F. (2012). Cortisol regulates Na+ uptake in zebrafish, Danio rerio, larvae via the glucocorticoid receptor. Molecular and Cellular Endocrinology *364*, 113–125.

Liu, N.-A., Huang, H., Yang, Z., Herzog, W., Hammerschmidt, M., Lin, S., and Melmed, S. (2003). Pituitary corticotroph ontogeny and regulation in transgenic zebrafish. Mol. Endocrinol. *17*, 959–966.

Liu, Y. (2007). Interrenal Organogenesis in the Zebrafish Model. Organogenesis *3*, 44.

Livak, K., and Schmittgen, T. (2001). Analysis of relative gene expression data using real-time quantitative PCR and the 2-[Delta][Delta] CT method. Methods *25*, 402–408.

Love, O.P., and Williams, T.D. (2008). The Adaptive Value of Stress‐Induced Phenotypes: Effects of Maternally Derived Corticosterone on Sex‐Biased Investment, Cost of Reproduction, and Maternal Fitness. Am Nat *172*, E135–E149.

Löhr, H., and Hammerschmidt, M. (2011). Zebrafish in Endocrine Systems: Recent Advances and Implications for Human Disease. Annu. Rev. Physiol. *73*, 183–211.

Machluf, Y., Gutnick, A., and Levkowitz, G. (2011). Development of the zebrafish hypothalamus. Annals of the New York Academy of Sciences *1220*, 93–105.

McCormick, S. (2001). Endocrine control of osmoregulation in teleost fish. Integrative and Comparative Biology *41*, 781.

Meylan, S., and Clobert, J. (2005). Is corticosterone-mediated phenotype development adaptive? Maternal corticosterone treatment enhances survival in male lizards. Hormones and Behavior *48*, 44–52.

Mommsen, T., Vijayan, M., and Moon, T. (1999). Cortisol in teleosts: dynamics, mechanisms of action, and metabolic regulation. Reviews in Fish Biology and Fisheries *9*, 211–268.

Müller, W., Lessells, C.K.M., Korsten, P., and Engelhardt, von, N. (2007). Manipulative signals in family conflict? On the function of maternal yolk hormones in birds. Am Nat *169*, E84–E96.

Nesan, D., and Vijayan, M.M. (2012a). Embryo exposure to elevated cortisol level leads to cardiac performance dysfunction in zebrafish. Molecular and Cellular Endocrinology *363*, 85–91.

Nesan, D., and Vijayan, M.M. (2012b). Role of glucocorticoid in developmental programming: Evidence from zebrafish. General and Comparative Endocrinology 1–10.

Nesan, D., Kamkar, M., Burrows, J., Scott, I.C., Marsden, M., and Vijayan, M.M. (2012). Glucocorticoid receptor signaling is essential for mesoderm formation and muscle development in zebrafish. Endocrinology *153*, 1288–1300.

Peterson, B.C., and Small, B.C. (2005). Effects of exogenous cortisol on the GH/IGF-I/IGFBP network in channel catfish. Domestic Animal Endocrinology *28*, 391–404.

Pierce, A.L., Breves, J.P., Moriyama, S., Hirano, T., and Grau, E.G. (2011). Differential regulation of Igf1 and Igf2 mRNA levels in tilapia hepatocytes: effects of insulin and cortisol on GH sensitivity. Journal of Endocrinology *211*, 201–210.

Pikulkaew, S., Benato, F., Celeghin, A., Zucal, C., Skobo, T., Colombo, L., and Valle, L.D. (2011). The knockdown of maternal glucocorticoid receptor mRNA alters embryo development in zebrafish. Dev. Dyn. *240*, 874–889.

Pippal, J.B., Cheung, C.M.I., Yao, Y.-Z., Brennan, F.E., and Fuller, P.J. (2011). Characterization of the zebrafish (Danio rerio) mineralocorticoid receptor. Molecular and Cellular Endocrinology *332*, 58–66.

Pottinger, T.G., and Carrick, T.R. (2001). Stress responsiveness affects dominant-subordinate relationships in rainbow trout. Hormones and Behavior *40*, 419–427.

Sathiyaa, R., and Vijayan, M. (2003). Autoregulation of glucocorticoid receptor by cortisol in rainbow trout hepatocytes. American Journal of Physiology- Cell Physiology *284*, C1508.

Sturm, A., Bury, N., Dengreville, L., (null), Flouriot, G., (null), and Prunet, P. (2005). 11-deoxycorticosterone is a potent agonist of the rainbow trout (Oncorhynchus mykiss) mineralocorticoid receptor. Endocrinology *146*, 47.

van der Boon, J., van den Thillart, G., and Addink, A. (1991). The effects of cortisol administration on intermediary metabolism in teleost fish. Comparative Biochemistry and Physiology Part a: Physiology *100*, 47–53.

Van Houdenhove, B., Van Den Eede, F., and Luyten, P. (2009). Does hypothalamic–pituitary–adrenal axis hypofunction in chronic fatigue syndrome reflect a “crash” in the stress system? Medical Hypotheses *72*, 701–705.

Veillette, P.A., Serrano, X., Garcia, M.M., and Specker, J.L. (2007). Evidence for the onset of feedback regulation of cortisol in larval summer flounder. General and Comparative Endocrinology *154*, 105–110.

Wendelaar Bonga, S. (1997). The stress response in fish. Physiological Reviews *77*, 591–626.

Westerfield, M. (2007). The Zebrafish Book (Eugene, Oregon: University of Oregon Press).

Yada, T., Muto, K., Azuma, T., Hyodo, S., and Schreck, C.B. (2005). Cortisol stimulates growth hormone gene expression in rainbow trout leucocytes in vitro. General and Comparative Endocrinology *142*, 248–255.

Young, G., Björnsson, B.T., Prunet, P., Lin, R.J., and Bern, H.A. (1989). Smoltification and seawater adaptation in coho salmon (Oncorhynchus kisutch): plasma prolactin, growth hormone, thyroid hormones, and cortisol. General and Comparative Endocrinology *74*, 335–345.

CHAPTER 6

Driever, W., Stemple, D., Schier, A., and Solnica-Krezel, L. (1994). Zebrafish: genetic tools for studying vertebrate development. Trends in Genetics *10*, 152–159.

Gilmour, K.M., Dibattista, J.D., and Thomas, J.B. (2005). Physiological causes and consequences of social status in salmonid fish. Integrative and Comparative Biology *45*, 263–273.

Hayward, L., and Wingfield, J. (2004). Maternal corticosterone is transferred to avian yolk and may alter offspring growth and adult phenotype. General and Comparative Endocrinology *135*, 365–371.

Hillegass, J., Villano, C., Cooper, K., and White, L. (2007). Matrix metalloproteinase-13 is required for zebra fish (Danio rerio) development and is a target for glucocorticoids. Toxicological Sciences *100*, 168.

Hillegass, J., Villano, C., Cooper, K., and White, L. (2008). Glucocorticoids alter craniofacial development and increase expression and activity of matrix metalloproteinases in developing zebrafish (Danio rerio). Toxicological Sciences.

Jowett, T. (1999). Transgenic zebrafish. Methods Mol. Biol. *97*, 461–486.

Krukowski, K., Eddy, J., Kosik, K.L., Konley, T., Janusek, L.W., and Mathews, H.L. (2011). Glucocorticoid dysregulation of natural killer cell function through epigenetic modification. Brain, Behavior, and Immunity *25*, 239–249.

Kumai, Y., Nesan, D., Vijayan, M.M., and Perry, S.F. (2012). Cortisol regulates Na+ uptake in zebrafish, Danio rerio, larvae via the glucocorticoid receptor. Molecular and Cellular Endocrinology *364*, 113–125.

Lillycrop, K.A., Slater-Jefferies, J.L., Hanson, M.A., Godfrey, K.M., Jackson, A.A., and Burdge, G.C. (2007). Induction of altered epigenetic regulation of the hepatic glucocorticoid receptor in the offspring of rats fed a protein-restricted diet during pregnancy suggests that reduced DNA methyltransferase-1 expression is involved in impaired DNA methylation and changes in histone modifications. Br. J. Nutr. *97*, 1064–1073.

Matthews, S.G. (2002). Early programming of the hypothalamo-pituitary-adrenal axis. Trends in Endocrinology & Metabolism *13*, 373–380.

McGowan, P.O., Sasaki, A., D'Alessio, A.C., Dymov, S., Labonté, B., Szyf, M., Turecki, G., and Meaney, M.J. (2009). Epigenetic regulation of the glucocorticoid receptor in human brain associates with childhood abuse. Nat. Neurosci. *12*, 342–348.

McLean, D.L., and Fetcho, J.R. (2008). Using imaging and genetics in zebrafish to study developing spinal circuits in vivo. Dev Neurobiol *68*, 817–834.

Moritz, K.M., Boon, W.M., and Wintour, E.M. (2005). Glucocorticoid programming of adult disease. Cell Tissue Res *322*, 81–88.

Nesan, D., and Vijayan, M.M. (2012). Embryo exposure to elevated cortisol level leads to cardiac performance dysfunction in zebrafish. Molecular and Cellular Endocrinology *363*, 85–91.

Oberlander, T.F., Weinberg, J., Papsdorf, M., Grunau, R., Misri, S., and Devlin, A.M. (2008). Prenatal exposure to maternal depression, neonatal methylation of human glucocorticoid receptor gene (NR3C1) and infant cortisol stress responses. Epigenetics *3*, 97–106.

Overli, O., Korzan, W.J., Höglund, E., Winberg, S., Bollig, H., Watt, M., Forster, G.L., Barton, B.A., ØVerli, E., Renner, K.J., et al. (2004). Stress coping style predicts aggression and social dominance in rainbow trout. Hormones and Behavior *45*, 235–241.

Pikulkaew, S., Benato, F., Celeghin, A., Zucal, C., Skobo, T., Colombo, L., and Valle, L.D. (2011). The knockdown of maternal glucocorticoid receptor mRNA alters embryo development in zebrafish. Dev. Dyn. *240*, 874–889.

Pottinger, T.G., and Carrick, T.R. (2001). Stress responsiveness affects dominant-subordinate relationships in rainbow trout. Hormones and Behavior *40*, 419–427.

Rasooly, R.S., Henken, D., Freeman, N., Tompkins, L., Badman, D., Briggs, J., Hewitt, A.T., National Institutes of Health Trans-NIH Zebrafish Coordinating Committee (2003). Genetic and genomic tools for zebrafish research: the NIH zebrafish initiative. Dev. Dyn. *228*, 490–496.

Seckl, J.R., and Meaney, M.J. (2004). Glucocorticoid Programming. Annals of the New York Academy of Sciences *1032*, 63–84.

Teh, C., Parinov, S., and Korzh, V. (2005). New ways to admire zebrafish: progress in functional genomics research methodology. Biotechniques *38*, 897–906.

Weaver, I.C.G. (2009). Epigenetic effects of glucocorticoids. Semin Fetal Neonatal Med *14*, 143–150.

Youngson, N.A., and Whitelaw, E. (2008). Transgenerational epigenetic effects. Annu. Rev. Genom. Human Genet. *9*, 233–257.

Zhang, T.-Y., and Meaney, M.J. (2010). Epigenetics and the environmental regulation of the genome and its function. Annu Rev Psychol *61*, 439–66–C1–3.